

---

Doctoral

Science

---

2007-01-01

## Rate and Equilibrium Constants for Reactions of Coordinated Cyclohexadienyl Cations

Martin Galvin

*Technological University Dublin*

Follow this and additional works at: <https://arrow.tudublin.ie/sciendoc>

 Part of the [Chemistry Commons](#)

---

### Recommended Citation

Galvin, Martin. *Rate and equilibrium constants for reactions of coordinated cyclohexadienyl cations*. Doctoral Thesis. Technological University Dublin. doi:10.21427/D7QG76

This Theses, Ph.D is brought to you for free and open access by the Science at ARROW@TU Dublin. It has been accepted for inclusion in Doctoral by an authorized administrator of ARROW@TU Dublin. For more information, please contact [arrow.admin@tudublin.ie](mailto:arrow.admin@tudublin.ie), [aisling.coyne@tudublin.ie](mailto:aisling.coyne@tudublin.ie), [vera.kilshaw@tudublin.ie](mailto:vera.kilshaw@tudublin.ie).



# **Rate and Equilibrium Constants for Reactions of Coordinated Cyclohexadienyl Cations**

By

**Martin Galvin BSc.**

A Thesis Submitted to the Dublin Institute of Technology,  
for the Degree of Doctor of Philosophy.

Supervised by Dr. Claire McDonnell

and

Prof. Rory More O'Ferrall (UCD)

School of Chemical and Pharmaceutical Sciences  
Dublin Institute of Technology  
Kevin Street, Dublin 8.


**May 2007**

I certify that this thesis which I now submit for the award of Doctor of Philosophy, is entirely my own work and has not been taken from the work of others save and to the extent that such work has been cited and acknowledged within the text of my work.

This thesis was prepared according to the regulations for postgraduate study by research of the Dublin Institute of Technology and has not been submitted in whole or in part for an award in any other Institute or University.

The work reported on in this thesis conforms to the principles and requirements of the Institute's guidelines for ethics in research.

The Institute has permission to keep, to lend or to copy this thesis in whole or in part, on condition that any such use of the material of the thesis be duly acknowledged.

Signature   
Candidate

Date 20/7/07

## Acknowledgements

The writing and completion of a thesis is the final act of a journey which begins many years prior. As one travels the path, one encounters numerous people along the way, many of which have a hand in shaping and moulding the research, the thesis or the researcher. This is my opportunity to acknowledge those people.

I owe a debt of gratitude to my supervisors Dr. Claire McDonnell and Prof. Rory More O'Ferrall. They not only readily provided advice and guidance on the material contained within these pages, they also endowed me with a view of the world I shall carry through life.

I would like to thank Dr. Dara Coyne for all his help over the years, especially for the time he dedicated instructing me in the use of UV-Vis software. Without his patient tutelage no results would have been obtained at all!

From Lab330, to G38 to the Focas Institute, one friend has been there through thick and thin. He stood by me in all aspects of my life including honouring me by being best man at my wedding. Ciarán Potter, you have been a wonderful friend, words fail me in trying to express my gratitude, all I can say is thank you.

The Focas institute is full of people I need to thank and I simply cannot name them all. A special thank you however to Patrick Lynch and Catriona O'Meara.

Finally I need to thank my family, my parents, Maire and Frank, who have always been a source of support. My gratitude also goes to my extended family, Noel, Rita and William, for all your encouragement. Above all I need to acknowledge my wife Anne-Margaret and my daughter Nerys. You are with me in every aspect of my life and your love is my inspiration.

*Dedicated to Kathleen McGuire*

1913 - 2000

“There are few earthly things more beautiful than a university, a place where those who hate ignorance may strive to know, where those who perceive truth may strive to make others see.”

John Masefield

# Table of Contents

Abbreviations	x
Abstract	xii
1 Introduction.....	1
1.1 Oxidative Metabolites of Aromatic Hydrocarbons.....	1
1.1.1 Arene Oxides .....	4
1.1.2 Arene <i>Cis</i> - and <i>Trans</i> -Dihydrodiols .....	6
1.1.3 Arene Hydrates .....	9
1.1.4 Reactivity of Arene Hydrates .....	10
1.2 Organometallic Chemistry .....	15
1.2.1 Tricarbonyliron Complexes-Initial Synthetic Methods .....	16
1.2.2 Tricarbonyliron Complexation Using Tricarbonyliron Transfer Reagents	18
1.2.2.1 ( $\eta^4$ -1-Oxabuta-1,3-diene)tricarbonyliron Complexes.....	18
1.2.2.2 Grevels' Reagent (Bis( $\eta^2$ - <i>cis</i> -cyclooctene)tricarbonyliron) .....	19
1.2.2.3 ( $\eta^4$ -1-Azabuta-1,3-diene)tricarbonyliron Complexes .....	20
1.2.2.4 Tricarbonyliron Complexes of Chiral 1-Azabuta-1,3-dienes .....	22
1.2.3 Synthetic Applications of Tricarbonyliron Complexes .....	23
1.2.3.1 The Tricarbonyliron Fragment as a Protecting Group.....	23
1.2.3.2 Stereochemical Control Using the Tricarbonyliron Group.....	24
1.2.3.3 The Tricarbonyliron Moiety as an Activating Group .....	25
1.2.3.4 Stabilising Ability of the Tricarbonyliron Unit .....	26
1.2.4 Cyclohexadienyl-tricarbonyliron Complexes .....	28
1.2.5 Cyclohexadienyl-tricarbonyliron Complexes in Synthesis.....	30
1.2.6 Ligand Exchange: Substitution of a Carbonyl Ligand by a Triarylphosphine or Trialkylphosphine Ligand .....	33
1.2.6.1 The Eighteen Electron Rule.....	34
1.2.6.2 Back Bonding .....	35
1.2.6.3 The Electron Environment in Cyclohexadiene Complexes.....	35
1.2.6.4 Reaction Conditions for Ligand Exchange .....	36
1.2.7 Decomplexation of Tricarbonyliron Complexes .....	37
1.3 Stability of Coordinated Cyclohexadienyl Cations .....	38

1.3.1	Direct Equilibrium Measurements.....	39
1.3.2	Kinetic Measurements .....	40
1.4	Organometallic Coordination of Oxidative Metabolites of Aromatic Hydrocarbons-Aims of this Study .....	42
2	Results.....	45
2.1	( $\eta^5$ -Cyclohexadienyl)dicarbonyltriphenylphosphineiron Cation.....	45
2.1.1	Equilibrium Constant for Hydrolysis.....	46
2.1.2	Rate Constants for Hydrolysis .....	48
2.1.3	Rate Constants for Ionisation of ( $\eta^4$ - <i>Exo</i> -5-hydroxy-1,3- cyclohexadiene)dicarbonyltriphenylphosphineiron.....	58
2.1.4	pH Profile.....	65
2.1.5	Evidence for Formation of the Metal Protonated Species .....	68
2.1.5.1	$^1\text{H}$ NMR Spectroscopic Data .....	69
2.1.5.2	IR Spectroscopic Data .....	70
2.2	( $\eta^5$ -Cyclohexadienyl)tricarbonyliron Cation - Hydrolysis Reaction .....	73
2.2.1	Rate Constants for Hydrolysis Below pH 8.....	74
2.2.2	Ionisation of ( $\eta^4$ - <i>Exo</i> -5-hydroxy-1,3-cyclohexadiene)tricarbonyliron.....	81
2.2.3	Kinetic Determination of $pK_R$ for ( $\eta^4$ - <i>Exo</i> -5-hydroxy-1,3- cyclohexadiene)tricarbonyliron .....	84
2.2.4	Spectroscopic Determination of $pK_R$ for ( $\eta^4$ - <i>Exo</i> -5-hydroxy-1,3- cyclohexadiene)tricarbonyliron .....	86
2.2.5	Kinetic Determination of $pK_R$ for ( $\eta^4$ - <i>Exo</i> -5-hydroxy-1,3- cyclohexadiene)tricarbonyliron in $\text{D}_2\text{O}$ .....	88
2.2.6	Spectroscopic Determination of $pK_R$ for ( $\eta^4$ - <i>Exo</i> -5-hydroxy-1,3- cyclohexadiene)tricarbonyliron in $\text{D}_2\text{O}$ .....	91
2.2.7	pH Profile Below pH 8 .....	92
2.2.8	pD Profile.....	95
2.2.9	Equilibrium Constants for Hydrolysis .....	97
2.2.10	Rate Constants for Hydrolysis Above pH 8.....	99
2.3	( $\eta^5$ -Cyclohexadienyl)tricarbonyliron Cation - Methanolysis Reaction .....	105
2.3.1	Equilibrium Constant for Cation Formation in Methanol .....	105
2.3.2	Equilibrium Constant for Cation Formation in 50% Aqueous Methanol. ....	107
2.4	( $\eta^5$ -Cyclohexadienyl)tricarbonyliron $^1\text{H}$ NMR Spectroscopic Study.....	111



3	Discussion.....	124
3.1	Cyclohexadienyl Complexes Examined.....	124
3.2	pH Profile for ( $\eta^5$ -Cyclohexadienyl)dicarbonyltriphenylphosphineiron.....	126
3.2.1	Protonated Iron Complex.....	130
3.3	Measurements of Rates and Equilibria for the Reaction of ( $\eta^5$ -Cyclohexadienyl)tricarbonyliron.....	133
3.3.1	pH Profile.....	136
3.3.2	Isotope Effects for Rate and Equilibrium Constants.....	138
3.3.3	Measurements of $pK_R$ in Methanol.....	140
3.4	Comparison of Measured Equilibrium Constants with Those in the Literature.....	142
3.5	Comparison of Rate Constants For the Coordinated and Uncoordinated Cyclohexadienyl Cations.....	147
3.6	Conversion of Arene <i>Cis</i> - to <i>Trans</i> - Dihydrodiols <i>via</i> their Tricarbonyliron Complexes.....	152
3.6.1	Isomerisation of <i>Exo</i> -substituent to <i>Endo</i> -substituent.....	152
3.6.2	Implications for the Conversion of Arene <i>Cis</i> -Dihydrodiols to <i>Trans</i> -Dihydrodiols <i>via</i> Coordination to Ironcarbonyls.....	154
3.7	Conclusion.....	155
4	Experimental Details.....	159
4.1	General Instrumentation.....	159
4.2	Synthesis of Organic Substrates for Kinetic and Equilibrium Measurements.....	159
4.2.1	( $\eta^5$ -Cyclohexadienyl)dicarbonyltriphenylphosphineiron Hexafluorophosphate.....	159
4.3	Other Organic Substrates for Kinetic and Equilibrium Measurements.....	164
4.4	Reagents Used for Kinetic and Equilibrium Measurements.....	164
4.4.1	Solvents.....	164
4.4.2	Acids and Bases.....	165
4.4.3	Buffers.....	165
4.4.4	Inorganic Reagents.....	166
4.4.5	Deuterated Buffer Solutions.....	166
4.5	Instrumentation.....	167

4.5.1	pH Measurement.....	167
4.5.2	UV Spectrophotometry.....	167
4.5.3	UV-Vis Spectrophotometry Using a Fast Mixing Apparatus.....	168
4.6	Kinetic and Equilibrium Measurements .....	170
4.6.1	Equilibrium Measurements.....	170
4.6.2	Calculation of Data for Equilibrium Measurements Using Sigmaplot Software .....	171
4.6.3	Kinetic Measurements .....	173
4.6.4	Calculations for Kinetic Measurements.....	174
	References	175
	Appendix	181

## Abbreviations and Symbols

<b>A</b>	absorbance
<b>Ac</b>	acetyl
<b>Ac<sub>2</sub>O</b>	acetic anhydride
<b>Ar</b>	aryl
<b>bda</b>	benzylideneacetone
<b>BH</b>	buffer acid
<b>br s</b>	broad singlet
<b>Bu</b>	butyl
<b>°C</b>	degree(s) celsius
<b>cm<sup>-1</sup></b>	wavenumbers
<b><sup>13</sup>C NMR</b>	carbon 13 nuclear magnetic resonance
<b>δ</b>	chemical shift
<b>d</b>	doublet
<b>dd</b>	doublet of doublets
<b>DME</b>	1,2-dimethoxyethane
<b>DMF</b>	dimethylformamide
<b>DMSO</b>	dimethylsulphoxide
<b>ε</b>	molar extinction coefficient / molar absorbtivity
<b>Et</b>	ethyl
<b>EtO</b>	ethoxy
<b>FTIR</b>	Fourier transform infrared spectroscopy
<b>g</b>	gram(s)
<b>GPR</b>	general purpose reagent
<b>h</b>	hour(s)
<b>HCl</b>	hydrochloric acid
<b><sup>1</sup>H NMR</b>	proton nuclear magnetic resonance
<b>H<sub>2</sub>SO<sub>4</sub></b>	sulphuric acid
<b>Hz</b>	hertz
<b>IR</b>	infrared
<b>J</b>	coupling constant
<b>k</b>	rate constant
<b>K</b>	equilibrium constant

$\lambda$	wavelength
l	litre(s)
lit.	literature
log	logarithm
M	moles / litre
m	multiplet
m.p.	melting point
Me	methyl
MeO	methoxy
$\mu$ l	microlitre(s)
ml	millilitre(s)
mmol	millimole(s)
NADPH	nicotinamide adenine dinucleotide phosphate
NaOH	sodium hydroxide
PAH(s)	polycyclic aromatic hydrocarbon(s)
Ph	phenyl
ppm	parts per million
R	alkyl substituent or buffer ratio
s	second(s) or singlet
t	triplet
TBSOTf	<i>tert</i> -butyldimethylsilyl trifluoromethanesulfonate
TFA	trifluoroacetic acid
THF	tetrahydrofuran
TLC	thin layer chromatography
TMS	tetramethylsilane
UV	ultraviolet

## Abstract

In this work, the nucleophilic reaction of ironcarbonyl coordinated cyclohexadienyl cations with water and hydroxide to produce the corresponding coordinated arene hydrate analogues was examined. These nucleophilic reactions are a key step in a synthetic route to convert arene *cis*-dihydrodiols to their *trans*-isomers *via* their tricarbonyliron coordinated complexes. The arene *trans*-dihydrodiols produced have significant potential to be used as chiral building blocks in synthetic chemistry and have the advantage that they are more stable than their *cis*- analogues.

The first cation studied was ( $\eta^5$ -cyclohexadienyl)dicarbonyltriphenylphosphineiron. An equilibrium constant,  $pK_R$ , for formation of the coordinated arene hydrate, ( $\eta^4$ -*exo*-5-hydroxy-1,3-cyclohexadiene)dicarbonyltriphenylphosphineiron, from this coordinated cation was determined spectrophotometrically to be 9.9. Rate constants were measured for the hydrolysis of the cationic species, ( $\eta^5$ -cyclohexadienyl)dicarbonyltriphenylphosphineiron, and for the ionisation of the corresponding hydrate, ( $\eta^4$ -*exo*-5-hydroxy-1,3-cyclohexadiene)dicarbonyltriphenylphosphineiron, allowing a pH-profile ( $\log k$  versus pH) to be constructed. In the acidic region of the profile, an additional reaction was found to be occurring and was assigned to protonation at the iron atom. Evidence supporting the existence of a protonated iron complex was obtained by examining the reaction with trifluoroacetic acid of a related complex, ( $\eta^4$ -cyclohexa-1,3-diene)-dicarbonyltriphenylphosphineiron, by means of FTIR and  $^1\text{H}$  NMR spectroscopy.

Similarly, the ( $\eta^5$ -cyclohexadienyl)tricarbonyliron cation was studied. An equilibrium constant,  $pK_R$ , of 4.8 was determined by both spectrophotometric and kinetic means. Equilibrium and kinetic solvent isotope effects were observed and the values measured were consistent with those expected for the hydrolysis of a carbocation. A spectrophotometric examination of the ( $\eta^5$ -cyclohexadienyl)tricarbonyliron cation in methanol provided a  $pK_R$  of 1.0 for the methanolysis reaction. A complementary  $^1\text{H}$  NMR examination in deuterated methanol showed that the changes observed correspond to those observed in the UV spectra. From the  $^1\text{H}$  NMR study, it can be concluded that the nucleophilic reaction of the coordinated

cyclohexadienyl cations with the nucleophiles in this study provide the kinetically favoured *exo*-substituted product.

A comparison of the rate constant for ionisation of the tricarbonyliron coordinated *exo*-hydrate measured in this work with that for the *endo*-hydrate previously determined<sup>85</sup> showed that the *exo*- isomer reacted more than  $10^6$  times more quickly. It can be concluded that the difficult step in the route to convert arene *cis*-dihydrodiols to their *trans* isomers will be reaction of the coordinated *endo* diol to give the corresponding cation. Thus, the best strategy for improving the process is to explore and optimise conditions for conversion of *cis*-diol complexes to their carbocations.

The equilibrium constants determined for both cations, ( $\eta^5$ -cyclohexadienyl)dicarbonyltriphenylphosphineiron and ( $\eta^5$ -cyclohexadienyl)tricarbonyliron, can be compared with that for the uncoordinated cyclohexadienyl cation (benzenonium ion) which is much less stable. The  $pK_R$  for this cation was previously determined to be -2.1.<sup>53</sup> The difference in stability amounts to factors of  $10^{12}$  and  $10^7$  respectively. However this large difference in stability fails to reflect the difference in reactivity of the species. The coordinated cations undergo a different reaction in aqueous solution to the uncoordinated cation, hydrolysis rather than deprotonation. When the acid dissociation constant,  $pK_a$ , of the cyclohexadienyl cation is compared with the  $pK_R$  values of the coordinated species, differences in reactivity of nearly 48 kcal mol<sup>-1</sup> and 40 kcal mol<sup>-1</sup> are observed. Comparisons were also made between the cations studied in this work and other coordinated and uncoordinated cations, including the tropylium ion. It can be inferred that if these coordinated cations underwent deprotonation to form the corresponding coordinated benzene complexes, two of the double bonds would be coordinated and the one remaining double bond would be olefinic.

## **CHAPTER 1**

### **INTRODUCTION**

# 1 Introduction

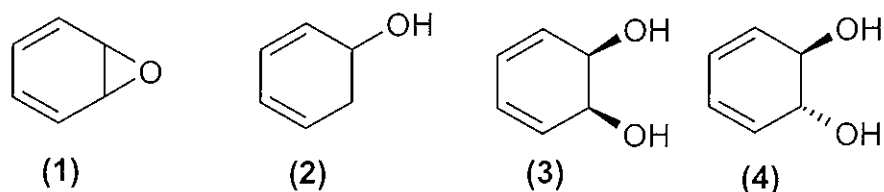
Oxidative products of aromatic hydrocarbons and the study of organometallic compounds are two areas that have long generated interest among organic chemists, the former particularly in regard to their role in the metabolism of polycyclic aromatic hydrocarbons (PAHs) and the latter in relation to their application to organic synthesis. In the work described in this thesis, aspects of both areas are examined, as the compounds of interest are iron complexes of oxidative metabolites of aromatic hydrocarbons. This chapter provides background information and a summary of the relevant previous work in these fields.

Oxidative biotransformations of aromatic substrates can yield a number of synthetically useful products and these will be discussed further in Section 1.1. The bioproducts formed can be subjected to further chemical and enzymatic transformations. The chemical transformations carried out include the use of metal complexed intermediates as the coordinated metal can exert a stereodirecting effect. The overall aims of research on these enzymatic and chemical transformations are the development of a greater scientific understanding of the processes involved and the examination of the potential for commercialisation of some of the bioproducts and their derivatives. This thesis describes a study of model compounds for chemical transformations using metal-coordinated intermediates of oxidative metabolites of aromatic hydrocarbons.

## 1.1 Oxidative Metabolites of Aromatic Hydrocarbons

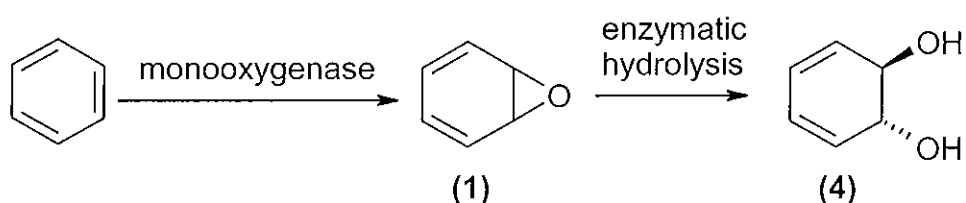
When mono- and dioxygenase enzymes act upon aromatic hydrocarbons, their oxidative metabolites are formed. These metabolites are arene oxides (**1**), arene hydrates (**2**), arene *cis*-dihydrodiols (**3**) and arene *trans*-dihydrodiols (**4**) and they are shown for the example of benzene derivatives in Chart 1.1.





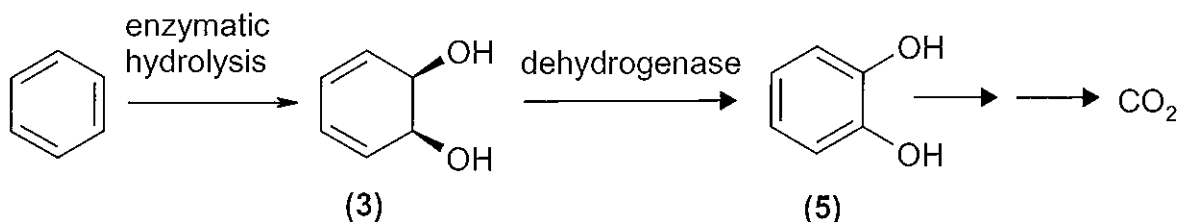
**Chart 1.1 Oxidative metabolites of benzene.**

The monooxygenase-catalysed oxidation of aromatic hydrocarbons in animals, plants and fungi (eukaryotes) is known to yield an arene oxide intermediate prior to enzymatic hydrolysis to form the arene *trans*-dihydrodiol.<sup>1</sup> In mammals, oxidative metabolites are produced as part of the body's natural process by which aromatic compounds are metabolised in the liver to give polar derivatives that are water soluble and that may then be excreted. This process is summarised in Scheme 1.1.



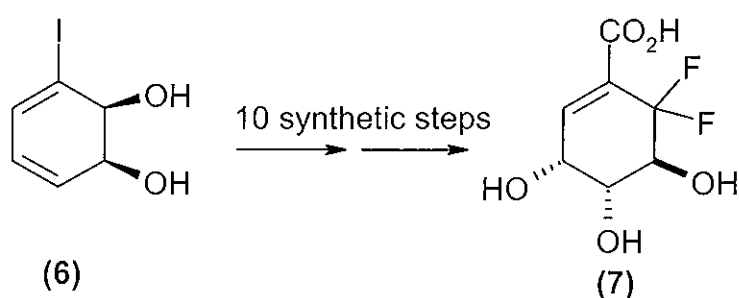
**Scheme 1.1 Degradation of aromatic hydrocarbons in mammals (eukaryotes).**

In bacterial systems (prokaryotes), arene *trans*-dihydrodiols are not produced when aromatic hydrocarbons are metabolised. Instead, dioxygenase-catalysed oxidation occurs and arene *cis*-dihydrodiols are formed.<sup>1</sup> Under normal conditions, the *cis*-dihydrodiols are dehydrogenated enzymatically to give a catechol (5) which is then degraded further as shown in Scheme 1.2.



**Scheme 1.2 Degradation of aromatic hydrocarbons in bacterial systems (prokaryotes).**

In 1968, Gibson *et al.*<sup>2</sup> first effected a biotransformation to produce benzene-*cis*-dihydrodiol (*cis*-3,5-cyclohexadiene-1,2-diol) (**3**) using a mutant strain of the bacterium *Pseudomonas putida*. This mutant strain possesses a non-functioning enzyme that would normally be responsible for catalysing the dehydrogenation step to give catechol (**5**) as shown in Scheme 1.2. The consequence of the mutation is that the benzene *cis*-dihydrodiol accumulates to appreciable concentrations and is excreted into the growth medium. The *cis*-dihydrodiols produced are optically pure and have found many applications in organic chemistry including the synthesis of biologically active compounds.<sup>3</sup> For example, as shown in Scheme 1.3, 6,6-difluoroshikimic acid (**7**), a compound with potential as an antifungal, antibacterial and antiparasitic agent, was synthesised in 10 steps from the enantiomerically pure diol (1*S*,2*S*)-3-iodocyclohexa-3,5-diene-1,2-diol (**6**) by Whitehead *et al.*<sup>4</sup>



**Scheme 1.3 Structure of the biologically active 6,6-difluoroshikimic acid (**7**) and the arene dihydrodiol, (1*S*,2*S*)-3-iodocyclohexa-3,5-diene-1,2-diol (**6**) from which it was synthesised.**

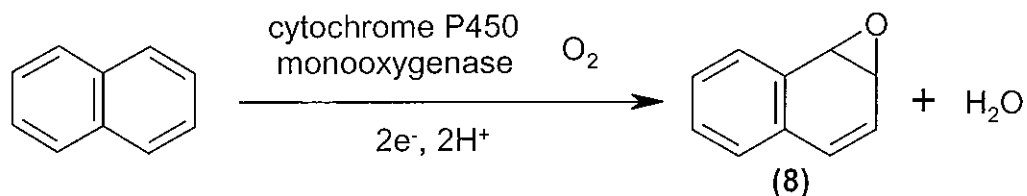
Arene hydrates are produced when the elements of water are added to a double bond of an aromatic compound. Benzene hydrate (**2**) shown in Chart 1.1 is an example. Unlike the arene oxides and dihydrodiols, arene hydrates are not usually produced directly by the oxidative metabolism of aromatic compounds. Benzylic or allylic hydroxylation of dihydroaromatic substrates, especially in bacterial metabolism, appears to be the route by which arene hydrates are formed.

The three classes of metabolites discussed, arene oxides, arene hydrates and the arene *cis*- and *trans*-dihydrodiols, will now be examined further with particular emphasis given to their respective roles in the metabolism of aromatic compounds.

### 1.1.1 Arene Oxides

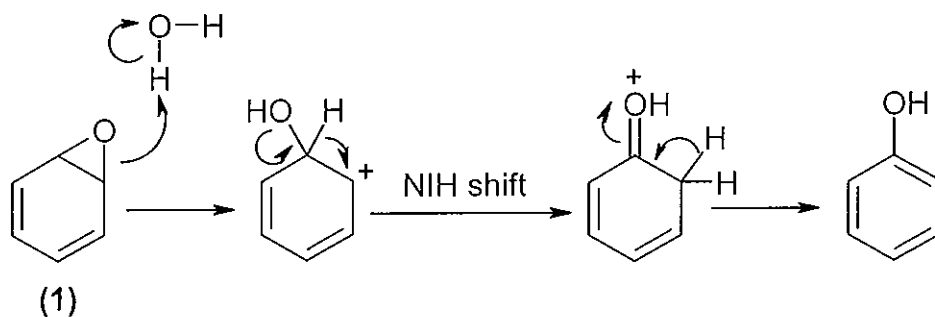
As shown in Scheme 1.1, benzene oxide (1), an epoxide, forms when one of the double bonds of benzene is oxidised by a monooxygenase enzyme in eukaryotes. The cytochrome P450 enzymes, primarily found in the liver, are responsible for this conversion.<sup>5</sup> A cytochrome is defined by Nelson and Cox as “a protein containing heme prosthetic groups”. A prosthetic group is the non-amino acid part of a conjugated protein.<sup>6</sup> Omura and Sato first discovered cytochrome P450 in 1962 and subsequently named it due to “a distinct absorption band at 450 nm” observed for the reduced form of the carbon monoxide complex.<sup>7</sup>

Extensive studies have been carried out into the process by which aromatic compounds are transformed to their oxide derivatives.<sup>8</sup> The transformation is catalysed by cytochrome P450 monooxygenase enzymes. A NADPH (nicotinamide adenine dinucleotide phosphate) supported reduction of one oxygen atom from an oxygen molecule to water accompanied by incorporation of the other oxygen atom into the substrate has been shown to occur in the mechanism.<sup>8</sup> Scheme 1.4 shows the example of the formation of naphthalene oxide (8) from treatment of naphthalene with the cytochrome P450 monooxygenase enzymes.



**Scheme 1.4 Formation of naphthalene oxide from the reaction of naphthalene with cytochrome P450 monooxygenase enzymes.**

The action of the cytochrome P450 enzymes is not always beneficial as the arene oxides produced can react in more than one way. One possibility is a rearrangement reaction involving a NIH shift<sup>9</sup> (a 1,2-hydride shift) that yields a phenol product as shown in Scheme 1.5 for benzene oxide (1).

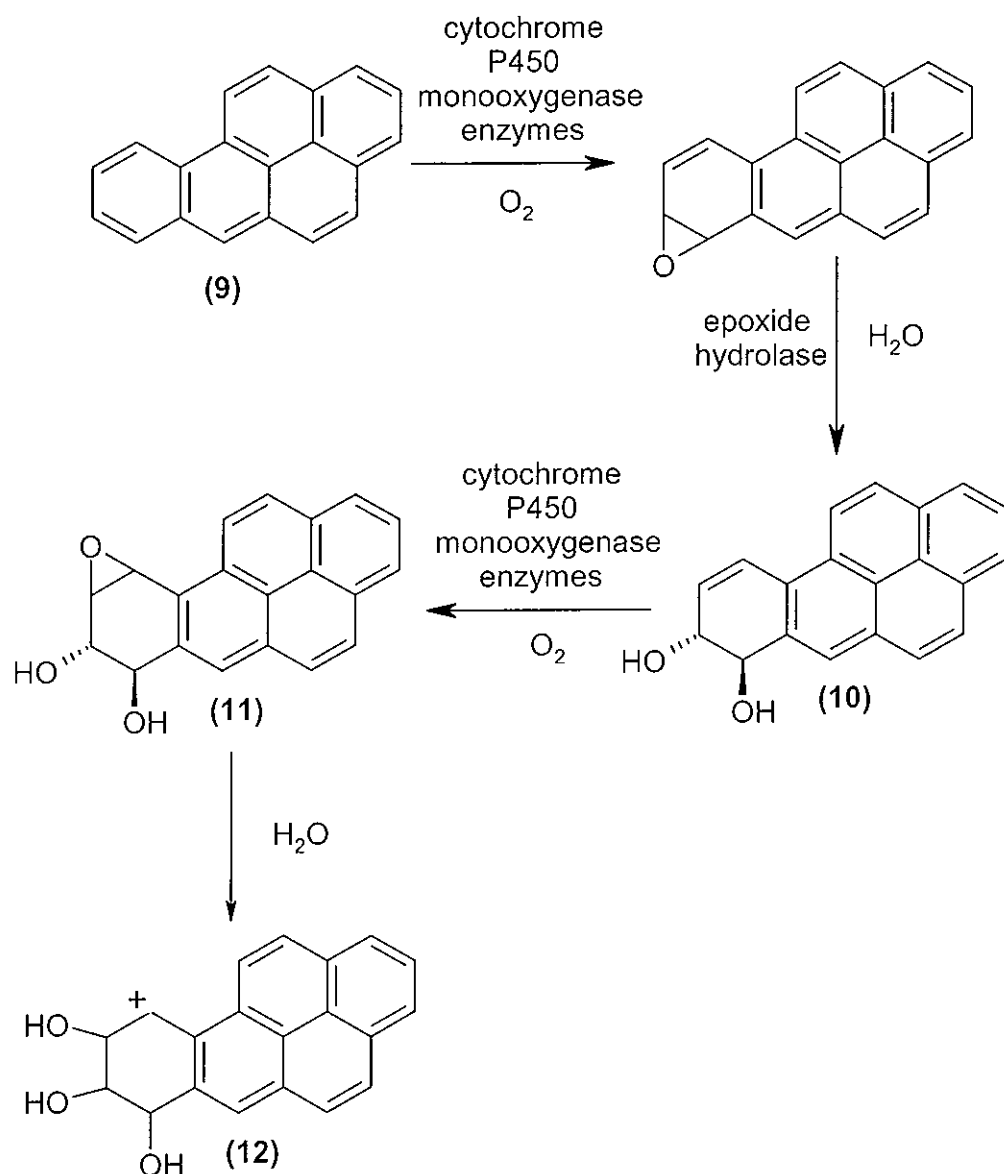


**Scheme 1.5 Rearrangement of benzene oxide (1) to yield a phenol product incorporating a NIH shift.**

The other pathway that arene oxides can react by is a nucleophilic addition reaction. It is this addition reaction that can be harmful as nucleophilic attack by the purine and pyrimidine bases of DNA may occur and this can result in cancer causing mutations. Consequently, many carcinogenic and mutagenic substances become so only after partial metabolism by the cytochrome P450 enzymes.<sup>10</sup>

One of the most carcinogenic of the polycyclic aromatic hydrocarbons is benzo[a]pyrene (9). It is formed from the incomplete combustion of fossil fuels and is present in car exhaust and cigarette smoke. Many arene oxides can be formed from benzo[a]pyrene, the two most harmful being the benzo[a]pyrene-4,5-oxide and the benzo[a]pyrene-7,8-oxide. Benzo[a]pyrene-7,8-oxide is particularly harmful and has been shown to be the “ultimate” carcinogen from benzo[a]pyrene.<sup>11</sup> The reason for this is that it reacts with water to form a diol (10) and then reacts further to give a diol epoxide (11) shown in Scheme 1.6. This diol epoxide is not readily rearranged *via* the NIH shift as the carbocation intermediate (12) that forms is unstable due to the effect of the nearby electron withdrawing hydroxyl groups. Instead, the diol epoxide (11) is more likely to undergo nucleophilic attack by DNA.

Thus, the relative stability of the carbocations formed when an arene oxide ring opens on being protonated is of great importance in determining whether the arene oxide is a carcinogen. The more stable the carbocation, the less potential it has to be a carcinogen.



**Scheme 1.6** Products formed from the action of cytochrome P450 monooxygenase enzymes on benzo[a]pyrene.

### 1.1.2 Arene *Cis-* and *Trans*-Dihydrodiols

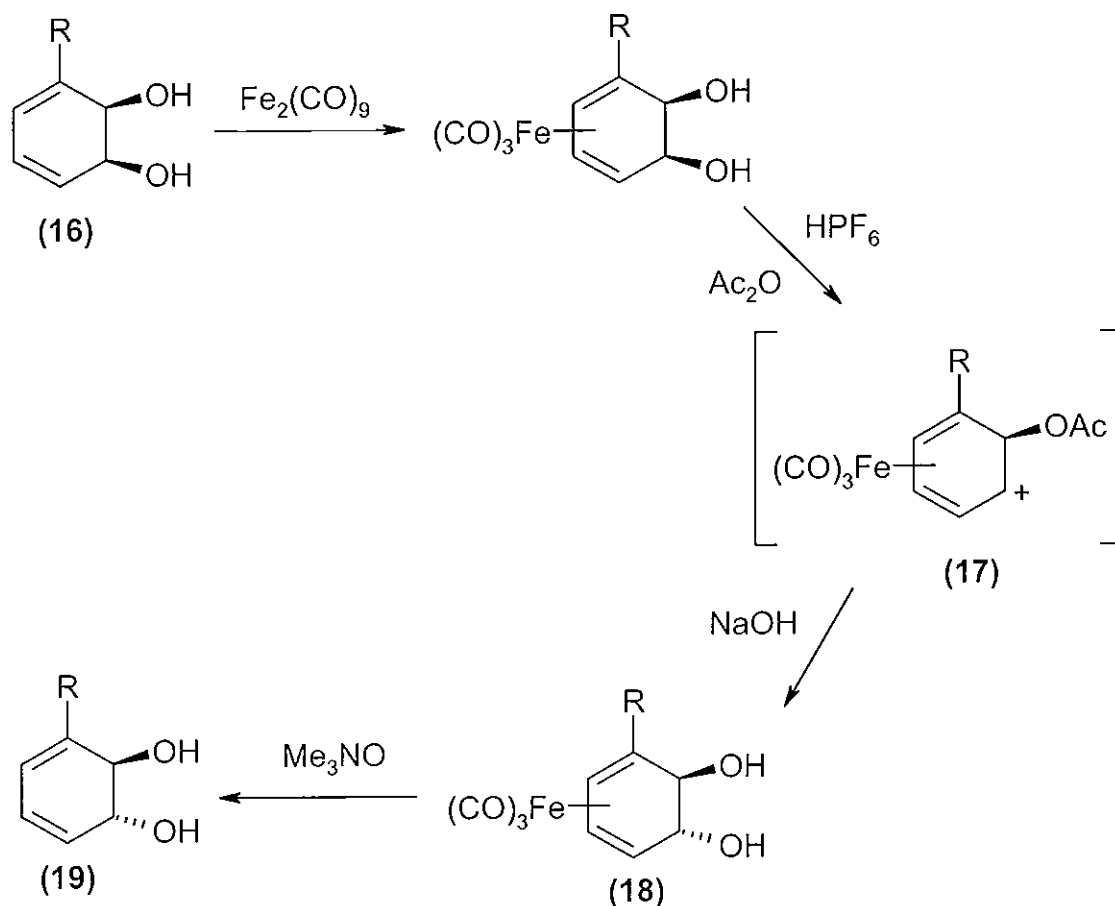
Boyland and Levi first demonstrated that arene oxides undergo enzyme catalysed hydrolysis to form arene *trans*-dihydrodiols (see Scheme 1.1) when they isolated *trans*-1,2-dihydroxy-1,2-dihydroanthracene (13), shown in Chart 1.2, as a metabolite formed from anthracene in both rats and rabbits.<sup>12</sup>



The *trans*-dihydrodiols, products of the oxidative metabolism of aromatic compounds in eukaryotes, are not as accessible as their *cis* counterparts as they cannot be produced by means of a biotransformation. The *trans*-dihydrodiols are however more stable than the corresponding *cis*-dihydrodiols. Boyd has commented on the restriction of their use that occurs as a result of the instability of some of the arene *cis*-dihydrodiols.<sup>17</sup>

This difference in stability and the potential use of the *trans*-dihydrodiols as chiral building blocks has led to a drive to synthesise the *trans*-dihydrodiols from their readily available *cis*-counterparts. Boyd and Sharma summarised many of the possible enzyme-catalysed routes and chemoenzymatic routes to the *trans*-dihydrodiols in a recent review.<sup>17</sup> One of the suggested pathways incorporates coordination of a tricarbonyliron moiety ( $\text{Fe}(\text{CO})_3$ ) and is shown in Scheme 1.7.

In this proposed synthetic route, an arene *cis*-dihydrodiol (**16**) is coordinated with a tricarbonyliron fragment and is then reacted with hexafluorophosphoric acid in the presence of acetic anhydride to form a cyclohexadienyl cation intermediate (**17**). This cation traps a nucleophile *anti* to the metal yielding an arene *trans*-dihydrodiol-tricarbonyliron complex (**18**). A subsequent decomplexation with trimethylamine-*N*-oxide affords the arene *trans*-dihydrodiol (**19**). In a preliminary study carried out by Boyd, it was found that an electron withdrawing group such as trifluoromethyl was required as a substituent on the ring. This conversion from the bioavailable arene *cis*-dihydrodiols to their *trans*-analogues, particularly the step involving trapping of the nucleophile by the carbocation intermediate (**17**), is of interest in this work and will be discussed in more detail at a later stage.



**Scheme 1.7** Chemoenzymatic synthesis of a benzene *trans*-dihydrodiol (19) from its *cis*-dihydrodiol (16) analogue

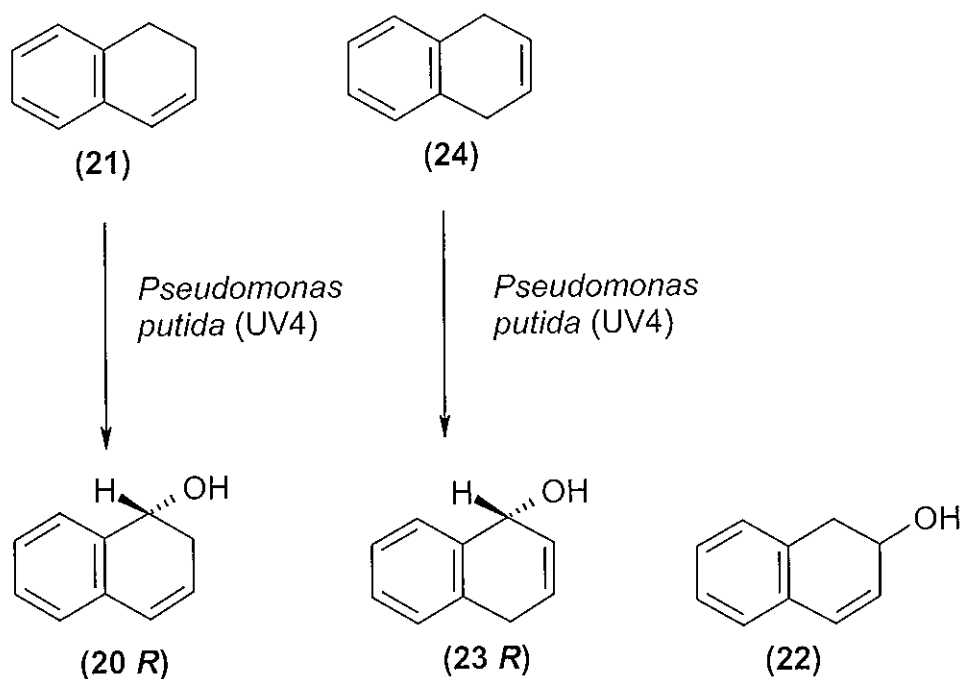
### 1.1.3 Arene Hydrates

In 1895, Bamberger *et al.* prepared the first known example of an arene hydrate, 1-hydroxy-1,2-dihydronaphthalene (20).<sup>18</sup> The synthetic pathway used by Bamberger involved dehydrohalogenation. A number of alternative routes have been developed since then, including one involving reduction of the corresponding arene oxide.<sup>19</sup> The arene hydrates have long been believed to be involved in the metabolism of polycyclic aromatic hydrocarbons.<sup>20</sup> Boyland and Solomon inferred that an arene hydrate was implicated in the metabolism of naphthalene by examining mammalian urine.<sup>20</sup> They found that liberation of naphthalene was achieved only after acidification of the urine. However, due to the instability of these metabolites, it was not until 1989 that Boyd and co-workers isolated (+)-(*R*)-1-hydroxy-1,2-dihydronaphthalene (20 *R*).



This compound was obtained as a metabolite formed from 1,2-dihydronaphthalene (**21**) using a mutant strain of *Pseudomonas putida*.<sup>21</sup>

There are three isomeric hydrates of naphthalene which have been isolated, 1-hydroxy-1,2-dihydronaphthalene (**20 R**), 2-hydroxy-1,2-dihydronaphthalene (**22**), and 1-hydroxy-1,4-dihydronaphthalene (**23 R**) and these are shown in Scheme 1.8. The *R* configurations of (**20**) and (**23**) are shown because, in 1990, Boyd *et al.* isolated (**20 R**) and (**23 R**) in optically pure form as intermediates from the metabolism of 1,2-dihydronaphthalene (**21**) and 1,4-dihydronaphthalene (**24**) respectively by the UV4 mutant strain of *Pseudomonas putida*.<sup>22</sup> Synthetic routes to each compound have also been developed.

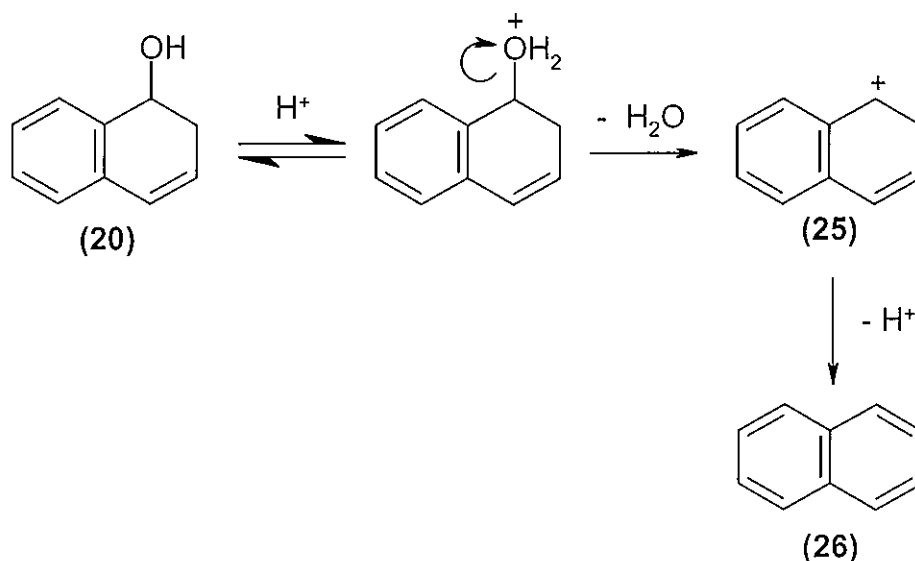


**Scheme 1.8** Formation of two of the arene hydrate derivatives of naphthalene using a mutant strain of *Pseudomonas putida* (UV4)

#### 1.1.4 Reactivity of Arene Hydrates

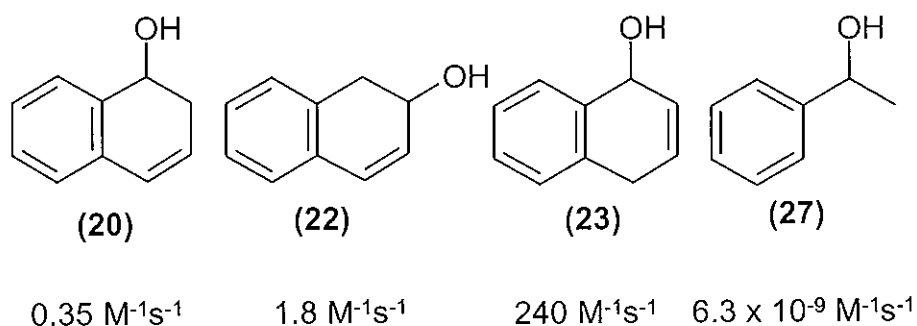
In acidic solutions, arene hydrates undergo dehydration to form aromatic products. Scheme 1.9 shows a mechanism for the dehydration of 1-hydroxy-1,2-dihydronaphthalene (**20**) based on the dehydration of alcohols to form alkenes. In the mechanism, it can be seen that formation of a carbocation (**25**) occurs following the loss

of water from the protonated alcohol. A subsequent deprotonation of the carbocation gives the aromatic product (26).



**Scheme 1.9** Dehydration of 1-hydroxy-1,2-dihydronaphthalene (20)

The most important difference between dehydration of alcohols and arene hydrates is that, for the hydrates, the reaction occurs by rate determining carbocation formation rather than rate determining deprotonation of the carbocation. This is because deprotonation of the carbocation produced in the case of an arene hydrate gives an aromatic compound. When the reactivity of the arene hydrates and alcohols to dehydration is compared, it is noted that the arene hydrates are generally much more reactive than their structurally related counterparts. In Chart 1.4, a comparison is made between the second order rate constants for dehydration ( $k_{\text{dehyd}}$ ) of the three isomeric hydrates of naphthalene, denoted  $\alpha$ -naphthalene hydrate (20),  $\beta$ -naphthalene hydrate (22), and  $\gamma$ -naphthalene hydrate (23) and an alcohol analogue, 1-phenylethanol (27).<sup>23</sup>



**Chart 1.4 Comparison of the second order rate constants for dehydration ( $k_{\text{dehyd}}$ ) of the three isomeric hydrates of naphthalene and the alcohol analogue 1-phenylethanol.**

It can be seen from Chart 1.4 that the rate constant for dehydration of the  $\alpha$ -naphthalene hydrate (**20**) to naphthalene is  $6 \times 10^7$  times greater than the rate constant observed for dehydration of 1-phenylethanol to styrene. The large increase in reactivity can be attributed to a number of factors each of which will be discussed.

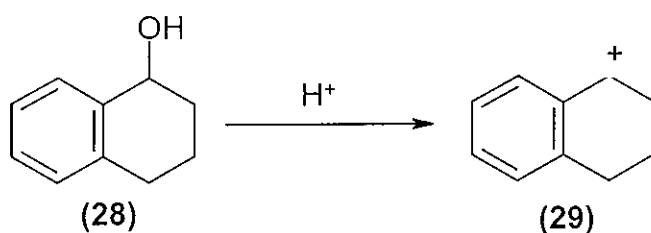
(i) Aromatic Stabilisation

When the dehydration of an arene hydrate is examined, one of the most obvious factors expected to contribute to the reactivity of the hydrates is the exceptional stability shown by the aromatic product. From the mechanism in Scheme 1.9, it can be seen that the dehydration of the arene hydrates proceeds *via* a carbocation intermediate. The product stability would be expected to influence the rate of deprotonation of the carbocation but not affect its rate of formation. The product stability is therefore limited to lowering the energy barrier for deprotonation of the carbocation provided no change in mechanism occurs. For 1-phenylethanol, the rate determining step is known to be loss of a proton from the carbocation and it has been shown to occur 700 times more slowly than the corresponding deprotonation of carbocation (**25**) from naphthalene hydrate.<sup>24,25</sup> The aromatic stabilisation of naphthalene is therefore responsible for only 700-fold of the  $6 \times 10^7$  fold difference in reactivity of the hydrate compared to the alcohol. Concerted elimination from the protonated hydrate would avoid the carbocation intermediate and in principle a faster reaction would be possible. This possibility is however excluded by the absence of general acid catalysis.<sup>23</sup>

(ii) Carbocation Stability

The stability of the carbocation intermediate formed during the dehydration of the alcohols will play an important role in the rate of hydration. Two factors which will influence the stability of the carbocation are (a) its cyclic nature and (b) the presence of a vinyl group *ortho* to the carbocation centre.

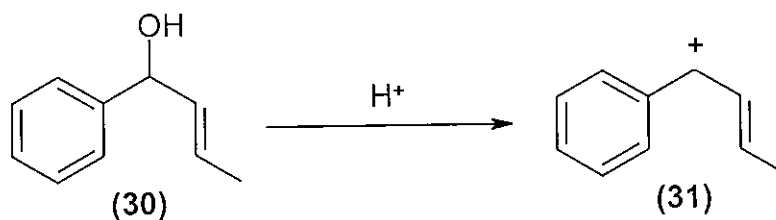
The rate constant for carbocation formation of the dihydro derivative of  $\alpha$ -naphthalene hydrate (20),  $\alpha$ -tetralol (28), is 200 times greater than for the corresponding reaction of 1-phenylethanol (27).<sup>23</sup> The increased reactivity of the cyclic  $\alpha$ -tetralol may be attributed to factors affecting the stabilisation of the carbocation (29).



Scheme 1.10 Carbocation (29) formation from  $\alpha$ -tetralol (28)

In the cyclic structure, there is less entropy loss than in the non-cyclic structure when the carbocation is generated. This is due to the phenyl ring being held in a favourable conformation for resonance. For the non-cyclic 1-phenylethanol structure (27) however resonance may only occur when free rotation of the phenyl ring ceases. Sterically, the non-cyclic structure is hindered for resonance as the methyl group hinders achievement of a planar structure. No such steric hindrance is present in the benzylic carbocation.

A vinyl substituent would also be expected to stabilise the carbocation intermediate. This is confirmed by comparing the rate of carbocation formation for the  $\gamma$ -naphthalene hydrate (23) and for its open chain analogue phenylpropenylcarbinol (30). It was found that the rate for the cyclic structure was 400 times faster. The measured 400-fold difference is not far from the difference of 200-fold for formation of the carbocations from 1-phenylethanol (27) and  $\alpha$ -tetralol (28). This implies that the activating effects of the vinyl groups in the  $\gamma$ -naphthalene hydrate (23) and phenylpropenylcarbinol are comparable.



**Scheme 1.11 Carbocation (31) formation from phenylpropenylcarbinol (30)**

In summary, the naphthalene hydrates show an increase in reactivity when compared to 1-phenylethanol. This may be attributed to a number of factors and aromatic stabilisation, the cyclic nature of naphthalene hydrates attributing to enhanced resonance and the effect of a vinyl substituent all play an important role.

Finally, it can be observed from Chart 1.4 that the  $\gamma$ -naphthalene hydrate (23) has a much greater reactivity than the  $\alpha$ - and  $\beta$ -naphthalene hydrates (20 and 22) by a factor of 680 and 130 respectively. The difference cannot lie with the carbocation stability, as the  $\beta$ - and  $\gamma$ -hydrates yield the same carbocation. Therefore it would almost certainly arise from a difference in reactant stabilities from conjugation of the double bond with the ring in the  $\alpha$ -hydrate (20) and  $\beta$ -hydrate (22) but not the  $\gamma$ -hydrate (23).

In this study, the species of interest are the tricarbonyliron coordinated oxidative metabolites of aromatic hydrocarbons. When the tricarbonyliron moiety is coordinated to the arene hydrates and arene *cis*- and *trans*-dihydrodiols, it confers upon the compounds properties which vary markedly from those usually expected in the absence of coordination. The effects of this coordination will be examined in the subsequent sections.

## 1.2 Organometallic Chemistry

The birth of modern day organometallic chemistry and the rapid development of this area in the latter half of the twentieth century have been attributed to the accidental discovery of ferrocene in 1951 by Kealy and Pauson.<sup>26</sup> Pearson<sup>30</sup> reports that, at the same time, a proposal by Orgel, Pauling and Zeiss allowed a greater understanding of metal-olefin complexes as they introduced the concept of  $\pi$ -backbonding in a model proposed for bonding in metal carbonyls. Many organometallic complexes were known before this time however and the first complex was synthesised in 1827 by Zeise.<sup>27</sup> It was an ionic compound,  $K[Pt(C_2H_4)Cl_3]$ , potassium trichloroethyleneplatinite (II).

Many metals have been used to produce complexes for synthetic purposes including chromium, magnesium, palladium and rhodium. This review will be restricted to examining organoiron complexes only. Pearson has remarked that "Iron forms stable complexes with a wide range of ligands, making this perhaps the most valuable metal in the periodic table".<sup>30</sup> The most common type of organoiron complexes are the iron carbonyls and the sandwich type complexes, for example, ferrocene.

Three stable carbonyls of iron are known, pentacarbonyliron ( $Fe(CO)_5$ ), nonacarbonyldiiron ( $Fe_2(CO)_9$ ) and dodecacarbonyltriiron ( $Fe_3(CO)_{12}$ ) and they are shown in Chart 1.5. Monde<sup>28</sup> and Bertholet<sup>29</sup> independently discovered pentacarbonyliron (**32**) in 1891 as a musty smelling yellow liquid prepared by a direct reaction between finely divided iron and carbon monoxide. Nonacarbonyldiiron (**33**) is prepared by photolysis of  $Fe(CO)_5$  in acetic acid using a medium pressure mercury lamp to give shiny gold platelets. Dodecacarbonyltriiron (**34**) is formed as a dark green solid in a variety of ways, one of which is the thermal decomposition of nonacarbonyldiiron.<sup>30</sup>

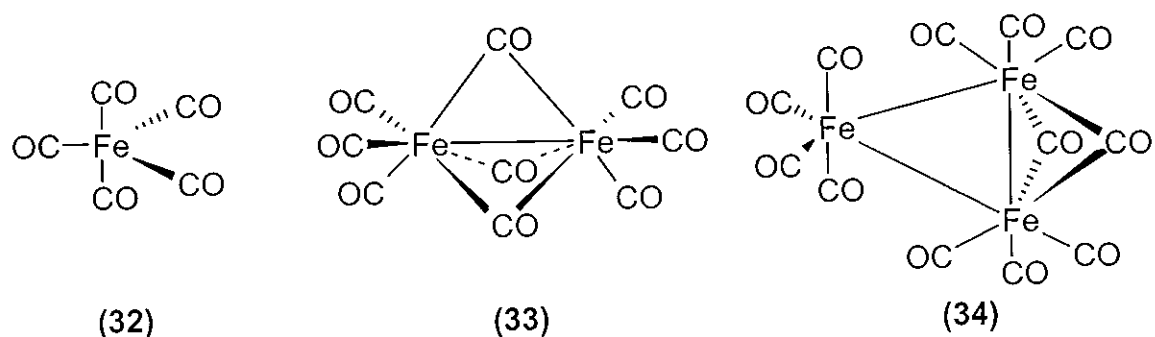
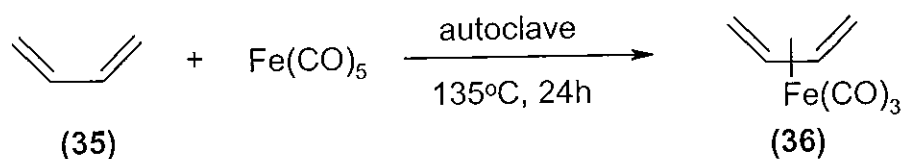


Chart 1.5 Structures of pentacarbonyliron (32), nonacarbonyldiiron (33) and dodecacarbonyltriiron (34).

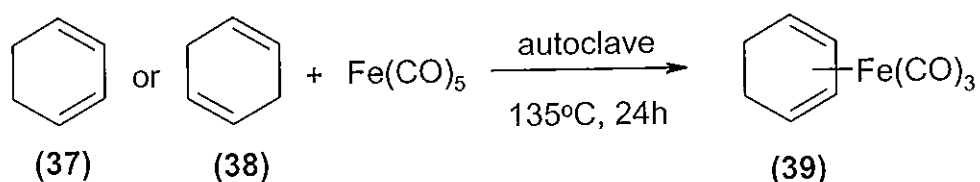
### 1.2.1 Tricarbonyliron Complexes-Initial Synthetic Methods

The first tricarbonyliron complex was synthesised by Reihlen and co-workers in 1930 when they isolated ( $\eta^4$ -buta-1,3-diene)tricarbonyliron (36) from the thermal reaction of buta-1,3-diene (35) with pentacarbonyliron as shown in Scheme 1.12.<sup>31</sup>



Scheme 1.12 Synthesis of ( $\eta^4$ -buta-1,3-diene)tricarbonyliron (36) from buta-1,3-diene (35) using pentacarbonyliron.

The procedure developed by Reihlen shown above was used to synthesise a broad range of tricarbonyliron-butadiene complexes. Hallam and Pauson extended the field further in 1958 when they prepared ( $\eta^4$ -cyclohexa-1,3-diene)tricarbonyliron (39) by heating an excess of cyclohexa-1,3-diene (37) with pentacarbonyliron.<sup>32</sup>



Scheme 1.13 Synthesis of the cyclic diene ( $\eta^4$ -cyclohexa-1,3-diene)tricarbonyliron (39) from either structural isomer of cyclohexadiene.

When investigating the further reaction of the product complexes formed, Hallam and Pauson found that these dienes resisted hydrogenation and Diels-Alder type reactions, reactions normally characteristic of alkene functionality, when they were complexed to the tricarbonyliron moiety. This resistance to these reactions leads to the conclusion that when the tricarbonyliron moiety is coordinated to the organic ligand, it acts as a protecting group.<sup>32</sup>

In 1961, Arnet and Pettit discovered that treatment of a non-conjugated diene with pentacarbonyliron resulted in rearrangement to give a conjugated isomer. In most cases the product was a stable diene-tricarbonyl iron complex.<sup>33</sup> Thus cyclohexa-1,4-diene (**38**) was found to react with pentacarbonyliron giving concomitant isomerisation of the diene to yield complex (**39**). A vast array of substituted cyclohexa-1,4-dienes are available by a Birch reduction of the corresponding benzene derivatives.<sup>52</sup> Therefore it became possible to synthesise a broad range of ( $\eta^4$ -cyclohexa-1,3-diene)tricarbonyliron complexes.

Various experimental methods were developed for complexing the dienes. The most common procedure was developed by Cais and Maoz and involved direct reaction of the diene with pentacarbonyliron in refluxing di-n-butyl ether.<sup>34</sup> In conjunction with the Birch reduction, many alkylbenzenes, alkoxybenzenes, alkoxyalkylbenzenes and benzoic acid derivatives were transformed into their corresponding substituted (cyclohexa-1,3-diene)tricarbonyliron complexes. Nonacarbonyldiiron and dodecacarbonyltriiron can also be used as sources for the tricarbonyliron moiety but the nonacarbonyldiiron reagent is limited to reaction with 1,3-dienes only. It has the advantage however of being employed under milder conditions than pentacarbonyliron and has been utilised for the complexation of more sensitive 1,3-dienes.<sup>30</sup> For each of the ironcarbonyl reagents used, the reactions are generally carried out under either thermal or photolytic conditions.

The yields obtained for the complexation reactions using any of the ironcarbonyl complexes are usually quite moderate (30-50%) with some exceptions. A major drawback in relation to these methods is that in order to achieve high yields a large excess of the ironcarbonyl reagent is required. This can result in the build up of

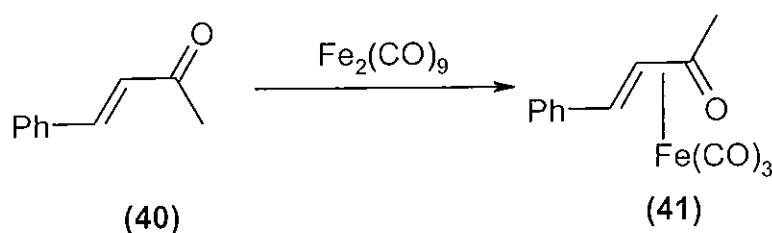


pyrophoric iron leading to a more hazardous work up.<sup>35</sup> However, complexation can usually be achieved under milder conditions and with greater selectivity by using a tricarbonyliron transfer reagent.<sup>36</sup>

## 1.2.2 Tricarbonyliron Complexation Using Tricarbonyliron Transfer Reagents

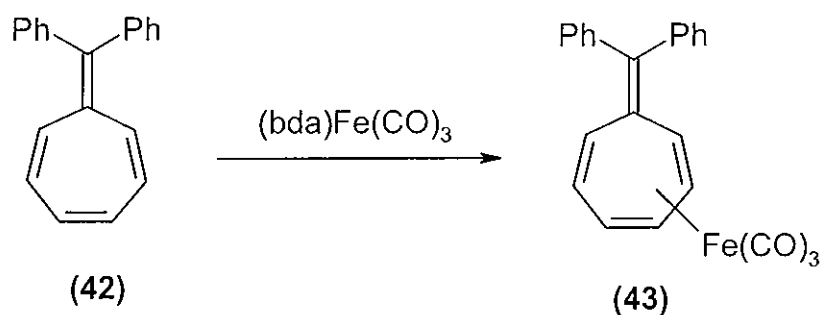
### 1.2.2.1 ( $\eta^4$ -1-Oxabuta-1,3-diene)tricarbonyliron Complexes

In 1964, Weiss first reported the ( $\eta^4$ -1-oxabuta-1,3-diene)tricarbonyliron complexes,<sup>37</sup> which were introduced by Lewis as transfer reagents in 1972.<sup>38</sup> The principal reagent in the series is ( $\eta^4$ -benzylideneacetone)tricarbonyliron, (bda)Fe(CO)<sub>3</sub> (**41**), synthesised from benzylideneacetone (**40**) and nonacarbonyldiiron as shown in Scheme 1.14.



Scheme 1.14 Synthesis of (bda)Fe(CO)<sub>3</sub> (**41**).

The (bda)Fe(CO)<sub>3</sub> acts as convenient source for the tricarbonyliron moiety under mild conditions. An example demonstrating how it has been utilised to good effect is the complexation of 8,8-diphenylheptafulvene (**42**) to produce its tricarbonyliron derivative (**43**) shown in Scheme 1.15. Due to the sensitivity of the free ligand to both heat and UV light, the Fe(CO)<sub>5</sub> and Fe<sub>3</sub>(CO)<sub>12</sub> reagents could not be used and reaction with Fe<sub>2</sub>(CO)<sub>9</sub> yielded an unstable hexacarbonyldiiron complex.<sup>38</sup>

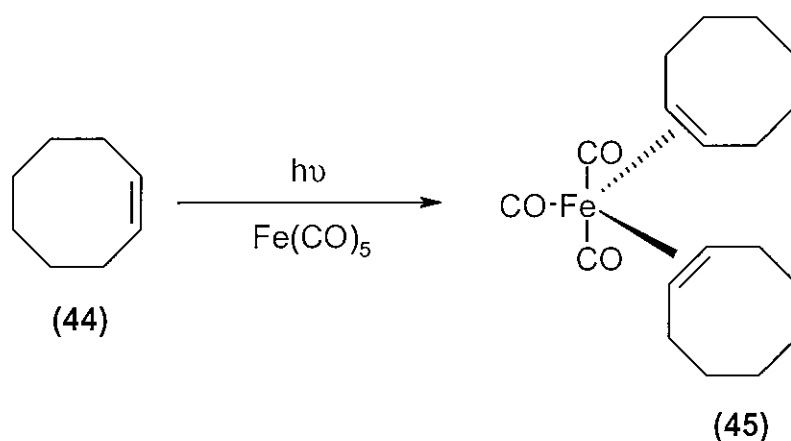


**Scheme 1.15** Synthesis of  $(\eta^4\text{-8,8-diphenylheptafulvene})\text{tricarbonyliron}$  (43) utilising the tricarbonyliron transfer reagent  $(\text{bda})\text{Fe}(\text{CO})_3$ .

A drawback of the  $(\text{bda})\text{Fe}(\text{CO})_3$  transfer reagent is that it will not transfer the tricarbonyliron fragment to non-conjugated dienes.<sup>39</sup>

#### 1.2.2.2 Grevels' Reagent (*Bis*( $\eta^2\text{-cis-cyclooctene}$ )tricarbonyliron)

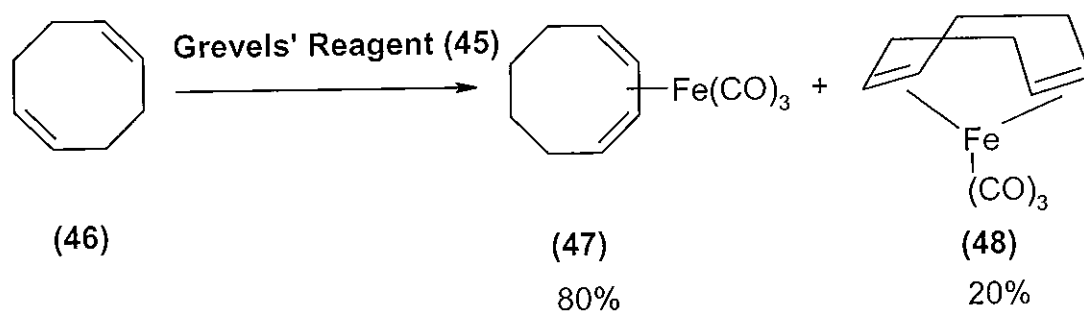
Another transfer reagent commonly used was synthesised by Grevels in 1984.<sup>40</sup> The eponymous Grevels' reagent is a bis( $\eta^2\text{-cis-cyclooctene}$ )tricarbonyliron complex (45) which was isolated from the photolytic reaction of pentacarbonyliron and *cis-cyclooctene* (44) as shown in Scheme 1.16.



**Scheme 1.16** Synthesis of Grevels' reagent (45) by direct reaction of pentacarbonyliron with *cis-cyclooctene*.

Grevels' reagent has two main advantages over the  $(\text{bda})\text{Fe}(\text{CO})_3$  transfer reagent. These are that it requires extremely mild conditions (temperatures below  $0^\circ\text{C}$ ) to transfer the tricarbonyliron fragment to 1,3-dienes and that it will react with non-

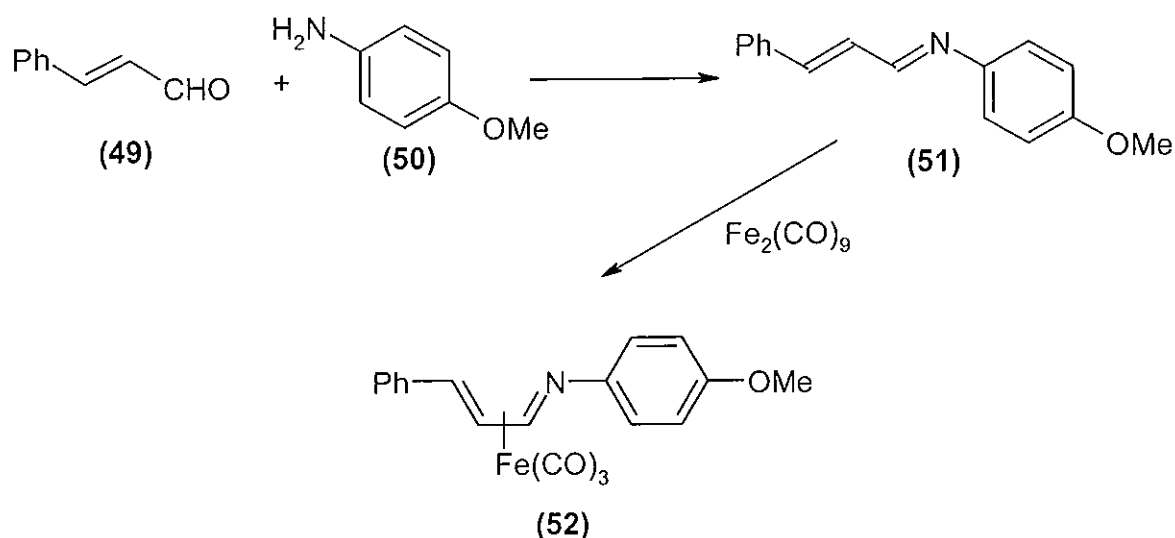
conjugated dienes. Scheme 1.17 demonstrates the transfer of the tricarbonyliron moiety from Grevels' reagent (45) to *cis*-cycloocta-1,5-diene (46) with concomitant isomerisation of the double bonds to give ( $\eta^4$ -cycloocta-1,3-diene)tricarbonyliron (47) and ( $\eta^4$ -cycloocta-1,5-diene)tricarbonyliron (48).



Scheme 1.17 Reaction of Grevels' reagent (45) with the non-conjugated *cis*-cycloocta-1,5-diene.

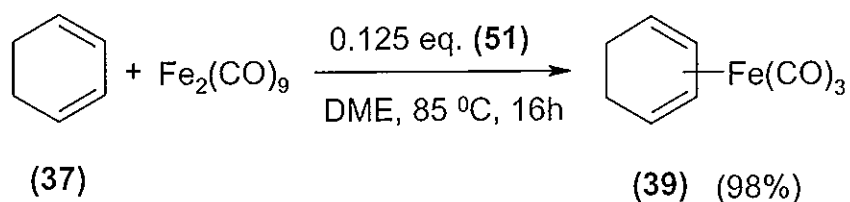
### 1.2.2.3 ( $\eta^4$ -1-Azabuta-1,3-diene)tricarbonyliron Complexes

The ( $\eta^4$ -1-azabuta-1,3-diene)tricarbonyliron transfer reagents were first reported by Otsuka<sup>41</sup> and Lewis<sup>42</sup> four decades ago. More recently, extensive work has been carried out by Knölker to develop the use of these complexes as transfer reagents.<sup>35,43,44,45</sup> Various methods have been reported for their synthesis. The most convenient approach is outlined in Scheme 1.18 for the example of ( $\eta^4$ -1-(4-methoxyphenyl)-4-phenyl-1-azabuta-1,3-diene)tricarbonyliron (52), the most efficient of the series of transfer reagents prepared by Knölker.<sup>45</sup> An imine condensation of *trans*-cinnamaldehyde (49) with *p*-anisidine (50) provides 1-(4-methoxyphenyl)-4-phenyl-1-azabuta-1,3-diene (51). Reaction of the diene with nonacarbonyldiiron affords the transfer reagent (52).



**Scheme 1.18** Synthesis of the tricarbonyliron transfer reagent, ( $\eta^4$ -1-(4-methoxyphenyl)-4-phenyl-1,3-diene)tricarbonyliron (**52**).

The major advantage noted for the use of the azabutadiene complexes of type (**52**) compared to the other transfer reagents discussed ((bda)Fe(CO)<sub>3</sub> and Grevels' reagent) is that when reacting the free ligands of type (**51**) with nonacarbonyldiiron, a sub-stoichiometric quantity of the free ligand may be used.<sup>36</sup> Also, the synthesis of ( $\eta^4$ -cyclohexa-1,3-diene)tricarbonyliron (**39**) from cyclohexa-1,3-diene shown in Scheme 1.13 can be performed using the azabutadiene complex (**51**) and nonacarbonyldiiron in one step and the yield increases from 21% to 98%.<sup>45</sup> This one step synthesis is represented in Scheme 1.19. When (bda)Fe(CO)<sub>3</sub> or Grevels' reagent are used, the yields are 95% and 78% respectively. The overall reaction times and conditions are quite different as both the (bda)Fe(CO)<sub>3</sub> and Grevels' reagent require a two step synthesis in which the initial step is isolation of the transfer reagent.<sup>36</sup>

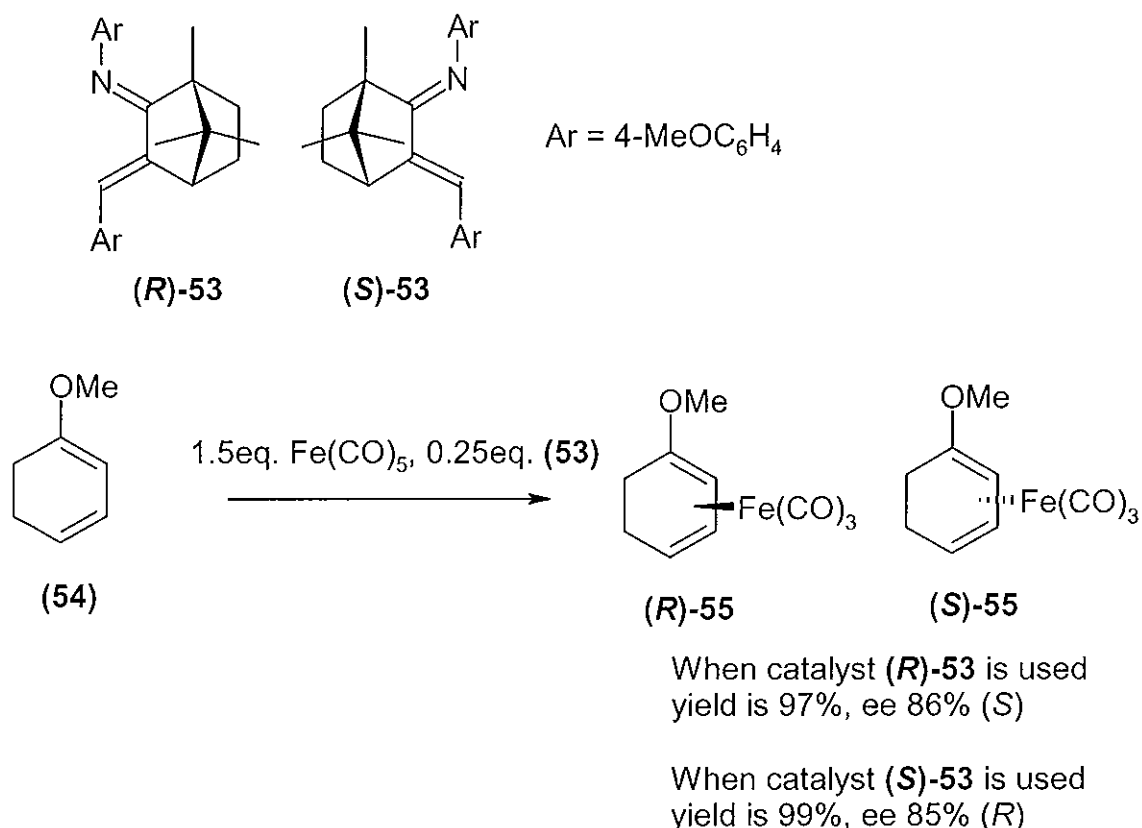


**Scheme 1.19** One step synthesis of ( $\eta^4$ -cyclohexa-1,3-diene)tricarbonyliron (**39**) using the tricarbonyliron transfer reagent (1-(4-methoxyphenyl)-4-phenyl-1,3-diene) (**51**).

The disadvantage associated with using the azadiene-tricarbonyliron transfer reagents is that, as is the case for (bda)Fe(CO)<sub>3</sub>, no reaction is observed with non-conjugated dienes.

#### *1.2.2.4 Tricarbonyliron Complexes of Chiral 1-Azabuta-1,3-dienes*

In recent years, a novel form of asymmetric catalysis has been realised by employing chiral 1-azabuta-1,3-dienes. It has been shown that by using the chiral 1-azabuta-1,3-dienes, planar chiral transition metal  $\pi$ -complexes may be afforded by an asymmetric complexation of prochiral dienes with the tricarbonyliron fragment.<sup>36</sup> An example of this asymmetric synthesis is shown in Scheme 1.20. The camphor derivatives of the 1-azabuta-1,3-diene catalysts (**53**) were initially prepared and reacted with a range of prochiral dienes, for example, 1-methoxycyclohexa-1,3-diene (**54**) which yields complexes such as ( $\eta^4$ -1-methoxycyclohexa-1,3-diene)tricarbonyliron (**55**). (**55**) has been used as a building block in the stereoselective synthesis of spirocyclic compounds.<sup>36,46</sup>



**Scheme 1.20** Asymmetric catalysis incorporating camphor derivatives (**53**) of the 1-azabuta-1,3-diene transfer reagents.

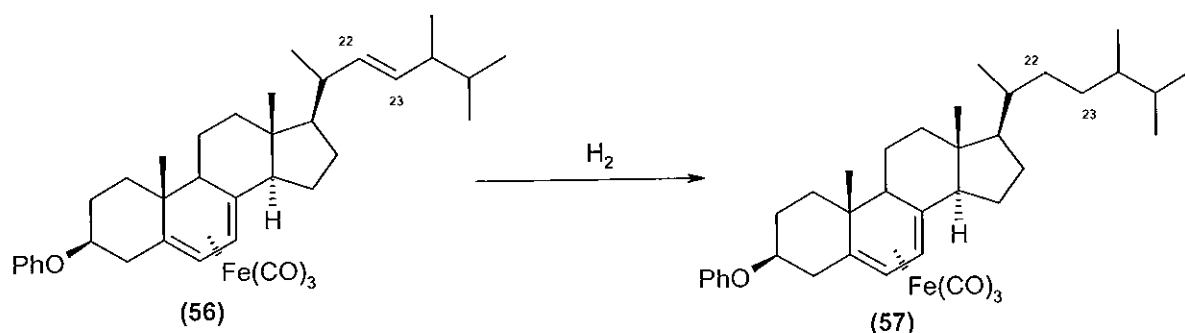
### 1.2.3 Synthetic Applications of Tricarbonyliron Complexes

The tricarbonyliron complexes have found many uses in organic synthesis, for example as protecting groups, activating groups and stereochemical controllers. An outline of some of the ways in which they have been utilised to date follows.

#### 1.2.3.1 The Tricarbonyliron Fragment as a Protecting Group

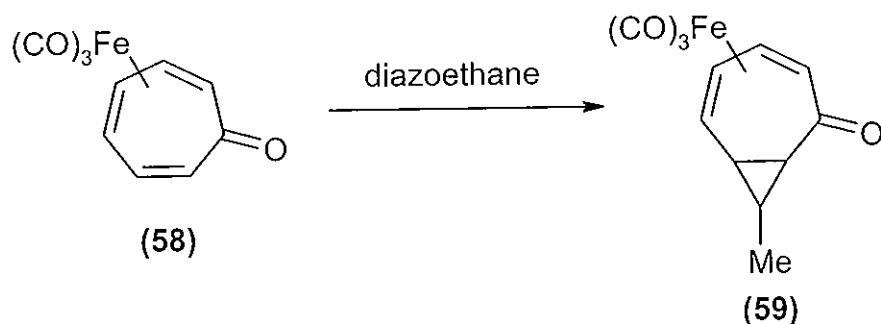
As mentioned in Section 1.2.1, it was Hallam and Pauson who first observed in 1958 that when a diene was co-ordinated to the tricarbonyliron moiety it resisted reactions which were characteristic of carbon-carbon double bonds.<sup>32</sup> Since then, many groups have utilised this change in reactivity which results from complexation. For example, it has been demonstrated that the ergosterol benzoate complex (**56**) undergoes hydroboration, osmylation and hydrogenation selectively at the 22,23-double bond as

shown for the example of hydrogenation in Scheme 1.21.<sup>47</sup> The diene double bonds coordinated to the  $\text{Fe}(\text{CO})_3$  group are unaffected by these reactions.



**Scheme 1.21** The tricarbonyliron moiety ( $\text{Fe}(\text{CO})_3$ ) acting as a protecting group in the ergosterol benzoate complex (56) allowing selective hydrogenation at the 22,23-double bond.

Carbon-carbon bond forming reactions have also been selectively performed with an uncomplexed double bond. One example is the cyclopropanation of the tropone- $\text{Fe}(\text{CO})_3$  complex (58) with diazoethane as described by Franck-Neumann and Martina affording complex (59). This transformation can be seen in Scheme 1.22.<sup>48</sup>

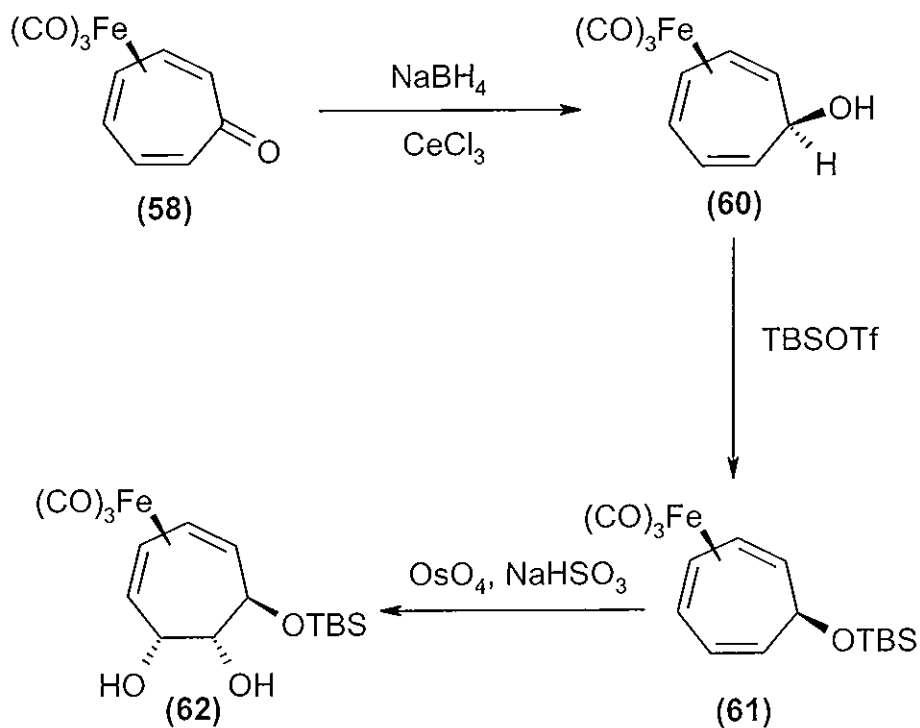


**Scheme 1.22** Cyclopropanation of the tropone- $\text{Fe}(\text{CO})_3$  complex (58).

### 1.2.3.2 Stereochemical Control Using the Tricarbonyliron Group

Stereochemical control has often been achieved by the use of tricarbonyliron complexes. An example of such control was reported by Pearson and Srinivasan and is shown in Scheme 1.23.<sup>49</sup> The tropone-tricarbonyliron complex (58) reacts to produce a single diastereomer (60) when reduced with sodium borohydride. Pearson and his group noted that when a ketone situated *alpha* to a tricarbonyliron-coordinated diene is

reduced, the reaction is stereochemically controlled. This effect was attributed to addition of hydride *anti* to the tricarbonyliron group.<sup>50</sup> Osmylation of the complex (61) protected by TBSOTf (*tert*-butyldimethylsilyl trifluoromethanesulfonate) afforded the triol derivative (62) shown.

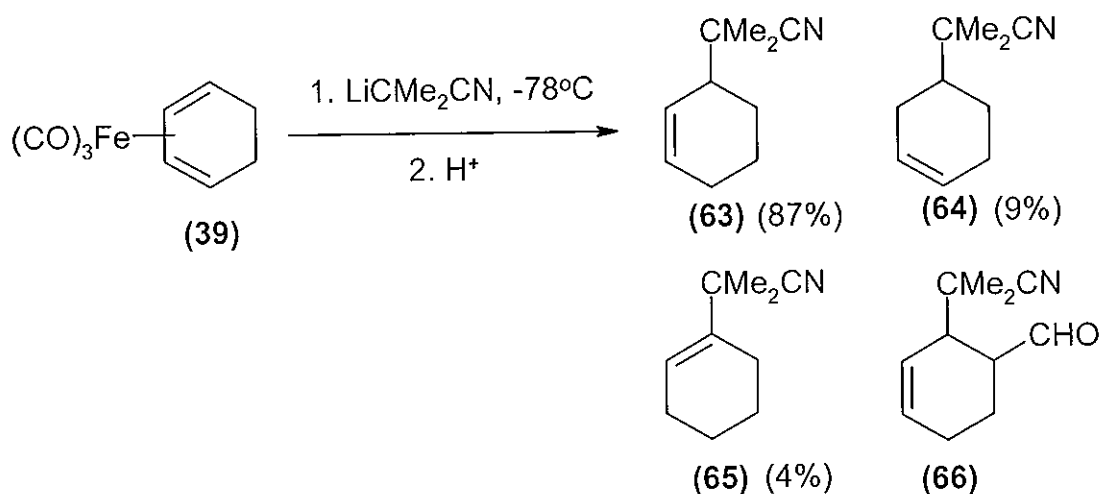


Scheme 1.23 Example of stereochemical control using the tricarbonyliron group.

### 1.2.3.3 The Tricarbonyliron Moiety as an Activating Group

The iron atom in tricarbonyliron complexes can act as an electron acceptor. This opens the possibility for nucleophilic addition to the diene carbon atoms and can, for example, allow the formation of new carbon-carbon bonds. Scheme 1.24 shows the nucleophilic addition of 2-lithio-2-methylpropionitrile ( $\text{LiCMe}_2\text{CN}$ ) to ( $\eta^4$ -cyclohexa-1,3-diene)tricarbonyliron (39) followed by decomplexation providing the four products shown, (63), (64), (65) and (66). ((66) is only isolated when the reaction mixture is allowed to warm to room temperature).<sup>51</sup>

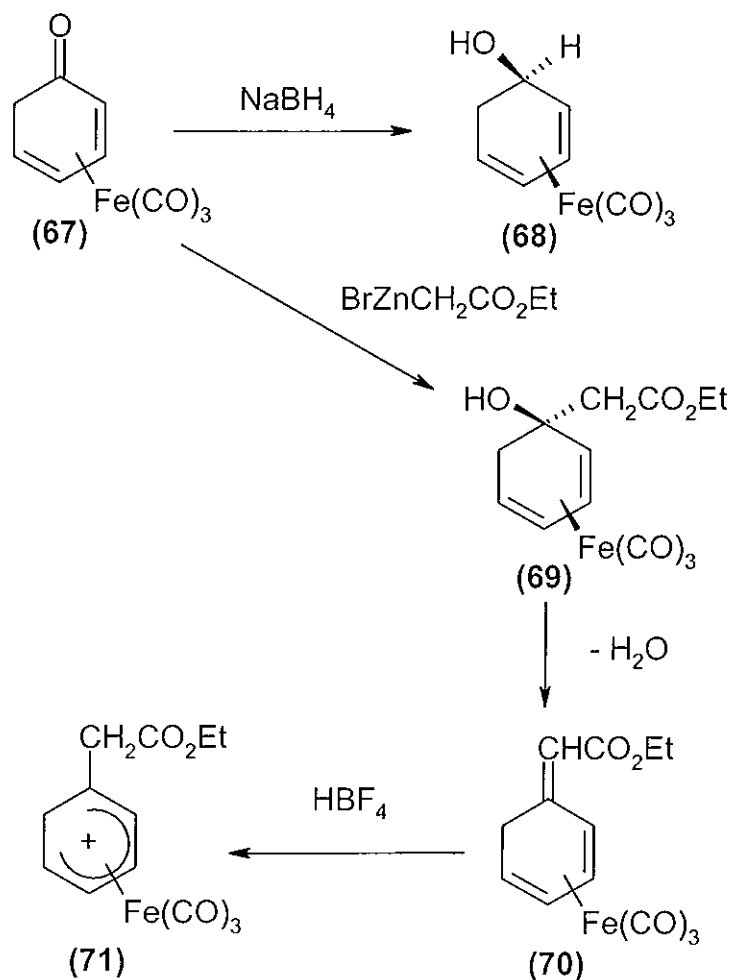




Scheme 1.24 Nucleophilic addition of 2-lithio-2-methyl-propionitrile to (η<sup>4</sup>-cyclohexa-1,3-diene)tricarbonyliron (39).

#### 1.2.3.4 Stabilising Ability of the Tricarbonyliron Unit

Cyclohexadienone, a tautomer of phenol, is stabilised by coordination to the tricarbonyliron fragment. Instead of tautomerising to phenol, which is the more stable tautomer in the uncomplexed state, the cyclohexadienone-tricarbonyliron complex (67) remains in the keto form and can be utilised in synthesis. It has been found to react with a limited number of nucleophiles, some of which are shown in Scheme 1.25.<sup>30</sup> When (67) is treated with a solution of sodium borohydride, an *endo* hydroxy complex (68) is formed by addition of the hydride nucleophile *anti* to the metal. Reaction of (67) with zinc ethyl bromoacetate gives the substituted complex (69) which dehydrates to yield complex (70). When (70) is reacted with tetrafluoroboric acid, the substituted (η<sup>5</sup>-cyclohexadienyl)-tricarbonyliron cation (71) is formed and this cation may be reacted further with a range of nucleophiles.



Scheme 1.25 The complexed keto tautomer of phenol, cyclohexadienone-tricarboxyliron (67), utilised for synthesis.

Another striking example of the stabilising effect of the tricarboxyliron moiety can be seen when one looks at the  $(\eta^5\text{-cyclohexadienyl})\text{tricarboxyliron}$  cation (72) complex in Chart 1.6. This complex can be readily isolated as the tetrafluoroborate or hexafluorophosphate salt and may be recrystallised from water.<sup>52</sup> The uncomplexed cation (73) however is very reactive and has been found to deprotonate in water at close to the limiting rate of relaxation of water (estimated as  $5 \times 10^{10} \text{ s}^{-1}$ ).<sup>53</sup>

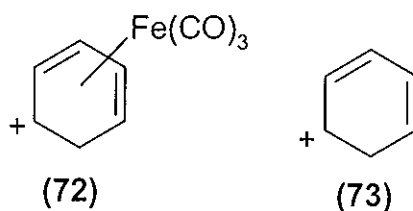
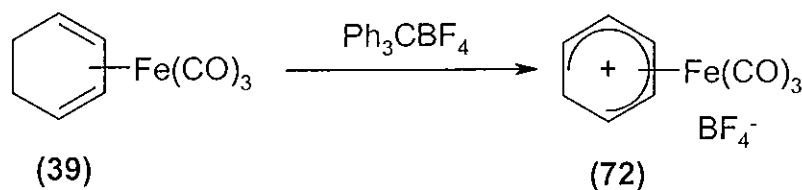


Chart 1.6 The complexed (72) and uncomplexed (73) cyclohexadienyl cations.

### 1.2.4 Cyclohexadienyl-tricarbonyliron Complexes

A significant synthetic breakthrough in the chemistry of tricarbonyliron complexes occurred in 1960 when Fischer and Fischer produced the tetrafluoroborate salt of ( $\eta^4$ -cyclohexa-1,3-diene)tricarbonyliron (**72**).<sup>54</sup> It was prepared by the hydride abstraction reaction of ( $\eta^4$ -cyclohexa-1,3-diene)tricarbonyliron (**39**) with triphenyl-carbenium tetrafluoroborate, as shown in Scheme 1.26. Evidence indicates that the iron is bonded to five  $sp^2$  carbon atoms simultaneously in the cyclohexadienyl complexes.<sup>55</sup> These five  $sp^2$  carbon atoms are planar but the sixth carbon in the cyclohexadienyl ring is  $sp^3$  hybridised and can occupy a position above (**72a**) or below (**72b**) the plane, as can be seen in Chart 1.7. Wilkinson and co-workers used  $^1\text{H}$  NMR data to demonstrate that, for the ( $\eta^5$ -cyclohexadienyl)tricarbonyliron tetrafluoroborate complex, the configuration is as shown in (**72b**).<sup>56</sup>



Scheme 1.26 Fischer and Fischer synthesis of ( $\eta^5$ -cyclohexadienyl)tricarbonyliron tetrafluoroborate (**72**).

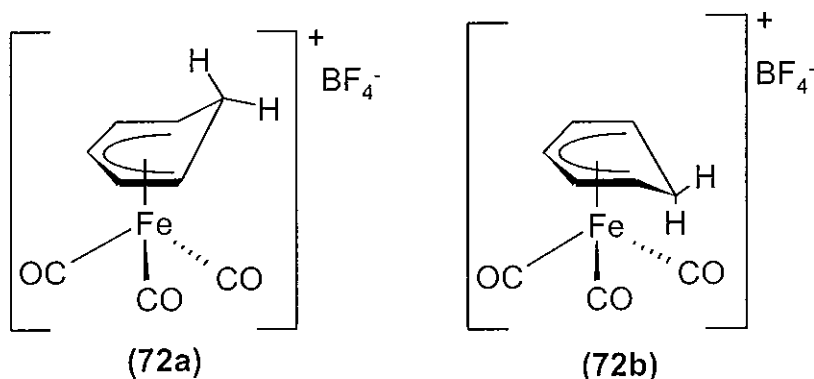
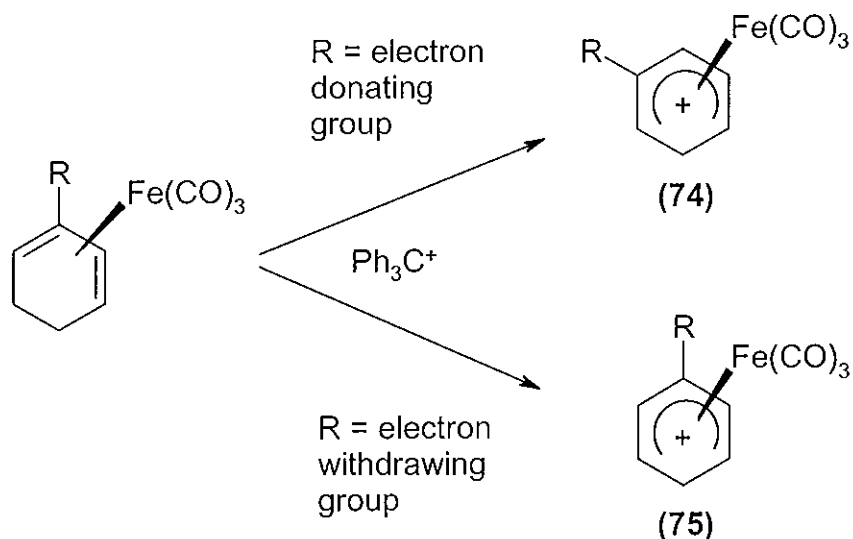


Chart 1.7 The  $sp^3$  carbon in the ( $\eta^5$ -cyclohexadienyl)tricarbonyliron tetrafluoroborate complex occupying a position above (**72a**) and below (**72b**) the plane of the five  $sp^2$  carbon atoms.

The dienyl complexes have found many uses in organic synthesis due to their strongly electrophilic nature. There are many conceivable pathways by which a

nucleophile may react with the complexes (for example, *anti* or *syn* attack on the ring, attack at the metal). However, most evidence collected to date would suggest nucleophilic attack on the ring at the face opposite the metal occurs as the majority of products have an *exo* configuration. The reactions of the dienyl complexes are characterised by high regio- and stereoselectivity.<sup>57</sup> It has not been established whether the initial attack of the nucleophile is onto the ring or onto a metal or carbonyl centre followed by rearrangement.

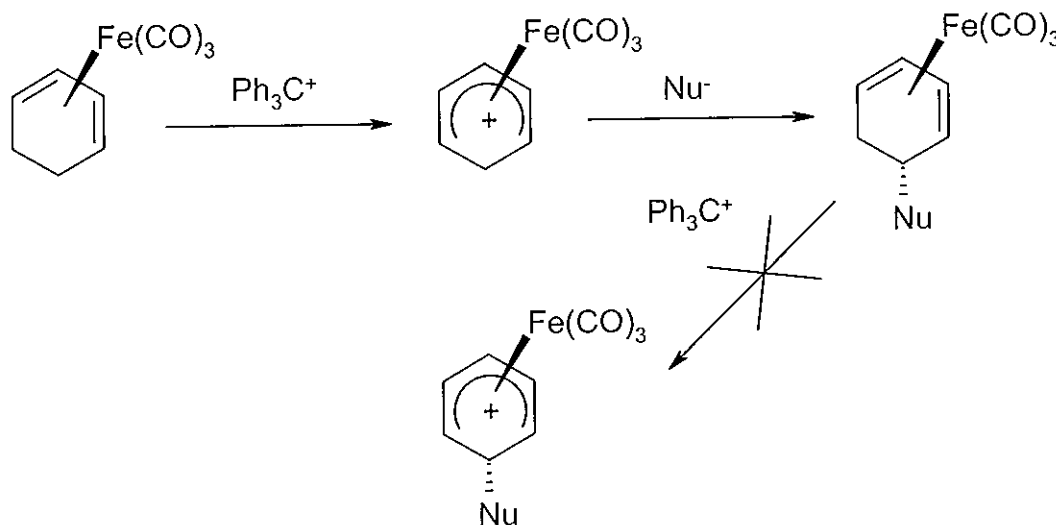
The dienyl complexes of many mono- and disubstituted cyclohexadiene complexes are known. The hydride abstraction process is regioselective and the product formed depends on the nature of the substituents (*i.e.* whether the substituent is an electron acceptor or electron donor). Steric factors also have an influence. This regioselectivity is illustrated in Scheme 1.27. When R is an electron donating group, the main product of hydride abstraction is 94% of complex (74); when R is an electron withdrawing group, the main product is 95% of complex (75).<sup>58</sup>



**Scheme 1.27** Substituent effect on hydride abstraction in substituted ( $\eta^4$ -cyclohexa-1,3-diene)tricarbonyliron complexes.

There is one limitation to the hydride abstraction process in cyclohexadienyl complexes. When a substituent is at the carbon-5 position, *anti* to the metal, the abstraction does not proceed. This means that in a sequential synthetic pathway involving addition of a nucleophile to a cyclohexadienyl complex, reactivation of the

neutral complex to a dienyl complex and further addition of a nucleophile is not possible.<sup>30</sup> This is illustrated in Scheme 1.28.



**Scheme 1.28** Pathway showing limitation of the hydride abstraction process for cyclohexadienyl complexes with substituents at carbon 5.

### 1.2.5 Cyclohexadienyl-tricarbonyliron Complexes in Synthesis

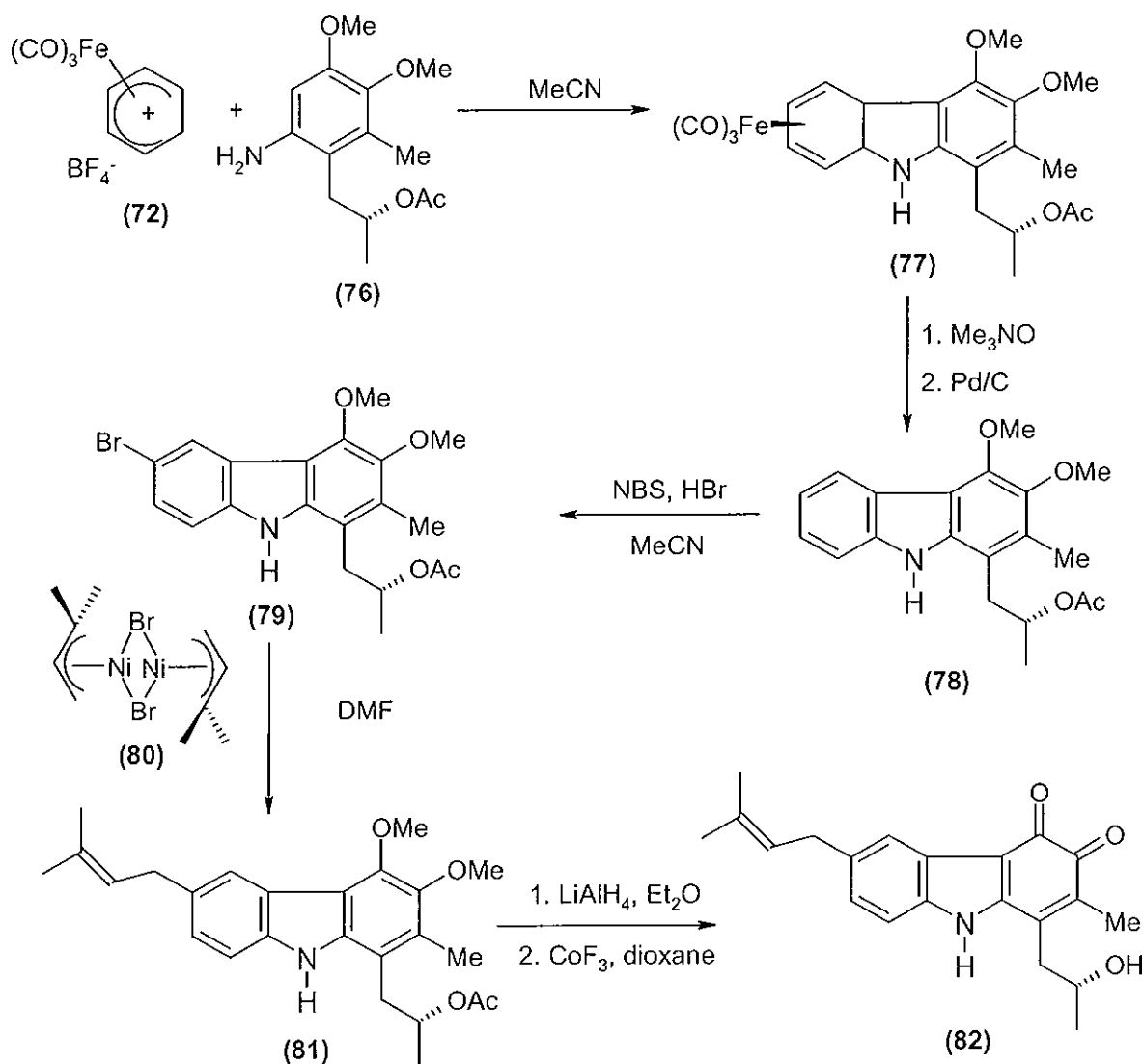
The cyclohexadienyl-tricarbonyliron complexes react with an almost inexhaustible range of nucleophiles. For most nucleophiles, the yields are quite high. A high regio- and stereoselectivity of reaction is also usually observed. An extensive review of reactions of nucleophiles with cyclohexadienyl complexes was carried out in 1994 by Pearson.<sup>30</sup>

Some examples of the utilisation of the cyclohexadienyl-tricarbonyliron complexes in a variety of chemical syntheses will now be described.

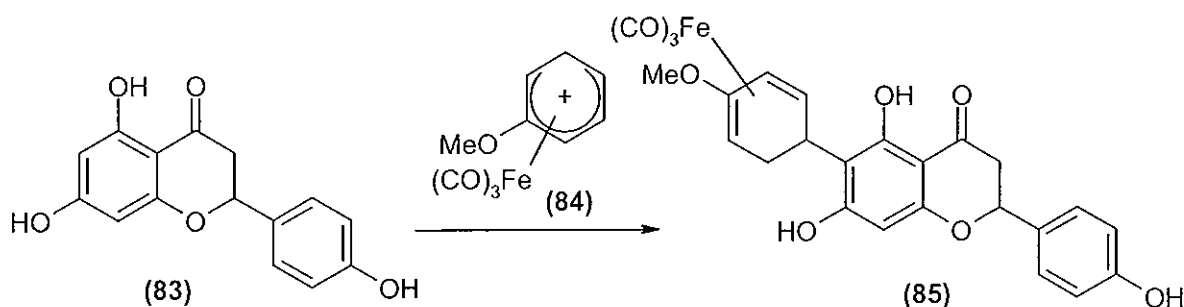
1. Many carbazole alkaloids have been isolated from natural sources. They are of interest due to their useful biological activities. They demonstrate potent neuronal cell protection and have been shown to exhibit free radical scavenging activity. Knölker *et al.* completed the first enantioselective total synthesis of the carbazole alkaloid carquinostatin A (**82**) in 2000. The synthetic route for this synthesis is laid out in Scheme 1.29.<sup>59</sup> Nucleophilic trapping of the cyclohexadienyl complex (**72**) by the enantiopure arylamine (**76**) followed by an

oxidative cyclization affords the tricarbonyliron complex (77). (77) is decomplexed using trimethylamine-*N*-oxide and aromatised by a dehydrogenation using 10% palladium on activated carbon yielding the carbazole (78). *N*-bromosuccinamide reacts with (78) by electrophilic aromatic substitution to produce the bromocarbazole (79). Coupling of the bromocarbazole (79) by the dimeric nickel complex (80) shown provides (81), which, on removal of the acetyl group by reduction with lithium aluminium hydride followed by oxidation using cobalt (III) fluoride affords the carbazole alkaloid carquinostatin A (82).

2. Stephenson and his group developed a synthesis of organometalcarbonyl probes (an example is 4',5,7-trihydroxy-6-{tricarbonyl[( $\eta^4$ -2"-methoxy-1",3"-cyclohexadien-5" $\alpha$ -yl]iron}flavanone (85) shown in Scheme 1.30) by reacting a cyclohexadienyl-tricarbonyliron complex (84) complex with a flavanone (83). The aim of producing the probes was to use them to explore the mode of action of nod gene induction in *Rhizobium leguminosarum* by attaching the probe to its protein binding site.<sup>60</sup> The vibrational modes of the carbonylmetal bands in the organometalcarbonyl probes undergo environment induced shifts when bound to their target sites. These shifts may be monitored by the carbonylmetal-immunoassay method (CMIA) which is used to exploit the low detection limits of the vibrational modes of carbonylmetal complexes by FT-IR spectroscopy.

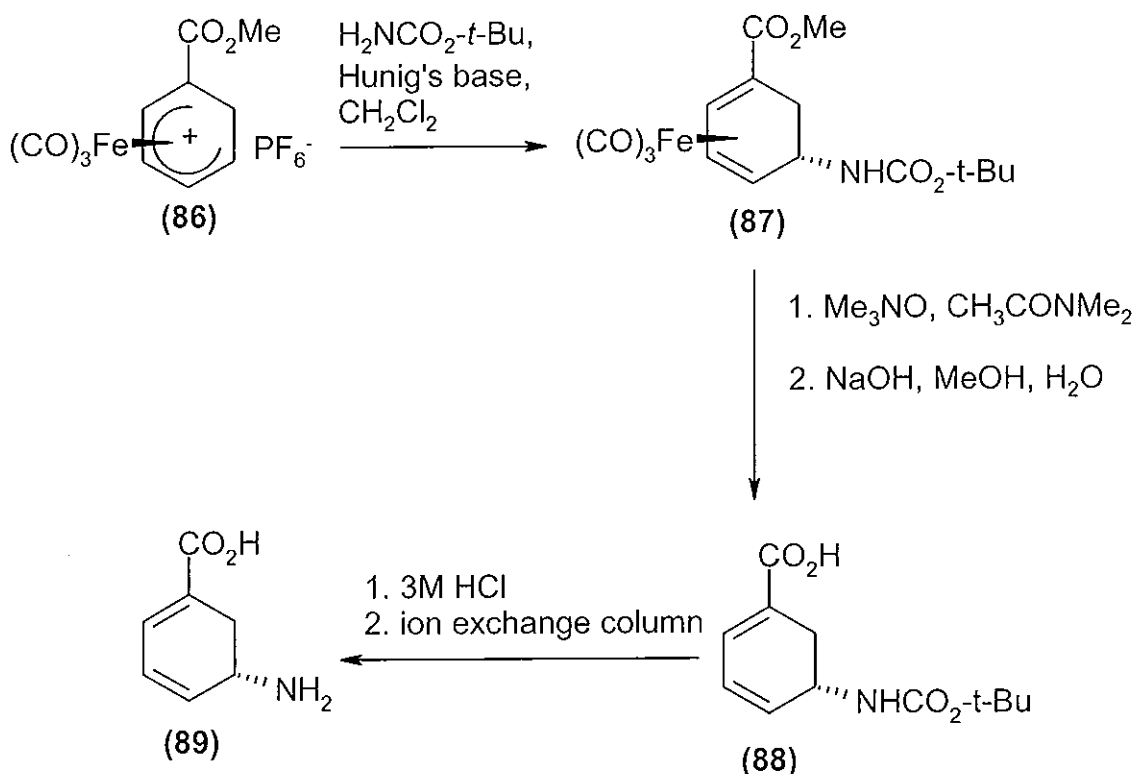


Scheme 1.29 Enantioselective synthesis of carquinostatin A (82) by Knölker *et al* utilising a cyclohexadienyl-tricarbonyliron complex.<sup>59</sup>



Scheme 1.30 Synthesis of an organometalprobe, 4',5,7-trihydroxy-6-{tricarbonyl[( $\eta^4$ -2"-methoxy-1",3"-cyclohexadien-5" $\alpha$ -yl]iron}flavanone (85) by Stephenson *et al* utilising a cyclohexadienyl-tricarbonyliron complex.<sup>60</sup>

3. Birch *et al.* used a cyclohexadienyl-tricarbonyliron complex (**86**) to prepare (-)-gabaculine (**89**), a naturally occurring amino acid. It is potentially useful in the treatment of Parkinsonism, schizophrenia and epilepsy.<sup>61</sup> Scheme 1.31 shows the steps followed by Birch to synthesise (-)-gabaculine (**89**). The complexed cyclohexadienyl cation (**86**) is trapped by the heteroatom nucleophile, *tert*-butyl carbamate, *anti* to the metal to yield the neutral complex (**87**). Decomplexation is achieved by dissolving (**87**) in dimethylacetamide and reacting with trimethylamine oxide. This is followed by hydroxide ion promoted ester hydrolysis to afford the gabaculine protected compound (**88**). Acid catalysed hydrolysis of (**88**) provides the (-)-gabaculine (**89**) product.



Scheme 1.31 Synthesis of the amino acid, (-)-gabaculine (**89**), by Birch *et al.* utilising a cyclohexadienyl-tricarbonyliron complex.

### 1.2.6 Ligand Exchange: Substitution of a Carbonyl Ligand by a Triarylphosphine or Trialkylphosphine Ligand

Replacement of one of the carbonyl ligands by triphenylphosphine ( $\text{PPh}_3$ ) has a marked effect on reactivity of the cyclohexadienyl tricarbonyliron complexes.



This is due to a change in the electron environment in the complex which increases the electron density around the metal. To understand where this increased electron density comes from, it is useful to take a closer look at bonding between the metal and carbonyl ligand. In order to do this, it is first necessary to consider two aspects of coordination complexes that govern their reactivity. They are the 18-electron rule and back bonding.

### 1.2.6.1 The Eighteen Electron Rule

The 18 electron rule for organometallic compounds is analogous to the octet rule for organic compounds. If a metal has a total electron count of 18 in its valence shell, the complex should be stable. The 18 electrons in the valence shell are comprised of the two *s* orbital electrons, six *p* orbital electrons and 10 *d* orbital electrons. Like the octet rule, the 18 electron rule is not always obeyed but it serves as a guide to predicting the stability of complexes.<sup>62,63</sup> Various methods exist for counting the electrons and an example is given in Chart 1.8 for nonacarbonyldiiron (33).

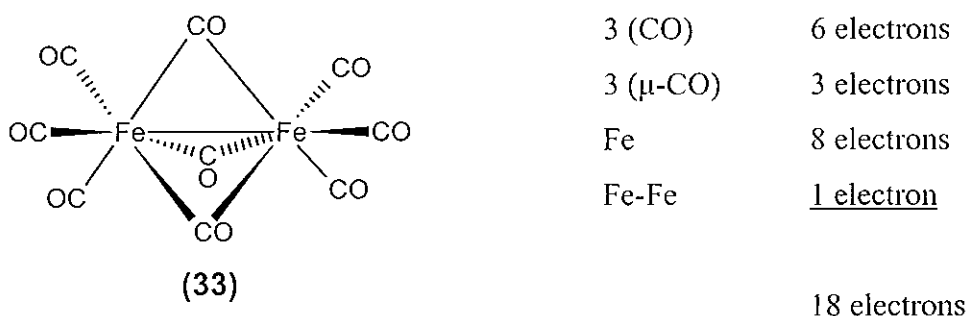


Chart 1.8 18 electron count for nonacarbonyldiiron (33).

The carbonyl ligands are each said to donate two electrons from a lone pair to an empty *d* orbital. The bridging carbonyls, denoted  $\mu$ -CO, donate one electron to each iron atom. Iron atoms have eight valence electrons as they are in group eight in the periodic table. The metal-metal bond is assumed to contribute one electron to each metal atom. That provides a total valence shell electron count of eighteen for the iron in the nonacarbonyldiiron complex.

### 1.2.6.2 Back Bonding

A sigma bond ( $\sigma$ ) is formed when a ligand (such as the carbonyl ligand) donates a pair of electrons to an empty orbital on the metal. Some ligands have empty antibonding orbitals (denoted  $\pi^*$ ) which are of suitable orientation to accept electrons back from the metal to form pi bonds. To use the carbonyl ligands as an example, this back donation of electrons strengthens the metal-carbon bond but weakens the carbon-oxygen bond. Not all ligands accept electrons back from the metal (called  $\pi$ -acceptance or  $\pi$ -acidity) in the same way as the carbonyl ligand. The trialkylphosphine or triarylphosphine ( $R_3P$ ) type ligands may be fine tuned by changing the R group to increase their ability to donate or accept electrons from the metal.  $P(CH_3)_3$  for example has a weak  $\pi$ -acidity in comparison to the carbonyl ligand whereas  $PF_3$  has a  $\pi$ -acidity which matches that of the carbonyl ligand.<sup>64</sup> An example of the formation of  $\pi$  bonds formed by back bonding from a metal is given in Figure 1.1, between a tetracarbonyliron moiety and a carbonyl ligand for the pentacarbonyliron complex (32).

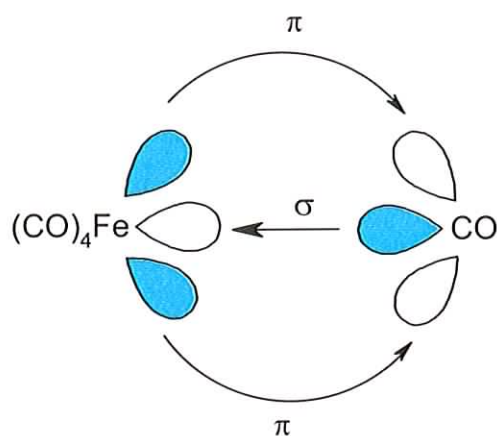
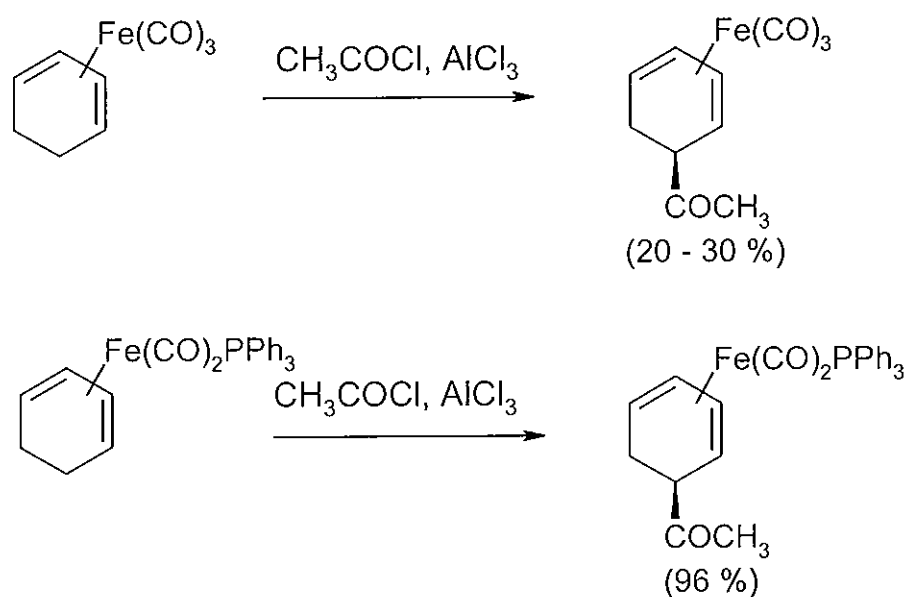


Figure 1.1 Formation of sigma and pi bonds in pentacarbonyliron (32).

### 1.2.6.3 The Electron Environment in Cyclohexadiene Complexes

To return to the  $(\eta^4\text{-cyclohexa-1,3-diene})\text{tricarbonyliron}$  complexes, the lone pair electrons situated on the carbon atom within the carbonyl molecule are donated to the metal to form a sigma bond. The metal can donate electrons back from a filled d orbital to the ligand's lowest unoccupied molecular orbital (LUMO). The result of this back bonding is an increase in the strength of the metal-carbon bond with a corresponding decrease for the carbon-oxygen bond.

When a carbonyl ligand is replaced by a triphenylphosphine ligand, this back bonding is reduced. This is due to a decreased  $\pi$ -acidity of the triphenylphosphine ligand. The effect is a decrease in the reactivity of the carbonyl ligand toward nucleophiles and a reduced capacity to undergo reductive dimerisation reactions as the ability to accept electrons has decreased.<sup>65</sup> For the neutral cyclohexadiene-tricarbonyliron complexes, an increase in reactivity towards electrophiles is also observed when a carbonyl ligand is replaced by triphenylphosphine.<sup>66</sup> This may be observed by examining the Friedel-Crafts acylation reactions in Scheme 1.32.



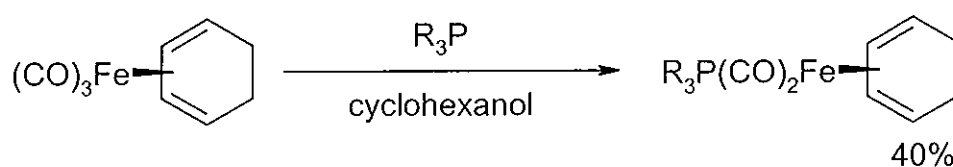
**Scheme 1.32 Comparison of Friedel-Crafts acylation of a cyclohexadiene-tricarbonyliron complex and a cyclohexadiene-dicarbonyltriphenylphosphineiron complex.**

#### 1.2.6.4 Reaction Conditions for Ligand Exchange

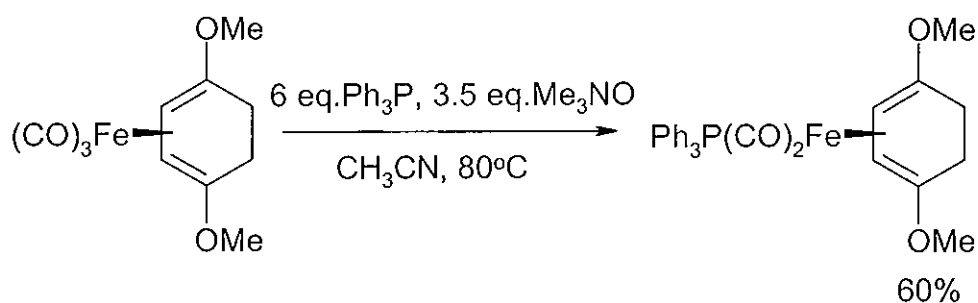
Various methods of ligand exchange have been developed and one of the most commonly used for the R<sub>3</sub>P type complexes was reported by Pearson and Raithby in 1981 and is shown in Scheme 1.33.<sup>107</sup> In this method, the cyclohexadiene-tricarbonyliron complexes are reacted with the R<sub>3</sub>P ligands in refluxing cyclohexanol. The yields are only 40% on average due to formation of a side product. The nature of the ligand and the substituents on the cyclohexadiene ring has an effect on the synthetic method to be used. For example, the Pearson and Raithby method gives a yield of only

15% when one tries to replace a carbonyl group with triphenylphosphine when a methoxy substituent is present on the cyclohexadiene ring. Guillou *et al.* found that the yield for the same ligand exchange on a similar type of cyclohexadiene complex with two methoxy substituents could be increased to 60% using different conditions.<sup>67</sup> In Guillou's method, six equivalents of triphenylphosphine and 3.5 equivalents of trimethylamine oxide were reacted with the substituted cyclohexadiene complex in acetonitrile at 80°C.

Pearson and Raithby



Guillou *et al.*



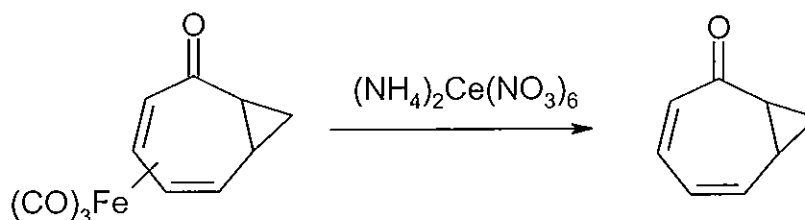
**Scheme 1.33 Comparison of the ligand substitution methods developed by Pearson and Raithby<sup>107</sup> and Guillou *et al.*<sup>67</sup>**

In all, a wide range of cyclic and acyclic (diene) $Fe(CO)_2L$  complexes have been prepared and phosphine, phosphite, isonitrile, arsine, stibine, and other ligands have been used.<sup>65,66,67,68,107</sup>

### 1.2.7 Decomplexation of Tricarbonyliron Complexes

In order for the tricarbonyliron fragment to be of use synthetically, it is important that this moiety can be added and removed easily and in good yield. Sections 1.2.1 and 1.2.2 detailed how the tricarbonyliron complexes may be synthesised as well as how the use of transfer reagents provides the complexes in high yield under mild

conditions. There are many examples of disengagement of organic ligands from the tricarbonyliron group in good yield, an example of which is shown in Scheme 1.34.<sup>69</sup>

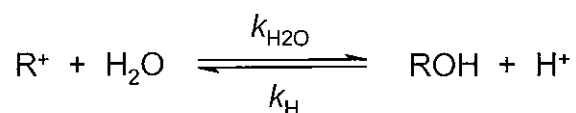


**Scheme 1.34 Demetallation of a tricarbonyliron complex using ceric ammonium nitrate.**

There are a number of other oxidising reagents that have been developed to remove the organic ligand from the tricarbonyliron complexes as well as ceric ammonium nitrate. They are trimethylamine-*N*-oxide, iron (III) chloride, copper (II) chloride and pyridinium chlorochromate.<sup>30</sup> The former, trimethylamine-*N*-oxide (Me<sub>3</sub>NO), was first utilised in 1963 by Shvo and Hazum<sup>70</sup> and it is by far the most widely used. Unlike the other decomplexing agents, it does not generate acidic conditions. This is an important consideration if the organic ligand being disengaged contains acid sensitive functional groups.

### 1.3 Stability of Coordinated Cyclohexadienyl Cations

The stability of the coordinated cyclohexadienyl carbocations can be determined by measurement of  $K_R$ , the equilibrium constant for formation of the coordinated benzene hydrates (ROH) from the coordinated cyclohexadienyl cations ( $R^+$ ), based on the reaction shown in Scheme 1.35. Schemes 2.1 (Section 2.1, page 45) and 2.4 (Section 2.2, page 71) in the results chapter show this equilibrium for the cyclohexadienyl cation complexes examined in this work.



**Scheme 1.35 Formation of a coordinated benzene hydrate (ROH) from a coordinated cyclohexadienyl cation ( $R^+$ ).**

In Scheme 1.35,  $k_{\text{H}_2\text{O}}$  is the rate constant for reaction of the coordinated cyclohexadienyl cation with water. The rate constant,  $k_{\text{H}}$ , refers to the acid catalysed formation of the coordinated cyclohexadienyl cation from the corresponding benzene hydrate. A convenient way to express the equilibrium constant,  $K_{\text{R}}$ , is in terms of its negative logarithm defined as  $\text{p}K_{\text{R}}$  ( $\text{p}K_{\text{R}} = -\log K_{\text{R}}$ ).

In principle, there are two methods by which the constant  $K_{\text{R}}$  can be determined. They are:

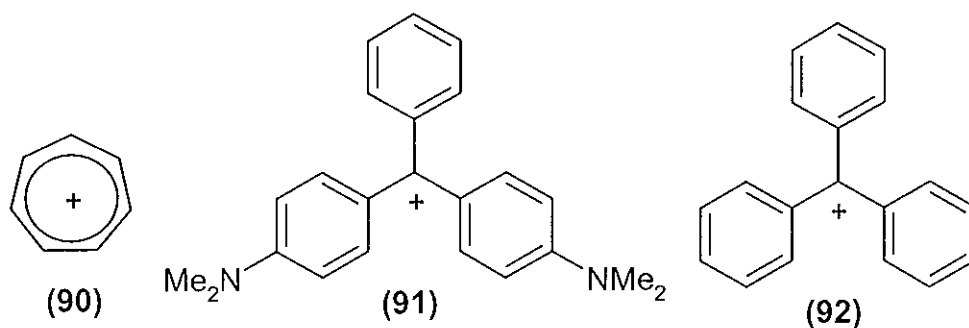
1. By a direct measurement of the equilibrium concentrations of the coordinated cyclohexadienyl cation and benzene hydrate.
2. By direct kinetic measurements of the forward and reverse rates of the coordinated cyclohexadienyl cation and benzene hydrate reactions respectively, under the same conditions.

### 1.3.1 Direct Equilibrium Measurements

The relationship between the concentrations of reactants and products for direct equilibrium measurements of the equilibrium constant  $K_{\text{R}}$ , from Scheme 1.35, is given by Equation 1.1.

$$K_{\text{R}} = [\text{ROH}] [\text{H}^+] / [\text{R}^+] \quad (1.1)$$

UV-Vis spectrophotometry is commonly used to carry out direct determinations of  $K_{\text{R}}$ . This is achieved by determining the relative concentrations of the carbocation and hydrate being studied at equilibrium at particular acid concentrations. An appreciable change in spectrum is required between the fully ionised and fully neutral species, and both species must be sufficiently stable to be directly observable. The tropylium cation (90) and the di-(*p*-dimethylaminophenyl)-phenylmethyl cation (91) are shown in Chart 1.9. They are examples of cations that are sufficiently stable to allow the concentrations of both the carbocation and corresponding alcohol to be measured in dilute acid solutions.<sup>71,72</sup>



**Chart 1.9 Tropylium (90), di-(*p*-dimethylaminophenyl)-phenylmethyl (91) and triphenylmethyl (92) cations.**

For cations such as the triphenylmethyl cation (92), their concentrations are too small to be measured in dilute acid solutions and solutions of concentrated acid are required (>45% H<sub>2</sub>SO<sub>4</sub>). As a result of medium effects, the  $K_R$  value deviates under these conditions from its value in water and the Hammett acidity function or the “excess acidity” method must be applied. By use of reference reactions, a plot of  $\log K_R$  versus the acidity function,  $X$ , can be obtained and the value of  $K_R$  extrapolated to pure water when  $X_0 = 0$  is determined.<sup>73,74,75</sup>

In most instances however it is generally not possible to determine the  $K_R$  of a carbocation in concentrated acid media. It is too far removed from aqueous solution and determination of  $X_0$  values has not always been carried out.

### 1.3.2 Kinetic Measurements

An alternative to employing equilibrium measurements to determine  $K_R$  is the use of kinetic measurements. In this approach, the rate constants for the forward and reverse reactions,  $k_{H_2O}$  and  $k_H$  respectively, are combined as is shown in Equation 1.2.

$$K_R = k_{H_2O} / k_H \quad (1.2)$$

For uncoordinated carbocations,  $k_{H_2O}$  can be difficult to measure as, in the case of very reactive carbocations, reaction of the carbocation with water is the

kinetically favoured direction of the equilibrium. Two general methods have traditionally been used to determine  $k_{\text{H}_2\text{O}}$ :

#### 1. Indirect Method

An example of an indirect method for determining the rate constant  $k_{\text{H}_2\text{O}}$  is the azide 'clock' technique. In this approach, the rate constant ratio for reaction of a carbocation with two nucleophiles (one of which is the azide ion) is determined by analysis of the products formed. The azide ion rate constant is diffusion controlled and is used as a 'clock' to estimate the reactivity of the carbocation in the presence of the second nucleophile. Richard and Jencks have used the azide clock technique for various carbocation systems.<sup>76</sup>

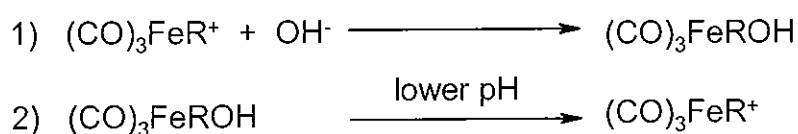
#### 2. Direct Method

An example of a direct method used to determine  $k_{\text{H}_2\text{O}}$  for very reactive carbocations is laser flash photolysis. The basis of this technique is that a laser pulse is used to produce a transient carbocation species in greater than equilibrium concentrations. The transient carbocation species produced can be monitored by means of absorption spectra and the rate of decay of the cationic species in pure solvent and in the presence of nucleophiles can be observed. McClelland *et al.* was one of the first groups to use laser flash photolysis for direct investigations of the reactivity of unstable carbocations in aqueous media in the late 1980's.<sup>77</sup>

In the case of the carbocations examined in this study, the stabilising ability of the tricarbonyliron moiety allowed the rate constant,  $k_{\text{H}_2\text{O}}$ , to be measured directly by reacting the coordinated cyclohexadienyl cations to yield the coordinated benzene hydrate product.

The rate constant,  $k_{\text{H}}$ , for carbocation formation from alcohols (including arene hydrates) has been determined by various methods. An example of one approach used is the monitoring of isotope exchange in dilute acid solutions. However, for the coordinated cyclohexadienyl cations being examined in this work,  $k_{\text{H}}$  can be measured by allowing the coordinated cation to react fully to form the hydrate and subsequently quenching this hydrate into a solution of sufficiently lower pH that will allow the reaction of the hydrate to cation to be observed, as shown in Scheme 1.36.



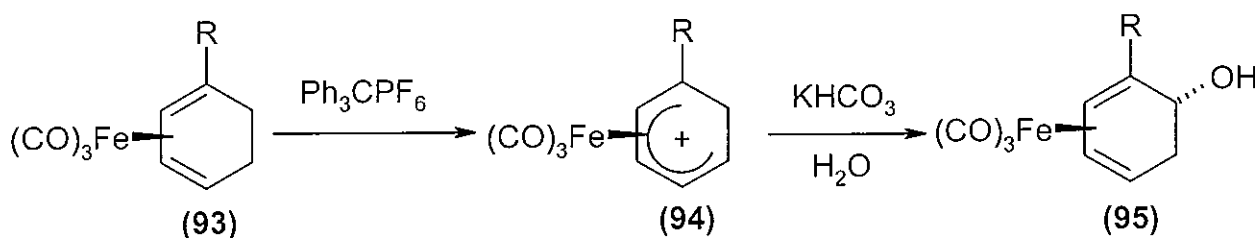


**Scheme 1.36** Formation of a solution of the coordinated arene hydrate and subsequent quenching into a solution of lower pH to allow conversion of the hydrate to the corresponding coordinated cyclohexadienyl cation to be monitored.

## 1.4 Organometallic Coordination of Oxidative Metabolites of Aromatic Hydrocarbons-Aims of this Study

As was discussed in Section 1.1.2, arene *cis*-dihydrodiols, which are readily accessible by large scale fermentation using mutant strains of bacteria, have found many uses as synthons in organic chemistry. The *trans*- analogues are not yet accessible on a commercial scale but a number of enzymatic and chemoenzymatic pathways that could be used to synthesise substituted arene *trans*-dihydrodiols have been described in a review by Boyd and Sharma.<sup>17</sup> Although a number of pathways are available, they are multistep in character and generally of limited synthetic scope and yield. One of the most promising and direct chemical routes was outlined in Scheme 1.7 and it involves coordination of an arene *cis*-dihydrodiol with a tricarbonyliron moiety. In a preliminary study of this synthetic route, two steps that could cause difficulties were identified. They were the trapping of the coordinated cyclohexadienyl cation by a nucleophile and the decomplexing step.

The principal goal of this study is to investigate the nucleophilic reaction of water and hydroxide with the coordinated cyclohexadienyl cation with a view to modifying the tricarbonyliron moiety to allow efficient reaction of the carbocation. A model reaction which was employed to monitor the nucleophilic trapping of various coordinated cyclohexadienyl cations (**94**) is shown in Scheme 1.37.

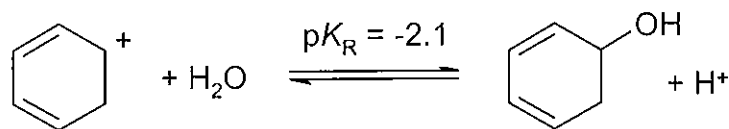


**Scheme 1.37** Model reaction to be used for investigating nucleophilic trapping of the coordinated cyclohexadienyl cations (94).

From Scheme 1.37, it can be seen that substituted 1,3-cyclohexadienes are used as the starting materials in the model reaction used in this work. This is because they are more readily available than the arene *cis*-dihydrodiols. When coordinated to the tricarbonyliron group, they form complexes of type (93). The product of the model reaction is a coordinated benzene hydrate (95). Decomplexation will provide a range of substituted arene hydrates. These are another form of oxidative metabolite from polycyclic aromatic hydrocarbons and they have also found uses in organic synthesis.

As has been discussed in Section 1.2.6, replacement of a carbonyl ligand by a triphenylphosphine ligand alters the reactivity of a coordinated cyclohexadienyl cation. Thus, a dicarbonyltriphenylphosphineiron-cyclohexadienyl cation was studied in addition to a tricarbonyliron-cyclohexadienyl cation.

Successful monitoring of the model reaction by UV-Vis spectrophotometry will allow a secondary benefit, a comparison of  $pK_R$  for the equilibrium of the coordinated and uncoordinated cyclohexadienyl cations.  $pK_R$  for the uncoordinated cyclohexadienyl cation was previously determined to be -2.1 by More O'Ferrall *et al.*<sup>53</sup>



**Scheme 1.38** Equilibrium of the cyclohexadienyl cation with benzene hydrate.

## **CHAPTER 2**

### **RESULTS**

## 2 Results

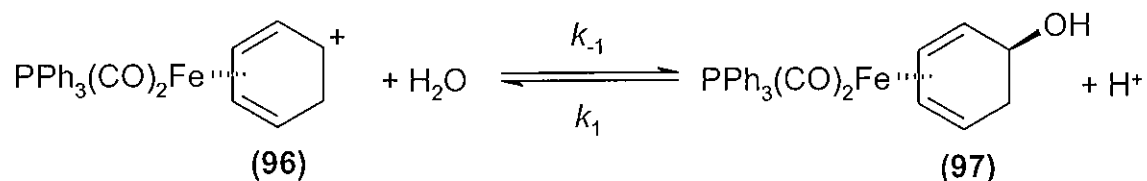
The principal aim of the work undertaken in this study was to investigate the nucleophilic trapping of two ironcarbonyl coordinated cyclohexadienyl cations. The ( $\eta^5$ -cyclohexadienyl)dicarbonyltriphenylphosphineiron cation (**96**) was examined initially. Once this triphenylphosphine substituted analogue had been studied, the parent carbocation (**72**) was examined. Interpretation of the results obtained for this tricarbonyliron substituted carbocation was easier when they were compared with those already determined for the dicarbonyltriphenylphosphineiron substituted cation (**96**).

### 2.1 ( $\eta^5$ -Cyclohexadienyl)dicarbonyltriphenylphosphineiron Cation

Rates and equilibria for hydrolysis of the ( $\eta^5$ -cyclohexadienyl)dicarbonyltriphenylphosphineiron cation (**96**) to its corresponding hydrate, shown in Scheme 2.1, have been studied. Measurements include:

- $pK_R$  for the hydrolysis of this coordinated cation to the hydrate.
- rate constants for the base catalysed hydrolysis of the ( $\eta^5$ -cyclohexadienyl)dicarbonyltriphenylphosphineiron cation (**96**).
- rate constants for the acid catalysed ionisation of ( $\eta^4$ -*exo*-5-hydroxy-1,3-cyclohexadiene)dicarbonyltriphenylphosphineiron (**97**).

A pH profile has been constructed from this data. In addition, a  $^1\text{H}$  NMR study investigating protonation of the iron atom during the ionisation reaction was undertaken.



Scheme 2.1

The stability of the coordinated cyclohexadienyl carbocation can be determined by measurement of  $K_R$ , the equilibrium constant for formation of the

coordinated benzene hydrate from the coordinated cyclohexadienyl cation. From Scheme 2.1, the equilibrium constant can be defined by Equation 2.1 below.

$$K_R = [97] [H^+] / [96] \quad (2.1)$$

As the rates of the forward and reverse reactions are equal at equilibrium, the equilibrium constant,  $K_R$ , may also be expressed in terms of the rate constants of the forward and reverse reactions as shown in Equation 2.2.

$$K_R = k_{-1} / k_1 \quad (2.2)$$

### 2.1.1 Equilibrium Constant for Hydrolysis

The  $pK_R$  value for the hydrolysis of the ( $\eta^5$ -cyclohexadienyl)dicarbonyltriphenylphosphineiron cation (used as its hexafluorophosphate salt) was determined by using UV-Vis absorption spectrophotometry. The result obtained was based upon the absorbance measurements made at the pHs indicated in Table 2.1. It was calculated from Equation 2.3 in which  $A$ ,  $A_1$  and  $A_m$  are the final absorbance for the partially hydrated species at the chosen pH, the absorbance for the coordinated cyclohexadienyl cation (96) and the absorbance for the fully formed neutral coordinated hydrate (97) respectively. The final absorbances observed in the UV-Vis spectra for the hydrolysis reaction of the ( $\eta^5$ -cyclohexadienyl)dicarbonyltriphenylphosphineiron cation (96) were used. The  $pK_R$  was determined to be  $9.87 \pm 0.36$ .

$$pK_R = \text{pH} + \log (A_m - A) / (A - A_1) \quad (2.3)$$

In aqueous solution, the coordinated cyclohexadienyl cation shows a UV spectrum with strong absorbances around 200 nm. In aqueous sodium hydroxide, the absorbance of this peak decreased and the quality of the UV spectrum below 210 nm deteriorated. The equilibrium constant measurement was based on absorbances recorded at 255 nm. When fully formed, the coordinated hydrate shows a UV spectrum with  $\epsilon = 3.85 \times 10^4 \text{ M}^{-1} \text{ cm}^{-1}$  at  $\lambda_{\text{max}} = 220 \text{ nm}$ . Figure 2.1 shows the UV-Vis spectra

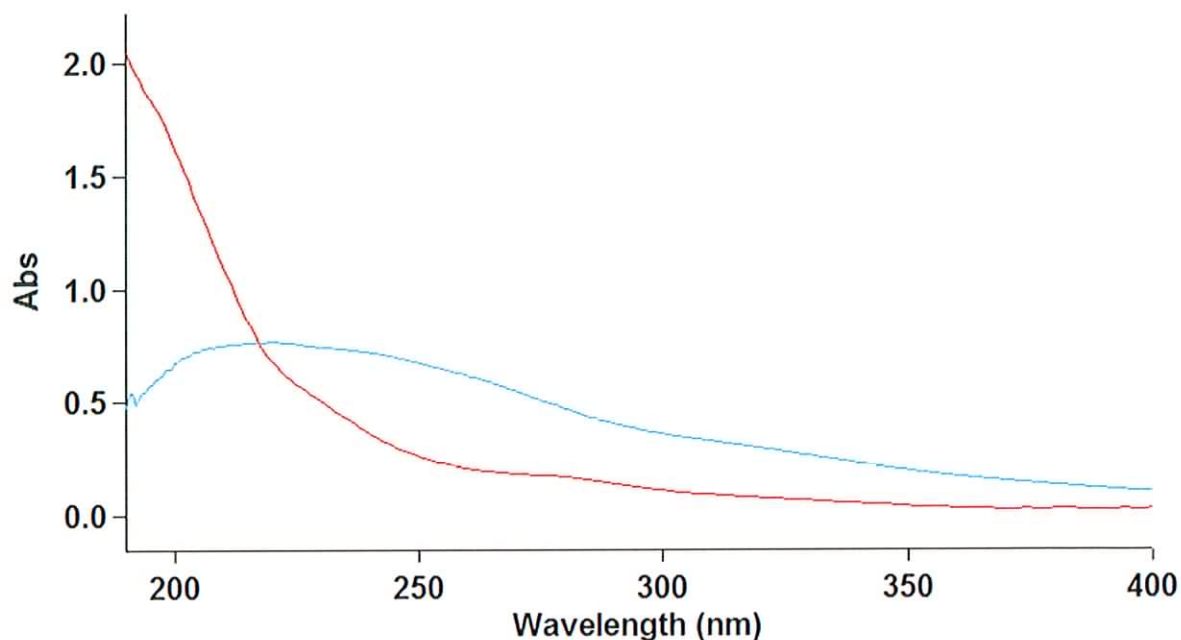
recorded for the coordinated cyclohexadienyl cation (**96**) and for the corresponding hydrate (**97**).

**Table 2.1** Absorbances of ( $\eta^5$ -cyclohexadienyl)dicarbonyltriphenylphosphineiron in aqueous borate buffer solutions at 25°C.<sup>a</sup>

pH	R <sup>b</sup>	Absorbance	pK <sub>R</sub>
7.10 <sup>c</sup>		0.23 <sup>d</sup>	
8.75 <sup>f</sup>		0.26	9.76
9.12 <sup>f</sup>	1.0	0.34	9.44
9.48 <sup>f</sup>	2.3	0.37	9.63
9.73 <sup>f</sup>	4.0	0.44	9.51
10.07 <sup>f</sup>	9.0	0.42	9.97
11.00 <sup>g</sup>		0.51	10.33
11.31 <sup>h</sup>		0.53	10.42
12.00 <sup>k</sup>		0.57 <sup>e</sup>	

Mean pK<sub>R</sub> = 9.87 ± 0.36

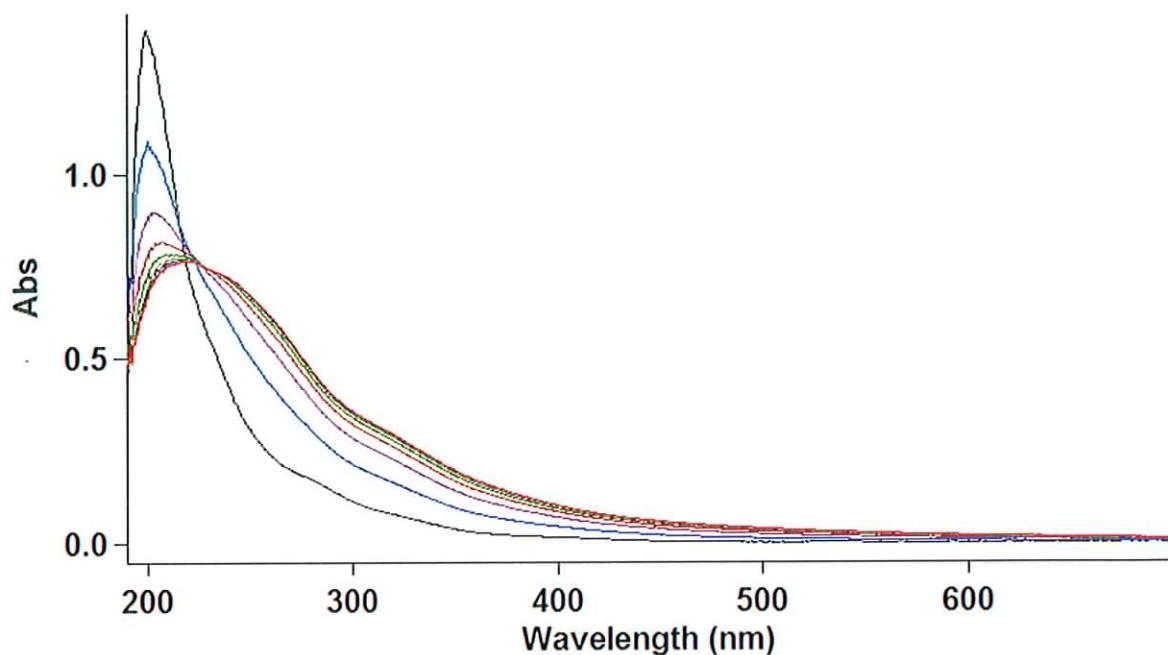
(a) Measurements were made at 255 nm, with a substrate concentration of  $2.0 \times 10^{-5}$  M and ionic strength 0.1M. (b) R = [buffer base]/[buffer acid]. (c) Unbuffered H<sub>2</sub>O. (d) Absorbance for fully formed coordinated cyclohexadienyl cation, A<sub>I</sub>. (e) Absorbance for fully formed neutral coordinated hydrate, A<sub>m</sub>. (f) Borate buffer. (g) 0.001M NaOH. (h) 0.002M NaOH. (k) 0.01M NaOH



**Figure 2.1** Overlay of UV-Vis spectra recorded for ( $\eta^5$ -cyclohexadienyl)-dicarbonyltriphenylphosphineiron cation ( $\lambda_{\text{max}}$  190nm) and the corresponding hydrate, ( $\eta^4$ -*exo*-5-hydroxy-1,3-cyclohexadiene)-dicarbonyltriphenylphosphineiron, ( $\lambda_{\text{max}}$  220 nm). Measurements were made at a substrate concentration of  $2 \times 10^{-5}$  M and ionic strength of 0.1 M.

### 2.1.2 Rate Constants for Hydrolysis

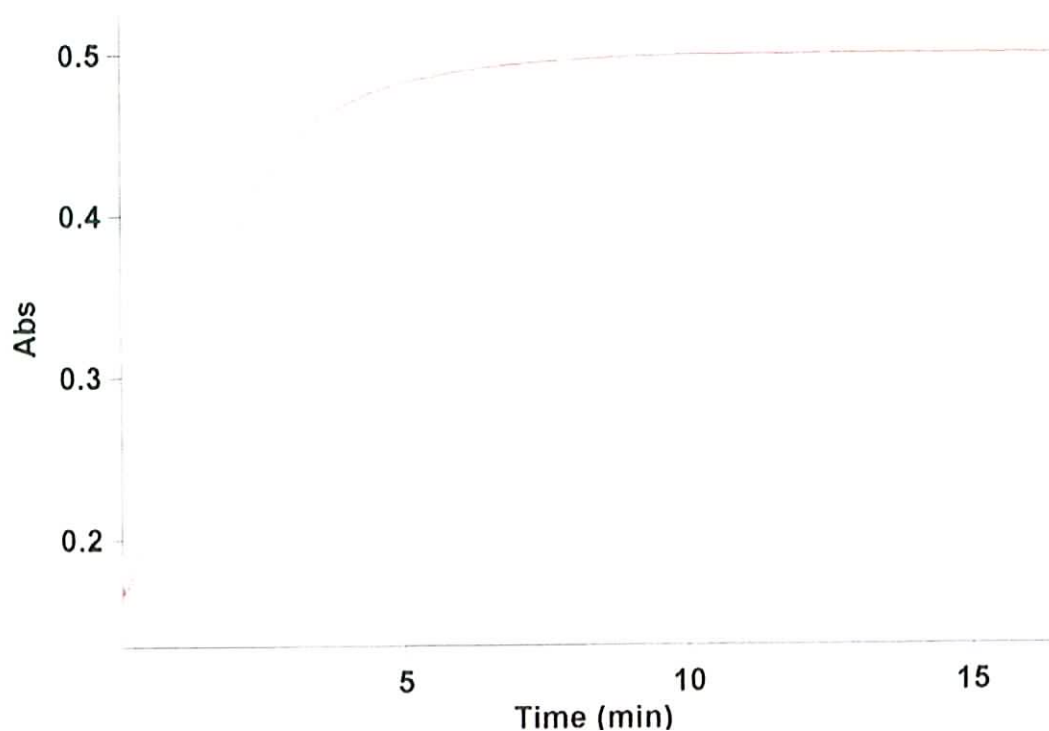
The rate of hydrolysis of ( $\eta^5$ -cyclohexadienyl)dicarbonyltriphenylphosphineiron (**96**) was measured in aqueous solutions of sodium hydroxide and carbonate and borate buffers by monitoring the increase in absorbance at 275 nm observed in the UV absorption spectra recorded. A typical example of the UV repetitive scan observed (cycle time 5 minutes) for the hydrolysis reaction is shown in Figure 2.2. Initial kinetic measurements obtained at the  $\lambda_{\text{max}}$  of the cation (202 nm) were found to be quite noisy with poor reproducibility. This was probably because the region below 210 nm is subject to interference from absorption by sodium hydroxide.



**Figure 2.2**      **Repetitive scan for the hydrolysis of ( $\eta^5$ -cyclohexadienyl)dicarbonyltriphenylphosphineiron in aqueous 0.001M sodium hydroxide (cycle time 5 minutes) at 25°C and a substrate concentration of  $2.0 \times 10^{-5}$  M**

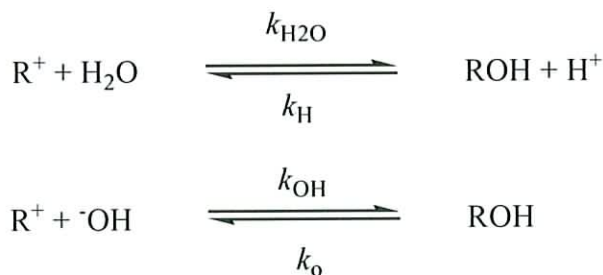
From Figure 2.2 it can be seen that the isosbestic point is not quite clear. This observation, combined with the occurrence of a small induction period on some of the kinetic scans, as shown in Figure 2.3, may indicate the presence of an initial reaction, possibly at the carbonyl carbon or the iron centre.<sup>78</sup>





**Figure 2.3** A kinetic scan observed for the hydrolysis of ( $\eta^5$ -cyclohexadienyl)dicarbonyltriphenylphosphineiron in aqueous 0.003 M hydroxide at 275 nm and 25°C with a substrate concentration of  $2.0 \times 10^{-5}$  M.

There are two hydrolysis reactions of the coordinated cation producing the coordinated hydrate complex. The first is direct addition of water to the cation with the equilibrium of the reaction defined by  $K_R$ , and the second is addition of hydroxide ( $\text{OH}^-$ ) to the cation with the equilibrium constant for the reaction,  $K_C$ . Both reactions are shown below with the corresponding rate constants for each step of the reaction provided.



Which reaction predominates will depend on the pH of the solution in which the reaction is taking place. In high hydroxide concentration the latter reaction will predominate with the contribution of reaction with water to the observed rate constant being negligible. In the reactions above it can be seen that two of the reactions are pH independent with rate constants  $k_{\text{H}_2\text{O}}$  and  $k_0$  respectively.

#### Hydroxide Ion Catalysed Reaction

Table 2.2 shows first order rate constants for the hydrolysis of ( $\eta^5$ -cyclohexadienyl)dicarbonyltriphenylphosphineiron in aqueous sodium hydroxide. The equilibrium constant,  $K_R$ , can be estimated by plotting the rate constants against hydroxide ion concentration as shown in Figure 2.4. According to Equation 2.4, the slope and intercept of this plot correspond to rate constants  $k_{\text{OH}} = 1.85 \text{ M}^{-1}\text{s}^{-1}$  and  $k_0 = 2.59 \times 10^{-3} \text{ s}^{-1}$  for hydroxide catalysed and pH independent reactions. The equilibrium constant,  $K_C$ , defined as the equilibrium constant for the reaction of electrophiles with nucleophiles, can be obtained from the observed rate constants as shown in Equation 2.5.<sup>79</sup> Bunting has pointed out that when the nucleophile involved in the reaction is a hydroxide ion,  $K_C$  and  $K_R$  provide equal measures of electrophile stability.<sup>80</sup> The relationship between  $K_C$  and  $K_R$  is thus described in Equation 2.6 where  $K_w$  is the autoprotolysis constant of water. The value of  $\text{p}K_R$  determined by applying this equation is 10.22.\*

---

\* The value of  $k_0$  obtained from Figure 2.4 was not used for this calculation due to the scatter of the points introducing a relatively large error. The value of  $k_0$  can also be obtained from the intercept of the pH profile (Section 3.2, Figure 3.1) and was found to be  $3.09 \times 10^{-4} \text{ s}^{-1}$ .

**Table 2.2** First order rate constants for the hydrolysis of ( $\eta^5$ -cyclohexadienyl)dicarbonyltriphenylphosphineiron in aqueous sodium hydroxide solutions at 25°C.<sup>a</sup>

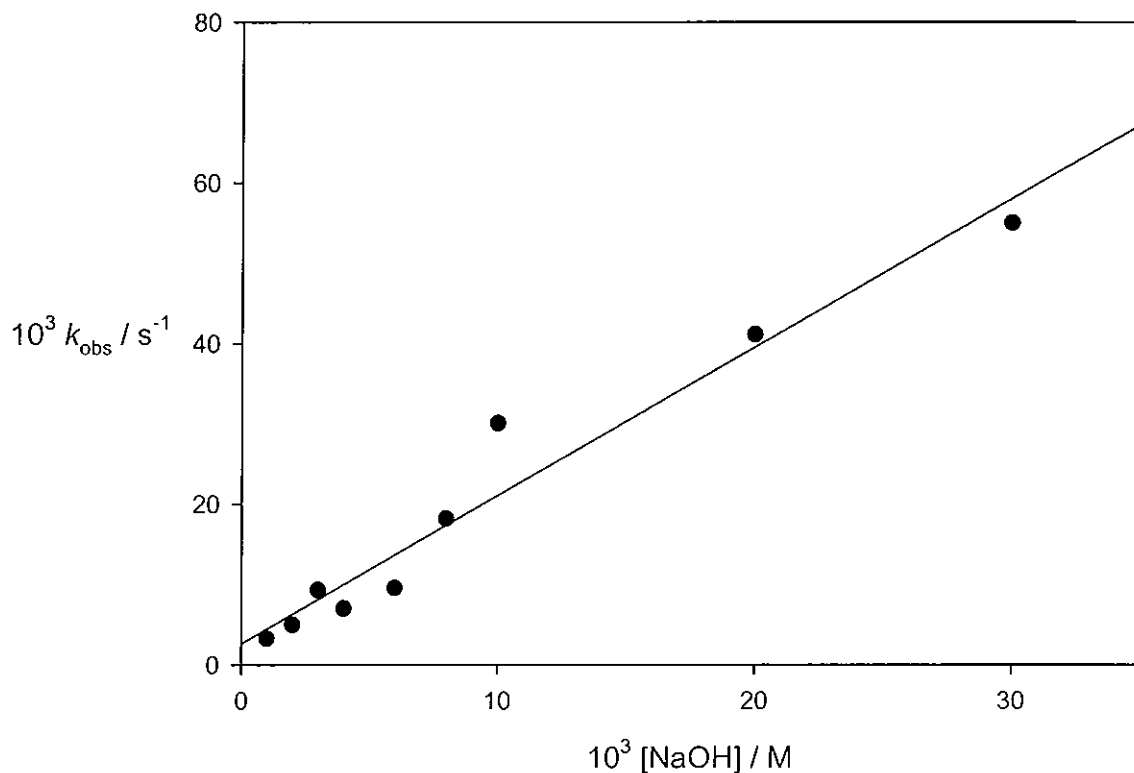
pH	$10^3$ [NaOH]/M	$10^3 k_{\text{obs}}/\text{s}^{-1}$
12.48	30.0	55.0
12.30	20.0	41.1
12.01	10.0	30.1
11.94	8.0	18.2
11.78	6.0	9.57
11.63	4.0	7.00
11.49	3.0	9.34
11.30	2.0	4.98
11.01	1.0	3.26

(a) Measurements were made at 275 nm with a substrate concentration of  $2.0 \times 10^{-5}$  M.

$$k_{\text{obs}} = k_{\text{OH}}[\text{OH}^-] + k_{\text{o}} \quad (2.4)$$

$$K_{\text{C}} = k_{\text{OH}} / k_{\text{o}} \quad (2.5)$$

$$K_{\text{R}} / K_{\text{C}} = K_{\text{w}} \quad (2.6)$$



**Figure 2.4** Plot of first order rate constants against hydroxide ion concentration for the hydrolysis of ( $\eta^5$ -cyclohexadienyl)dicarbonyltriphenylphosphineiron (**96**) in aqueous sodium hydroxide at 25°C.

#### Reaction in Carbonate Buffers

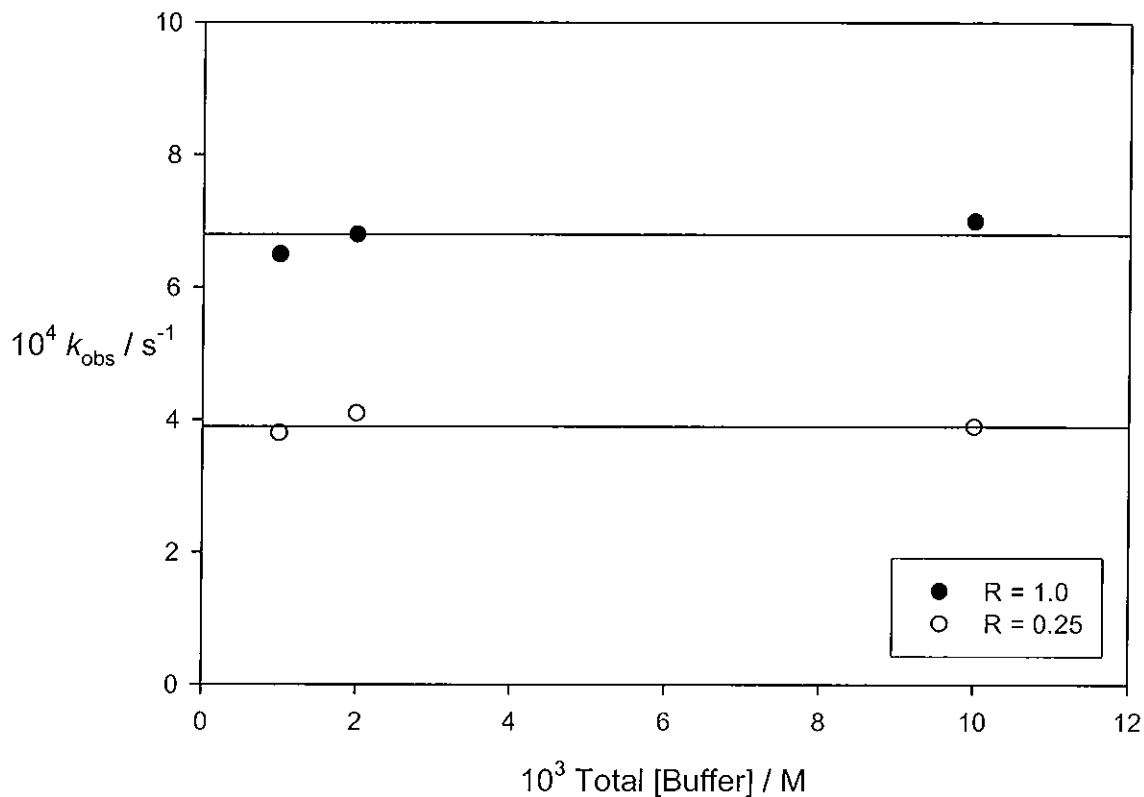
Rate constants for the hydrolysis of ( $\eta^5$ -cyclohexadienyl)dicarbonyltriphenylphosphineiron in aqueous carbonate buffers were also measured. The first order rate constants obtained are shown in Table 2.3 and are plotted against total buffer concentration for different buffer ratios ( $R = [\text{buffer base}] / [\text{buffer acid}]$ ) in Figure 2.5.

**Table 2.3** First order rate constants for the hydrolysis of ( $\eta^5$ -cyclohexadienyl)dicarbonyltriphenylphosphineiron in aqueous carbonate buffers at 25°C.<sup>a</sup>

pH	R <sup>b</sup>	10 <sup>3</sup> [CO <sub>2</sub> <sup>2-</sup> ]/M	10 <sup>3</sup> [HCO <sub>3</sub> <sup>-</sup> ]/M	10 <sup>4</sup> k <sub>obs</sub> /s <sup>-1</sup>
10.69	2.33	7.0	3.0	12.2
10.51	1.50	6.0	4.0	9.5
10.33	1.00	5.0	5.0	7.0
10.33	1.00	1.0	1.0	6.8
10.33	1.00	0.5	0.5	6.5
9.96	0.43	3.0	7.0	4.7
9.73	0.25	2.0	8.0	3.9
9.73	0.25	0.4	1.6	4.1
9.73	0.25	0.2	0.8	3.8

(a) Measurements were made at 275 nm with a substrate concentration of  $2.0 \times 10^{-5}$  M and ionic strength 0.1 M. (b) R = [buffer base] / [buffer acid].

It can be seen from the plots in Figure 2.5 that general acid or base catalysis is not observed as lines of slope zero are obtained. The intercepts of these plots are a contribution from both the hydroxide catalysed reaction ( $k_{OH}[\text{OH}^-]$ ) and the pH independent reaction of water ( $k_o$ ) as described by the equation  $k_{obs} = k_{OH}[\text{OH}^-] + k_o$ . Using this equation  $k_o$  was found to be  $2.9 \times 10^{-4}$  s<sup>-1</sup> for both R = 0.25 and 1.0 respectively and it represent the pH independent reaction rate.



**Figure 2.5** Plot of first order rate constants against total buffer concentration at fixed buffer ratios for the hydrolysis of ( $\eta^5$ -cyclohexadienyl)dicarbonyltriphenylphosphineiron in aqueous carbonate buffers at 25°C.

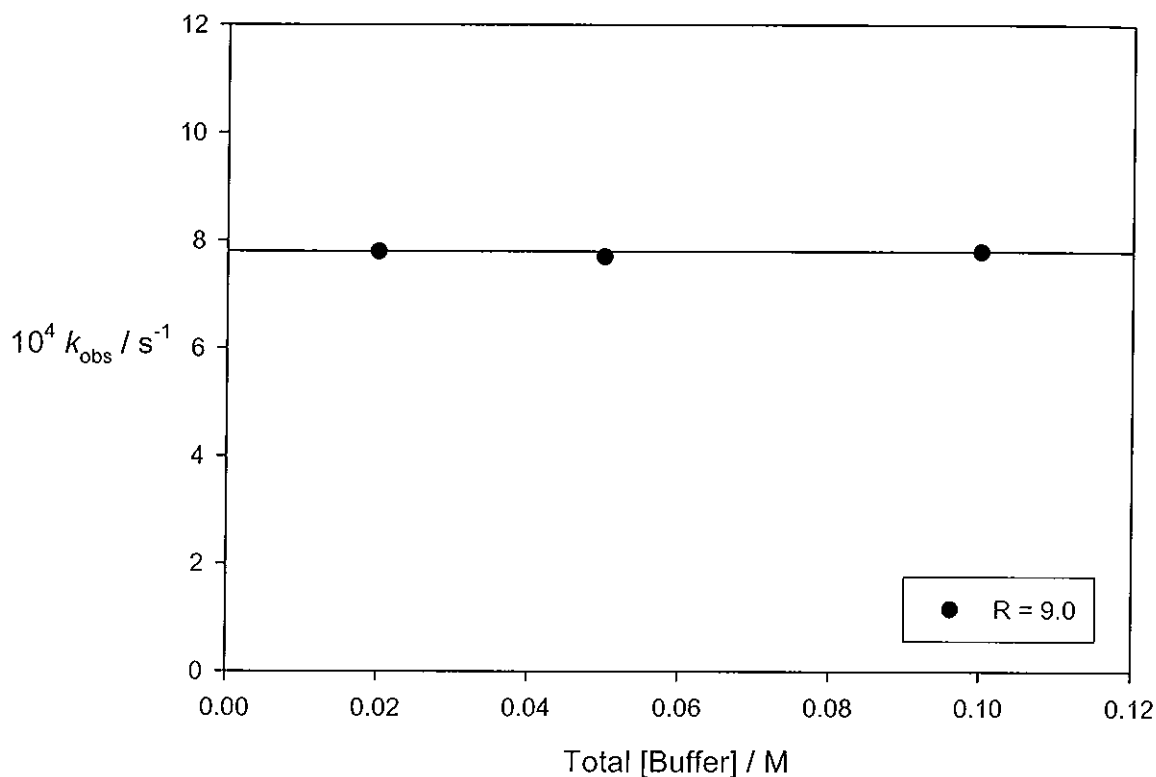
Reaction in Borate Buffers

Rate constants for the hydrolysis of ( $\eta^5$ -cyclohexadienyl)dicarbonyltriphenylphosphineiron were measured in a range of borate buffers. First order rate constants for this reaction are presented in Table 2.4 and a plot of the first order rate constants against total buffer concentration for pH 10.07 is shown in Figure 2.6.

**Table 2.4** First order rate constants for the hydrolysis of ( $\eta^5$ -cyclohexadienyl)dicarbonyltriphenylphosphineiron in aqueous borate buffers at 25°C.<sup>a</sup>

pH	R <sup>b</sup>	[H <sub>2</sub> BO <sub>3</sub> <sup>-</sup> ]/M	[H <sub>3</sub> BO <sub>3</sub> ]/M	10 <sup>4</sup> <i>k</i> <sub>obs</sub> /s <sup>-1</sup>
10.07	9.0	0.090	0.010	7.8
10.07	9.0	0.045	0.005	7.7
10.07	9.0	0.018	0.002	7.8
9.48	2.3	0.070	0.030	3.7
9.12	1.0	0.050	0.050	3.5

(a) Measurements were made at 275 nm with a substrate concentration of  $2.0 \times 10^{-5}$  M and ionic strength 0.1 M. (b) R = [buffer base] / [buffer acid].



**Figure 2.6** Plot of first order rate constants against total buffer concentration at a fixed buffer ratio of 9.0 for the hydrolysis of ( $\eta^5$ -cyclohexadienyl)dicarbonyltriphenylphosphineiron in aqueous borate buffer at 25°C.

The plot in Figure 2.6 shows that for borate buffers, as for carbonate buffers, general acid or base catalysis is not observed as a line of slope zero was obtained. The buffer independent rate constant,  $k_{\text{obs}}$ , was found to be  $(7.80 \pm 0.05) \times 10^{-4} \text{ s}^{-1}$  for  $R = 9.0$ . The pH independent rate constant,  $k_o$ , can be determined from the equation  $k_{\text{obs}} = k_{\text{OH}}[\text{OH}^-] + k_o$  and was found to be  $5.6 \times 10^{-4} \text{ s}^{-1}$ . Observed rate constants of  $3.7 \times 10^{-4} \text{ s}^{-1}$  and  $3.5 \times 10^{-4} \text{ s}^{-1}$  for  $R = 2.3$  and 1.0 respectively were measured.



### 2.1.3 Rate Constants for Ionisation of ( $\eta^4$ -Exo-5-hydroxy-1,3-cyclohexadiene)dicarbonyltriphenylphosphineiron

Rate constants for the ionisation of the coordinated arene hydrate, ( $\eta^4$ -exo-5-hydroxy-1,3-cyclohexadiene)dicarbonyltriphenylphosphineiron (**97**), were measured in aqueous solutions of hydrochloric acid and chloroacetate, acetate and cacodylate buffers. The coordinated arene hydrate was generated by allowing a solution of the coordinated cyclohexadienyl cation in acetonitrile to be hydrolysed fully in 0.001M aqueous sodium hydroxide. When the hydrolysis reaction was complete, this solution was quenched into various buffer or hydrochloric acid solutions containing sufficient excess acid to neutralise the sodium hydroxide present. In this way, the rate of formation of the coordinated cyclohexadienyl cation could be monitored by following a decrease in absorbance at 275 nm using UV spectrophotometry. Attempts were made to prepare a sample of the coordinated arene hydrate (**97**) so that it could be used directly. However, a sufficiently pure sample was not isolated.

An example of a repetitive scan for this ionisation reaction is shown in Figure 2.7. Below 220 nm the spectra are affected by absorption of the cacodylate buffer. Taking this into account, Figures 2.2 and 2.7 are consistent with the expected relationship between ionisation and hydrolysis as forward and reverse reactions.

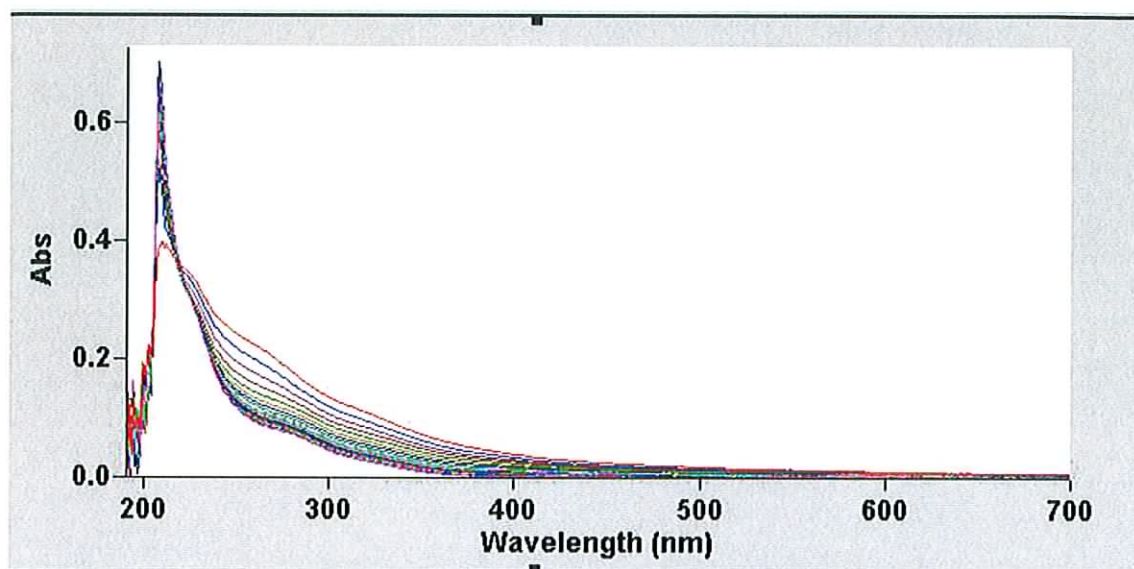


Figure 2.7      Repetitive scan (cycle time 1.5 minutes) for the ionisation of ( $\eta^4$ -*exo*-5- hydroxycyclohexa-1,3-diene)dicarbonyltriphenylphosphineiron (97) in aqueous cacodylate buffer at 25°C and a substrate concentration of  $1.0 \times 10^{-5}$  M.

### Reaction in Borate Buffers

Table 2.5 contains the first order rate constants measured for the ionisation of the coordinated hydrate complex in borate buffer solutions. First order rate constants were measurable for both the hydrolysis reaction of the coordinated cation (see Table 2.4) and the ionisation reaction of the coordinated hydrate. For example, if we consider the borate buffer solution at pH 9.12, the first order rate constants were found to be  $3.4 \times 10^{-4}$  and  $3.5 \times 10^{-4} \text{ s}^{-1}$  for the ionisation and hydrolysis reactions respectively. Obtaining a very similar rate constant regardless of whether the forward (hydrolysis) or reverse (ionisation) reactions were being monitored confirms that the reactions are reversible.

**Table 2.5** First order rate constants for the ionisation of ( $\eta^4$ -*exo*-5-hydroxy-1,3-cyclohexadiene)dicarbonyltriphenylphosphineiron (**97**) in aqueous borate buffers at 25°C.<sup>a</sup>

pH	R <sup>b</sup>	[H <sub>2</sub> BO <sub>3</sub> <sup>-</sup> ]/M	[H <sub>3</sub> BO <sub>3</sub> ]/M	10 <sup>4</sup> k <sub>obs</sub> /s <sup>-1</sup>
9.12	1.0	0.050	0.050	3.4
8.39	0.25	0.020	0.080	2.6
8.16	0.11	0.010	0.090	3.2

(a) Measurements were made at 275 nm, with a substrate concentration of  $2.0 \times 10^{-5}$  M and ionic strength 0.1 M. (b) R = [buffer base] / [buffer acid].

### Reaction in Cacodylate Buffers

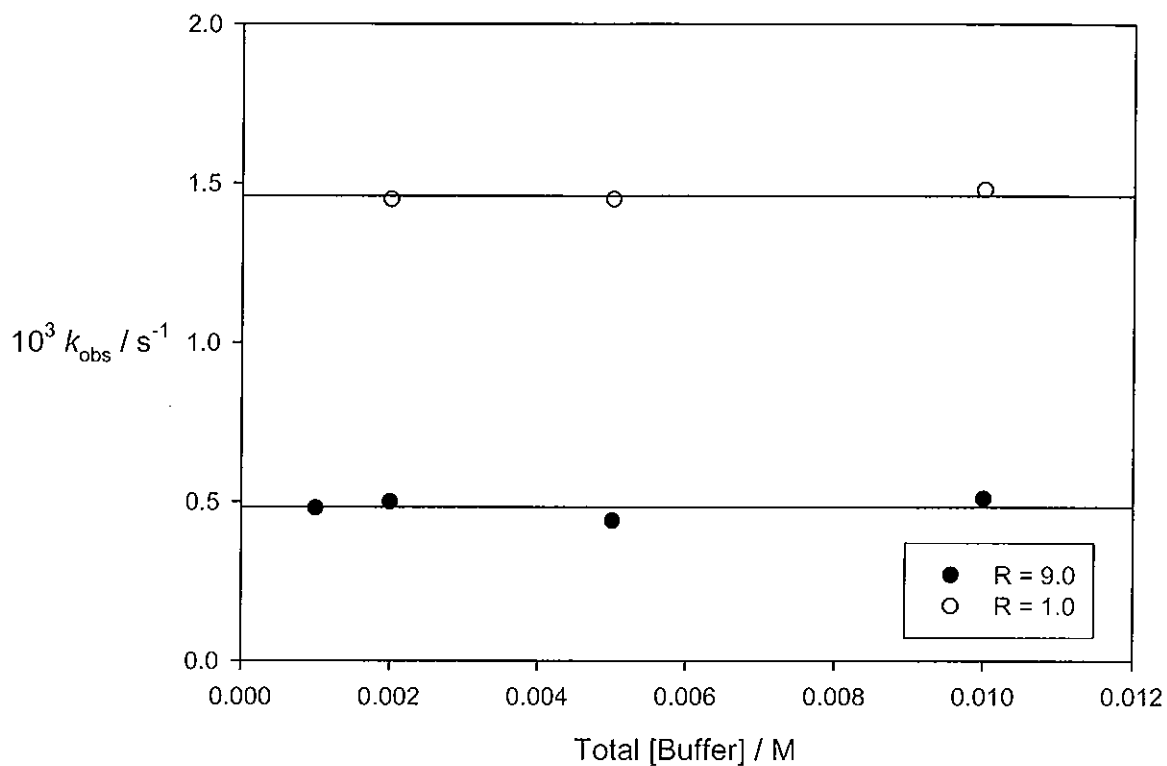
Table 2.6 shows first order rate constants for the ionisation of ( $\eta^4$ -*exo*-5-hydroxy-1,3-cyclohexadiene)dicarbonyltriphenylphosphineiron (**97**) in aqueous cacodylate buffer solutions. A plot of first order rate constants against total buffer concentration for [buffer base] / [buffer acid] ratios of 9.0 and 1.0 is shown in Figure 2.8. No evidence of general acid or base catalysis of the reaction of the coordinated hydrate to give the corresponding cation is observed in the plots in Figure 2.8 as both

give lines of slope zero. The intercepts of these plots are  $(0.48 \pm 0.03) \times 10^{-3} \text{ s}^{-1}$  and  $(1.46 \pm 0.01) \times 10^{-3} \text{ s}^{-1}$  for buffer ratios 9.0 and 1.0 respectively.

**Table 2.6** First order rate constants for the ionisation of ( $\eta^4$ -*exo*-5-hydroxy-1,3-cyclohexadiene)dicarbonyltriphenylphosphineiron in aqueous cacodylate buffers at 25°C.<sup>a</sup>

pH	R <sup>b</sup>	[(CH <sub>3</sub> ) <sub>2</sub> AsO <sub>2</sub> <sup>-</sup> ]/M	[(CH <sub>3</sub> ) <sub>2</sub> AsO <sub>2</sub> H]/M	10 <sup>3</sup> <i>k</i> <sub>obs</sub> /s <sup>-1</sup>
7.11	9.0	0.009	0.001	0.51
7.11	9.0	0.0045	0.0005	0.44
7.11	9.0	0.0018	0.0002	0.50
7.11	9.0	0.0009	0.0001	0.48
6.54	2.3	0.007	0.003	0.73
6.11	1.0	0.005	0.005	1.48
6.11	1.0	0.0025	0.0025	1.45
6.11	1.0	0.001	0.001	1.45

(a) Measurements were made at 275 nm with a substrate concentration of  $2.0 \times 10^{-5} \text{ M}$  and ionic strength 0.1 M. (b) [buffer base] / [buffer acid].



**Figure 2.8** Plot of first order rate constants against total buffer concentration at fixed buffer ratios of 9.0 and 1.0 for the ionisation of ( $\eta^4$ -*exo*-5-hydroxy-1,3-cyclohexadiene)-dicarbonyltriphenylphosphineiron in aqueous cacodylate buffers at 25°C.

#### Reaction in Acetate and Chloroacetate Buffers

Tables 2.7 and 2.8 show first order rate constants for the ionisation of ( $\eta^4$ -*exo*-5-hydroxy-1,3-cyclohexadiene)dicarbonyltriphenylphosphineiron (**97**) in acetate buffers and chloroacetate buffers respectively.

**Table 2.7** First order rate constants for the ionisation of ( $\eta^4$ -*exo*-5-hydroxy-1,3-cyclohexadiene)dicarbonyltriphenylphosphineiron in aqueous acetate buffers at 25°C.<sup>a</sup>

pH	R <sup>b</sup>	10 <sup>3</sup> [CH <sub>3</sub> CO <sub>2</sub> <sup>-</sup> ] /M	10 <sup>3</sup> [CH <sub>3</sub> CO <sub>2</sub> H] /M	10 <sup>3</sup> <i>k</i> <sub>obs</sub> /s <sup>-1</sup>
5.60	9.0	9.0	1.0	1.20
5.25	4.0	8.0	2.0	1.26
4.65	1.0	5.0	5.0	1.37
4.04	0.25	2.0	8.0	2.29

(a) Measurements were made at 275 nm with a substrate concentration of  $2.0 \times 10^{-5}$  M and ionic strength 0.1 M. (b) [buffer base] / [buffer acid].

**Table 2.8** First order rate constants for the ionisation of ( $\eta^4$ -*exo*-5-hydroxy-1,3-cyclohexadiene)dicarbonyltriphenylphosphineiron in aqueous chloroacetate buffers at 25°C.<sup>a</sup>

pH	R <sup>b</sup>	10 <sup>3</sup> [ClCH <sub>2</sub> CO <sub>2</sub> <sup>-</sup> ] /M	10 <sup>3</sup> [ClCH <sub>2</sub> CO <sub>2</sub> H] /M	10 <sup>3</sup> k <sub>obs</sub> /s <sup>-1</sup>
3.21	4.0	8.0	2.0	11.5
3.15	2.3	7.0	3.0	6.90
3.15	2.3	3.5	1.5	6.99
2.77	1.0	5.0	5.0	16.8
2.16	0.25	2.0	8.0	29.9

(a) Measurements were made at 275 nm with a substrate concentration of  $2.0 \times 10^{-5}$  M and ionic strength of 0.1 M. (b) [buffer base] / [buffer acid].

The average rate constant when the buffer ratio is 2.3 is  $6.95 \times 10^{-3} \text{ s}^{-1}$

Although the measurements are made at a single buffer concentration, on the basis of the lack of general acid or base catalysis observed in other buffers (cacodylate and borate) and the close agreement of the two rate constants at buffer ratio 2.3, it can be concluded that no buffer catalysis is occurring in acetate or chloroacetate buffers either. The average of the two rate constants measured at R = 2.3 for chloroacetate is  $6.95 \times 10^{-3} \text{ s}^{-1}$ . Buffer independent rate constants at this and other buffer ratios are taken to be the value obtained for the single measurements reported.

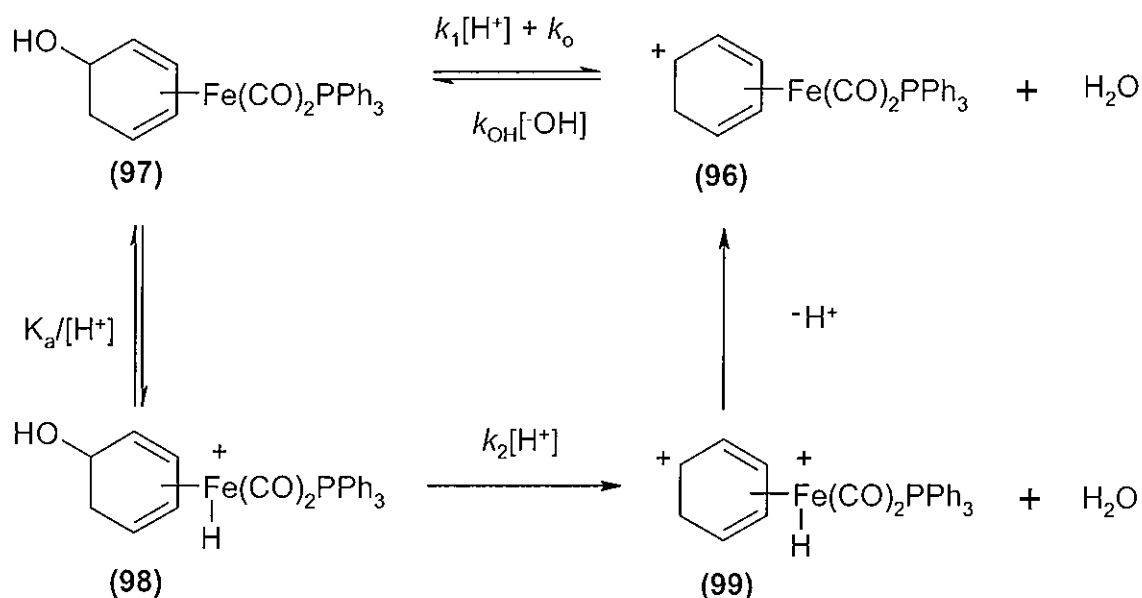
### H<sup>+</sup> Catalysed Reaction

Only one first order rate constant was measured in aqueous hydrochloric acid solution at an acid concentration of 0.001 M. The rate constant was  $1.15 \times 10^{-2} \text{ s}^{-1}$ . When hydrochloric acid solutions of higher concentration were examined, the observed rate constants exhibited poor reproducibility.

#### 2.1.4 pH Profile

The buffer independent rate constants for the hydrolysis of ( $\eta^5$ -cyclohexadienyl)dicarbonyltriphenylphosphineiron may be combined with first order rate constants measured in hydrochloric acid and sodium hydroxide to construct a pH-profile for the reaction. These rate constants are recorded in Tables 2.2 to 2.8 and are shown plotted as  $\log k$  versus pH in Figure 3.1 (Section 3.2, page 127).

The structure of the pH-profile is believed to reflect the changes in mechanism or reactant species that occur on changing the acidity of the medium. These changes have been interpreted as shown in Scheme 2.2.



Scheme 2.2

In the left hand portion of Scheme 2.2, the acid dissociation constant,  $K_a$ , refers to dissociation of the protonated iron complex (98). From the dissociation constant the



ratio of reactant (98) and product (97) present at a given pH can be calculated using the following expression:

$$K_a / [H^+] = [97] / [98]$$

Kinetic expressions for the different regions of the pH-profile that allow rate constants for the processes involved to be determined may be derived as follows:

(i) pH < 4

Based on Scheme 2.2, at pH values below 4, catalysis by acid is observed as shown in Equation 2.7. The reactive species is the iron protonated complex cation (98) which has fully formed. Further protonation of the complex leads to the loss of water and a di-cation species (99) is formed. This intermediate is quickly deprotonated to give the coordinated cyclohexadienyl cation (96).

$$k_{\text{obs}} = k_2[H^+] \quad (2.7)$$

(ii) pH 4 to 6

In the region from pH 4 to 8 of the pH profile, the rate equation may be derived based on the equilibrium between the coordinated hydrate (97) and the protonated metal species (98) shown in Scheme 2.2. The rate law is given in Equation 2.8. In the pH range 4 to 6, the metal protonated species is the predominant species and this undergoes deprotonation followed by acid catalysed reaction of (97) to form the product (96). In this region,  $[H^+] \gg K_a$  for the metal protonated iron complex (98) and Equation 2.8 can be simplified to Equations 2.9 and 2.10.

$$k_{\text{obs}} = k_1 K_a [H^+] / \{K_a + [H^+]\} \quad (2.8)$$

$$k_{\text{obs}} = k_1 K_a [H^+] / [H^+] \quad (2.9)$$

$$k_{\text{obs}} = k_1 K_a \quad (2.10)$$

(iii) pH 6 to 8

From pH 6 to 8, the predominant species is the coordinated hydrate (97), some of which undergoes protonation to form the metal protonated species (98). Therefore  $K_a$  for the metal protonated iron complex  $\gg [H^+]$  and Equation 2.8 reduces to Equations 2.11 and 2.12.

$$k_{\text{obs}} = k_1 K_a [H^+] / K_a \quad (2.11)$$

$$k_{\text{obs}} = k_1 [H^+] \quad (2.12)$$

(iv) pH 8 to 10

The equilibrium constant for the formation of the coordinated benzene hydrate (97),  $pK_R$ , was estimated to be  $9.87 \pm 0.36$ , in Section 2.1.1. The implication is that an equilibrium exists between the coordinated cation and hydrate species in the region of the pH profile around pH 10. In the pH range from 8 to 10, a pH independent reaction takes place that involves ionisation of the coordinated hydrate (97) to give the coordinated cyclohexadienyl cation (96). Water is the predominant reacting species. The rate law for this region is given in Equation 2.13.

$$k_{\text{obs}} = k_o \quad (2.13)$$

(v) pH > 10

Above pH 10, the coordinated cation species (96) undergoes a hydroxide ion promoted reaction to form the coordinated hydrate (97). Equation 2.14 describes the rate law for formation of the hydrate species above pH 10.

$$k_{\text{obs}} = k_{\text{OH}} [\text{OH}^-] \quad (2.14)$$

A rate equation which describes reactions over the entire pH range of the profile is produced by combining Equations 2.7, 2.10, 2.12, 2.13 and 2.14 to give the rate law 2.15.

$$k_{\text{obs}} = k_2[\text{H}^+] + \{k_1K_a[\text{H}^+]\} / \{K_a + [\text{H}^+]\} + k_o + k_{\text{OH}}[\text{OH}^-] \quad (2.15)$$

In Table 2.9, rate constants are presented for the limiting pH-dependent and pH-independent regions of the pH profile.

**Table 2.9** Rate constants obtained from the pH-independent and pH-dependent regions of the pH-profile for the reaction of ( $\eta^5$ -cyclohexadienyl)dicarbonyltriphenylphosphineiron cation.

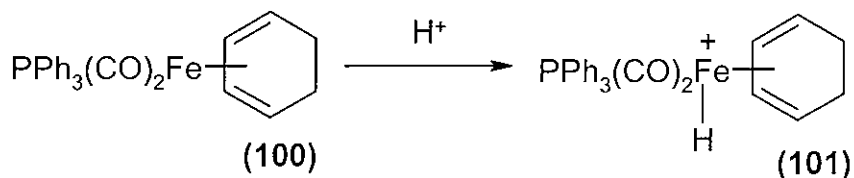
pH Range	pH-Dependence	Rate Expression	Rate Constant ( $\text{M}^{-1} \text{s}^{-1}$ )
<4	$\text{H}^+$	$k_2[\text{H}^+]$	8.2
4 – 6	$\text{H}_2\text{O}$	$k_1K_a^{\text{a,b}}$	$1.3 \times 10^3$
6 – 8	$\text{H}^+$	$k_1[\text{H}^+]$	$3.6 \times 10^3$
8 – 10	$\text{H}_2\text{O}$	$k_o$	$3.1 \times 10^{-4} \text{ s}^{-1}$
>10	$\text{OH}^-$	$k_{\text{OH}}[\text{OH}^-]$	2.1

(a) The rate expression obtained from the pH profile is  $1.28 \times 10^{-3} \text{ s}^{-1}$ . (b) The  $\text{p}K_a$  for the protonated iron complex (98) in Scheme 2.2 was estimated to be 6.0 from the point of inflection on the pH profile.

### 2.1.5 Evidence for Formation of the Metal Protonated Species

In Figure 3.1, a downward bend is observed in the pH-profile at a pH of 6. A downward bend on a pH-profile can be indicative of either a change in rate limiting step in the observed reaction mechanism or a substrate titration.<sup>81</sup> It has been reported in the literature that metal hydrides such as  $\text{HMn}(\text{CO})_5$  and  $\text{H}_2\text{Fe}(\text{CO})_4$  have  $\text{p}K_a$  values of between 4 and 7.<sup>82</sup> A characteristic of metal hydride complexes is a large high-field  $^1\text{H}$  NMR shift for the signal produced by the proton attached to the metal.<sup>82</sup>

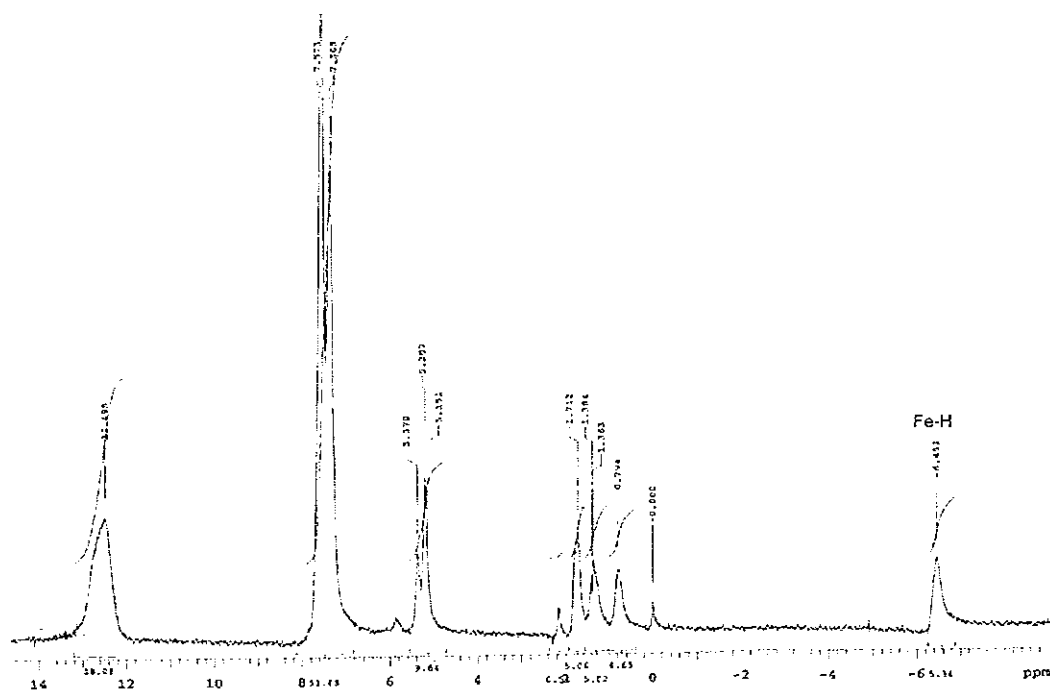
In Scheme 2.2, it is shown that the proposed mechanism involves protonation of the neutral coordinated hydrate (97) at iron. It was not possible to produce a sample of this iron protonated species for  $^1\text{H}$  NMR analysis. Therefore, it was decided to check to see if NMR studies could be performed on the neutral complex (100) to see if formation of a metal hydride (protonation at iron) occurred under acidic conditions.



**Scheme 2.3 Protonation at iron of the neutral complex ( $\eta^4$ -cyclohexa-1,3-diene)dicarbonyltriphenylphosphineiron.**

#### 2.1.5.1 $^1\text{H}$ NMR Spectroscopic Data

A  $^1\text{H}$  NMR signal in the range -5 to -15 ppm is expected for the proton attached to the iron atom in a metal hydride.<sup>82</sup> A  $^1\text{H}$  NMR spectrum of the neutral complex, ( $\eta^4$ -cyclohexa-1,3-diene)dicarbonyltriphenylphosphineiron (100), in deuterated chloroform was recorded using an increased scanning width to ensure that no signals were present in this region. One drop of trifluoroacetic acid was then added to the NMR tube and the solution was shaken vigorously. A solution colour change from yellow to orange was noted. When a  $^1\text{H}$  NMR spectrum of this acidified solution was recorded, a signal had appeared at -6.45 ppm as can be seen in Figure 2.9. An attempt was made to monitor the formation of this signal but it was not successful. The main problem encountered was locking the solvent signal of the sample. Locking this signal can be time consuming when metals are present in the sample due to the effect a metal can have on the spectrometer's magnet. This delay resulted in the hydride signal being fully formed by the time the spectrum was recorded. As an alternative, IR spectroscopy was then used in order to attempt to monitor the progress of the reaction.



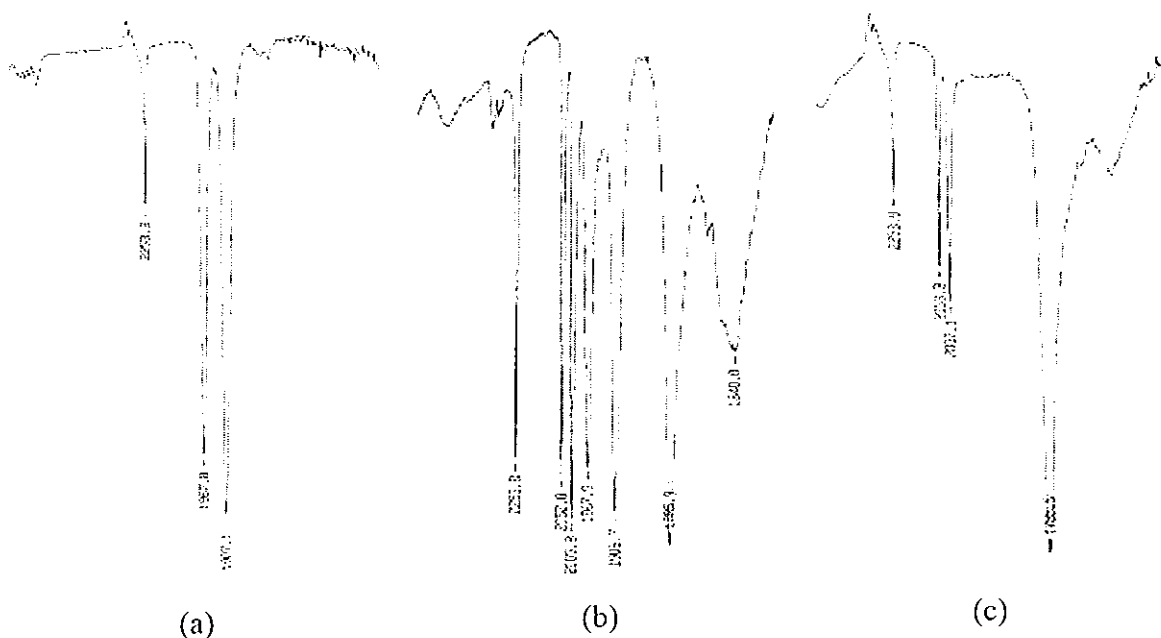
**Figure 2.9** Iron hydride signal at -6.45 ppm in the <sup>1</sup>H NMR spectrum of ( $\eta^4$ -cyclohexa-1,3-diene)dicarbonyltriphenylphosphineiron (100) to which trifluoroacetic acid has been added.

#### 2.1.5.2 IR Spectroscopic Data

IR spectroscopy is ideal for monitoring reactions which involve formation, loss or changes to carbonyl groups, due to their intense absorption in the IR region between 1600 and 2100  $\text{cm}^{-1}$ . For iron carbonyl compounds, an increase in frequency of the carbonyl absorption bands is noted when a conversion from a neutral to a charged species occurs.<sup>52</sup> This change in the carbonyl absorption bands would be expected to occur for the reaction presented in Scheme 2.3.

The neutral ( $\eta^4$ -cyclohexa-1,3-diene)dicarbonyltriphenylphosphineiron complex was dissolved in the minimum volume of chloroform and an IR spectrum was obtained by preparing a thin film of a neat sample of the solution on calcium fluoride plates. Some trifluoroacetic acid (TFA) was dissolved in chloroform and added drop wise to the sample solution. An IR spectrum of the solution was run after each addition

of TFA. The IR spectra obtained are displayed in Figure 2.10 and the data are summarised in Table 2.10.



**Figure 2.10** IR spectra obtained when monitoring the formation of the iron-hydride bond by following changes in the carbonyl absorption bands on addition of TFA to a solution of (100). Spectra (a), (b) and (c) represent the neutral complex (100), a mixture of the neutral (100) and protonated complexes (101) and the fully formed protonated species (101) respectively.

**Table 2.10** IR spectra obtained on addition of TFA to (100). Spectra (a), (b) and (c) represent the neutral complex (100), a mixture of the neutral and protonated (101) complexes and the fully formed protonated species respectively.

Solution	Carbonyl Stretch Absorption Bands (cm <sup>-1</sup> )	Assignment	Reference
(100) in chloroform	1968, 1907	Complex (100)	Figure 2.10 (a)
(100) in chloroform + 2 drops of TFA solution	2052, 2005 1968, 1907 1785	Complex (101) Complex (100) Trifluoroacetic Acid	Figure 2.10 (b)
(100) in chloroform + 6 drops of TFA solution	2052, 2005 1785	Complex (101) Trifluoroacetic Acid	Figure 2.10 (c)

In Figure 2.10(a), two carbonyl absorption bands at 1968 and 1907 cm<sup>-1</sup> are visible on the spectrum which are due to the carbonyl groups of the neutral complex (100). On addition of TFA, giving a solution containing approximately 10% TFA, the intensity of these two bands are observed to decrease whilst three new carbonyl absorption bands appear, as can be seen in Figure 2.10(b). The three new bands are at 2052, 2005 and 1785 cm<sup>-1</sup> respectively. The absorption bands at 2052 and 2205 cm<sup>-1</sup> are due to the carbonyl groups of the charged complex (101) which are found at a higher frequency than the neutral complex (100), as previously noted for similar complexes by Birch.<sup>52</sup> The carbonyl absorption band at 1785 cm<sup>-1</sup> is due to the TFA. On addition of more TFA, increasing the concentration in the sample solution to approximately 20%, complete conversion of (100) to (101) has occurred, noted by the disappearance of the

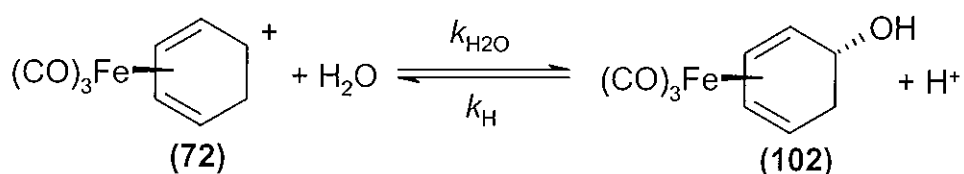
absorption bands at 1968 and 1907  $\text{cm}^{-1}$ . The carbonyl absorption bands (2052 and 2205  $\text{cm}^{-1}$ ) of the charged complex have subsequently increased in intensity.

## 2.2 ( $\eta^5$ -Cyclohexadienyl)tricarbonyliron Cation - Hydrolysis Reaction

Rates and equilibria for hydrolysis of the ( $\eta^5$ -cyclohexadienyl)tricarbonyliron cation (**72**) to its hydrate analogue (**102**), shown in Scheme 2.4, have been studied. Measurements include:

- $pK_R$  for the hydrolysis of this coordinated cation to the hydrate determined by both kinetic and equilibrium methods
- measurement of a kinetic isotope effect for hydrolysis of the coordinated cation and determination of  $pK_R$  in deuterated solutions.
- rate constants for the base catalysed hydrolysis of the ( $\eta^5$ -cyclohexadienyl)tricarbonyliron cation.
- rate constants for the acid catalysed ionisation of ( $\eta^4$ -*exo*-5-hydroxycyclohexa-1,3-diene)tricarbonyliron.

A pH profile has been constructed from this data. In addition a  $^1\text{H}$  NMR study was carried out to investigate whether the UV-Vis spectrophotometry changes track those observed by NMR.



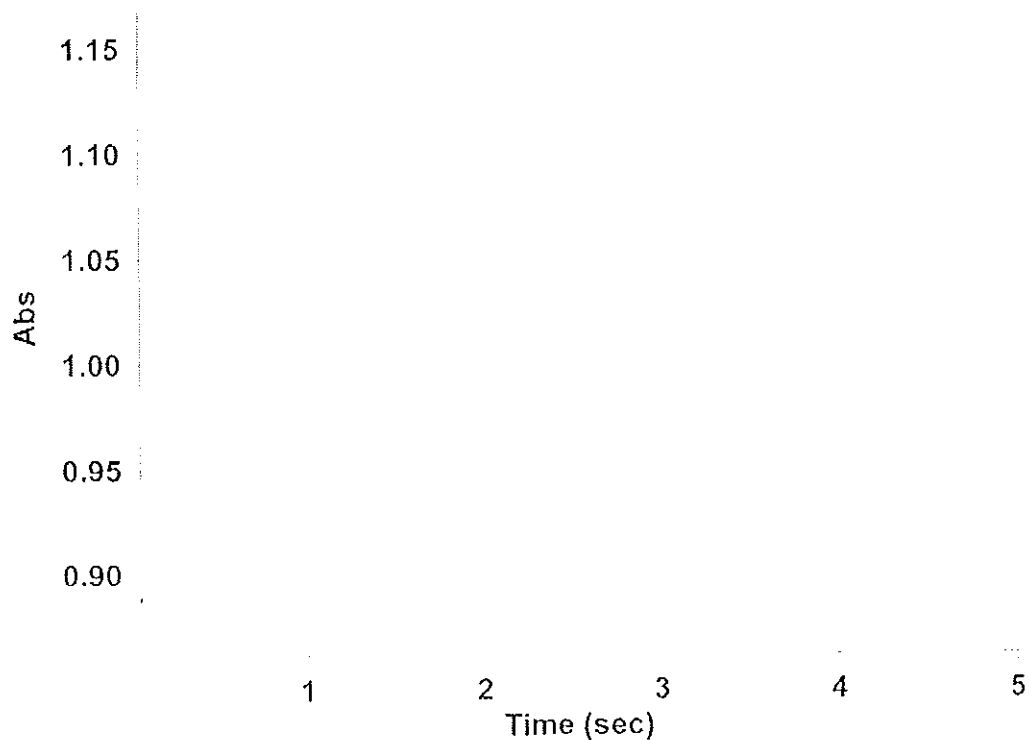
Scheme 2.4



### 2.2.1 *Rate Constants for Hydrolysis Below pH 8*

The results measured in the pH range from 3 to 8 showed no buffer catalysis and were found to be reversible. These findings are consistent with the hydrolysis reaction and will be presented first. By contrast, above pH 8, in borate and carbonate buffers, strong buffer catalysis consistent with reaction with the buffer was observed and the reactions were not reversible. For this reason, the results for these more basic buffers will be dealt with after those between pH 4 to 8.

As the reaction was too fast to measure by injecting the substrate into a UV cell containing aqueous buffer and monitoring the absorbance change, the rate of hydrolysis of the ( $\eta^5$ -cyclohexadienyl)tricarbonyliron cation (**72**) was determined using a rapid mixing accessory. Kinetic data was obtained in aqueous cacodylate, phosphate, acetate, borate and carbonate buffers as well as hydroxide solutions. The substrate injection syringe on the fast mixing accessory was filled with the required amount of the ( $\eta^5$ -cyclohexadienyl)tricarbonyliron cation solution (made up in either acetonitrile or water as its tetrafluoroborate salt) together with a little dilute acid to ensure the substrate remained in its cationic form. The second syringe contained a buffer solution with an excess of buffer base. After mixing, an increase in absorbance at 250 nm was monitored and an example of a kinetic scan observed is shown in Figure 2.11.



**Figure 2.11** A kinetic scan observed at 250 nm using a fast mixing apparatus for the hydrolysis of ( $\eta^5$ -cyclohexadienyl)-tricarbonyliron in aqueous borate buffer of pH 9.23 at 25°C with a substrate concentration of  $2.0 \times 10^{-5}$  M and ionic strength of 0.1 M.

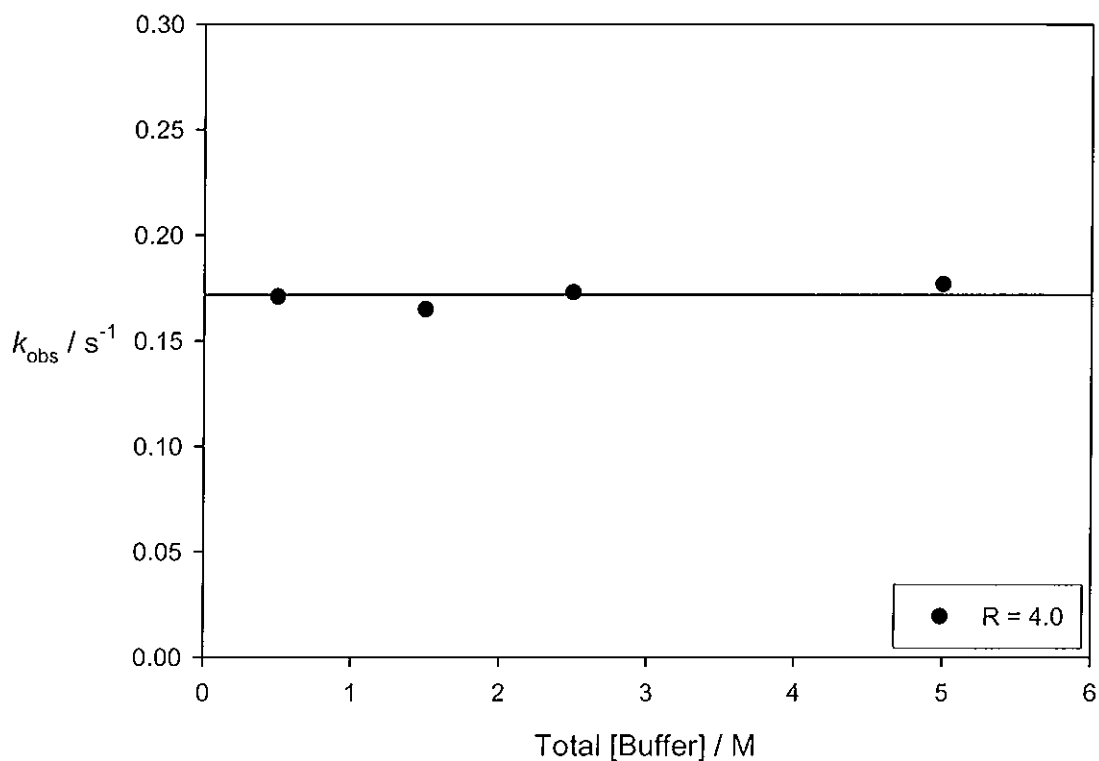
#### Reaction in Cacodylate Buffers

The observed rate constants for the hydrolysis of ( $\eta^5$ -cyclohexadienyl)tricarbonyliron (**72**) in a range of aqueous cacodylate buffers is presented in Table 2.11. A check for buffer catalysis was carried out at a buffer ratio of 4.0 and a plot of the observed rate constants against total buffer concentration is shown in Figure 2.12.

**Table 2.11** First order rate constants for the hydrolysis of ( $\eta^5$ -cyclohexadienyl)tricarbonyliron (72) in aqueous cacodylate buffers at 25°C.<sup>a</sup>

pH	R <sup>b</sup>	10 <sup>2</sup> [(CH <sub>3</sub> ) <sub>2</sub> AsO <sub>2</sub> <sup>-</sup> ]/M	10 <sup>2</sup> [(CH <sub>3</sub> ) <sub>2</sub> AsO <sub>2</sub> H]/M	<i>k</i> <sub>obs</sub> /s <sup>-1</sup>
6.76	4.0	4.0	1.0	0.177
6.76	4.0	2.0	0.50	0.173
6.76	4.0	1.2	0.30	0.165
6.76	4.0	0.4	0.10	0.171
6.34	1.5	0.60	0.40	0.180
6.09	0.66	0.40	0.60	0.174
5.98	0.43	0.30	0.70	0.180
5.56	0.25	0.20	0.80	0.190

(a) Measurements were made at 250 nm with a substrate concentration of  $2.0 \times 10^{-5}$  M and ionic strength 0.1 M, using a fast mixing apparatus. (b) [buffer base] / [buffer acid].



**Figure 2.12** Plot of first order rate constants against total buffer concentration at a fixed buffer ratio of 4.0 for the hydrolysis of ( $\eta^5$ -cyclohexadienyl)tricarbonyliron (72) in aqueous cacodylate buffers at 25°C.

A straight line of zero slope confirms the absence of general base or acid catalysis. As no buffer catalysis was observed when the buffer ratio  $R = [\text{buffer base}] / [\text{buffer acid}]$  was 4.0, buffer solutions prepared with other buffer ratios were not investigated to check for buffer catalysis. The pH independent rate constant for pH 6.76 is  $0.171 \pm 0.004 \text{ s}^{-1}$ .

### Reaction in Phosphate Buffers

Rate constants for the hydrolysis of ( $\eta^5$ -cyclohexadienyl)tricarbonyliron (72) in aqueous phosphate buffers were also measured. First order rate constants for this reaction are presented in Table 2.12. For the two buffer concentrations examined at a buffer ratio of  $R=1.0$ , the similarity between the observed rate constants led to the conclusion that general acid or base catalysis was not occurring.

**Table 2.12** First order rate constants for the hydrolysis of ( $\eta^5$ -cyclohexadienyl)tricarbonyliron in aqueous phosphate buffers at 25°C.<sup>a</sup>

pH	R <sup>b</sup>	[HPO <sub>4</sub> <sup>2-</sup> ]/M	[H <sub>2</sub> PO <sub>4</sub> <sup>-</sup> ]/M	<i>k</i> <sub>obs</sub> /s <sup>-1</sup>
7.80	4.0	0.032	0.008	0.200
7.20	1.0	0.020	0.020	0.179
7.20	1.0	0.004	0.004	0.169

(a) Measurements were made at 250 nm with a substrate concentration of  $2.0 \times 10^{-5}$  M and ionic strength 0.1 M, using a fast mixing apparatus. (b) [buffer base] / [buffer acid].

The average rate constant when the buffer ratio is 1.0 is  $0.174 \text{ s}^{-1}$ .

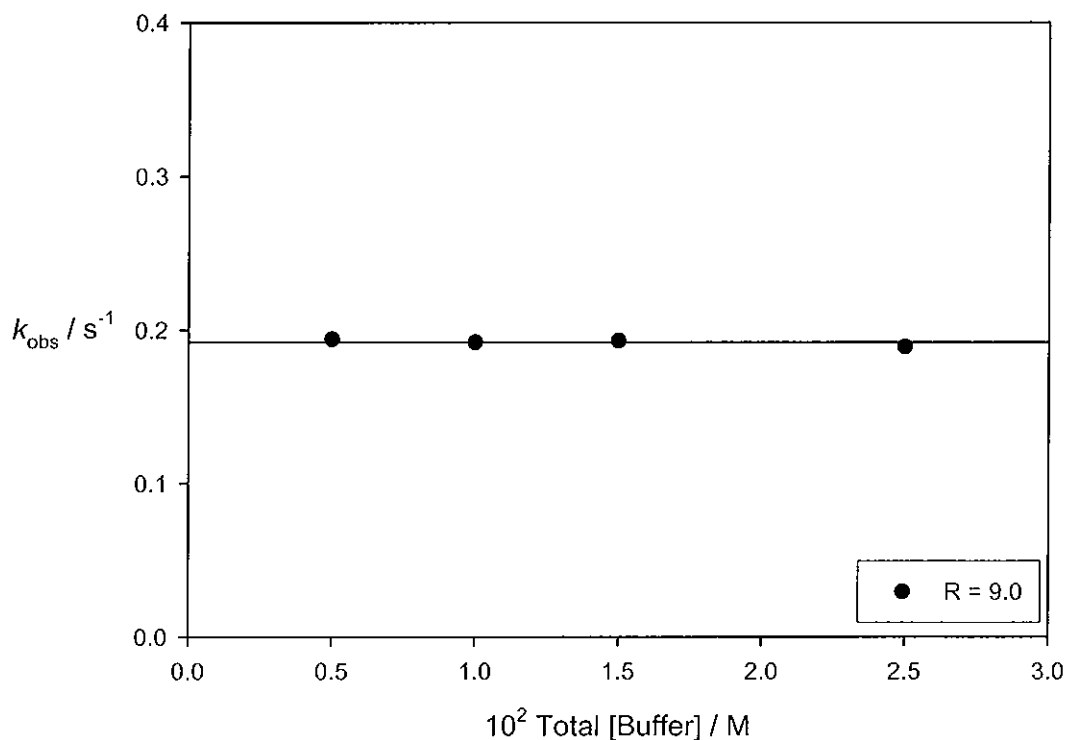
### Reaction in Acetate Buffers

The first order rate constants observed when the hydrolysis of ( $\eta^5$ -cyclohexadienyl)tricarbonyliron (72) was investigated in a number of aqueous acetate buffer solutions are presented in Table 2.13. The first order rate constants when the buffer ratio,  $R = [\text{buffer base}] / [\text{buffer acid}]$  was 9.0 are plotted against total buffer concentration in Figure 2.13.

**Table 2.13** First order rate constant for the hydrolysis of ( $\eta^5$ -cyclohexadienyl)tricarbonyliron in aqueous acetate buffers at 25°C.<sup>a</sup>

pH	R <sup>b</sup>	10 <sup>2</sup> [CH <sub>3</sub> CO <sub>2</sub> <sup>-</sup> ] /M	10 <sup>2</sup> [CH <sub>3</sub> CO <sub>2</sub> H] /M	<i>k</i> <sub>obs</sub> /s <sup>-1</sup>
5.60	9.0	2.25	0.25	0.189
5.60	9.0	1.35	0.15	0.193
5.60	9.0	0.90	0.10	0.192
5.60	9.0	0.45	0.05	0.194
5.25	4.0	0.80	0.20	0.212
4.83	1.5	0.60	0.40	0.285
4.47	0.66	0.40	0.60	0.421
4.04	0.25	0.20	0.80	0.991

(a) Measurements were made at 250 nm with a substrate concentration of  $2.0 \times 10^{-5}$  M and ionic strength 0.1 M, with a fast mixing apparatus. (b) [buffer base] / [buffer acid].



**Figure 2.13** Plot of first order rate constants against total buffer concentration at a fixed buffer ratio of 9.0 for the hydrolysis of ( $\eta^5$ -cyclohexadienyl)tricarbonyliron (72) in aqueous acetate buffers at 25°C.

In acetate buffers the straight line of zero slope observed for the plot of observed rate constants against buffer concentration at constant buffer ratio in Figure 2.13 again shows that no general acid or base catalysis is occurring. As no catalysis was observed at a buffer ratio of 9.0, measurements made at other acetate buffer ratios were not checked for catalysis. A single measurement was made at all other buffer ratios. The pH independent rate constant for pH 5.6 is  $0.192 \pm 0.001 \text{ s}^{-1}$ .

### 2.2.2 Ionisation of ( $\eta^4$ -*exo*-5-hydroxy-1,3-cyclohexadiene)tricarbonyliron

The absorbance change observed at higher pHs began to decrease as the acetate buffers became more acidic. This decrease in absorbance change is ascribed to an incomplete conversion of the coordinated cyclohexadienyl cation to its hydrate analogue occurring as the  $pK_R$  for the formation of the coordinated hydrate was approached. To maximise the absorbance change observed, further results were obtained by monitoring the reaction in the reverse direction *i.e.* ionisation of the coordinated hydrate to give the coordinated cation

Rate constants for the ionisation of ( $\eta^4$ -*exo*-5-hydroxy-1,3-cyclohexadiene)tricarbonyliron (**102**) to give the coordinated cation were measured in aqueous acetate and methoxyacetate buffers. The equilibrium between the two species is shown in Scheme 2.4 (Section 2.2). The coordinated arene hydrate was generated as a reactant by dissolving the ( $\eta^5$ -cyclohexadienyl)tricarbonyliron (**72**) substrate in water and injecting this solution into a dilute cacodylate buffer solution in the substrate syringe of the UV-Vis spectrophotometer fast mixing accessory. The pH of the cacodylate buffer was sufficiently high to ensure that all of the coordinated cation was converted to the coordinated arene hydrate. This solution of coordinated arene hydrate was quenched into various methoxyacetate and acetate buffers and the formation of the ( $\eta^5$ -cyclohexadienyl)tricarbonyliron cation was monitored by following a decrease in absorbance at 240 nm. The concentration of these buffers was much greater than that of the cacodylate buffer in the substrate syringe.

#### Reaction in Methoxyacetate Buffers

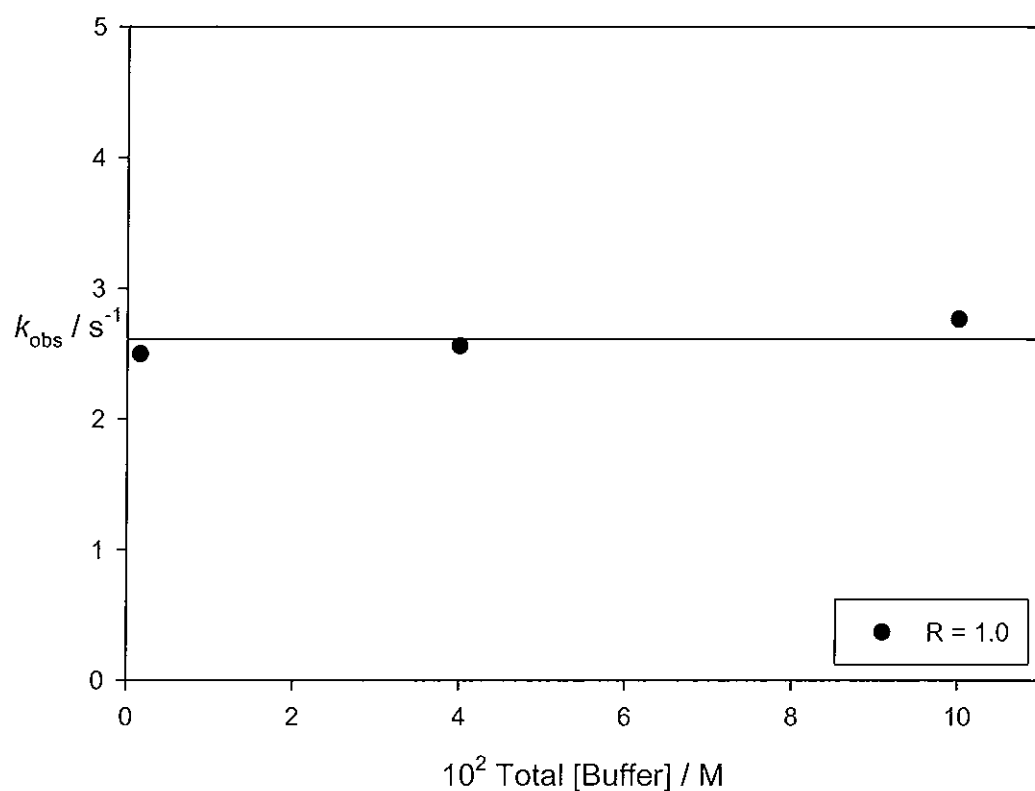
Table 2.14 shows first order rate constants for the ionisation of ( $\eta^4$ -*exo*-5-hydroxy-1,3-cyclohexadiene)tricarbonyliron in aqueous methoxyacetate buffer solutions. Figure 2.14 displays a plot of first order rate constants against total buffer concentration for a [buffer base] / [buffer acid] ratio of 1.0. Again there is no indication of buffer catalysis and the average rate constant is  $2.61 \pm 0.11 \text{ s}^{-1}$ .



**Table 2.14** First order rate constants for the ionisation of ( $\eta^4$ -*exo*-5-hydroxy-1,3-cyclohexadiene)tricarbonyliron (102) in aqueous methoxyacetate buffers at 25°C.<sup>a</sup>

pH	R <sup>b</sup>	10 <sup>2</sup> [CH <sub>3</sub> OCH <sub>2</sub> CO <sub>2</sub> <sup>-</sup> ] /M	10 <sup>2</sup> [CH <sub>3</sub> OCH <sub>2</sub> CO <sub>2</sub> H] /M	<i>k</i> <sub>obs</sub> /s <sup>-1</sup>
4.27	5.0	5.0	1.0	0.701
3.79	1.7	5.0	3.0	1.80
3.57	1.0	5.0	5.0	2.77
3.57	1.0	2.0	2.0	2.56
3.57	1.0	0.80	0.80	2.50

(a) Measurements were made at 240 nm with a substrate concentration of  $2.0 \times 10^{-5}$  M and ionic strength 0.1 M, using a fast mixing apparatus. (b) [buffer base] / [buffer acid].



**Figure 2.14** Plot of first order rate constants against total buffer concentration at a fixed buffer ratio of 1.0 for the ionisation of ( $\eta^4$ -*exo*-5-hydroxy-1,3-cyclohexadiene)tricarbonyliron (**102**) in aqueous methoxyacetate buffers at 25°C.

#### Reaction in Acetate Buffers

Rate constants for the ionisation of ( $\eta^4$ -*exo*-5-hydroxy-1,3-cyclohexadiene)tricarbonyliron (**102**) in aqueous acetate buffers are presented in Table 2.15. As general acid or base catalysis was not observed for the hydrolysis reaction in acetate buffers which had been examined previously (see Table 2.13), a check for buffer catalysis was not undertaken for the ionisation reaction in acetate buffers.

**Table 2.15** First order rate constants for the ionisation of ( $\eta^4$ -*exo*-5-hydroxy-1,3-cyclohexadiene)tricarbonyliron in aqueous acetate buffers at 25°C.<sup>a</sup>

pH	R <sup>b</sup>	[CH <sub>3</sub> OCH <sub>2</sub> CO <sub>2</sub> <sup>-</sup> ]/M	[CH <sub>3</sub> OCH <sub>2</sub> CO <sub>2</sub> H]/M	$k_{\text{obs}}/\text{s}^{-1}$
4.65	1.0	0.025	0.025	0.346
3.99	0.25	0.010	0.040	1.01

(a) Measurements were made at 240 nm with a substrate concentration of  $2.0 \times 10^{-5}$  M and ionic strength 0.1 M, using a fast mixing apparatus. (b) [buffer base] / [buffer acid].

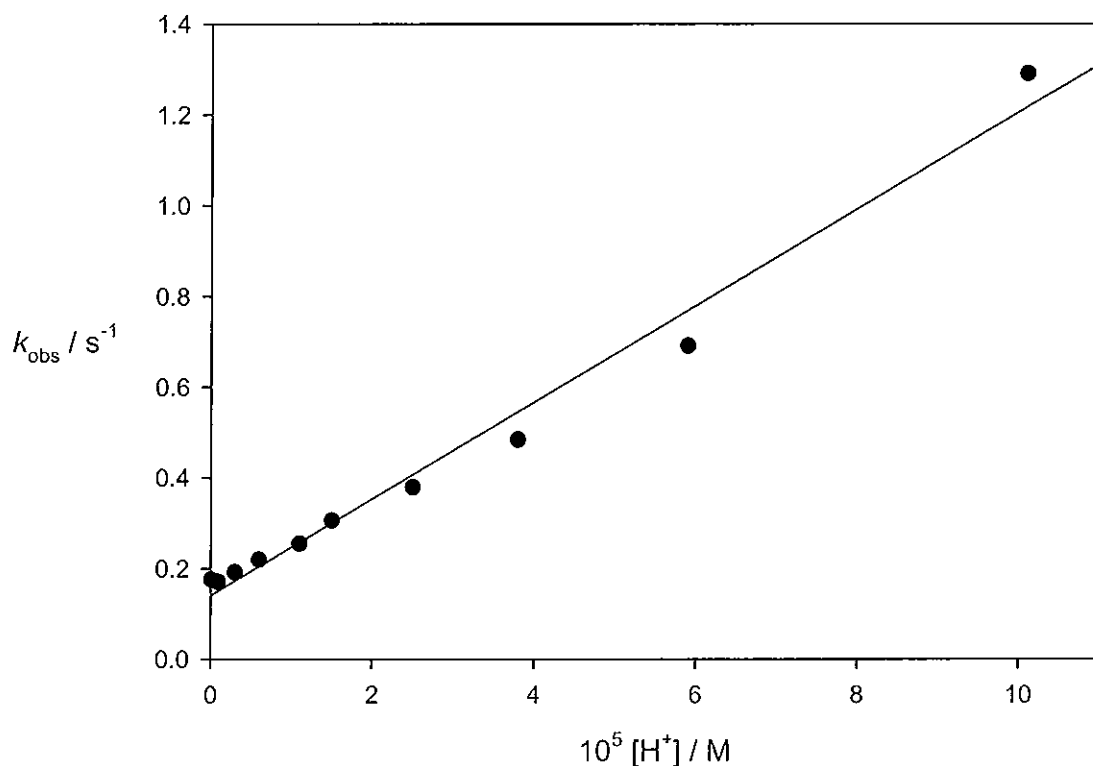
### 2.2.3 Kinetic Determination of $pK_R$ for ( $\eta^4$ -*Exo*-5-hydroxy-1,3-cyclohexadiene)tricarbonyliron

The equilibrium constant,  $K_R$ , can be determined kinetically as a ratio of rate constants for hydrolysis and ionisation reactions, *i.e.*  $K_R = k_{\text{H}_2\text{O}}/k_{\text{H}}$ . For coordinated cyclohexadienyl cations such as (72),  $k_{\text{H}_2\text{O}}$  is determined from the reaction of the coordinated cation with water. From the results of the investigation of the effect of changing pH on the equilibrium between the coordinated cation (72) and the coordinated hydrate (102) which was monitored by changes in absorbance, the  $pK_R$  value was found to be 4.77 (these results are presented in Section 2.2.9, page 95). This implied that the  $pK_R$  could be determined kinetically in a range of mildly acidic buffer solutions (pH 4 to 6). A determination of the  $pK_R$  was then carried out by both kinetic and spectroscopic means in aqueous and deuterated solutions one after the other to allow for a direct comparison to be made between the data obtained. In Table 2.16, the observed rate constants for the hydrolysis of ( $\eta^5$ -cyclohexadienyl)tricarbonyliron (72) in aqueous acetate, cacodylate and phosphate buffers are presented. These rate constants are plotted against hydrogen ion concentration in Figure 2.15.

**Table 2.16** First order rate constants for the hydrolysis of the ( $\eta^5$ -cyclohexadienyl)tricarbonyliron cation (72) in aqueous acetate, cacodylate and phosphate buffers at 25°C.<sup>a</sup>

pH	R <sup>b</sup>	10 <sup>5</sup> [H <sup>+</sup> ]/M	<i>k</i> <sub>obs</sub> /s <sup>-1</sup>
8.10	2.3	0.01	0.176
6.10	1.0	0.09	0.171
5.43	0.11	0.3	0.192
5.13	0.25	0.6	0.220
4.91	0.40	1.1	0.255
4.73	0.66	1.5	0.306
4.56	1.0	2.5	0.379
4.37	1.5	3.8	0.484
4.18	2.3	5.9	0.691
3.92	4.0	10.1	1.29

(a) Measurements were made at 250 nm with a substrate concentration of  $2.0 \times 10^{-4}$  M and ionic strength 0.1 M. (b) [buffer acid] / [buffer base].



**Figure 2.15** Plot of first order rate constants against  $[\text{H}^+]$  for the hydrolysis of  $(\eta^5\text{-cyclohexadienyl})\text{tricarbonyliron}$  (72) in aqueous acetate, cacodylate and phosphate buffers at 25°C.

The straight line plot observed in Figure 2.15 is summarised in Equation 2.17 based on Equation 2.16.  $K_{\text{R}} = k_{\text{H}_2\text{O}} / k_{\text{H}} = 0.140 \text{ s}^{-1} / 1.07 \times 10^4 \text{ s}^{-1} = 1.31 \times 10^{-5}$  and thus a value of  $\text{p}K_{\text{R}} = 4.87$  is obtained using this method.

$$k_{\text{obs}} = k_{\text{H}}[\text{H}^+] + k_{\text{H}_2\text{O}} \quad (2.16)$$

$$k_{\text{obs}} = (1.07 \pm 0.02) \times 10^4 \text{ M}^{-1} \text{ s}^{-1} [\text{H}^+] + 0.140 \pm 0.004 \text{ s}^{-1} \quad (2.17)$$

#### 2.2.4 Spectroscopic Determination of $\text{p}K_{\text{R}}$ for $(\eta^4\text{-Exo-5-hydroxy-1,3-cyclohexadiene})\text{tricarbonyliron}$

The  $\text{p}K_{\text{R}}$  value obtained from Figure 2.15 can be verified by determining the  $\text{p}K_{\text{R}}$  using a spectroscopic method. Table 2.17 presents absorbance changes observed while monitoring the hydrolysis of  $(\eta^5\text{-cyclohexadienyl})\text{tricarbonyliron}$  in aqueous acetate, cacodylate and phosphate buffers. The absorbance change reported is the difference between the final absorbance and initial absorbance for a kinetic scan at 250

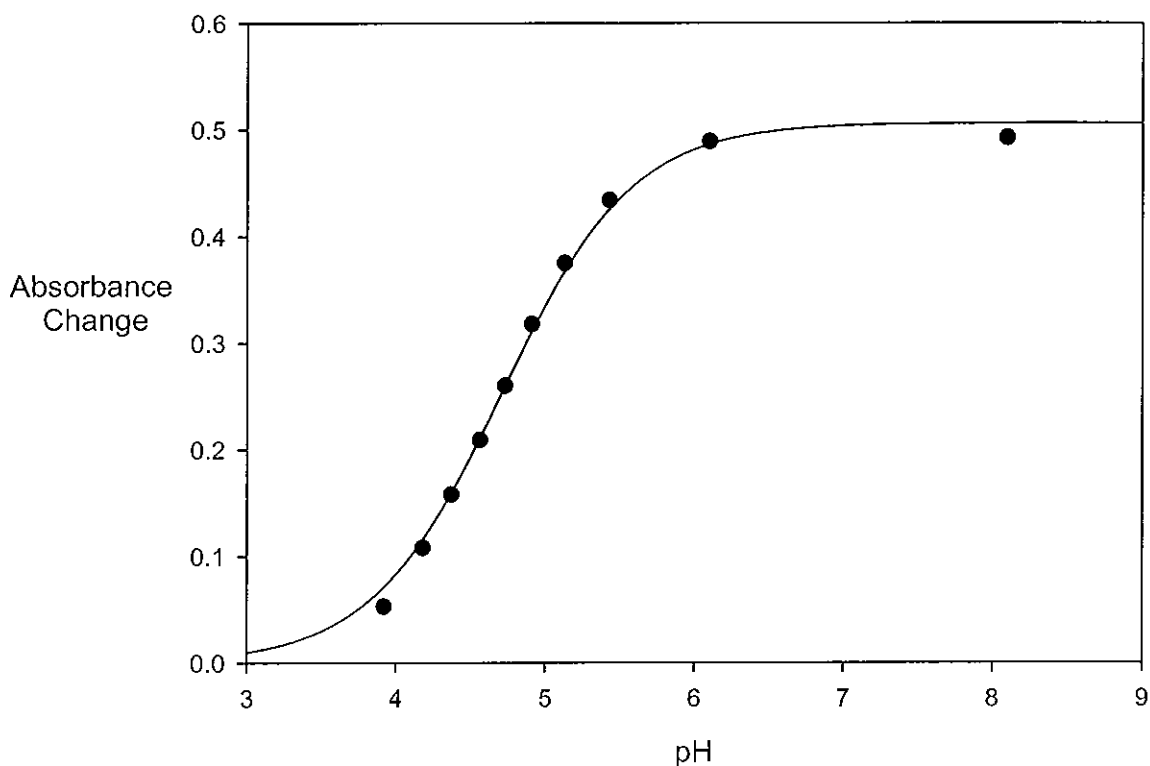
nm. An example of a kinetic scan was shown previously in Figure 2.11. Figure 2.16 is a plot of absorbance change against pH. The inflection point on the curve represents the equilibrium constant. The best fit line to the data points in Figure 2.16 was fitted using Equation 2.18. (Refer to Section 4.6.2 for more detail about Equation 2.18).

$$\Delta\text{Abs} = A_{\infty} \times \{K_R / (K_R + [\text{H}^+])\} \quad (2.18)$$

**Table 2.17**      **Absorbance measurements for the hydrolysis of the ( $\eta^5$ -cyclohexadienyl)tricarbonyliron cation in aqueous acetate, cacodylate and phosphate buffers.<sup>a</sup>**

pH	R <sup>b</sup>	Absorbance Change
8.10	0.43	0.492
6.10	1.0	0.489
5.43	9.0	0.434
5.13	4.0	0.375
4.91	2.3	0.318
4.73	1.5	0.260
4.56	1.0	0.209
4.37	0.66	0.158
4.18	0.43	0.108
3.92	0.25	0.053

(a) Measurements were made at 250 nm with a substrate concentration of  $2 \times 10^{-4}$  M and ionic strength 0.1 M. (b) [buffer base] / [buffer acid]

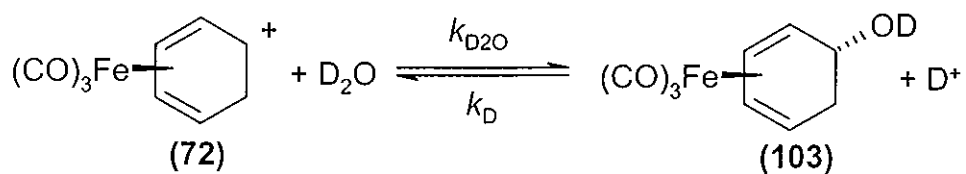


**Figure 2.16** Plot of absorbance change against pH for the hydrolysis of ( $\eta^5$ -cyclohexadienyl)tricarbonyliron (**72**) in aqueous acetate, cacodylate and phosphate buffers at 25°C.

The equilibrium constant,  $pK_R$ , determined from the inflection point on Figure 2.16, is equal to 4.71. This is in very close agreement with the equilibrium constant determined kinetically as described in Section 2.2.3.

### 2.2.5 Kinetic Determination of $pK_R$ for ( $\eta^4$ -Exo-5-hydroxy-1,3-cyclohexadiene)tricarbonyliron in $D_2O$

The equilibrium constant,  $pK_R$ , was measured in deuterated solutions by both kinetic and spectroscopic means. This allows the determination of equilibrium and kinetic isotope effects. The kinetic determination was carried out by measuring the observed rate constants for the hydrolysis of ( $\eta^5$ -cyclohexadienyl)tricarbonyliron (**72**) in acetate and cacodylate buffer solutions prepared in deuterium oxide. It can be seen from Scheme 2.5, that  $K_R = k_{D_2O}/k_D$ . Table 2.18 lists the observed rate constants for the hydrolysis of the coordinated cation (**72**) to the coordinated deuterated hydrate (**103**) and they are shown plotted against the deuterium ion concentration in Figure 2.17.



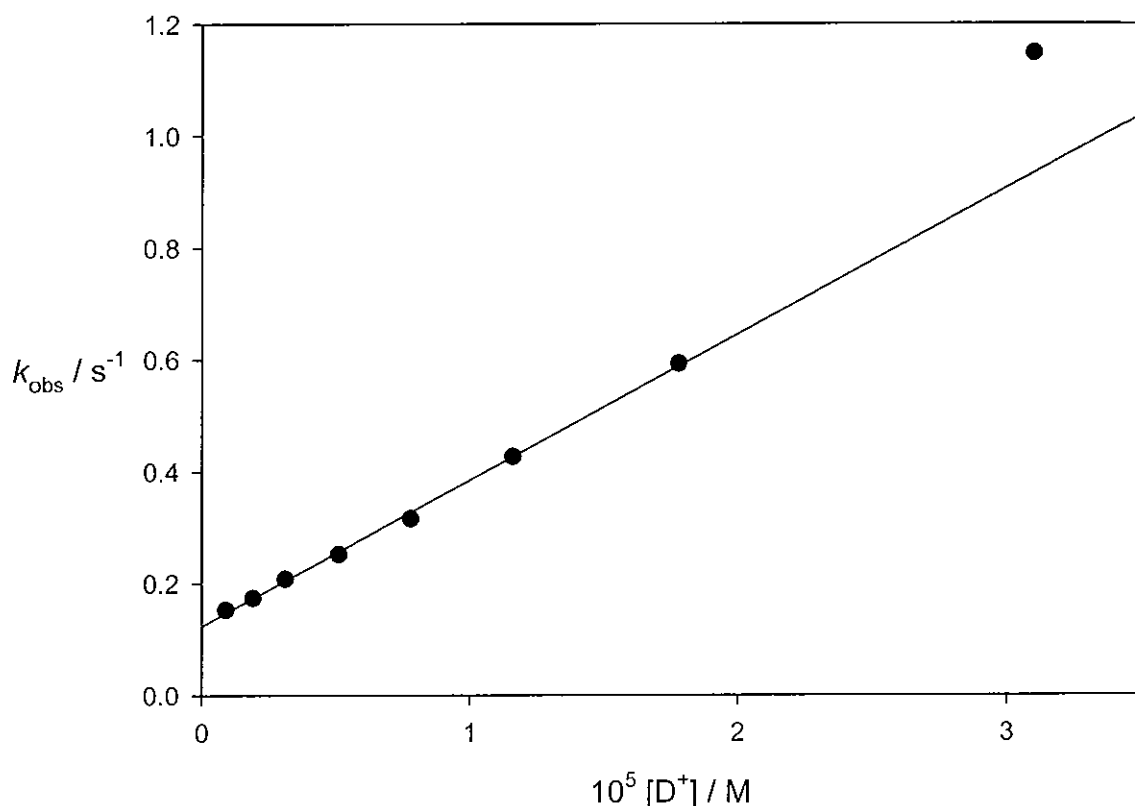
Scheme 2.5

**Table 2.18** First order rate constants for the hydrolysis of the ( $\eta^5$ -cyclohexadienyl)tricarbonyliron cation (72) in acetate and cacodylate buffer solutions prepared in deuterium oxide at 25°C.<sup>a</sup>

pD	R <sup>b</sup>	10 <sup>5</sup> [D <sup>+</sup> ]/M	k <sub>obs</sub> /s <sup>-1</sup>
5.90	0.11	0.09	0.153
5.61	0.25	0.19	0.174
5.40	0.40	0.31	0.208
5.21	0.66	0.51	0.252
5.04	1.0	0.78	0.316
4.86	1.5	1.16	0.427
4.66	2.3	1.78	0.593
4.32	4.0	3.10 <sup>c</sup>	1.147 <sup>c</sup>

(a) Measurements were made at 250 nm with a substrate concentration of  $2.0 \times 10^{-4}$  M and ionic strength 0.1 M. (b) [buffer acid] / [buffer base]. (c) This point was omitted when the straight line was plotted in Figure 2.17; see Appendix.





**Figure 2.17** Plot of first order rate constants against  $[D^+]$  for the hydrolysis of  $(\eta^5\text{-cyclohexadienyl})\text{tricarbonyliron}$  (72) in acetate and cacodylate buffer solutions prepared in deuterium oxide at  $25^\circ\text{C}$ .

The straight line plot observed in Figure 2.17 is summarised in Equation 2.20 based on Equation 2.19.  $K_R = k_{D2O} / k_D = 0.124 \text{ s}^{-1} / (2.61 \times 10^4) \text{ s}^{-1} = 4.75 \times 10^{-6}$ . Therefore  $pK_R = 5.32$ .

$$k_{obs} = k_D[D^+] + k_{D2O} \quad (2.19)$$

$$k_{obs} = (2.61 \pm 0.05) \times 10^4 \text{ s}^{-1} [D^+] + 0.124 \pm 0.004 \text{ s}^{-1} \quad (2.20)$$

The kinetic solvent isotope effect is calculated from  $k_D/k_H$  and this is equal to  $2.61 \times 10^4 \text{ s}^{-1} / 1.07 \times 10^4 \text{ s}^{-1} = 2.4$ . This is of the magnitude expected for hydrolysis of a carbocation.<sup>83</sup>

**2.2.6 Spectroscopic Determination of  $pK_R$  for ( $\eta^4$ -Exo-5-hydroxy-1,3-cyclohexadiene)tricarbonyliron in  $D_2O$**

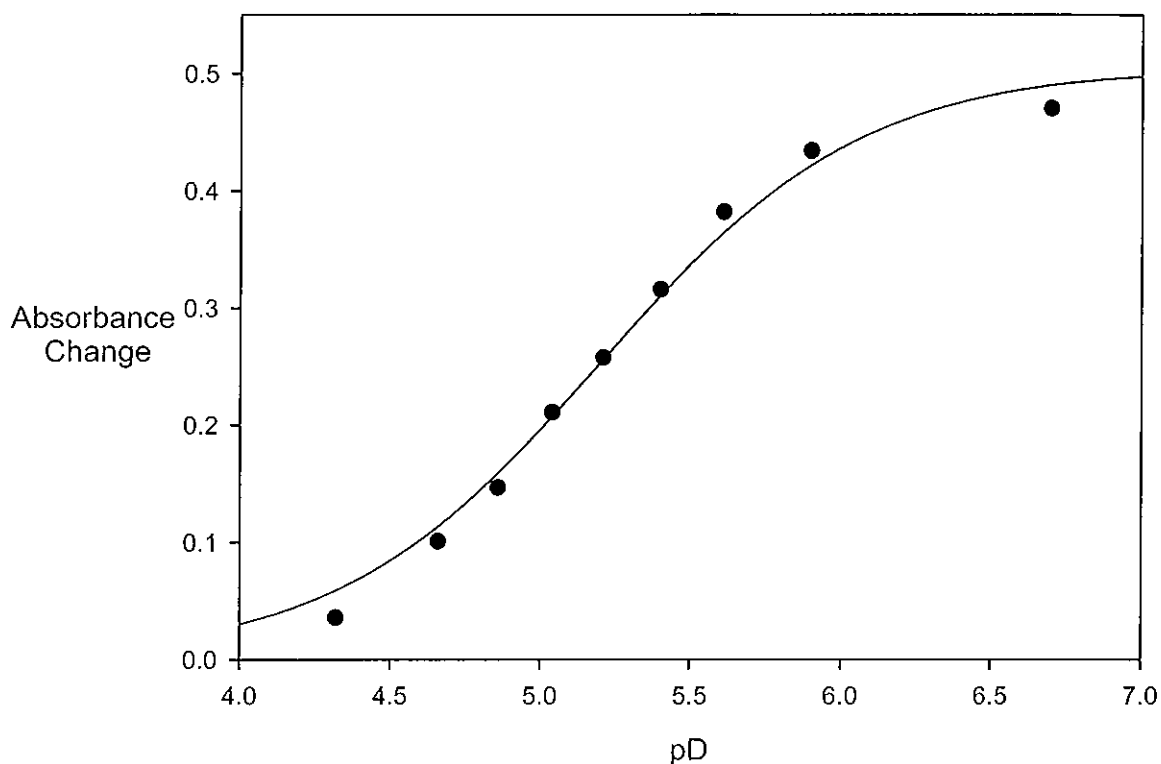
Acetate and cacodylate buffer solutions prepared in deuterium oxide were used to determine the equilibrium constant,  $pK_R$ , using a spectroscopic method. Table 2.19 records the difference ( $\Delta A$ ) between the final absorbance and initial absorbance at 250 nm for a kinetic measurement for the hydrolysis reaction of ( $\eta^5$ -cyclohexadienyl)tricarbonyliron (**72**). In Figure 2.18, this absorbance change is plotted against pD and the equilibrium constant  $pK_R$  corresponds to the point of inflection. The best fit of the line to the measured values of  $\Delta A$  in Figure 2.18 was obtained using Equation 2.21. (Refer to Section 4.6.2 for more detail about Equation 2.21).

$$\Delta \text{Abs} = A_\infty \times \{K_R / (K_R + [H^+])\} \quad (2.21)$$

**Table 2.19** Absorbance measurements for the hydrolysis of the ( $\eta^5$ -cyclohexadienyl)tricarbonyliron cation (**72**) in acetate and cacodylate buffer solutions prepared in deuterium oxide.<sup>a</sup>

pD	R <sup>b</sup>	Absorbance Change
6.70	1.0	0.470
5.90	9.0	0.434
5.61	4.0	0.382
5.40	2.3	0.316
5.21	1.5	0.258
5.04	1.0	0.211
4.86	0.66	0.147
4.66	0.43	0.101
4.32	0.25	0.036

(a) Measurements were made at 250 nm with a substrate concentration of  $2 \times 10^{-4}$  M and ionic strength 0.1 M. (b) [buffer base] / [buffer acid]



**Figure 2.18** Plot of absorbance change against pD for the hydrolysis of ( $\eta^5$ -cyclohexadienyl)tricarbonyliron in acetate and cacodylate buffer solutions prepared in deuterium oxide at 25°C.

The point of inflection on Figure 2.18, which represents the equilibrium constant  $pK_R$  in deuterated solutions, is 5.20. This value is in good agreement with the  $pK_R$  value of 5.32 obtained using a kinetic method in Section 2.2.6.

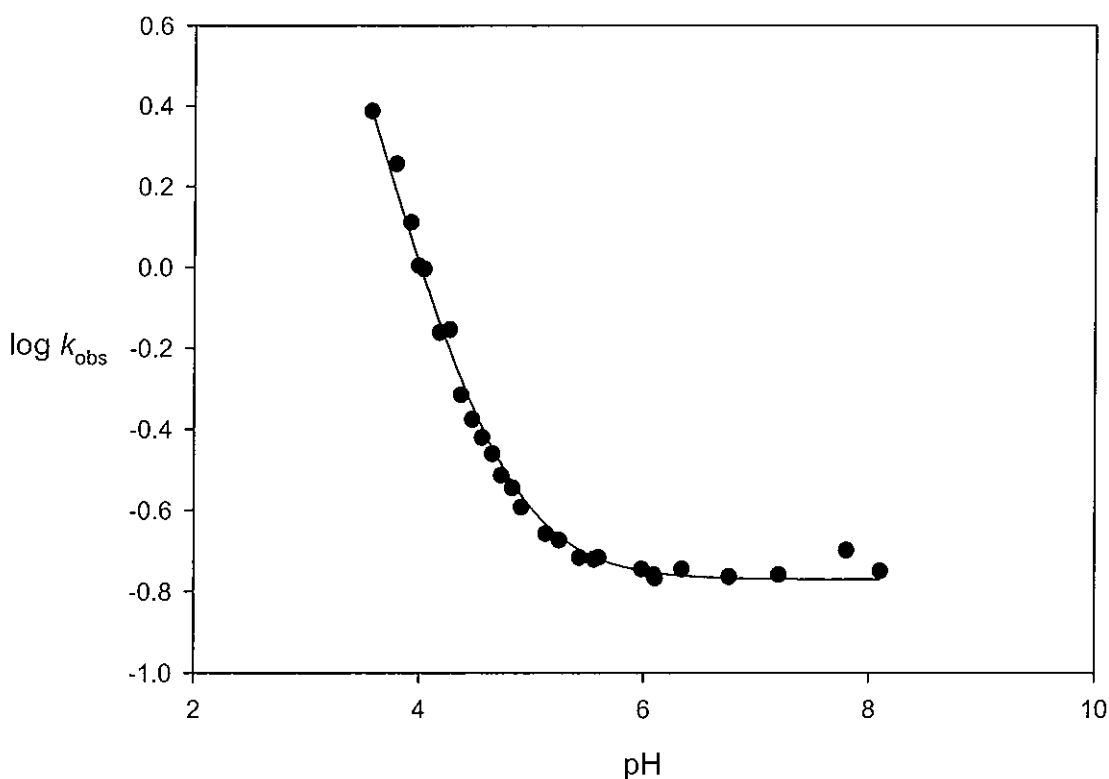
The equilibrium solvent isotope effect can be estimated from  $K_R^{H_2O}/K_R^{D_2O} = 1.31 \times 10^{-5} / 4.75 \times 10^{-6} = 2.76$ . An equilibrium solvent isotope effect of 2.76 is of the magnitude expected for hydrolysis of a carbocation.<sup>83</sup>

### 2.2.7 pH Profile Below pH 8

The buffer independent rate constants for the hydrolysis reaction of ( $\eta^5$ -cyclohexadienyl)tricarbonyliron (**72**) can be used to construct a pH rate profile for the reaction. The pH profile, a plot of  $\log k$  against pH, is shown in Figure 2.19 and is based on the rate constants recorded in Tables 2.11 to 2.16.

Below pH 4, the measured rate constants correspond to the ionisation of the coordinated arene hydrate to the coordinated cation. In the pH range 4 to 6, the measured rate constants represent the sum of the forward and reverse reaction rate constants for the hydrolysis of the ( $\eta^5$ -cyclohexadienyl)tricarbonyliron cation (72) and ionisation reaction of ( $\eta^4$ -*exo*-5-hydroxy-1,3-cyclohexadiene)tricarbonyliron (102) respectively. Above pH 6, the measured rate constants are for the hydrolysis reaction of the coordinated cation.

The structure of the pH profile is believed to reflect changes observed in the mechanism or the reactant species on varying the acidity of the reaction medium. These changes are interpreted as shown in Scheme 2.4 (Section 2.2, page 71) which includes the relevant reactions of  $\text{H}_3\text{O}^+$  and  $\text{H}_2\text{O}$  as acid or base species.



**Figure 2.19** pH profile ( $\log k$  against pH) for the hydrolysis of the ( $\eta^5$ -cyclohexadienyl)tricarbonyliron cation to the coordinated arene hydrate.

Kinetic expressions for the different regions of the pH-profile may be derived as follows, allowing rate constants for the process to be determined:

(i) pH < 5

Below pH 5, catalysis by acid is observed. This is shown in Equation 2.22 which is based on Scheme 2.4.

$$k_{\text{obs}} = k_{\text{H}} [\text{H}^+] \quad (2.22)$$

(ii) pH 5 to 9

In the region from pH 5 to 9, H<sub>2</sub>O is the species promoting the hydrolysis of the ( $\eta^5$ -cyclohexadienyl)tricarbonyliron cation. The rate law for this region of the pH profile is shown in Equation 2.23.

$$k_{\text{obs}} = k_{\text{H}_2\text{O}} \quad (2.23)$$

Combining Equations 2.22 and 2.23 gives Equation 2.24, the rate law which describes reactions observed on the pH profile below pH 8.

$$k_{\text{obs}} = k_{\text{H}} [\text{H}^+] + k_{\text{H}_2\text{O}} \quad (2.24)$$

The limiting pH-dependent and pH-independent regions of the pH-profile allow the rate constants which are presented in Table 2.20 to be determined.

**Table 2.20** Rate constants obtained from the pH-independent and pH-dependent regions of the pH-profile for the reaction of the ( $\eta^5$ -cyclohexadienyl)tricarbonyliron cation (72).

pH Range	pH-Dependence	Rate Expression	Rate Constant ( $M^{-1} s^{-1}$ )
< 5	$H^+$	$k_H [H^+]$	$8.3 \times 10^3$
5 - 8	$H_2O$	$k_{H_2O}$	0.177

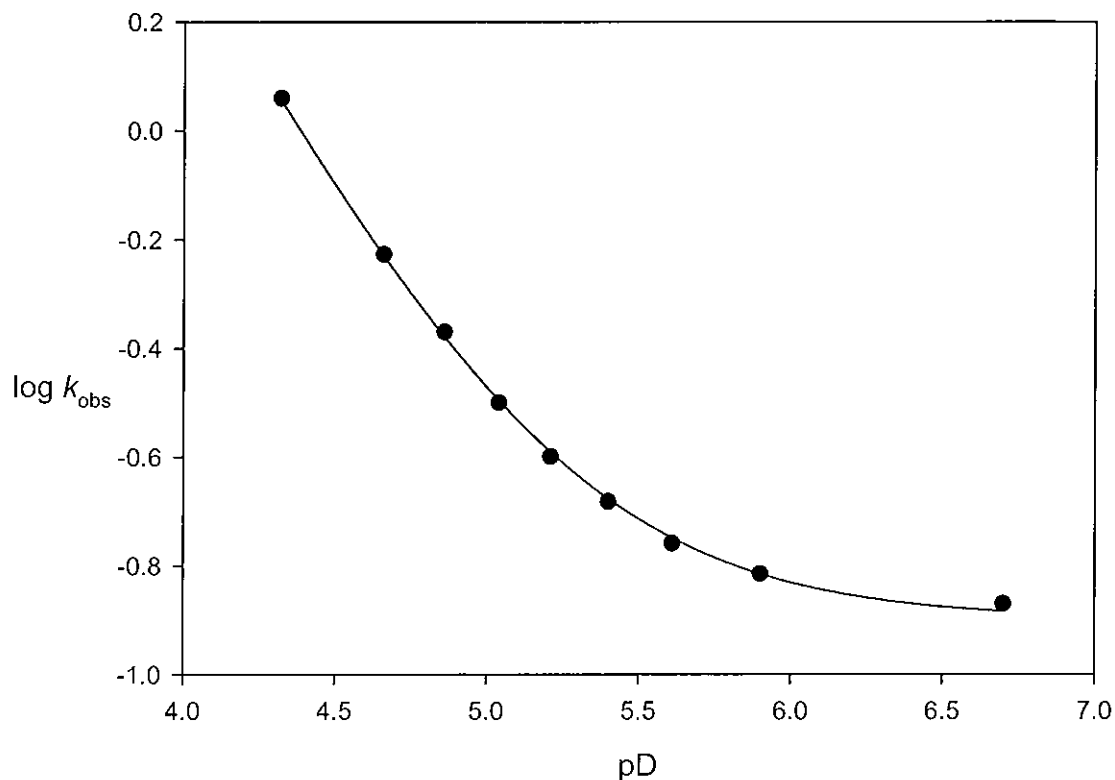
### 2.2.8 pD Profile

The hydrolysis reaction of the ( $\eta^5$ -cyclohexadienyl)tricarbonyliron cation (72) was measured in deuterated acetate and cacodylate buffer solutions in the pD range from 4 to 6.5. The first order rate constants obtained are presented in Table 2.21 and from them a pD profile for the pH range monitored can be prepared. This pD-profile is shown in Figure 2.20 and comprises a plot of  $\log k$  against pD.

**Table 2.21** First order rate constants for the hydrolysis of the ( $\eta^5$ -cyclohexadienyl)tricarbonyliron cation (72) in acetate and cacodylate buffer solutions prepared in deuterium oxide at 25°C.<sup>a</sup>

pD	$k_{\text{obs}} / \text{s}^{-1}$
6.70	0.135
5.90	0.153
5.61	0.174
5.40	0.208
5.21	0.252
5.04	0.316
4.86	0.427
4.66	0.593
4.32	1.15

(a) Measurements were made at 250 nm with a substrate concentration of  $2.0 \times 10^{-4}$  M and ionic strength 0.1 M, using a fast mixing apparatus.



**Figure 2.20** pD profile ( $\log k_{obs}$  against pD) for the hydrolysis of the ( $\eta^5$ -cyclohexadienyl)tricarbonyliron cation (**72**) to form the deuterated coordinated arene hydrate.

### 2.2.9 Equilibrium Constants for Hydrolysis

UV-Vis absorption spectrophotometry was used to determine  $pK_R$  for the hydrolysis of the ( $\eta^5$ -cyclohexadienyl)tricarbonyliron cation (**72**). The reaction was monitored in a range of aqueous buffer solutions (borate, phosphate, cacodylate and acetate). The pH and absorbance change (the difference between the initial and final absorbance on a kinetic scan) were recorded and are shown in Table 2.22. Figure 3.2 (Section 3.3) is a plot of absorbance change *versus* pH for the reaction in the buffers examined.



**Table 2.22** Absorbance change measurements for the hydrolysis of the ( $\eta^5$ -cyclohexadienyl)tricarbonyliron cation (**72**) in aqueous borate, phosphate, cacodylate and acetate buffers at 25°C.<sup>a</sup>

Buffer	R <sup>b</sup>	10 <sup>2</sup> [B] / M	pH	Absorbance Change
Borate	4.0	20.0	9.83	0.314
Borate	1.5	7.50	9.41	0.370
Borate	1.0	5.00	9.23	0.290
Borate	0.66	4.00	9.05	0.326
Borate	0.45	3.00	8.86	0.315
Borate	0.25	2.00	8.63	0.300
Borate	0.11	1.00	8.28	0.270
Phosphate	4.0	8.00	7.80	0.210
Phosphate	1.0	5.00	7.20	0.180
Cacodylate	4.0	2.00	6.76	0.177
Cacodylate	1.5	6.00	6.34	0.171
Cacodylate	0.66	4.00	5.98	0.168
Cacodylate	0.25	2.00	5.56	0.146
Acetate	4.0	8.00	5.25	0.132
Acetate	1.5	6.00	4.83	0.099
Acetate	0.66	4.00	4.47	0.053
Acetate	0.25	2.00	4.05	0.014

(a) Measurements were made at 250 nm with a substrate concentration of  $2.0 \times 10^{-5}$  M and ionic strength 0.1 M and were performed using a fast mixing accessory. (b) [buffer base] / [buffer acid]

The plot in Figure 3.2 shows two  $pK$  values,  $pK_1$  and  $pK_2$  respectively, as two inflection points are observed. The  $pK_R$  value that was required for the equilibrium between the tricarbonyliron coordinated cation (**72**) and the corresponding hydrate is believed to be  $pK_1$  which equals 4.77. This is in close agreement with the equilibrium constant determined by both kinetic (Section 2.2.3) and spectroscopic methods (Section

2.2.4) of 4.77. The second  $pK$  value,  $pK_2$ , is for to an as yet unidentified reaction and was found to be 8.05.

### 2.2.10 Rate Constants for Hydrolysis Above pH 8

Above pH 8, the rate constants determined for the hydrolysis of the ( $\eta^5$ -cyclohexadienyl)tricarbonyliron were measured using a fast mixing accessory attached to a UV-Vis spectrophotometer as already described in Section 2.2.1.

#### Hydroxide Ion Catalysed Reaction

Table 2.23 shows the first order rate constants observed for the hydrolysis of ( $\eta^5$ -cyclohexadienyl)tricarbonyliron (**72**) in aqueous hydroxide solutions. Above pH 11, the hydrolysis became too fast to be measured using the fast mixing accessory. Therefore it was not possible to measure many rates in hydroxide solutions.

**Table 2.23** First order rate constants for the hydrolysis of ( $\eta^5$ -cyclohexadienyl)tricarbonyliron in aqueous hydroxide solution at 25°C.<sup>a</sup>

pH	$10^3 [\text{OH}^-] / \text{M}$	$k_{\text{obs}} / \text{s}^{-1}$
11.0	1.0	4.7
10.6	0.2	2.5

(a) Measurements were made at 250 nm with a substrate concentration of  $2.0 \times 10^{-5}$  M and ionic strength 0.1 M, using a fast mixing apparatus.

#### Reaction in Borate Buffers

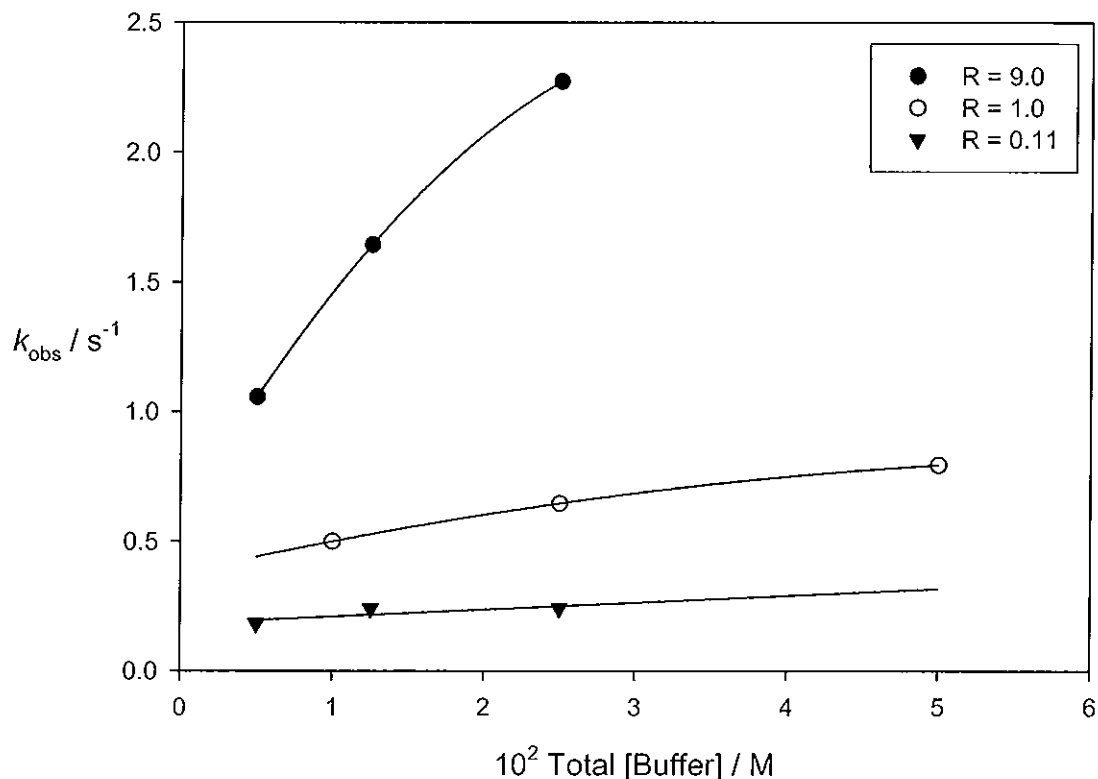
Table 2.24 shows first order rate constants for the hydrolysis of ( $\eta^5$ -cyclohexadienyl)tricarbonyliron (**72**) in aqueous borate buffers. Figure 2.21 shows a plot of first order rate constants against the total buffer concentration over a range of buffer ratios. As can be seen, the slopes of the plots representing each buffer ratio increase as the percentage of buffer base increases. This implies that buffer catalysis occurs for the hydrolysis reaction in borate buffers and is due to the buffer base. As buffer base catalysis is occurring, the buffer independent rate constants are obtained

from the intercepts of a plot of observed rate constants against buffer base concentration. These plots against buffer base concentration are shown in Figure 2.22. The slopes ( $k$ ) and intercepts ( $k_0$ ) of the plots in Figure 2.22 are summarised in Equations 2.26, 2.27 and 2.28, based on Equation 2.25. For the buffer ratio  $R = 0.11$ , a straight line is plotted of slope zero and a general base catalysed reaction is not observed.

**Table 2.24** First order rate constants for the hydrolysis of ( $\eta^5$ -cyclohexadienyl)tricarbonyliron in aqueous borate buffers at 25°C.<sup>a</sup>

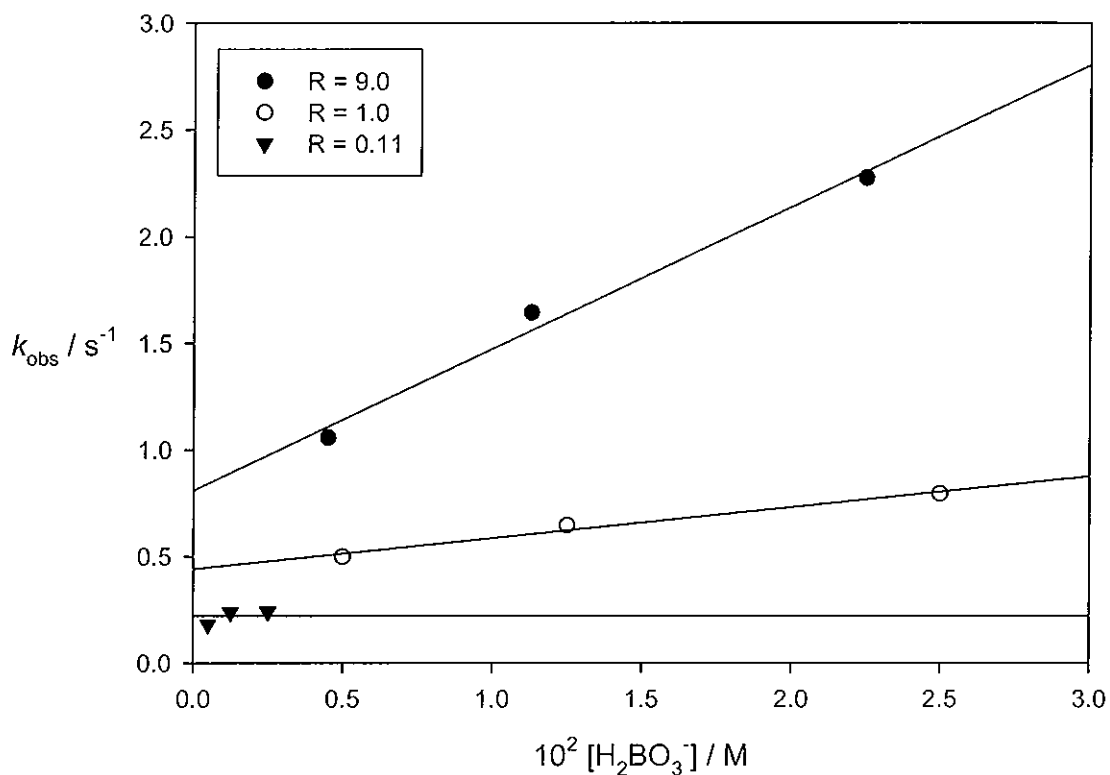
pH	R <sup>b</sup>	10 <sup>2</sup> [H <sub>2</sub> BO <sub>3</sub> <sup>-</sup> ]/M	10 <sup>2</sup> [H <sub>3</sub> BO <sub>3</sub> ]/M	$k_{\text{obs}}/\text{s}^{-1}$
10.18	9.0	2.25	0.25	2.27
10.18	9.0	1.125	0.125	1.64
10.18	9.0	0.45	0.05	1.06
9.23	1.0	2.50	2.50	0.794
9.23	1.0	1.25	1.25	0.646
9.23	1.0	0.50	0.50	0.499
8.23	0.11	0.25	2.25	0.241
8.23	0.11	0.125	1.13	0.239
8.23	0.11	0.05	0.45	0.182

(a) Measurements were made at 250 nm with a substrate concentration of  $2.0 \times 10^{-5}$  M and ionic strength 0.1 M using a fast mixing apparatus. (b) [buffer base] / [buffer acid].



**Figure 2.21** Plot of first order rate constants against total buffer concentration at fixed buffer ratios for the hydrolysis of ( $\eta^5$ -cyclohexadienyl)tricarbonyliron in aqueous borate buffers at 25°C. (Best fit lines (curved))

In Figure 2.21, it can be seen that the best fit to the data points for each buffer ratio are not straight lines as would have been expected. Instead there is some curvature in the plots. This is an indication that the buffer catalysis is not as straight forward as expected. One possibility is that a change in the mechanism of buffer catalysis is occurring. In Figure 2.22, where observed rate constants are plotted against buffer base concentration, the best fit straight lines are imposed on the data points.



**Figure 2.22** Plot of first order rate constants against buffer base concentration at fixed buffer ratios for the hydrolysis of ( $\eta^5$ -cyclohexadienyl)tricarbonyliron in aqueous borate buffers at 25°C. (Best fit straight lines imposed on the data points)

$$k_{\text{obs}} = k[\text{H}_2\text{BO}_3^-] + k_0 \quad (2.25)$$

$$(R=9.0) \quad k_{\text{obs}} = 6.64 \pm 0.08 \text{ M}^{-1}\text{s}^{-1} [\text{H}_2\text{BO}_3^-] + 0.81 \pm 0.12 \text{ s}^{-1} \quad (2.26)$$

$$(R=1.0) \quad k_{\text{obs}} = 4.42 \pm 0.33 \text{ M}^{-1}\text{s}^{-1} [\text{H}_2\text{BO}_3^-] + 0.44 \pm 0.03 \text{ s}^{-1} \quad (2.27)$$

$$(R=0.11) \quad k_{\text{obs}} = 0.22 \text{ s}^{-1} \quad (2.28)$$

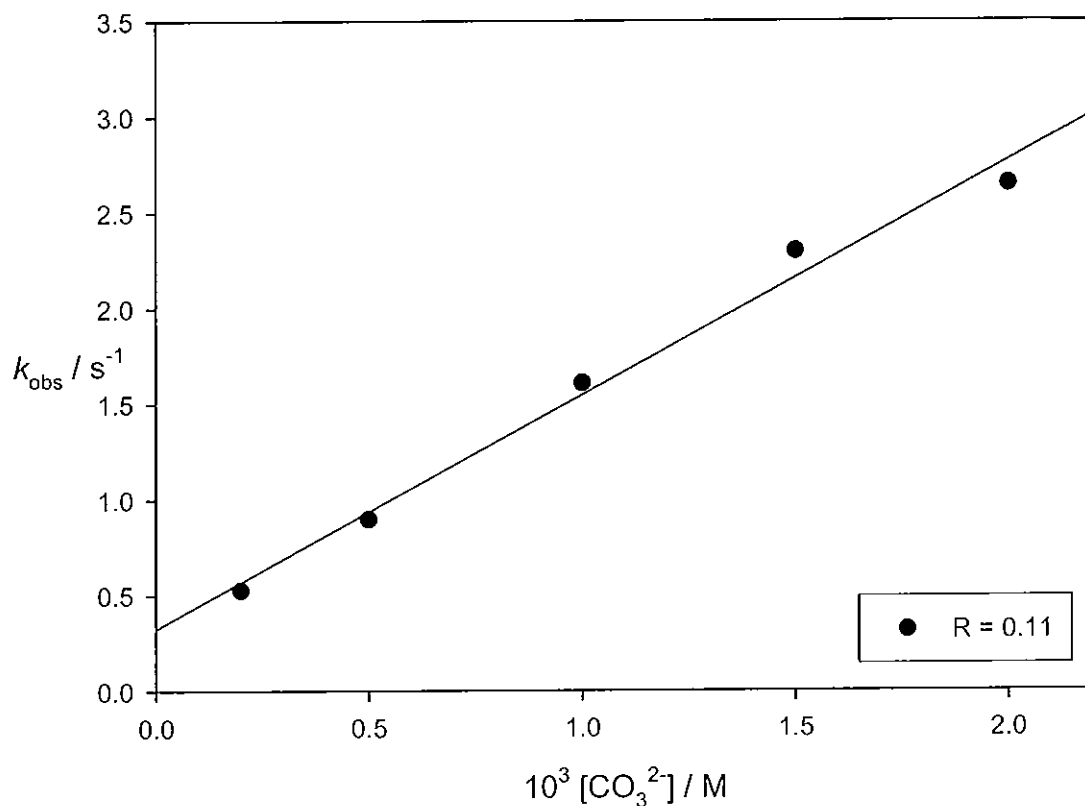
### Reaction in Carbonate Buffers

The hydrolysis of ( $\eta^5$ -cyclohexadienyl)tricarbonyliron was also monitored in aqueous carbonate buffers. The first order rate constants measured are shown in Table 2.25 and are plotted against buffer base concentration in Figure 2.23.

**Table 2.25** First order rate constants for the hydrolysis of ( $\eta^5$ -cyclohexadienyl)tricarbonyliron in aqueous carbonate buffers at 25°C.<sup>a</sup>

pH	R <sup>b</sup>	10 <sup>3</sup> [CO <sub>3</sub> <sup>2-</sup> ]/M	10 <sup>3</sup> [HCO <sub>3</sub> <sup>-</sup> ]/M	k <sub>obs</sub> /s <sup>-1</sup>
9.38	0.11	2.00	18.0	2.65
9.38	0.11	1.50	13.5	2.30
9.38	0.11	1.00	9.00	1.61
9.38	0.11	0.50	4.50	0.90
9.38	0.11	0.20	1.80	0.53

(a) Measurements were made at 250 nm, a substrate concentration of  $2.0 \times 10^{-5}$  M and ionic strength of 0.1 M using a fast mixing apparatus. (b) [buffer base] / [buffer acid].



**Figure 2.23** Plot of first order rate constants against buffer base concentration at a fixed buffer ratio of 0.11 for the hydrolysis of ( $\eta^5$ -cyclohexadienyl)tricarbonyliron in aqueous carbonate buffers at 25°C.

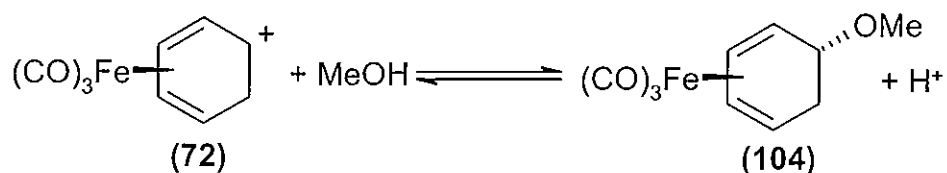
It can be seen in the plot in Figure 2.23 that buffer base catalysis is observed as the observed rate constant ( $k_{\text{obs}}$ ) increases as the buffer base concentration rises. The intercept of the plot in Figure 2.23 is summarised in Equation 2.30 based on Equation 2.29. As was observed in the borate buffer solutions, some curvature is noted at higher buffer base concentrations on the buffer catalysis plot.

$$k_{\text{obs}} = k[\text{CO}_3^{2-}] + k_0 \quad (2.29)$$

$$(R=0.11) \quad k_{\text{obs}} = (1.22 \pm 0.08) \times 10^{-3} \text{ M}^{-1} \text{ s}^{-1} [\text{CO}_3^{2-}] + 0.32 \pm 0.09 \text{ s}^{-1} \quad (2.30)$$

## 2.3 ( $\eta^5$ -Cyclohexadienyl)tricarbonyliron Cation - Methanolysis Reaction

An equilibrium constant,  $pK_R$ , was determined for the methanolysis reaction shown in Scheme 2.6.



Scheme 2.6

### 2.3.1 Equilibrium Constant for Cation Formation in Methanol

The equilibrium constant for this reaction was determined by taking spectrophotometric measurements in methanol containing 5% aqueous acid (perchloric acid). The coordinated cation (72) was initially dissolved in methanol. This provided the methoxy substituted complex (104). Addition of portions of the methoxy substituted complex solution to a cuvette containing 5% aqueous acid in methanol allowed the equilibrium between ( $\eta^4$ -exo-5-methoxycyclohexa-1,3-diene)tricarbonyliron (104) and the ( $\eta^5$ -cyclohexadienyl)tricarbonyliron cation (72) to be monitored.

The changes observed track those expected as a result of analysis of the NMR spectra recorded for this transformation (see Section 2.4). Table 2.27 lists the absorbance measurements observed for the equilibrium between the coordinated cation and the corresponding methoxy substituted complex in methanol at different acid concentrations. A spectrophotometric titration curve in which absorbance is plotted against pH is shown in Figure 2.24. The best fit line to the data points in Figure 2.24 was fitted using Equation 2.31. (Further information on Equation 2.31 is provided in Section 4.6.2).

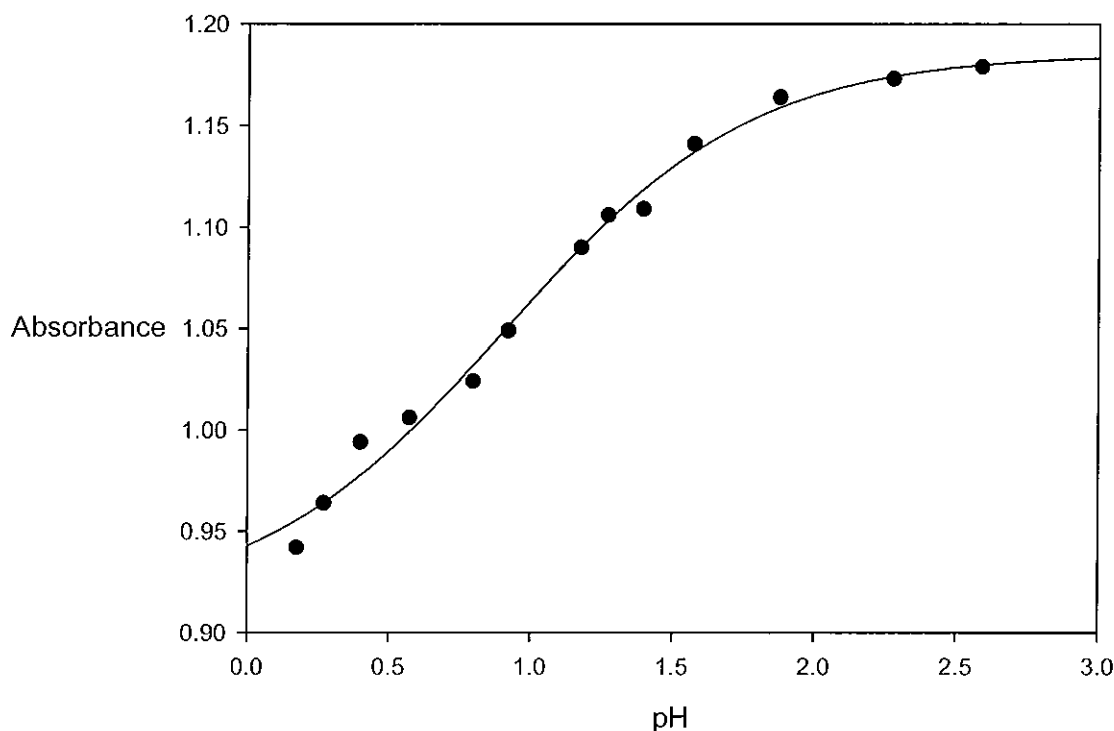
$$A = \{K_R A_B + A_{BH^+} [H^+]\} / \{K_R + [H^+]\} \quad (2.31)$$



**Table 2.27** Absorbance measurements for ( $\eta^5$ -cyclohexadienyl)-tricarbonyliron cation formation from the reaction of the ( $\eta^4$ -*exo*-5-methoxycyclohexa-1,3-diene)tricarbonyliron complex (104) with aqueous acid in methanol at 25°C.<sup>a</sup>

$10^4$ [H <sup>+</sup> ]/M	pH	Absorbance
0.03	2.59	1.179
0.05	2.28	1.173
0.13	1.88	1.164
0.25	1.57	1.141
0.38	1.40	1.109
0.51	1.27	1.106
0.63	1.18	1.090
1.14	0.92	1.049
1.52	0.80	1.024
2.53	0.57	1.006
3.79	0.40	0.994
5.06	0.27	0.964
6.32	0.18	0.942

(a) Measurements were made at 217 nm with a substrate concentration of  $4.6 \times 10^{-5}$  M.

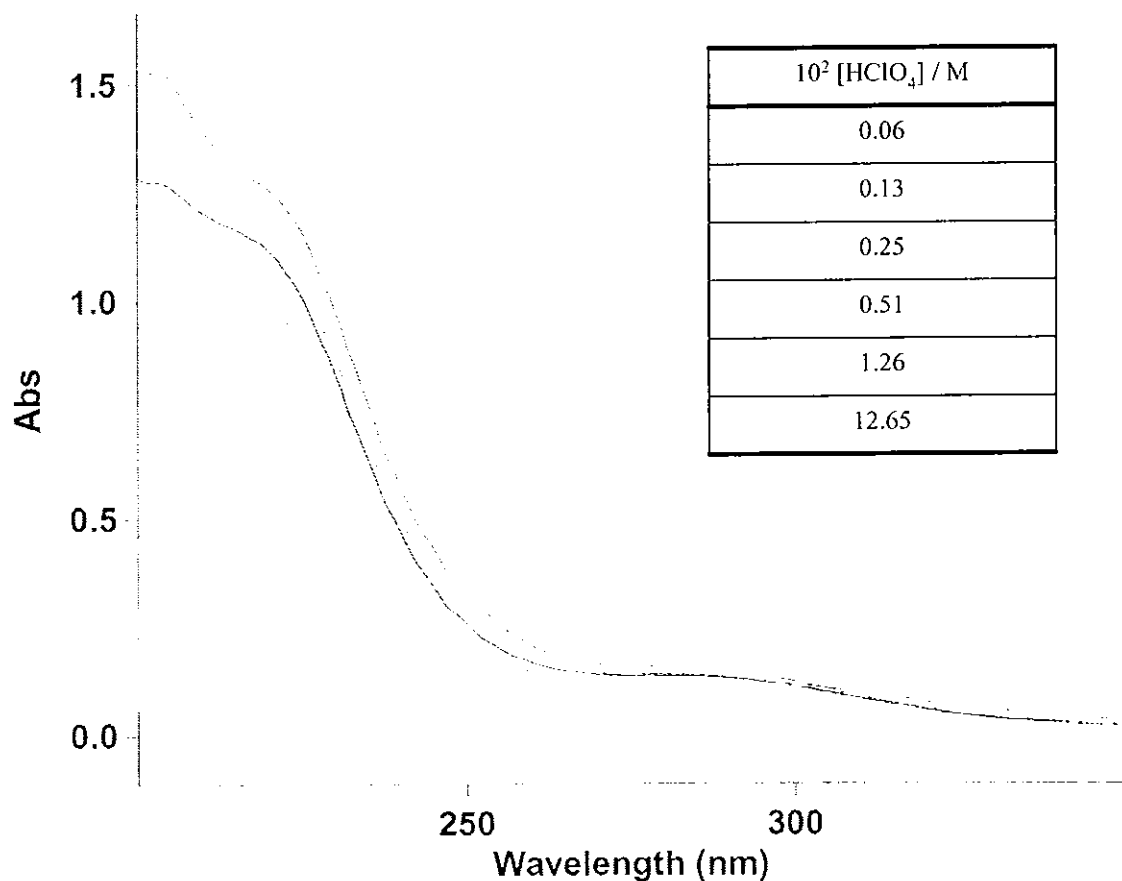


**Figure 2.24** Plot of absorbance against pH for carbocation formation from the reaction of the ( $\eta^4$ -*exo*-5-methoxycyclohexa-1,3-diene)tricarbonyliron complex (**104**) with aqueous acid in methanol at 25°C.

The equilibrium constant,  $pK_R$ , determined from the inflection point on the spectrophotometric titration curve is 0.91.

### 2.3.2 Equilibrium Constant for Cation Formation in 50% Aqueous Methanol

Absorbance measurements were also made for the equilibrium between ( $\eta^4$ -*exo*-5-methoxycyclohexa-1,3-diene)tricarbonyliron (**104**) and the ( $\eta^5$ -cyclohexadienyl)-tricarbonyliron cation (**72**) in 50% aqueous methanol solutions. An example of the UV spectra observed for this reaction is shown in Figure 2.25. The observed absorbances are presented in Table 2.28 and are plotted against pH in Figure 2.26. The best fit line to the data points in Figure 2.26 was fitted using Equation 2.32. (Further information on Equation 2.32 is provided in Section 4.6.2).



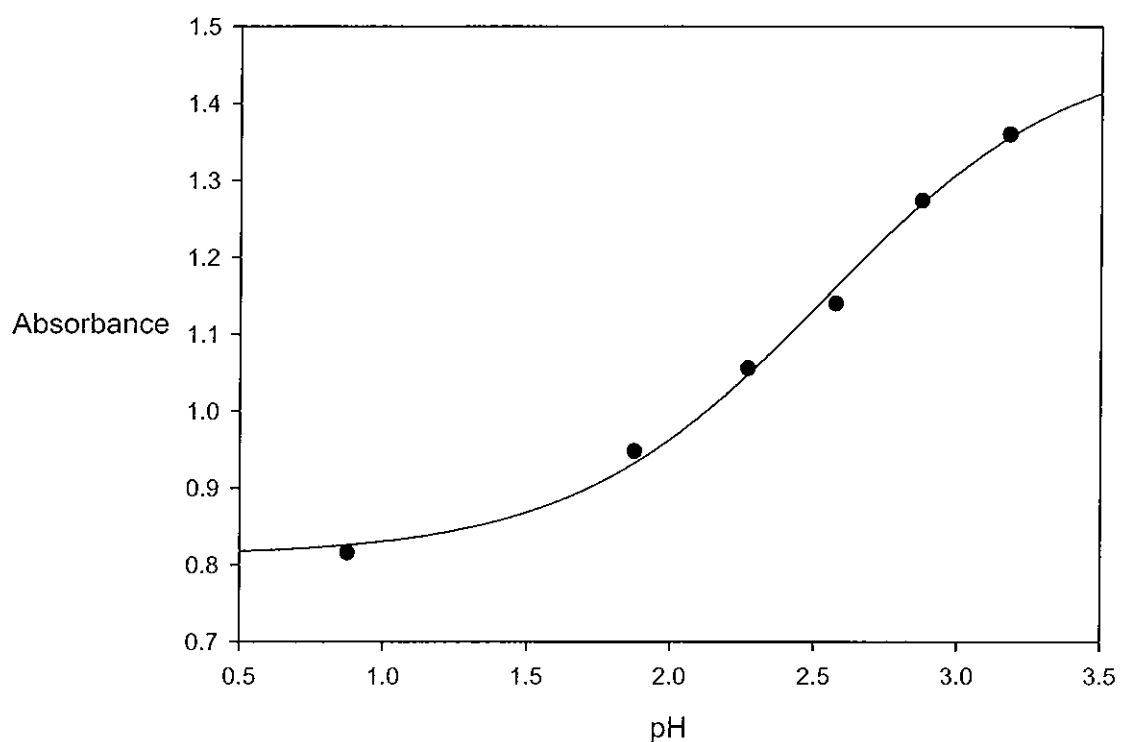
**Figure 2.25** UV-Vis spectra recorded for methanolysis of the ( $\eta^5$ -cyclohexadienyl)tricarbonyliron cation (72) in varying concentrations of acid in 50% aqueous methanol at 25°C and a substrate concentration of  $6 \times 10^{-5}$  M.

$$A = \{K_{\text{R}}A_{\text{B}} + A_{\text{BH}^+}[\text{H}^+]\} / \{K_{\text{R}} + [\text{H}^+]\} \quad (2.32)$$

**Table 2.28** Absorbance measurements for carbocation formation from the reaction of the ( $\eta^4$ -*exo*-5-methoxycyclohexa-1,3-diene)tricarbonyliron complex (104) with aqueous acid in 50% aqueous methanol at 25°C.<sup>a</sup>

$10^2 [\text{H}^+]/\text{M}$	pH	Absorbance
0.06	3.18	1.360
0.13	2.88	1.274
0.25	2.57	1.140
0.51	2.27	1.056
1.26	1.88	0.948
12.64	0.88	0.816

(a) Measurements were made at 204 nm with a substrate concentration of  $4.6 \times 10^{-5}$  M.



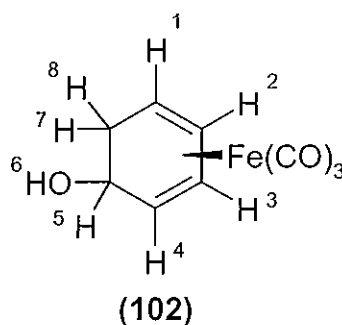
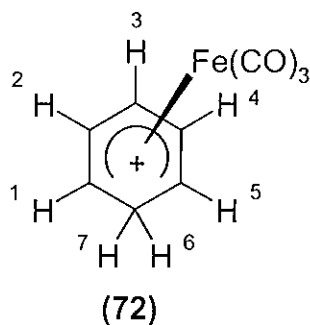
**Figure 2.26** Plot of absorbance against pH for carbocation formation from the reaction of the ( $\eta^4$ -*exo*-5-methoxycyclohexa-1,3-diene)tricarbonyliron complex (104) with aqueous acid in 50% aqueous methanol.

The inflection point on the spectrophotometric titration curve in Figure 2.26 gives the equilibrium constant,  $pK_R$ , for 50% aqueous methanol and it was found to be 2.53.

## 2.4 ( $\eta^5$ -Cyclohexadienyl)tricarbonyliron $^1\text{H}$ NMR Spectroscopic Study

A study was undertaken on the ( $\eta^5$ -cyclohexadienyl)tricarbonyliron cation (**72**) to ensure that changes inferred from monitoring the hydrolysis and methanolysis reactions by UV-Vis and IR spectrophotometry were also observed by  $^1\text{H}$  NMR spectroscopy.

Table 2.29 presents  $^1\text{H}$  NMR data for the ( $\eta^5$ -cyclohexadienyl)tricarbonyliron cation (**72**), ( $\eta^4$ -*exo*-5-hydroxycyclohexa-1,3-diene)tricarbonyliron (**102**) and ( $\eta^4$ -*exo*-5-methoxycyclohexa-1,3-diene)tricarbonyliron (**104**) complexes reported by Birch *et al.*<sup>52</sup> and Wilkinson *et al.*<sup>56</sup> The structures of complexes (**72**) and (**102**) are shown below and the structure of (**104**) is given at the beginning of Section 2.3.

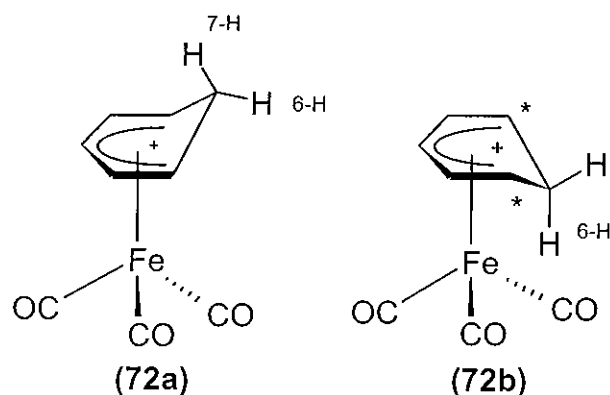


**Table 2.29**  $^1\text{H}$  NMR data reported by Wilkinson *et al.*<sup>56</sup> and Birch *et al.*<sup>52</sup> for the ( $\eta^5$ -cyclohexadienyl)tricarbonyliron cation (**72**), ( $\eta^4$ -*exo*-5-hydroxycyclohexa-1,3-diene)tricarbonyliron (**102**) and ( $\eta^4$ -*exo*-5-methoxycyclohexa-1,3-diene)tricarbonyliron (**104**).

Complex	$\delta$ / ppm <sup>a,b</sup>				
<b>72</b> <sup>c</sup>	2.02 (d, 6-H)	3.01 (dt, 7-H)	4.27 (t, 1-H, 5-H)	5.82 (t, 2-H, 4-H)	7.22 (t, 3-H)
<b>102</b> <sup>d</sup>	1.27 (7-H)	1.55 (6-H, 8-H)	2.82 (1-H, 4-H)	4.16 (5-H)	5.30 (2-H, 3-H)
<b>104</b> <sup>d</sup>	1.68 (7-H, 8-H)	2.90 (1-H, 4-H)	3.15 (6-H)	3.70 (5-H)	5.37 (2-H, 3-H)

(a) The solvent used to prepare the NMR samples was not specified. (b) Data was collected at an operating frequency of 60 MHz. (c) Wilkinson *et al.*<sup>56</sup> (d) Birch *et al.*<sup>52</sup>

Wilkinson *et al.*<sup>56</sup> were the first group to study the  $^1\text{H}$  NMR spectrum of the ( $\eta^5$ -cyclohexadienyl)tricarbonyliron cation (**72**), shortly after it was first prepared by Fischer and Fischer.<sup>54</sup> Wilkinson noted that the methylene protons labelled 6-H and 7-H provided two signals, one at 2.02 ppm and the other further downfield at 3.01 ppm. He attributed this feature of the spectrum to the non-equivalency of the protons due to the non-planarity of the ring. The ( $\eta^5$ -cyclohexadienyl)tricarbonyliron cation (**72**) may either have the methylene carbon pointing towards the cyclohexadienyl face to which the tricarbonyliron fragment is attached (**72b**) or pointing away from the face to which the tricarbonyliron fragment (**72a**) is attached. Wilkinson noted that in structure (**72b**), 6-H has a dihedral angle of approximately  $90^\circ$  relative to the protons on the two adjacent  $\text{sp}^2$  carbons (labelled with \*) and would not be expected to couple with them. 7-H on the other hand has a dihedral angle of approximately  $30^\circ$  relative to the protons on the neighbouring carbons and would be expected to couple with the adjacent protons. Wilkinson observed a doublet at 2.02 ppm and a doublet of triplets at 3.01 ppm, leading him to the conclusion that the ( $\eta^5$ -cyclohexadienyl)tricarbonyliron cation exists as structure (**72b**).



In this study, the tricarbonyliron coordinated cation (**72**) was dissolved in a number of solvents; deuterated acetonitrile ( $\text{CD}_3\text{CN}$ ), deuterated methanol ( $\text{CD}_3\text{OD}$ ) and deuterium oxide ( $\text{D}_2\text{O}$ ), and the  $^1\text{H}$  NMR spectrum in each solvent recorded. Tables 2.30 to 2.35 provide a summary of the spectroscopic data and the corresponding spectra are shown in Figures 2.27 to 2.32.

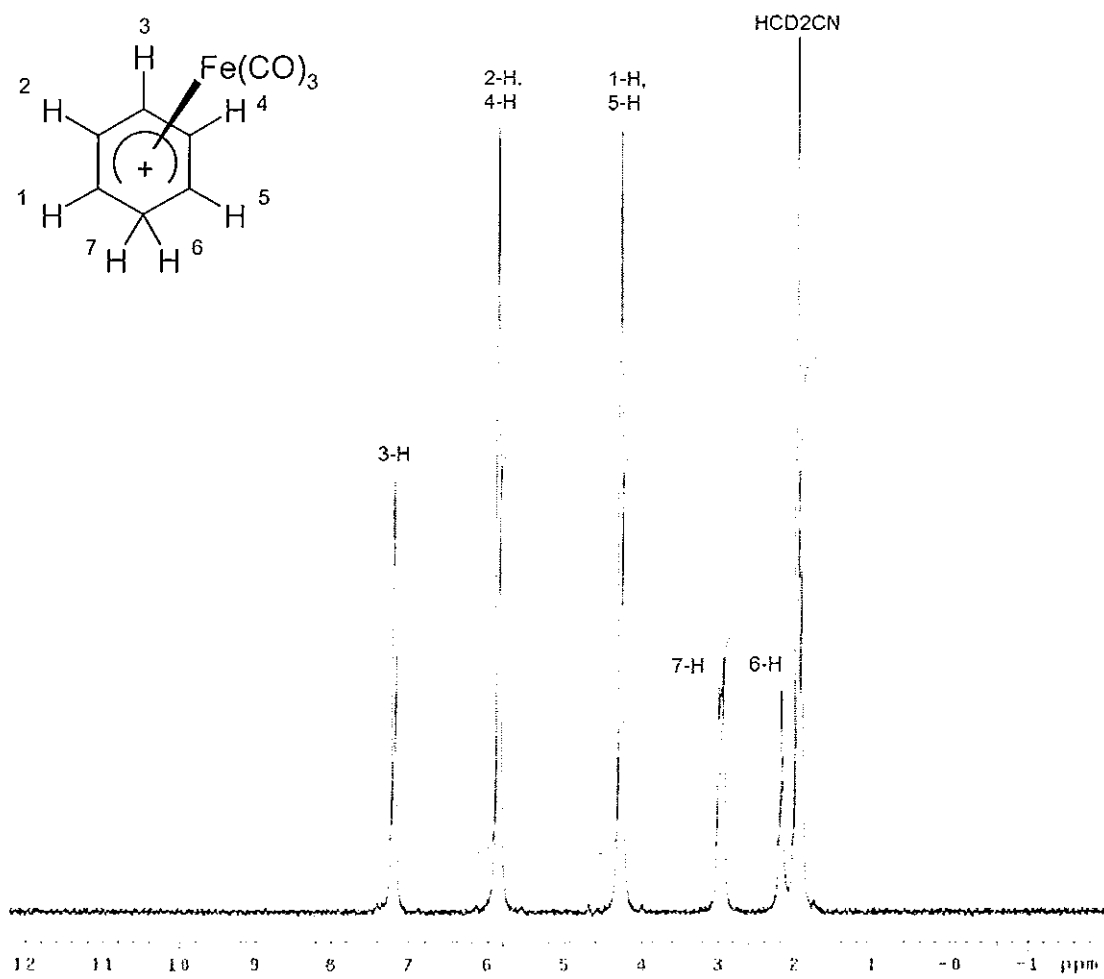
**Table 2.30**  $^1\text{H}$  NMR spectral data for  $(\eta^5\text{-cyclohexadienyl})\text{tricarbonyliron}$  in deuterated acetonitrile at a substrate concentration of 10 mg / 0.7 ml and in 50:50 deuterated acetonitrile/deuterium oxide at a substrate concentration of 10 mg / ml.

Complex	$\delta\text{H} / \text{ppm}^{\text{a,b}}$					Solvent
<b>72</b>	2.19	2.99	4.28	5.86	7.19	deuterated acetonitrile
	(6-H)	(7-H)	(1-H, 5-H)	(2-H, 4-H)	(3-H)	
<b>72</b>	2.08	3.08	4.41	6.03	7.34	50:50 deuterated acetonitrile/deuterium oxide
	(6-H)	(7-H)	(1-H, 5-H)	(2-H, 4-H)	(3-H)	

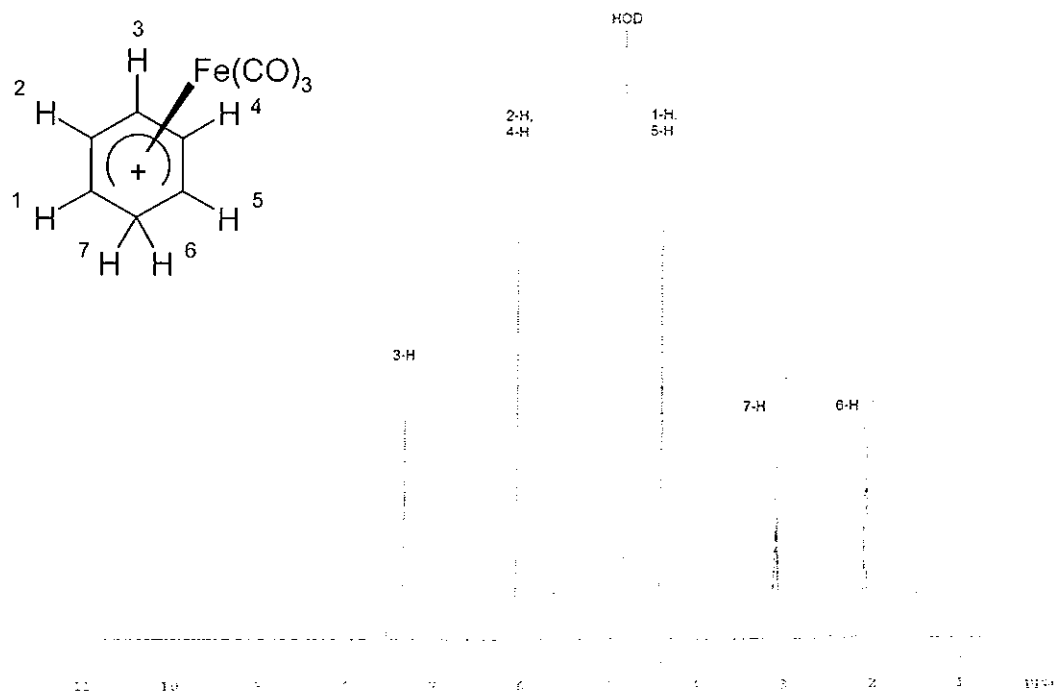
(a) Hydrogen numbering refers to the numbering system outlined for (**72**) outlined at the beginning of Section 2.4. (b) Spectrum was recorded at an operating frequency of 300 MHz in deuterated acetonitrile and at 500 MHz in 50:50 deuterated acetonitrile/deuterium oxide.



It has been noted by Gibson that the signals of complexes similar to those of interest in this study can be broadened significantly, masking the multiplicity of the signals. The broadening is a result of small amounts of paramagnetic iron salts present in the sample.<sup>84</sup> The <sup>1</sup>H NMR spectrum recorded for the coordinated cation (**72**) in deuterated acetonitrile (Figure 2.27) shows that the complex remained unchanged in this solvent. The signal observed at 1.98 ppm is due to a small amount of residual protons in the deuterated acetonitrile solvent. A check was performed to ensure that the same <sup>1</sup>H NMR spectrum is obtained when the coordinated cation is dissolved in a 50:50 ratio of deuterated acetonitrile and deuterium oxide. The spectrum recorded in this mixed solvent system is shown in Figure 2.28. The signal that occurs at 4.80 ppm is due to the presence of water. The spectrum is essentially the same as that recorded in deuterated acetonitrile except that there is a variation in chemical shifts of the signals of up to 0.17 ppm.



**Figure 2.27**  $^1\text{H}$  NMR spectrum of the  $(\eta^5\text{-cyclohexadienyl})\text{tricarbonyliron}$  cation (72) in deuterated acetonitrile.



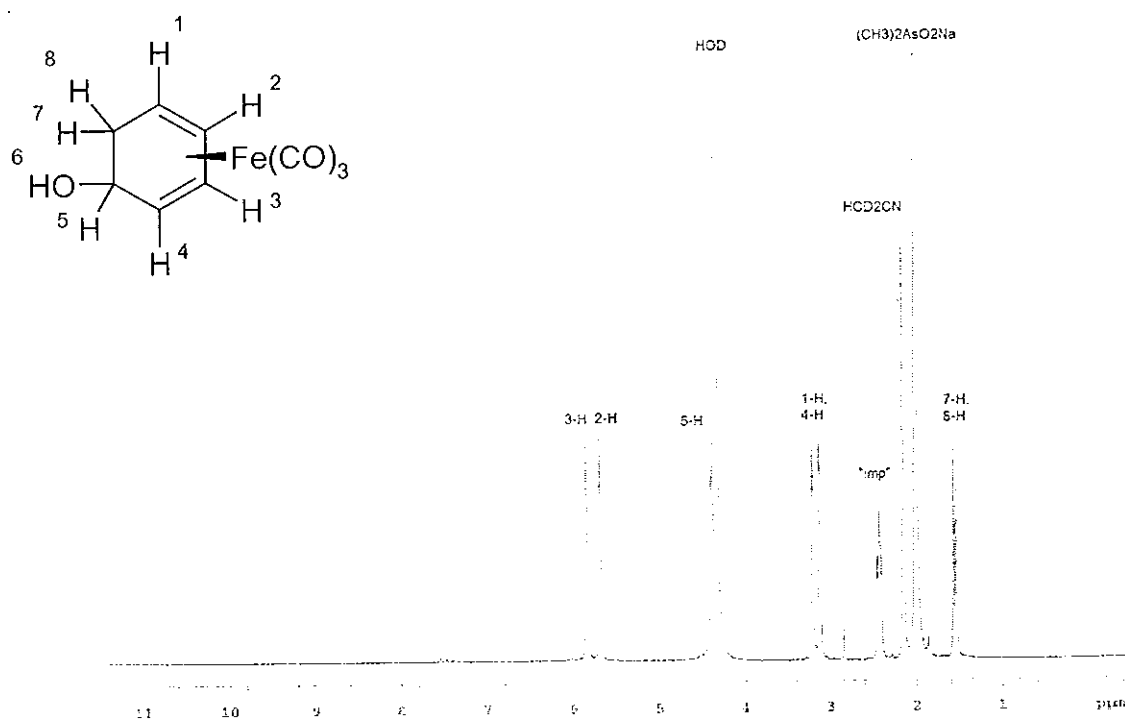
**Figure 2.28**  $^1\text{H}$  NMR spectrum of the ( $\eta^5$ -cyclohexadienyl)tricarbonyliron cation (**72**) in 50:50 deuterated acetonitrile/deuterium oxide.

In Figure 2.29, the  $^1\text{H}$  NMR spectrum recorded for the coordinated cation (**72**) in 50:50 deuterated acetonitrile and deuterium oxide buffered with sodium cacodylate ( $(\text{CH}_3)_2\text{AsO}_2\text{Na}$ ) is shown. Addition of sodium cacodylate shifts the equilibrium between the coordinated cation (**72**) and coordinated hydrate (**102**) to favour the hydrate. This would be expected on examination of the pH profile shown in Figure 2.19. Thus the  $^1\text{H}$  NMR spectrum for the coordinated benzene hydrate (**102**) and not that of the coordinated cation is observed. Table 2.32 summarises the spectroscopic data from Figure 2.29. Solvent signals found at 2.15 and 4.30 ppm are due to residual protons in the deuterated acetonitrile and water respectively. The signal at 2.00 ppm is due to sodium cacodylate whilst the signal at 2.4 ppm is due to an impurity which is unassigned. The hydroxyl proton (6-H) is absent in Figure 2.29 as expected because deuterium exchange with the solvent occurs.

**Table 2.32**  $^1\text{H}$  NMR spectral data for ( $\eta^4$ -*exo*-5-hydroxycyclohexa-1,3-diene)tricarbonyliron in 50:50 deuterated acetonitrile/deuterium oxide buffered with sodium cacodylate at a substrate concentration of 10 mg / ml.

Complex	$\delta\text{H} / \text{ppm}^{\text{a,b}}$				
<b>103</b>	1.56	3.19	4.40	5.68	5.84
	(7-H, 8-H)	(1-H, 4-H)	(5-H)	(2-H)	(3-H)

(a) Hydrogen numbering refers to the numbering system outlined for (**102**) at the beginning of Section 2.4. (b) Spectrum was recorded at an operating frequency of 500 MHz.



**Figure 2.29**  $^1\text{H}$  NMR spectrum of ( $\eta^4$ -*exo*-5-hydroxycyclohexa-1,3-diene)tricarbonyliron (**102**), formed by dissolving the corresponding cation in 50:50 deuterated acetonitrile/deuterium oxide buffered with sodium cacodylate.

When the ( $\eta^5$ -cyclohexadienyl)tricarbonyliron cation, in the form of its tetrafluoroborate salt, was dissolved in deuterated methanol to which deuterium chloride had been added, the  $^1\text{H}$  NMR spectrum shown in Figure 2.30 was obtained. The spectrum is that of the cation (**72**). The signal observed at 3.31 ppm is due to the residual solvent,  $\text{HCD}_2\text{OD}$ , and the signal at 4.87 ppm is due to water and residual  $\text{CD}_3\text{OH}$ . When the ( $\eta^5$ -cyclohexadienyl)tricarbonyliron cation is dissolved in methanol buffered with sodium cacodylate, the  $^1\text{H}$  NMR spectrum shown in Figure 2.31 was obtained. The spectrum is of the methoxy substituted complex ( $\eta^4$ -*exo*-5-methoxycyclohexa-1,3-diene)tricarbonyliron (**104**). No signal for the methoxy group in complex (**104**) is observed as it is actually the deuterated methoxy ( $\text{CD}_3\text{O}$ -) substituted complex that forms. The signal observed at 3.31 ppm is due to residual solvent,  $\text{HCD}_2\text{OD}$ , whilst the signal at 2.3 ppm is for an unassigned impurity.

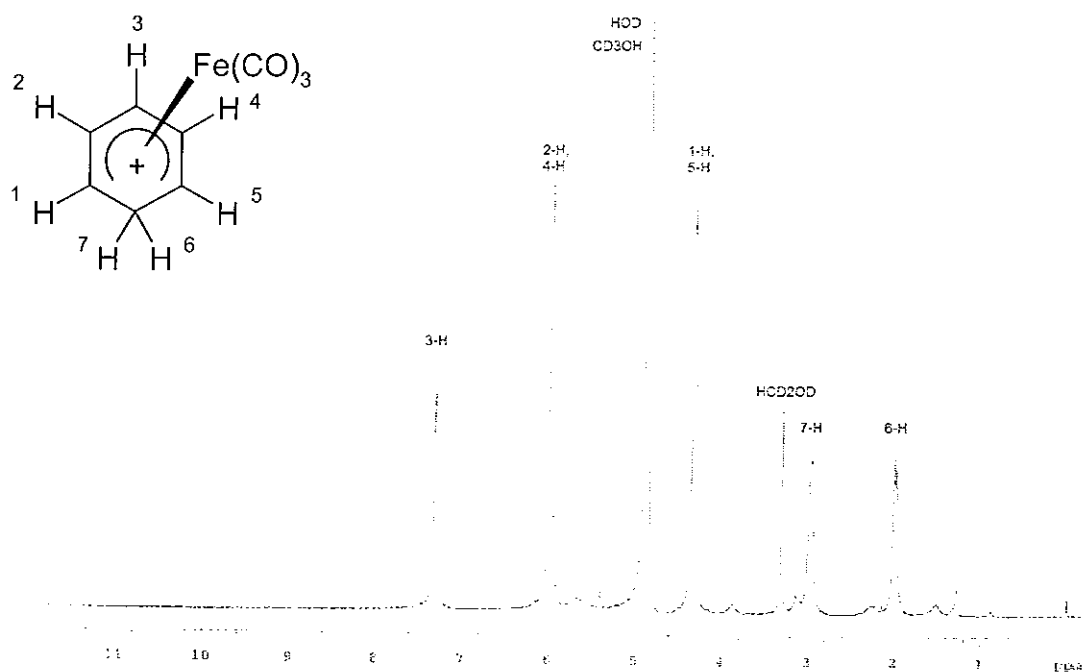
When the ( $\eta^5$ -cyclohexadienyl)tricarbonyliron cation, in the form of its tetrafluoroborate salt, was dissolved in deuterated methanol, the  $^1\text{H}$  NMR spectrum shown in Figure 2.32 was obtained. The spectrum contains signals for the coordinated cation (**72**) as well as the methoxy substituted complex ( $\eta^4$ -*exo*-5-methoxycyclohexa-1,3-diene)tricarbonyliron (**104**). The ratio of the two species is approximately 65:35 for the coordinated cation to the methoxy substituted complex. The signal that appears at 4.81 ppm is due to the presence of water. Again no signal for the methoxy group in complex (**104**) is observed as the solvent is deuterated methanol and thus it is actually the deuterated methoxy ( $\text{CD}_3\text{O}$ -) substituted complex that forms. The signal observed at 3.31 ppm is due to residual solvent,  $\text{HCD}_2\text{OD}$ . Two unassigned impurities are present in the spectrum at 2.3 ppm and 3.1 ppm respectively.

Table 2.33 summarises the spectroscopic data from the  $^1\text{H}$  NMR spectra in Figures 2.30, 2.31 and 2.32.

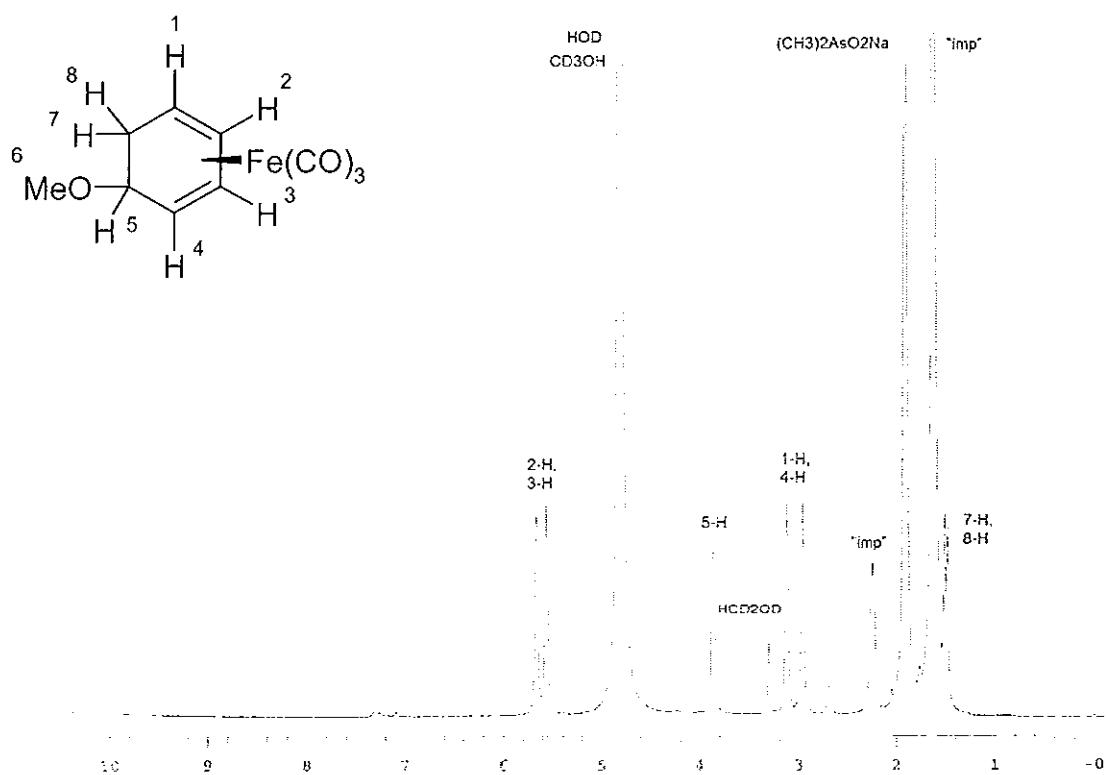
**Table 2.33**  $^1\text{H}$  NMR spectral data for the ( $\eta^5$ -cyclohexadienyl)tricarbonyl-iron cation (**72**) recorded in deuterated methanol, deuterated methanol with added DCl and deuterated methanol buffered with sodium cacodylate.

Complex	$\delta\text{H} / \text{ppm}^{\text{a}}$					Solvent	Figure
<b>72</b>	1.98 (6-H)	2.97 (7-H)	4.32 (1-H, 5-H)	5.98 (2-H, 4-H)	7.30 (3-H)	Deuterated methanol with added DCl	2.31
<b>72</b>	1.98 (6-H)	2.97 (7-H)	4.32 (1-H, 5-H)	5.98 (2-H, 4-H)	7.31 (3-H)	Deuterated methanol	2.30
<b>104</b>	1.51 (7-H, 8-H)	2.97, 3.13 (1-H, 4-H)	3.88 (5-H)	5.57, 5.67 (2-H, 3-H)		Deuterated methanol	2.30
<b>104</b>	1.49 (7-H, 8-H)	2.97, 3.10 (1-H, 4-H)	3.88 (5-H)	5.67, 5.57 (2-H, 3-H)		Deuterated methanol buffered with sodium cacodylate	2.32

(a) Spectra were recorded at an operating frequency of 500 MHz.

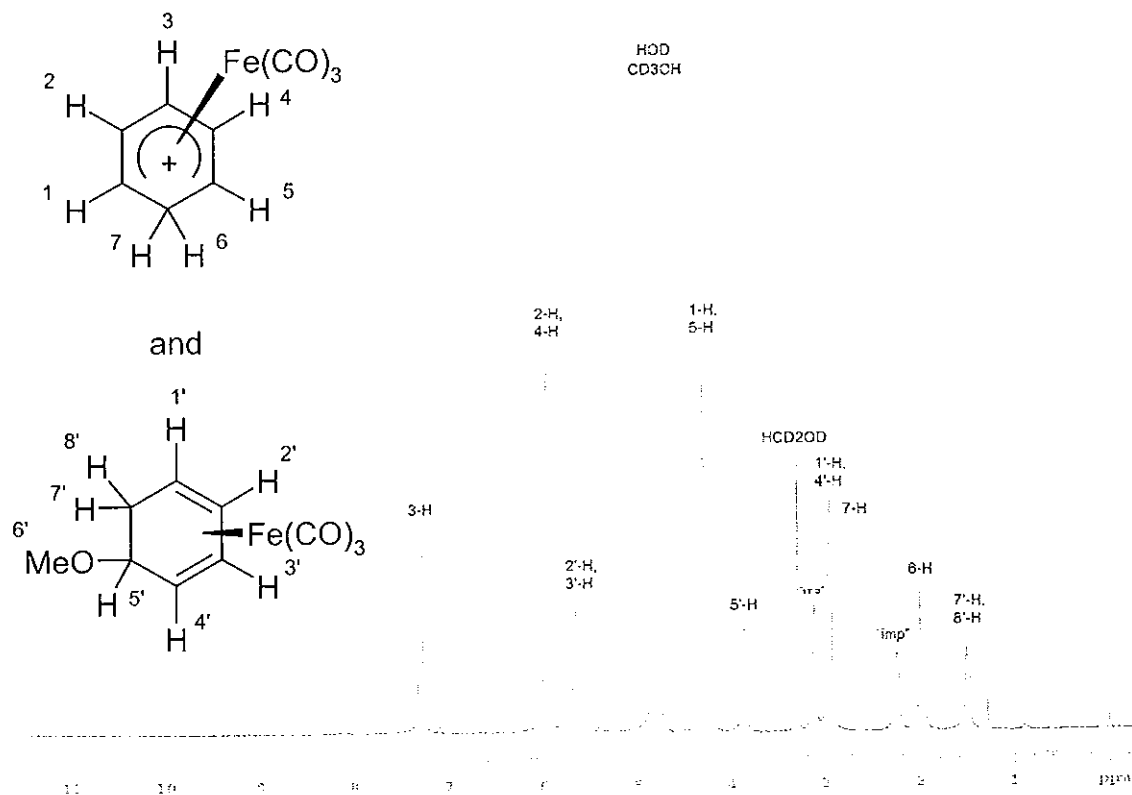


**Figure 2.30**  $^1\text{H}$  NMR spectrum of the  $(\eta^5\text{-cyclohexadienyl})\text{Fe}(\text{CO})_3^+$  cation (72) in deuterated methanol to which deuterium chloride has been added.



**Figure 2.31**  $^1\text{H}$  NMR spectrum of  $(\eta^4\text{-exo-5-methoxycyclohexa-1,3-diene})\text{tricarbonyliron}$  in deuterated methanol buffered with sodium cacodylate.





**Figure 2.32**  $^1\text{H}$  NMR spectrum of a mixture of the  $\eta^5$ -cyclohexadienyl)tricarbonyliron cation (72) and  $\eta^4$ -*exo*-5-methoxycyclohexa-1,3-diene)tricarbonyliron (104) in deuterated methanol.

## **CHAPTER 3**

### **DISCUSSION**

### 3 Discussion

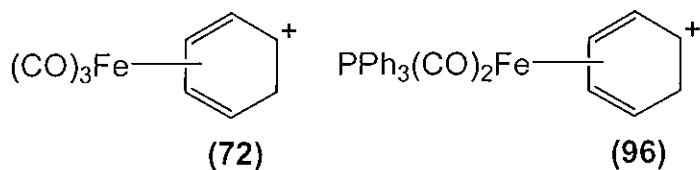
This chapter contains a discussion on the rates and equilibria for the hydrolysis of the ironcarbonyl-cyclohexadienyl cations investigated in this work. A synthetic pathway (Scheme 1.7) that can potentially be used to produce arene *trans*-dihydrodiols from their readily available *cis*-analogues utilises complexation to the tricarbonyliron moiety. An understanding of the mechanism of this pathway, a key step of which is the trapping of an ironcarbonyl coordinated cyclohexadienyl cation by a hydroxide nucleophile, is required however. The principal aim of this study was to investigate this trapping step by means of examining a model reaction. Thus the focus was on the tricarbonyliron complexed cyclohexadienyl cation (**72**) and some of its analogues. A quantitative study of their reactions with water was undertaken. In particular, the measurement of the equilibrium constant,  $pK_R$ , for the coordinated cations allows the stability of this species and the previously studied uncoordinated analogue to be compared. Implications for the arene *cis* to *trans*-dihydrodiol isomerisation by means of the ironcarbonyl-coordinated pathway will be examined.

#### 3.1 Cyclohexadienyl Complexes Examined

The complexes examined in this study are ironcarbonyl-coordinated analogues of the cyclohexadienyl cation (benzenonium ion). The uncoordinated cyclohexadienyl cation serves as a useful comparison to evaluate the effect of coordination to iron carbonyls on instability and reactivity. This cation has been studied previously by More O'Ferrall *et al.* and the equilibrium constants  $pK_R$  and  $pK_a$  for this species were determined.<sup>53</sup> It has been shown that in one molar acid, less than one molecule per mole of benzene exists in the protonated cyclohexadienyl cation form and, in aqueous solution, it is deprotonated at a rate close to the limiting rate of relaxation of the solvent.<sup>53</sup> A striking contrast is observed when the tricarbonyliron-coordinated cyclohexadienyl cation is examined. The coordinated species has been shown to be stable at mildly acidic pH and it can be recrystallised from water.<sup>52</sup> Moreover in the presence of bases it undergoes not deprotonation but nucleophilic addition. It is this stability and the electrophilic nature of these coordinated cyclohexadienyl cations that make them versatile reagents when reacting with nucleophiles. Some examples

showing how the coordinated cyclohexadienyl complexes have been utilised in syntheses were outlined in Section 1.2.5 (page 30).<sup>59,60,61</sup>

In this study, the two complexes ( $\eta^5$ -cyclohexadienyl)dicarbonyl-triphenylphosphineiron (**96**) and ( $\eta^5$ -cyclohexadienyl)tricarbonyliron (**72**) were examined.

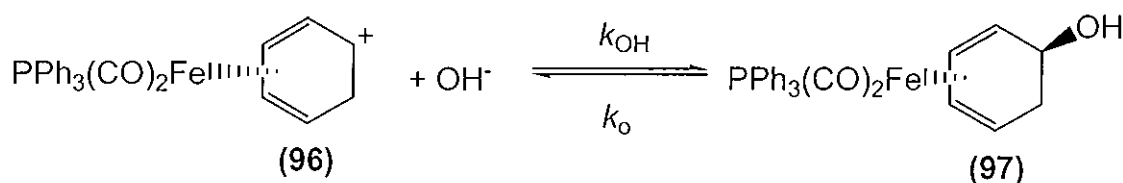


Initial work carried out previously in the group seemed to suggest that the tricarbonyliron coordinated cation (**72**) might be subject to nucleophilic attack by the hydroxide ion at the metal or carbonyl group.<sup>85</sup> Many research groups have reported that nucleophilic attack on ironcarbonyl complexes results in addition at various sites on the complexes including the ring and the carbonyl carbon.<sup>86,87</sup> Due to the uncertainty over the initial site of nucleophilic attack in the case of the coordinated cyclohexadienyl-tricarbonyliron cation, it was decided to replace one carbonyl ligand with a triphenylphosphine ligand to direct nucleophilic attack to the cyclohexadienyl ring and thus provide a model system that was expected to be relatively straightforward to examine. The directing effect of the triphenylphosphine group is due to both the steric hindrance to nucleophilic approach towards this bulky ligand and to an increased electron density on the iron atom that results. The increased electron density on iron is caused by the decreased  $\pi$ -acidity of the triphenylphosphine ligand compared to the carbonyl ligand it replaced.

### 3.2 pH Profile for ( $\eta^5$ -Cyclohexadienyl)dicarbonyltriphenylphosphineiron

When the hydrolysis reaction of ( $\eta^5$ -cyclohexadienyl)dicarbonyltriphenylphosphineiron (**96**) was monitored in aqueous sodium hydroxide at pH 11, a repetitive scan with an absorbance change of approximately 0.3 at 275 nm was observed (see Figure 2.2). As the hydroxide concentration of the aqueous solution decreased so too did the observed absorbance change.

The hydrolysis reaction was also monitored in aqueous carbonate and borate buffer solutions and the absorbance change grew smaller as the pH of the buffer solutions decreased. The decreasing change in absorbance is consistent with a reaction that is in equilibrium. In both carbonate and borate buffers, the reaction was reversible, allowing the ionisation of the coordinated hydrate (**97**) to be monitored. The reaction under examination is shown in Scheme 3.1 for which the equilibrium constant is  $K_C$ .



Scheme 3.1

The equilibrium constant for the reaction was obtained from absorbance changes accompanying the hydrolysis of ( $\eta^5$ -cyclohexadienyl)dicarbonyltriphenylphosphineiron as described by Albert and Serjeant.<sup>109</sup> The ratio of the absorbance changes is related to the equilibrium constant  $pK_R$  using the equation;

$$pK_R = \text{pH} + \log \left\{ \frac{(A_m - A)}{(A - A_l)} \right\}$$

The equilibrium constant determined by this method was found to be 9.87.

The equilibrium constant,  $K_C$ , could also be determined from the ratio of the forward and reverse rate constants. The observed rate constant,  $k_{\text{obs}}$ , is the sum of the forward and reverse reactions as shown in Equation 3.1. The rate constants ( $k_{\text{OH}}$  and  $k_0$ )

were measured as the slope and intercept of a plot of measured first order rate constants against the concentration of hydroxide ions (Section 2.1.2, Figure 2.4, page 52). The hydroxide catalysed rate constant,  $k_{\text{OH}}$ , was determined to be  $1.85 \text{ M}^{-1} \text{ s}^{-1}$  and the hydroxide independent rate constant,  $k_{\text{o}}$ , was found to be  $3.09 \times 10^{-4} \text{ s}^{-1\dagger}$ . Their ratio provides  $K_{\text{C}} = k_{\text{OH}} / k_{\text{o}}$ .

The equilibrium constant  $K_{\text{R}}$  is related to  $K_{\text{C}}$  by the equation;  $K_{\text{R}} / K_{\text{C}} = K_{\text{w}}$ , where  $K_{\text{w}}$  is the autoprotolysis constant of water. The equilibrium constant,  $\text{p}K_{\text{R}}$ , determined from kinetic measurements was 10.22.

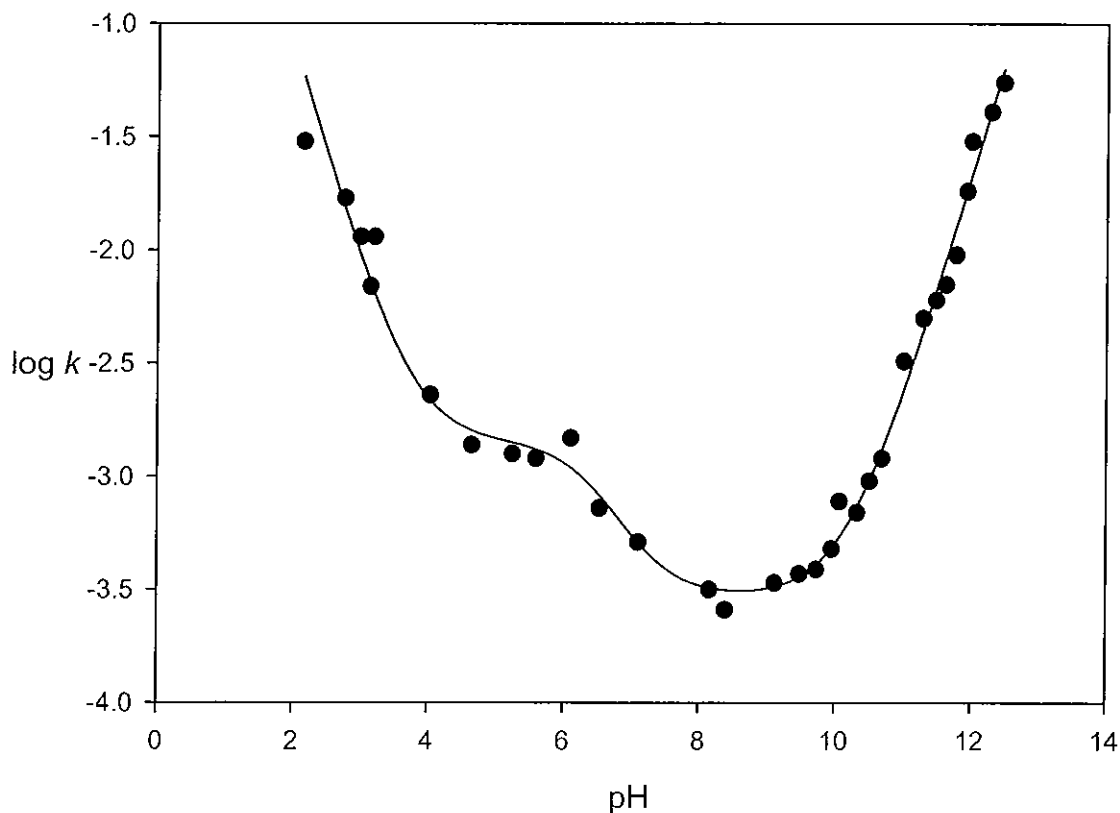
$$k_{\text{obs}} = k_{\text{OH}}[\text{OH}^-] + k_{\text{o}} \quad (3.1)$$

The hydrolysis of the coordinated cation (**96**) could be monitored in the pH range 9 – 12.5. At lower pHs the absorbance change became too small to measure accurately. Below pH 9 therefore, the hydrate (**97**) was generated by allowing the coordinated cation to hydrolyse fully in aqueous 0.001 M sodium hydroxide. The ionisation of the coordinated arene hydrate, ( $\eta^4$ -*exo*-5-hydroxy-1,3-cyclohexadiene)dicarbonyltriphenylphosphineiron (**97**), was then monitored at 275 nm by quenching into aqueous hydrochloric acid in chloroacetate, acetate, cacodylate and borate buffer solutions. Measurements at different buffer concentrations showed that the reaction did not show buffer catalysis.

A pH-profile for these reactions was prepared by plotting logs of the first order rate constants observed in sodium hydroxide, hydrochloric acid and buffer solutions against pH. This pH-profile is shown in Figure 3.1.

---

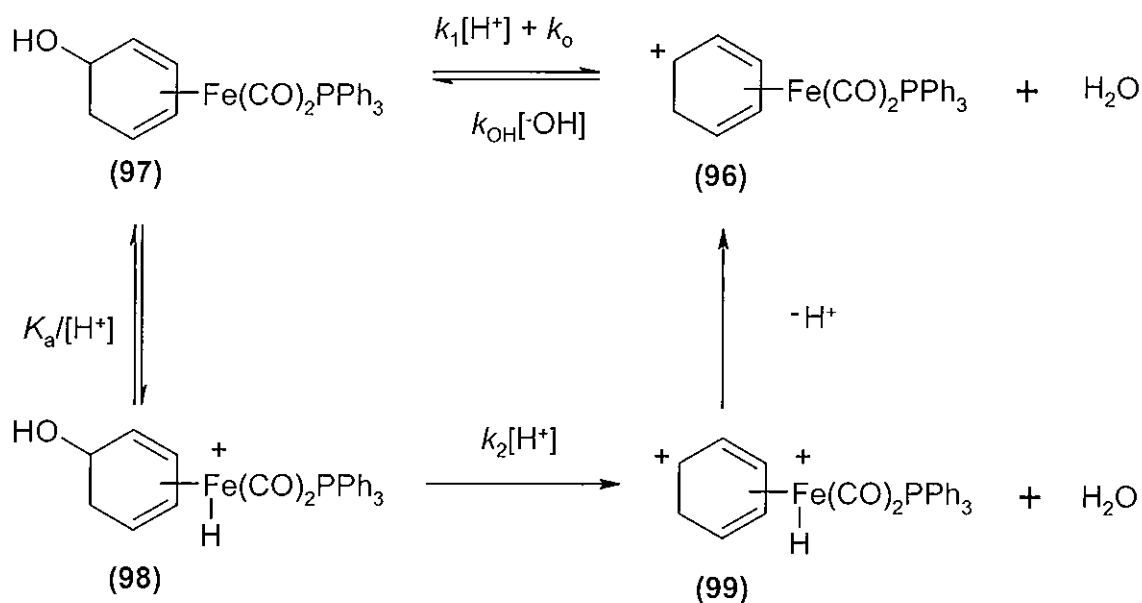
<sup>†</sup> See footnote, page 51 in relation to the value of  $k_{\text{o}}$  used here.



**Figure 3.1** pH profile ( $\log k_{\text{obs}}$  against pH) for the hydrolysis of ( $\eta^5$ -cyclohexadienyl)dicarbonyltriphenylphosphineiron (**96**) to the coordinated arene hydrate (**97**).

The changes in slope observed on the pH profile reflect changes to the mechanism of the reactions or of the reactant species undergoing reaction.<sup>88</sup> In the range from pH 10-14 the dependence of  $\log k_{\text{obs}}$  upon pH is consistent with the reaction shown in Scheme 3.1. A slope of 1 is observed indicating that the hydrolysis of ( $\eta^5$ -cyclohexadienyl)dicarbonyltriphenylphosphineiron (**96**) in this region of the profile is hydroxide ion dependent (OH<sup>-</sup>).

The remainder of the pH profile can be interpreted with reference to Scheme 3.2. The forward and reverse reactions of Scheme 3.1 are included at the top of Scheme 3.2 but with the hydrate (**97**) rather than the cation (**96**) as reactant and including acid catalysed formation of the cation with rate constant  $k_1$ .



Scheme 3.2

Between pH 8 and 10 on the pH profile, a pH independent reaction is observed in which water is the predominant reacting species. The water ionises the coordinated hydrate (97) to give the cation species (96). The rate constant for the reaction,  $k_0$ , is  $3.09 \times 10^{-4} \text{ M}^{-1} \text{ s}^{-1}$ .

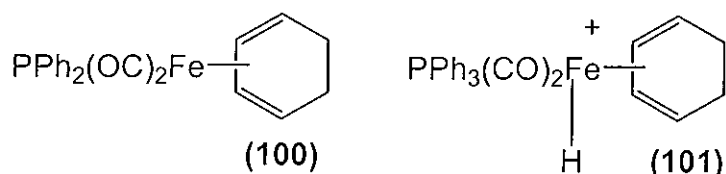
In the pH range 6 to 8, the predominant reactant species is the coordinated arene hydrate (97). The hydrate is ionised to the coordinated cation by an acid catalysed process and the rate constant determined for this reaction,  $3.59 \times 10^3 \text{ M}^{-1} \text{ s}^{-1}$ , can be assigned as  $k_1$ . Between pH 4 and pH 6 however the reaction becomes pH-independent. This is consistent with inactivation of the hydrate by a competing protonation equilibrium. The most plausible site for such a protonation is the iron atom as shown as (98) in Scheme 3.2. Between pH 4 and 6 the coordinated hydrate (97) and the metal protonated species (98) are in equilibrium. The predominant species is (98) which deprotonates to the hydrate (97), and is subsequently ionised to the coordinated cation *via* an acid-catalysed process. The equilibrium is shown on the left hand side of Scheme 3.2 and, from a best fit of the measured rate constants to a kinetic expression based on Scheme 3.2, a  $pK_a = 6.0$  is assigned to the protonated species. The reasonableness of this  $pK_a$  and the site of formation will be discussed in the following section.



Below pH 4, the predominant species is the fully formed protonated iron complex (**98**). Surprisingly, this undergoes an acid catalysed reaction for which it is difficult to think of a mechanism other than one similar to the ionisation of the parent hydrate to form the dication species (**99**). This dication is quickly deprotonated to give the coordinated ( $\eta^5$ -cyclohexadienyl)dicarbonyltriphenylphosphineiron cation (**96**). The acid catalysed rate constant for the reaction,  $k_2$ , was found to be  $8.2 \text{ M}^{-1} \text{ s}^{-1}$ . The reaction is shown at the bottom and right hand side of Scheme 3.2.

### 3.2.1 Protonated Iron Complex

As the metal protonated hydrate species (**98**) was not isolable, protonation of the corresponding ( $\eta^4$ -cyclohexa-1,3-diene)dicarbonyltriphenylphosphineiron (**100**) lacking a hydroxyl group was studied. Both  $^1\text{H}$  NMR and FTIR spectroscopic evidence for the formation of the metal protonated complex (**101**) were obtained.



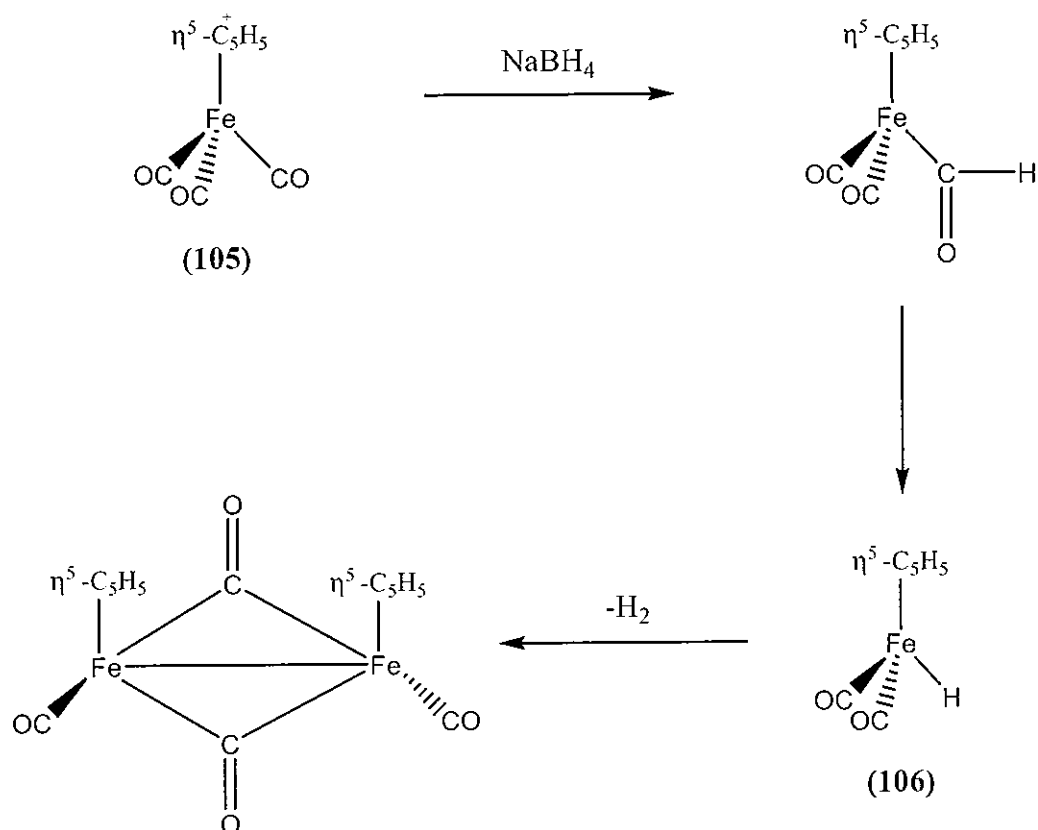
The  $^1\text{H}$  NMR signal for the proton bonded to the metal is a characteristic of metal hydride complexes and is usually observed as a high field shift between -5 and -15 ppm. For the  $^1\text{H}$  NMR studies carried out, the neutral complex (**100**) was dissolved in deuterated chloroform and a drop of trifluoroacetic acid added. The flask was shaken vigorously and a colour change was noted immediately indicating that a reaction was occurring. On examination of the resulting  $^1\text{H}$  NMR spectrum, a high field signal at -6.45 ppm was observed. An attempt was made to monitor the reaction as it occurred by diluting some trifluoroacetic acid in deuterated chloroform (~10%) and then adding this diluted acid solution drop wise to a freshly prepared solution of (**100**) but a systematic growth in the hydride signal was not observed.

It was however possible to monitor the progress of the protonation reaction using FTIR spectroscopy. The neutral complex (**100**) was dissolved in chloroform and a solution of trifluoroacetic acid in chloroform was then added drop-wise. The spectra

recorded show the intensity of the carbonyl absorption band increasing in frequency as the charge on the iron atom develops. This is in keeping with observations made by Birch *et al.* who reported that positively charged tricarbonyliron complexes show higher frequency absorption bands for their carbonyl ligands than their neutral analogues.<sup>52</sup>

Thus, this observation of metal hydride formation by protonation of the neutral ( $\eta^4$ -cyclohexa-1,3-diene)dicarbonyltriphenylphosphineiron complex supports the formation of the metal hydride complex proposed in Scheme 3.2.

In the literature, examples of metal hydrides have been known for many decades. Two species of hydrides which have been observed for ironcarbonyl complexes are  $\text{H}_2\text{Fe}(\text{CO})_4$  and  $[\text{HFe}(\text{CO})_3(\text{PPh}_3)_2]^+$ . These have been shown to provide high field  $^1\text{H}$  NMR signals of -11.1 and -7.6 ppm respectively.<sup>82</sup> A complex which leads to a more pronounced high field shift is ( $\eta^5$ -cyclopentadienyl)tricarbonyliron (**105**) whose hydride complex (**106**) was observed as an intermediate, during the reaction of (**105**) with sodium borohydride ( $\text{NaBH}_4$ ) in acetone to produce a dimer complex. The reaction is shown in Scheme 3.3.



Scheme 3.3

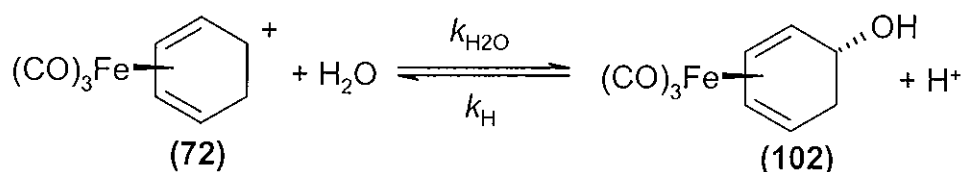
The reaction outlined in Scheme 3.3 was followed by both  $^1\text{H}$  NMR and FTIR spectroscopy.<sup>89</sup> The  $^1\text{H}$  NMR signal for the hydride proton in complex **(106)** occurred at -15.34 ppm. The carbonyl bands of  $(\eta^5\text{-cyclopentadienyl})\text{tricarbonyliron}$  **(105)** have a frequency of 2125 and 2075  $\text{cm}^{-1}$ , which reduced in frequency to 2014 and 1952  $\text{cm}^{-1}$  on formation of the metal hydride complex. This is a similar pattern to the one observed in this study and both correlate to the observations made by Birch *et al.*<sup>52</sup> The chemical shift of the hydride proton of **(101)** studied in this work is at lower field (-6.3 ppm) than most previously studied hydride complexes. This is consistent with its positive charge, and bears a close similarity to the chemical shift of -7.6 for  $[\text{HFe}(\text{CO})_3(\text{PPh}_3)_2]^+$ .<sup>82</sup>

Attempts to monitor protonation of **(100)** by UV-Vis spectroscopy in mixed aqueous solvents were unsuccessful. As far as can be determined, more acidic solutions were required for the protonation of **(100)** than the arene hydrate complex **(97)**. Nevertheless the clear evidence of protonation of **(100)** at the iron atom from FTIR and

$^1\text{H}$  NMR spectroscopy offers strong support for interpretation of the acid region of the pH profile of Figure 3.1 as shown in Scheme 3.2.

### 3.3 Measurements of Rates and Equilibria for the Reaction of ( $\eta^5$ -Cyclohexadienyl)tricarbonyliron

The completion of the pH profile for the ( $\eta^5$ -cyclohexadienyl)-dicarbonyltriphenylphosphineiron cation complex (**96**) provided a starting point to allow the parent iron tricarbonyl cation complex (**72**) to be analysed with greater confidence. It had been reported by Birch *et al.* that the coordinated benzene hydrate complex (**102**) can be precipitated from a solution of the corresponding cation (**72**) by addition of sodium bicarbonate.<sup>52</sup> This implies that the equilibrium constant,  $pK_R$ , for the cation is below 10 (the  $pK_a$  of the bicarbonate anion) and should be measurable at mildly acidic pHs.

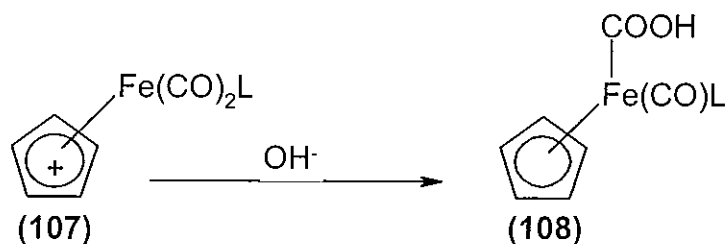


Scheme 3.4

It would also be expected that complex (**102**), ( $\eta^4$ -*exo*-5-hydroxy-1,3-cyclohexadiene)tricarbonyliron, would be less easily ionised than ( $\eta^4$ -*exo*-5-hydroxy-1,3-cyclohexadiene)dicarbonyltriphenylphosphineiron (**97**), where a carbonyl ligand has been replaced by a triphenylphosphine ligand. This is due to a lower electron density in complex (**102**) when compared to (**97**) as triphenylphosphine is electron donating relative to a carbonyl group.<sup>30</sup>

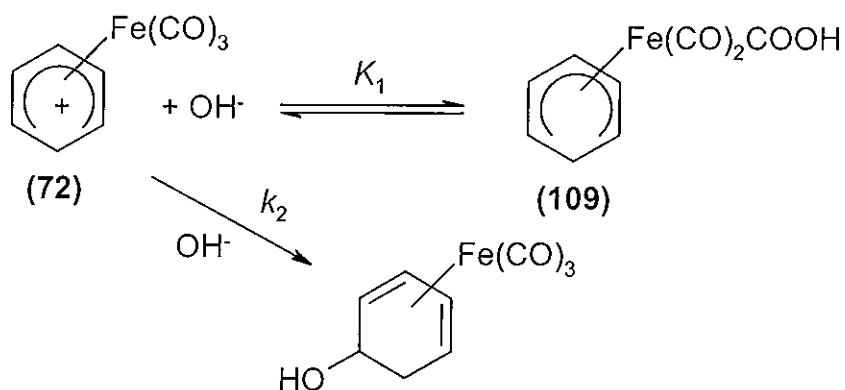
Hydroxide attack at the carbonyl carbon of irontricarbonyl complexed cyclic dienyl cations has previously been reported by Pettit *et al.*<sup>90</sup> and Atton and Kane-Maguire.<sup>78</sup> Pettit and his co-workers isolated metalcarboxylic acids (**108**) by reacting ( $\eta^5$ -cyclopentadienyl)-carbonyliron complexes of type (**107**) with sodium hydroxide as shown in Scheme 3.5, where L = CO or PPh<sub>3</sub>. Interestingly one of the complexes

studied in this work had a carbonyl ligand replaced by a triphenylphosphine, ( $\eta^5$ -cyclopentadienyl)dicarbonyltriphenylphosphineiron (**108**, when L = PPh<sub>3</sub>).



Scheme 3.5

Atton and Kane-Maguire examined the mechanism of addition of the hydroxide nucleophile to the carbonyl carbon of ( $\eta^5$ -cyclohexadienyl)tricarbonyliron (**72**). From their mechanistic studies, they came to the conclusion that a carboxylic acid species (**109**) is formed in a rapid pre-equilibrium and this is followed by hydroxide addition to the ring which proved to be an irreversible step. The mechanism deduced by Atton and Kane-Maguire is presented in Scheme 3.6. The hydroxide catalysed rate constant, denoted  $k_2$  in Scheme 3.6, was determined to be  $1 \times 10^5 \text{ M}^{-1} \text{ s}^{-1}$  at 0°C. Estimating that an increase of 10°C doubles the rate constant, a value of  $5.6 \times 10^5 \text{ M}^{-1} \text{ s}^{-1}$  is obtained. This is as expected, much faster than the hydroxide catalysed rate constant determined for the hydrolysis of ( $\eta^5$ -cyclohexadienyl)dicarbonyltriphenylphosphineiron (**96**) of  $2.06 \text{ M}^{-1} \text{ s}^{-1}$



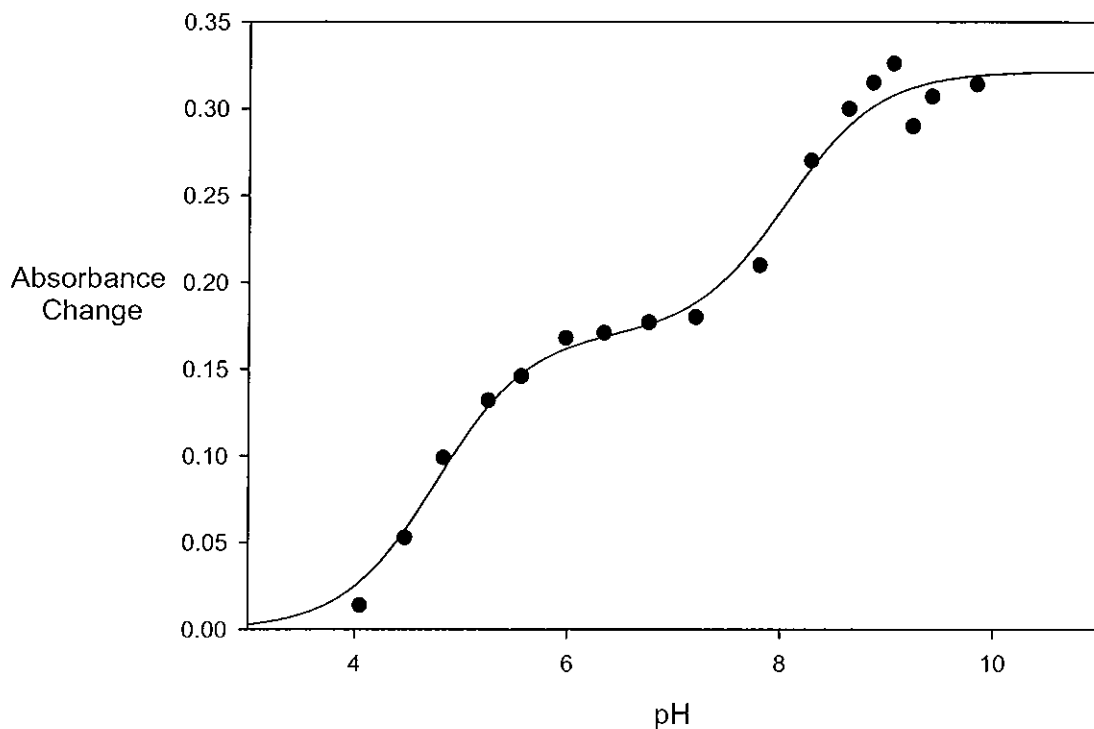
Scheme 3.6

Thus, hydroxide attack at the carbonyl group has been reported by two research groups independently but it is worth noting that these observations were made

at high hydroxide ion concentrations (~0.1M) only. Thus, the initial concern over competing hydroxide attack at the carbonyl ligand that led to the decision to examine the dicarbonyltriphenylphosphineiron complexed cation (**96**) first was misplaced.

On monitoring the hydrolysis of the ( $\eta^5$ -cyclohexadienyl)tricarbonyliron (**72**) cation, it was found that only a small absorbance change in the UV spectrum accompanied the reaction. Nevertheless, it was possible to monitor absorbance changes at 250 nm. Initial measurements in borate and carbonate buffers showed that the rate of reaction depended on buffer concentration and was not reversible. However this contrasted with studies carried out below pH 8 in cacodylate, phosphate, acetate and methoxyacetate buffers for which no dependence on buffer concentration occurred. The results obtained below pH 8 are consistent with interconversion between the coordinated cation (**72**) and the coordinated benzene hydrate (**102**) taking place (see Scheme 3.4, p 131). The irreversible reaction that occurred in borate and carbonate buffers also caused a change in the UV spectrum, as shown in Figure 3.2.

The plot in Figure 3.2 was constructed from data collected during the monitoring of the hydrolysis reaction of the cation (**72**), as well as the ionisation reaction of the hydrate (**102**). The reactions were monitored by UV-Vis absorption spectrophotometry with the aid of a fast mixing accessory in a range of buffer solutions. The absorbance change for reaction (the difference between the final and initial absorbance) on a kinetic time scan at 250 nm was plotted against the pH of the buffers in which the reaction was occurring. As can be seen in Figure 3.2, two inflection points are observed, an indication of two different reactions taking place. The lower inflection point provides an equilibrium constant  $pK_R = 4.77$ . The absorbance change above pH 8 is likely to be a result of reaction between the buffer bases and the cation.



**Figure 3.2** A plot of absorbance changes at 250 nm against pH for the hydrolysis of ( $\eta^5$ -cyclohexadienyl)tricarbonyliron in aqueous buffers at 25°C.

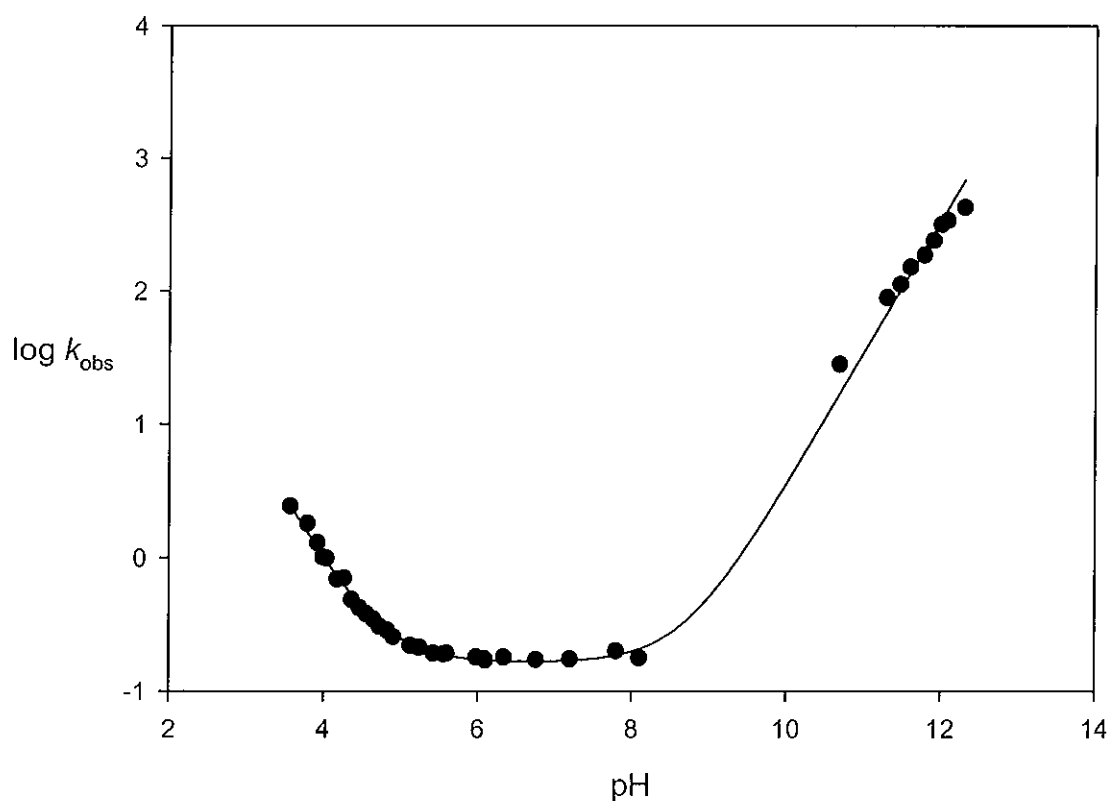
Using the results obtained below pH 8, it was possible to determine the rate constants for the conversion of hydrate to cation and for the reverse reaction. The reverse reaction was studied by quenching the coordinated hydrate species (72), generated by quenching the cation in a dilute cacodylate buffer, into excess acetate or methoxyacetate buffers. The rate constant for conversion of the cation to the hydrate,  $k_{H_2O}$ , was found to be  $0.177 \text{ s}^{-1}$  and the acid catalysed rate constant,  $k_H$ , measured for the reaction of the hydrate to form the coordinated cation, was  $8.3 \times 10^3 \text{ M}^{-1} \text{ s}^{-1}$ . The equilibrium constant,  $pK_R$ , for formation of the coordinated benzene hydrate from the corresponding cation determined from these results was 4.71. This is in good agreement with the spectrophotometrically determined value of 4.87.

### 3.3.1 pH Profile

All of the evidence obtained with respect to the reaction of ( $\eta^5$ -cyclohexadienyl)tricarbonyliron (72) with water and methanol supports the proposal that in acidic media the reactions proceed directly by *anti* addition to the formal

carbocation centre providing the *exo* substituted complex. Addition of a nucleophile to other sites in the complex was not observed. The observed data for the reaction of water with the coordinated cation can be combined with the data reported by Atton and Kane-Maguire<sup>78</sup> to provide the pH profile shown in Figure 3.3. As noted above the latter measurements were multiplied by a factor of 5.6 to allow for the difference between 0° and 25°C. The line drawn through the points in Figure 3.3 represents a best fit of observed to calculated rate constants based on the expression shown in Equation 3.2.

$$k_{\text{obs}} = k_{\text{H}_2\text{O}} + k_{\text{H}}[\text{H}^+] + k_2[\text{OH}^-] \quad (3.2)$$

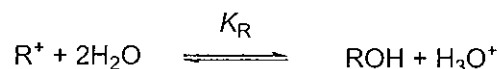


**Figure 3.3** pH profile ( $\log k$  against pH) for the hydrolysis of the ( $\eta^5$ -cyclohexadienyl)tricarbonyliron cation to the coordinated arene hydrate. Prepared from observed data and data previously reported by Atton and Kane-Maguire.<sup>78</sup>



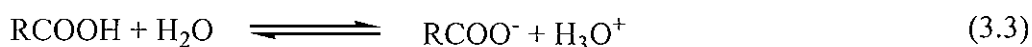
### 3.3.2 Isotope Effects for Rate and Equilibrium Constants

The hydrolysis of ( $\eta^5$ -cyclohexadienyl)tricarbonyliron (**72**) to form the coordinated hydrate (**102**) can be expressed as shown in Scheme 3.7, in which the hydrate and cation structures (in Scheme 3.4) are replaced by ROH and  $R^+$  respectively.



Scheme 3.7

Considering the water molecules on the left hand side of Scheme 3.7, one effectively converts three O-H bonds to three O-H<sup>+</sup> bonds on reaction of the cation (**72**) to produce the hydrate (**102**) while one OH of water is converted to that of the hydrate. The O-H bond in  $H_3O^+$  is weaker than in water and this leads to an isotope effect when a hydrogen atom is replaced by a deuterium, accompanying a change in solvent from  $H_2O$  to  $D_2O$ . The main factor which controls the solvent isotope effect for such a reaction is a contribution of 0.7 per hydrogen to  $k_{D_2O}/k_{H_2O}$  for the conversion of O-H to O-H<sup>+</sup>. The calculated equilibrium solvent isotope effect is therefore  $K_R^{D_2O}/K_R^{H_2O} = 0.7^3 = 0.35$ .<sup>83</sup> The ionisation of carboxylic acids can be considered as an analogous reaction as shown in Equation 3.3.

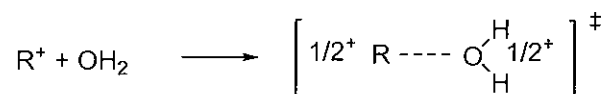


When carboxylic acids are ionised three O-H to O-H<sup>+</sup> bond conversions occur. Calculating the solvent isotope effect when the reaction is carried out contributes  $0.7^3 = 0.35$  to  $K_{D_2O}/K_{H_2O}$  as above. Gold determined the solvent isotope effect for the ionisation of acetic acid and found  $K_{D_2O}/K_{H_2O} = 0.30$ , close to the calculated value.<sup>91</sup> This may also be expressed as  $K_{H_2O}/K_{D_2O} = 3.27$ .

To return to the hydrolysis of (**72**) examined in this study, a similar factor of  $1/(0.7)^3$  is expected to contribute to the solvent isotope effect. The measured value of the equilibrium solvent isotope effect,  $K_R^{H_2O}/K_R^{D_2O} = 2.8$ , which is also close to the expected value. Variations between measurements have been attributed to small

contributions to the isotope effects from the OH bond of the product or water molecules in the solvation shells of reactants or products.

The kinetic solvent isotope effect on the rate constant for the forward reaction,  $k_1$ , is estimated from the difference between the transition state and reactants as shown in Scheme 3.8.

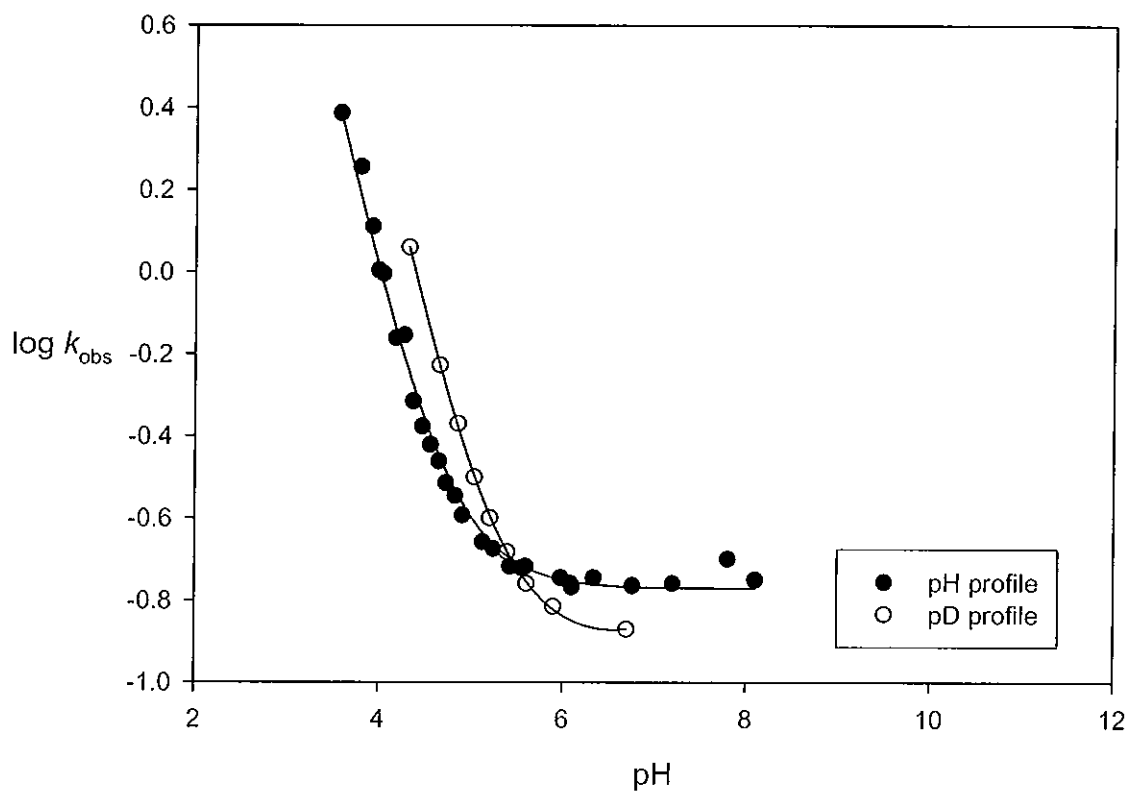


Scheme 3.8

At the transition state, two O-H bonds are partially converted to two O-H<sup>+</sup> bonds and this contribution may be approximated as  $k_1^{D_2O}/k_1^{H_2O} = 0.7^{0.5} \times 0.7^{0.5} = 0.7$ . To estimate the solvent isotope effect in the reverse direction, *i.e.* ionisation of the coordinated hydrate (102), Equation 3.4 is used which provides a value of  $k_{-1}^{D_2O}/k_{-1}^{H_2O} = 0.7/0.35 = 2.0$ . The kinetic solvent isotope effect observed in this study was 2.4, close to the calculated value.

$$k_{-1}^{D_2O}/k_{-1}^{H_2O} = (k_1^{D_2O}/k_1^{H_2O}) / (K_R^{D_2O}/K_R^{H_2O}) \quad (3.4)$$

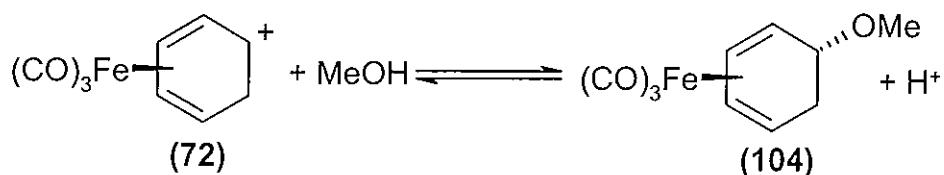
The effect of carrying out the hydrolysis and ionisation reactions in either water or deuterium oxide can be graphically represented by plotting the log of the observed rate constants for reaction against pH (or pD). In Figure 3.4, the pH and pD-profiles constructed from the observed experimental data are overlaid. It can be seen from the overlay that, to the left of the inflection points of both profiles, the reaction being observed (ionisation of the hydrate to cation) proceeds faster in D<sub>2</sub>O than in water. To the right of the inflection points, the opposite observation is made. Thus, on reaction of the cation to hydrate, the reaction is faster in water than it is in D<sub>2</sub>O.



**Figure 3.4** Combined pH and pD profile for the hydrolysis of the ( $\eta^5$ -cyclohexadienyl)tricarbonyliron cation to the coordinated arene hydrate.

### 3.3.3 Measurements of $pK_R$ in Methanol

The reaction of ( $\eta^5$ -cyclohexadienyl)tricarbonyliron (**72**) in methanol was also examined. This allowed the equilibrium constant,  $pK_R$ , for the interconversion shown in Scheme 3.9 between the cation and the methoxy substituted analogue (**104**) of the hydrate (**102**) to be determined.



Scheme 3.9

Measurements of  $pK_R$  in methanol proved to be easier to perform than those in water as buffered solutions were not required. Another advantage was that the results obtained in methanol could be directly compared with those from a  $^1\text{H}$  NMR study performed in the same solvent. This is important as UV spectra provide no structural information about the species that are being examined.

Analysis of spectrophotometric measurements for ( $\eta^5$ -cyclohexadienyl)-tricarbonyliron (**72**) in methanol containing (a) 5% aqueous perchloric acid and (b) 50% aqueous perchloric acid provided equilibrium constant values,  $pK_R = 0.91$  and  $2.53$  respectively. The difference in  $pK_R$  between the reactions with water ( $pK_R = 4.77$ ) and with the methanol containing 5% aqueous perchloric acid is  $\Delta pK_R = 3.8$ . This difference is characteristic of a reaction occurring at a carbocation centre and reflects the greater 'carbon' than proton basicity of a methoxide anion of 100-fold.<sup>92</sup> Another factor influencing the difference is the greater (proton) basicity of methanol than water. The equilibrium constant,  $pK_a$ , for the conjugate acid of methanol,  $\text{MeOH}_2^+$ , has been shown by Perdoncin and Scorrano to be  $-2.05$ .<sup>93</sup> This contributes a factor of  $10^{2.05}$  to the difference between  $pK_R$ s in methanol and water. The influence of these factors is seen from writing the ratio of  $K_R$  values in  $\text{H}_2\text{O}$  and methanol as in Equation 3.6 in which ROH and ROME represent the coordinated hydrate and methyl ether respectively. The ratio corresponds to the equilibrium shown in Equation 3.5. Thus, the relative values determined for  $pK_R$  in water and methanol are as expected.



$$K_R^{\text{H}_2\text{O}} / K_R^{\text{MeOH}} = [\text{H}_3\text{O}^+][\text{ROH}][\text{MeOH}] / [\text{H}_2\text{O}][\text{ROME}][\text{MeOH}_2^+] \quad (3.6)$$

The  $^1\text{H}$  NMR spectra recorded confirmed that the transformation being monitored in the UV spectrophotometric measurements was the methanolysis reaction shown in Scheme 3.9. The spectrum of a solution of the cation (**72**) in deuterated methanol was found to contain a mixture of the cation and the methoxy substituted complex (**104**). Modification of the pH of the deuterated methanol solution by addition of acid (deuterium chloride) or a buffer base (sodium cacodylate) resulted in spectra that respectively showed the fully formed coordinated cation (**72**) only and the methoxy

substituted complex (104) only (Section 2.4, Figures 2.30, 2.31 and 2.32, pages 118 - 120).

### 3.4 Comparison of Measured Equilibrium Constants with Those in the Literature

Table 3.1 lists equilibrium constants,  $pK_R$ , for a range of coordinated and uncoordinated carbocations. A comparison between the species included in the table allows the effects of coordination with tricarbonyliron and dicarbonyltriphenylphosphineiron to be explored. In the table,  $C_7H_7^+$  is the tropylium ion and  $C_7H_9^+Fe(CO)_3$  is the tricarbonyliron coordinated cycloheptadienyl cation.

**Table 3.1** Comparison of the equilibrium constants,  $pK_R$ , between various coordinated and uncoordinated carbocations.

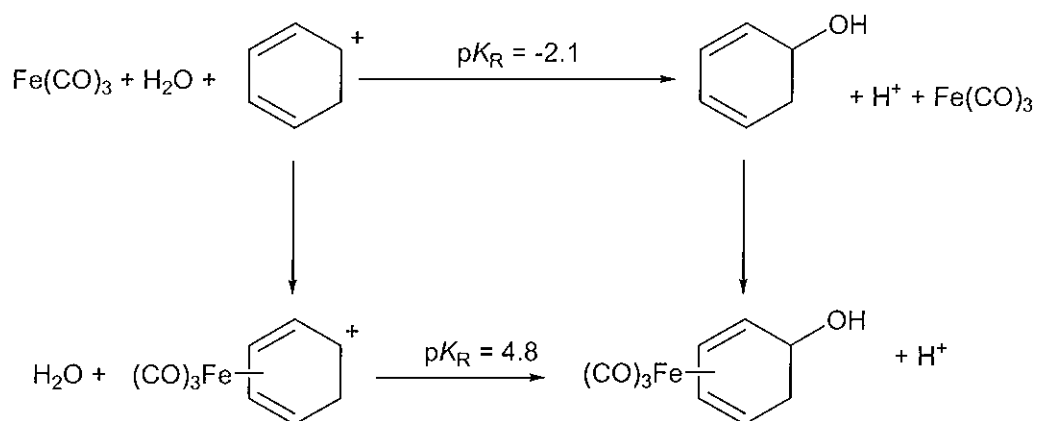
Complex	$pK_R$
$C_6H_7^+$	-2.1 <sup>a</sup>
$C_6H_7^+Fe(CO)_3$	4.8
$C_6H_7^+Fe(CO)_2PPh_3$	9.9
$C_7H_7^+$	4.7 <sup>b</sup>
$C_7H_7^+Fe(CO)_3$	4.5 <sup>b</sup>
$C_7H_9^+Fe(CO)_3$	4.7 <sup>b</sup>

(a) More O'Ferrall *et al.*<sup>53</sup>

(b) Pettit *et al.*<sup>94</sup>

To begin with, the  $pK_R$  values for the two cations examined in this study, ( $\eta^5$ -cyclohexadienyl)tricarbonyliron (72) and its triphenylphosphine substituted analogue, ( $\eta^5$ -cyclohexadienyl)dicarbonyltriphenylphosphineiron (96), may be compared. The values measured were 4.7 and 9.9 respectively and show that the triphenylphosphine substituted cation complex (96) is the more stable. This is an expected result as the triphenylphosphine ligand is electron donating and stabilises the formal carbocation centre on the cyclohexadienyl cation.

The  $pK_R$  values for (72) and (96) can also be compared with  $pK_R = -2.1$  for the uncoordinated cyclohexadienyl cation previously determined by More O’Ferrall *et al.*<sup>53</sup> The difference in  $pK_R$  values ( $\Delta pK_R$ ) between the tricarbonyliron coordinated and the uncoordinated cyclohexadienyl cation is 6.9. The positive value for this difference shows that coordination of the tricarbonyliron group has a greater stabilising effect on the cation than the cyclohexadienyl moiety of the hydrate. This becomes clear if the reactions are written as a thermodynamic cycle as in Scheme 3.10. If it is recognised that the  $pK_R$  values correspond to differences in free energy, then the differences in  $pK_R$  values for the horizontal reactions in the scheme are equal to the difference in “ $pK$ s” for the vertical reactions representing coordination of the tricarbonyliron group.

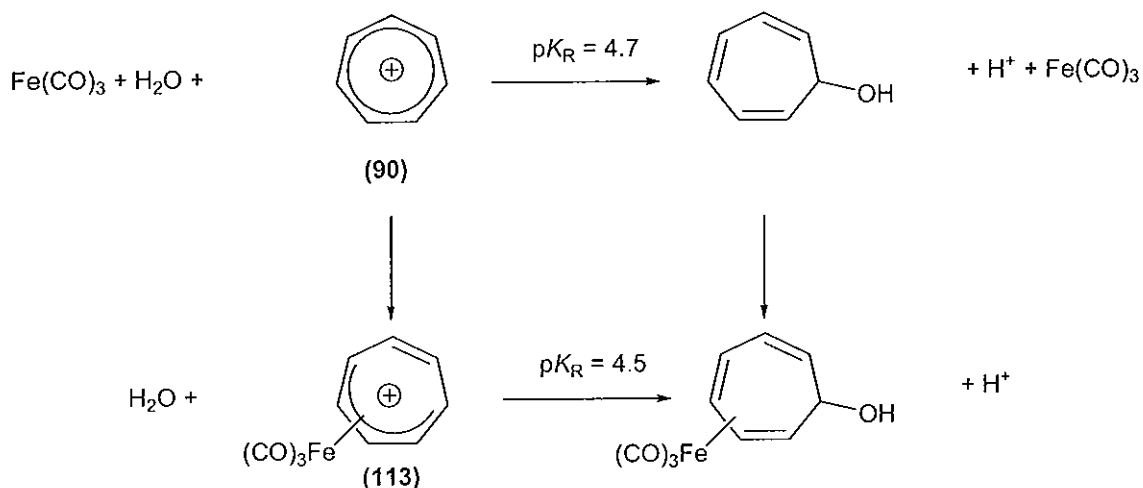


**Scheme 3.10**

A greater difference,  $\Delta pK_R = 12.0$ , is obtained between the cyclohexadienyl cation and the same cation coordinated to dicarbonyltriphenylphosphineiron. This represents an even greater relative stabilisation of the cation.

The comparison between the uncoordinated and tricarbonyliron-coordinated cyclohexadienyl cations is complemented by a similar comparison between coordinated and uncoordinated cycloheptatrienyl cations (tropylium ions), (90) and (113). The value of  $pK_R$  for the uncoordinated tropylium ion is 4.7 and that for the coordinated cation was determined by Pettit to be 4.5.<sup>94</sup> These values are shown in Table 3.1. In contrast to the cyclohexadienyl example  $\Delta pK_R = -0.2$  and is close to zero and  $pK_R$  is practically unchanged between the coordinated and uncoordinated cations. As

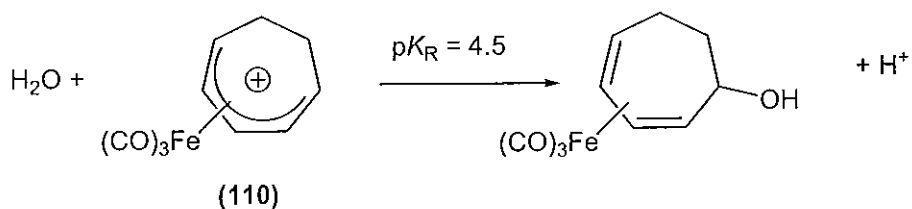
confirmed in Scheme 3.11 this means that the stabilising effect of tricarbonyliron on the neutral cycloheptatriene and tropylium ion is the same.



Scheme 3.11

The reason for this must be that the stabilising effect of coordination in the tropylium ion is offset by a loss of aromaticity in the uncoordinated cation. This is emphasised by writing the coordinated cation as non-aromatic with the tricarbonyliron group coordinated to a pentadienyl cation segment of the ion and an unconjugated double bond.

The correctness of this interpretation is confirmed by the fact that the cation (110) formed from the tricarbonyliron coordinated cycloheptadienol has the same  $pK_R$  (= 4.5) as the coordinated tropylium ion as shown in Scheme 3.12.<sup>94</sup> This means that the “unconjugated” double bond in the tropylium ion has a resonance interaction with the coordinated fragment of the iron that is no stronger than a terminal double bond of cycloheptatriene.



Scheme 3.12

This analysis has implications for the original comparison between coordinated and uncoordinated cyclohexadienyl cations.

Mayr<sup>95</sup> investigated the kinetics of reactions between a range of uncharged nucleophiles and the coordinated and uncoordinated tropylium cations. From this study, Mayr concluded that coordination of tricarbonyliron to the aromatic tropylium cation had little effect on the cation's electrophilicity, resulting in the two species having a similar reactivity towards nucleophiles. This result would have been predicted on the basis of the equilibrium values reported by Pettit.<sup>94</sup> Extending the comparison to the uncoordinated and tricarbonyliron coordinated dihydrotropylium ions, a similar pattern of reactivity to that observed for the coordinated and uncoordinated cyclohexadienyl cations is noted as the free ion is  $10^5$  to  $10^6$  times more reactive towards nucleophiles. (See below for the reactivity of the cyclohexadienyl cation)

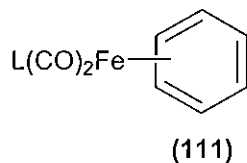
It should be noted however that the coordinated cyclohexadienyl cation undergoes different reactions to the uncoordinated analogue. The uncoordinated cation is deprotonated in aqueous solution to form benzene whilst the coordinated cations undergo nucleophilic attack in the same solvent. It may be more appropriate therefore to compare the  $pK_R$  values for the coordinated cation with the  $pK_a$  rather than  $pK_R$  of the cyclohexadienyl cation.

The  $pK_a$  of the cyclohexadienyl cation was previously determined by More O'Ferrall *et al.*<sup>53</sup> by combining a rate constant for protonation of benzene with an estimated value for deprotonation of the cyclohexadienyl cation ( $5 \times 10^{10} \text{ s}^{-1}$ ) close to the limit for solvent relaxation. The value obtained was -24.3. This corresponds to a difference of 35 units between ( $\eta^5$ -cyclohexadienyl)dicarbonyltriphenylphosphineiron (**96**) and the cyclohexadienyl cation and of 29 units between ( $\eta^5$ -cyclohexadienyl)tricarbonyliron (**72**) and the cyclohexadienyl cation. This represents a difference in stability of nearly  $48 \text{ kcal mol}^{-1}$  in the former case and  $40 \text{ kcal mol}^{-1}$  for the latter.

The fact that nucleophilic attack occurs in preference to deprotonation of the coordinated cations is characteristic of carbocations that react to form a non-aromatic double bond.<sup>23,96</sup> This suggests the conclusion that if the coordinated cations underwent

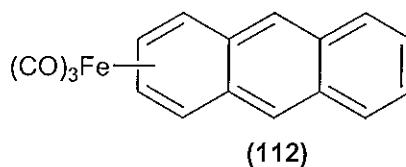


deprotonation to produce a coordinated benzene complex (111), two of the double bonds would be coordinated to the ironcarbonyl moiety whilst the one remaining double bond would be essentially olefinic in character.



(L = CO or PPh<sub>3</sub>)

The coordinated benzene complex has not yet been isolated but tricarbonyliron complexes of methyl naphthalenes<sup>97</sup> and anthracene (112)<sup>98</sup> have been reported. Manuel was able to prepare the tricarbonyliron coordinated anthracene by a direct reaction of anthracene with dodecacarbonyltriiron in refluxing cyclohexane for 48 hours.<sup>98</sup> Manuel did not succeed in preparing the coordinated naphthalene complex by the same method but methylnaphthalenes coordinated to tricarbonyliron have subsequently been reported.<sup>97</sup>



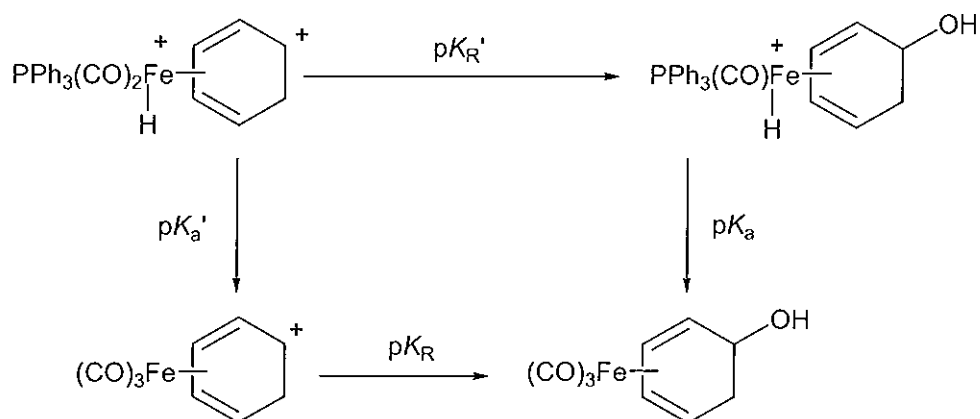
### 3.5 Comparison of Rate Constants For the Coordinated and Uncoordinated Cyclohexadienyl Cations

A comparison between the rate constants determined in this study for the hydrolysis reactions of the coordinated cations ( $\eta^5$ -cyclohexadienyl)-dicarbonyltriphenylphosphineiron (**96**) and ( $\eta^5$ -cyclohexadienyl)tricarbonyliron (**72**), and the rate constants for the uncoordinated cyclohexadienyl cation, previously determined by More O'Ferrall *et al.* can be made.<sup>53</sup> Such a comparison allows the effect of coordination to the tricarbonyliron and dicarbonyltriphenylphosphineiron moieties on the reactivity of the cyclohexadienyl ring to be explored. Table 3.2 lists the acid catalysed rate constants,  $k_H$ , for formation of the carbocations from their corresponding hydrates, the rate constants for the attack of water on the carbocations,  $k_{H_2O}$ , and their equilibrium constants,  $pK_R$ .

**Table 3.2** Rate constants for a range of coordinated and uncoordinated carbocations.

Complex	$10^{-3} k_H (M^{-1} s^{-1})$	$k_{H_2O} (s^{-1})$	$pK_R$
$C_6H_7^+$	0.18	$2.3 \times 10^4$	-2.1
$C_6H_7^+Fe(CO)_3$	8.3	0.177	4.7
$C_6H_7^+Fe(CO)_2PPh_3$	3.6	$4.53 \times 10^{-7}$	9.9
$C_6H_7^+Fe^+H(CO)_2PPh_3$	0.008	-	-

Also included in Table 3.2 is the rate constant,  $k_H$ , attributed to the reaction of the dicarbonyltriphenylphosphineiron complex protonated on the iron atom. The  $pK_a$  of this protonated complex could be determined by taking the cation, ( $\eta^5$ -cyclohexadienyl)dicarbonyltriphenylphosphineiron (**96**), and investigating its protonation in aqueous solution. Once the  $pK_a$  was known the  $pK_R$  value of this protonated complex could be estimated from the thermodynamic cycle in Scheme 3.13. Combining  $K_R$  with  $k_H$  then gives a value for  $k_{H_2O}$ .



**Scheme 3.13**

The rate constant,  $k_{\text{H}_2\text{O}}$ , listed for the cyclohexadienyl cation in Table 3.2 has been estimated from data for  $pK_R$  and  $k_{\text{H}}$  for the formation of this ion by More O'Ferrall *et al.*<sup>53</sup> The rate constant is  $2.3 \times 10^4 \text{ s}^{-1}$ , which is  $10^5$  times faster than the tricarbonyliron coordinated cation and  $10^{10}$  times faster than the dicarbonyltriphenylphosphineiron cation. This difference in reactivity with water of the three carbocations is expected from their equilibrium constants and reflects the stability of the different species. The acid catalysed rate constants would be expected to follow the opposite pattern with the more stable carbocation forming more rapidly. Interestingly, however  $(\eta^5\text{-cyclohexadienyl})\text{tricarbonyliron}$  (**72**) and its triphenylphosphine substituted analogue (**96**) are formed at almost the same rate from their hydrate complexes.

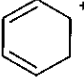
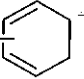
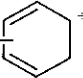

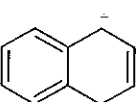
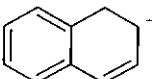
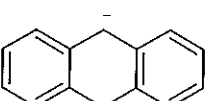
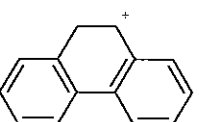
A more dramatic result is apparent when one extends the comparison to the uncoordinated cyclohexadienyl cation. The carbocation is formed only slightly more slowly than the coordinated cations and the uncoordinated cation is formed only 20 times more slowly than the dicarbonyltriphenylphosphineiron cation, despite a difference of twelve units in  $pK_R$ . This is a striking observation as the equilibrium constant for the cyclohexadienyl cation shows it to be far less stable than the coordinated species. Recall that the uncoordinated cation undergoes deprotonation at a rate close to the limiting rate of relaxation of the solvent in water whereas the tricarbonyliron complexed cation can be recrystallised in aqueous solution. This leads to the conclusion that the acid catalysed rate constants change only slightly on moving from the uncoordinated to coordinated cations whilst the rate constant for attack of water on the cations increases sharply as the equilibrium constant increases. At present

there is no obvious explanation for this behaviour and further measurements will be required to interpret it.

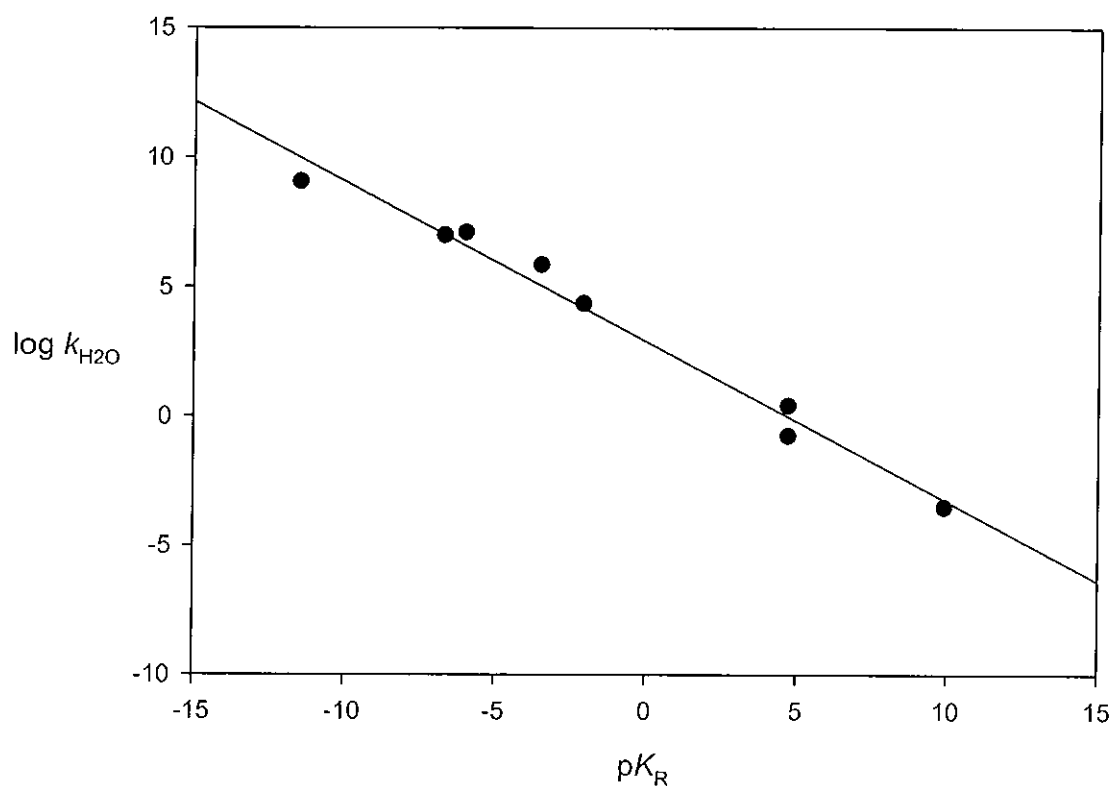
In Table 3.2, it is noticeable on examination of the acid-catalysed rate constants that  $k_{\text{H}}$  for formation of the protonated iron complex has a significantly lower value than for the other carbocations. This may be a result of the positive charge on the complex making attack of  $\text{H}^+$  less favourable.

The normal behaviour of values of  $k_{\text{H}_2\text{O}}$  for attack of water on the carbocation is confirmed by the fact that a linear free energy correlation exists between logs of these rate constants and the equilibrium constants,  $\text{p}K_{\text{R}}$ , for a range of protonated aromatic molecules. Such correlations are described in a review by McClelland where plots of  $\log k_{\text{H}_2\text{O}}$  versus  $\text{p}K_{\text{R}}$  are reported for a wide range of cations.<sup>99</sup> For the carbocations studied in this work, Table 3.3 lists the rate and equilibrium constants together with a range of protonated aromatic molecules and the plot is given in Figure 3.4.

**Table 3.3** Logs of rate constants,  $\log k_{\text{H}_2\text{O}}$ , and equilibrium constants,  $\text{p}K_{\text{R}}$ , for a range of coordinated and uncoordinated carbocations.

Complex	$\log k_{\text{H}_2\text{O}}$	$\text{p}K_{\text{R}}$
	4.36 <sup>a</sup>	-2.1 <sup>a</sup>
$(\text{CO})_3\text{Fe}$ - 	-0.75	4.7
$\text{PPh}_3(\text{CO})_2\text{Fe}$ - 	-6.34	9.9
	0.42 <sup>b</sup>	4.7 <sup>c</sup>
	5.86 <sup>d</sup>	-3.5 <sup>e</sup>
	7.0 <sup>a</sup>	-6.7 <sup>a</sup>
	7.11 <sup>a</sup>	-6.0 <sup>a</sup>
	9.07 <sup>d</sup>	-11.5 <sup>d</sup>

(a) More O'Ferrall *et al.*<sup>53</sup> (b) Ritchie and Fleischhauer.<sup>100</sup> (c) Mayr *et al.*<sup>95</sup> (d) More O'Ferrall *et al.*<sup>101</sup> (e) More O'Ferrall *et al.*<sup>23</sup>



**Figure 3.4** Plot of  $\log k_{H_2O}$  versus  $pK_R$  for protonated aromatic cations and their coordinated complexes.

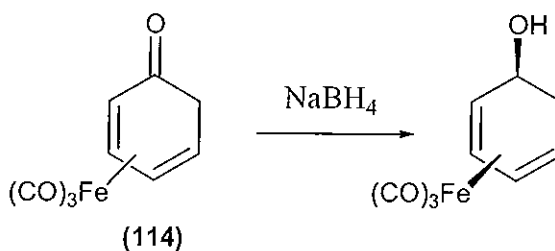
The slope of the plot in Figure 3.4 is  $-0.62 \pm 0.03$ . This value corresponds well with values obtained for similar plots of a wide range of structurally related carbocations as reported by McClelland, Pettit and Taft. The points for the coordinated cations lie to the right of the plot. The plot would suggest that the coordinated cations are behaving as normal carbocations.

### 3.6 Conversion of Arene *Cis*- to *Trans*- Dihydrodiols via their Tricarbonyliron Complexes

A principal aim of carrying out this study was to obtain mechanistic information pertinent to the synthesis of arene *trans*-dihydrodiols from their *cis*-counterparts. A potential pathway for the conversion of the isomers is *via* their tricarbonyliron coordinated complexes (*cf* Section 1.1.2, Scheme 1.7). The step of this synthetic scheme of most interest in this study was the trapping of the coordinated cation intermediates by water and hydroxide nucleophiles. The intermediates contain a hydroxyl group  $\beta$  to the charge centre. A model reaction was examined which did not contain the  $\beta$ -hydroxyl group, the products of which were coordinated arene hydrates. Coordination of the cyclohexadienyl cation by both the tricarbonyliron group and dicarbonyltriphenylphosphineiron moiety was examined. Taking the information obtained in this study, the implications for the *cis* to *trans* conversion will be discussed.

#### 3.6.1 Isomerisation of *Exo*-substituent to *Endo*-substituent

The nucleophilic attack of hydroxide on ( $\eta^5$ -cyclohexadienyl)tricarbonyliron (**72**) investigated in this study produces the hydroxyl substituted complex in which the hydroxyl substituent is *exo* to the tricarbonyliron fragment. Evidence to support the production of the *exo* isomer comes from  $^1\text{H}$  NMR spectroscopy data. Birch has shown that direct addition of hydroxide to (**72**) provides only the *exo* isomer.<sup>52</sup> This observation was supported independently by Atton and Kane-Maguire who isolated only the *exo* isomer on addition of hydroxide to (**72**).<sup>78</sup> The *endo* isomer has been previously prepared by Birch *et al.*<sup>52</sup> by sodium borohydride reduction of the tricarbonyliron coordinated keto complex (**114**) as shown in Scheme 3.14.



Scheme 3.14

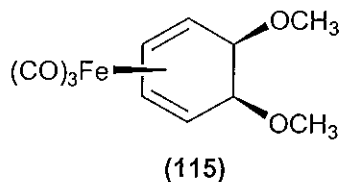
The rate constant,  $k_H$ , for the acid-catalysed reaction of the *endo*-substituted complex to form the tricarbonyliron coordinated cyclohexadienyl cation has been measured previously and found to be  $2.0 \times 10^{-3} \text{ M}^{-1} \text{ s}^{-1}$ .<sup>85</sup> This implies that the *endo* isomer is more than  $10^6$  times less reactive than its *exo* analogue for which  $k_H$  was found to be  $8.3 \times 10^3 \text{ M}^{-1} \text{ s}^{-1}$ . A comparison of the relative stabilities of both isomers has not yet been carried out but a possible explanation for the increased reactivity of the *exo* isomer would be a favourable interaction between the hydroxyl group of the *endo* isomer and the tricarbonyliron moiety

The *exo* and *endo* isomers of the corresponding methoxy substituted tricarbonyliron-cyclohexadiene complexes (shown below) have however been examined by Johnson *et al.*<sup>102</sup> In this investigation, it was found that after reacting ( $\eta^5$ -cyclohexadienyl)tricarbonyliron in refluxing methanol for 20 minutes, TLC analysis showed that the major product formed was the *exo* substituted complex and only small amounts of the *endo* isomer were present. However, when the reaction was allowed to continue to reflux for a total of 23 hours, the isomeric *endo* complex was obtained as the major product. An additional experiment carried out on ( $\eta^4$ -*exo*-5-methoxycyclohexa-1,3-diene)tricarbonyliron, showed that addition of one drop of tetrafluoroboric acid to a methanol solution followed by stirring at 20°C gave the *endo* complex initially but, when stirring was continued for 23 days, an equilibrium ratio of [*endo*] / [*exo*] of approximately 2 was reached. If it is assumed that a similar ratio occurred for the isomers of ( $\eta^4$ -5-hydroxycyclohexa-1,3-diene)tricarbonyliron, it can be concluded that they differ little in stability. A larger *kinetic* barrier to reaction for the *endo* isomer would therefore be implied. This larger kinetic barrier could be a result of the difference in how the species are formed, e.g. if the *endo* isomer is formed by initial attack of water or methanol on the metal centre.<sup>52</sup> It could also be because coordination by the tricarbonyliron group severely inhibits attack from the *endo* direction.

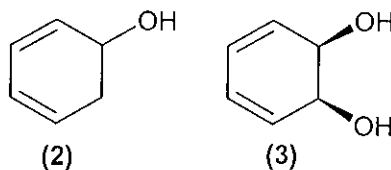




Recently, a sample of the complex, ( $\eta^4$ -*endo-cis*-5,6-dimethoxycyclohexa-1,3-diene)-tricarbonyliron (115) has been synthesised and an initial kinetic investigation has shown that the acid catalysed rate constant is 100 times smaller<sup>103</sup> than that of the tricarbonyliron coordinated *endo*-cyclohexadiene hydrate.<sup>85</sup>

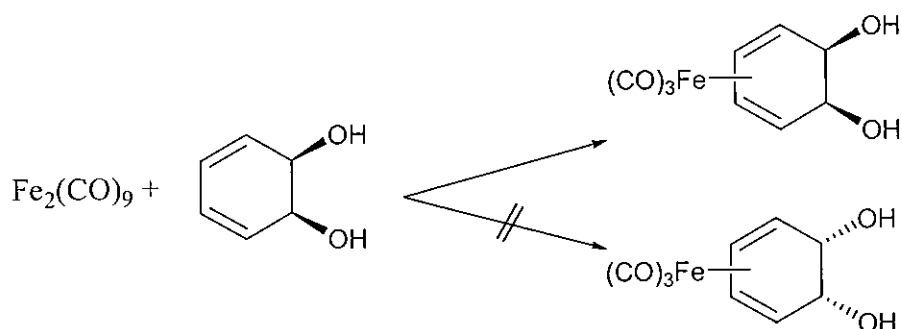


It would not be expected that a large difference in reactivity would be observed between the hydroxy and methoxy leaving groups. Therefore, it can be concluded that the second  $\beta$ -oxygen slows the reaction. A similar observation has been previously reported for the uncoordinated species. Benzene hydrate (2) was found to react 1600 times faster than *cis*-benzene dihydrodiol (3).<sup>104</sup> The structures of these compounds are shown below.



### 3.6.2 Implications for the Conversion of Arene *Cis*-Dihydrodiols to *Trans*-Dihydrodiols via Coordination to Ironcarbonyls

From these results, we can draw some inferences about the mechanism of interconversion of *cis*- and *trans*- benzene dihydrodiols. In the first place, if there is little difference in stability of *exo* and *endo* complexes, it is perhaps not surprising that reaction of the *cis*-diol with pentacarbonyliron ( $\text{Fe}(\text{CO})_5$ ) or nonacarbonyliron diiron ( $\text{Fe}_2(\text{CO})_9$ ) yield an *endo* complex in preference to the *exo* complex (Scheme 3.15). However it seems clear that the *endo* complex does not experience any strong stabilisation from interaction between the iron atom and hydroxyl groups.



Scheme 3.15

Secondly, it is apparent that the difficult step in the isomerisation is conversion of an *endo* diol to a cyclohexadienyl cation complex. This will require relatively strong acid (TFA or  $\text{HPF}_6$ ).<sup>105</sup> The synthetic conditions reported in the literature involve reaction with hexafluorophosphoric acid in acetic anhydride solvent. Under these conditions the hydroxyl groups will be acetylated but it is not clear how this will affect the reaction. If the acetylation promotes a solvolysis reaction, a stronger carboxylic acid such as trifluoroacetic acid might be more effective.

However what is clear is that once the carbocation is formed, quenching in a nucleophilic solvent will rapidly lead to reaction at the *exo* position forming the coordinated *trans* product.

The main conclusion to be drawn therefore is that the best strategy for improving the synthetic procedure is to explore and optimise conditions for conversion of *cis*-diol complexes to their carbocations.

### 3.7 Conclusion

The work carried out in this study has allowed the determination of the extent to which the cyclohexadienyl cation is stabilised by coordination to a tricarbonyliron or a dicarbonyltriphenylphosphineiron group. The equilibrium constants,  $\text{p}K_{\text{R}}$ , for formation of the coordinated arene hydrates from the coordinated cations, were found to be 9.9 and 4.8 respectively. Comparison to the uncoordinated cyclohexadienyl cation ( $\text{p}K_{\text{R}} = -2.1$ ) indicates a difference in stability of  $10^7$  and  $10^{12}$  respectively.

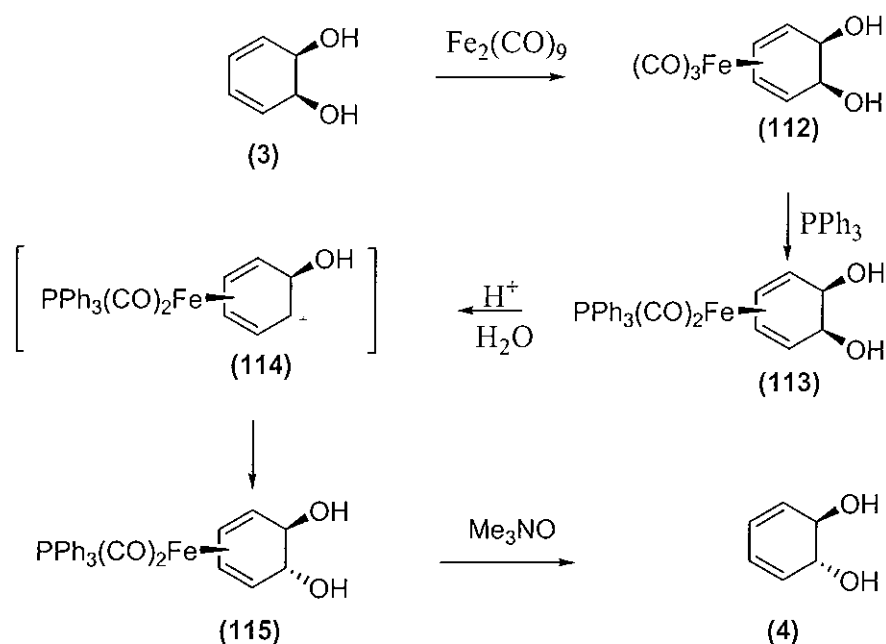
However, this large difference in stability fails to reflect the difference in reactivity of the species. The coordinated cations undergo a different reaction in aqueous solution to the uncoordinated cation, hydrolysis rather than deprotonation, and if the acid dissociation constant,  $pK_a$ , of the cyclohexadienyl cation is compared with the  $pK_R$  values of the coordinated species, differences in reactivity of nearly 48 kcal mol<sup>-1</sup> and 40 kcal mol<sup>-1</sup> are observed. Thus, it can be inferred that if these coordinated cations underwent deprotonation to form the corresponding coordinated benzene complexes, two of the double bonds would be coordinated and the remaining double bond would be olefinic

Comparisons were made between the cations studied in this work and other coordinated and uncoordinated cations. In the case of the tricarbonyliron coordinated tropylium ion, it was found that it had a similar  $pK_R$  value (4.5) to the corresponding coordinated cyclohexadienyl cation. Interestingly, the uncoordinated tropylium ion ( $pK_R = 4.7$ ) has a similar stability to its coordinated analogue. This is attributed to the aromatic stabilisation for the tropylium ion being comparable to the stabilising effect of tricarbonyl coordination on a dienyl system

Investigation of the reaction of the ( $\eta^5$ -cyclohexadienyl)tricarbonyliron cation in methanol provided a  $pK_R$  for the methanolysis reaction of 1.0. A comparison was made between the spectrophotometric measurements and <sup>1</sup>H NMR spectra obtained and the changes observed were consistent. From this comparison of data, it can be concluded that trapping of the coordinated cations by the nucleophiles examined in this study provides the kinetically favoured *exo* substituted products.

A full pH profile for reaction of the dicarbonyltriphenylphosphineiron coordinated cyclohexadienyl cation to form the coordinated arene hydrate was developed in this study. In the acidic region of the profile, an additional reaction was found to be occurring and was assigned to protonation at the iron atom. Evidence supporting the existence of a protonated iron complex was obtained by examining the reaction with trifluoroacetic acid of a related complex, ( $\eta^4$ -cyclohexa-1,3-diene)-dicarbonyltriphenylphosphineiron, by means of FTIR and <sup>1</sup>H NMR spectroscopy.

There are also implications from the work performed for the development of the synthetic route to convert arene *cis*-dihydrodiols to their *trans*-isomers via their tricarbonyliron coordinated complexes. The pH profile for the dicarbonyltriphenylphosphineiron coordinated cyclohexadienyl cation indicates that above pH 6, nucleophilic attack occurs at the cyclohexadienyl ring with no indication of any other reaction occurring. Future work would therefore include an undertaking to carry out the conversion of arene *cis*-dihydrodiols (3) to the *trans*-dihydrodiols (4) using the dicarbonyltriphenylphosphineiron moiety as shown in Scheme 3.16. In addition, it can be concluded that the *endo* complex does not experience any strong stabilisation from interaction between the iron atom and hydroxyl groups and that the nucleophilic capture of the coordinated carbocation is via kinetically favoured *exo* substitution (Section 1.1.2, Scheme 1.7). The difficult step in the isomerisation route will be the conversion of the coordinated *endo* diol to the corresponding cation. Thus the best strategy for improving the process is to explore and optimise conditions for conversion of *cis*-diol complexes to their carbocations.



Scheme 3.16

## **CHAPTER 4**

### **EXPERIMENTAL**

## 4 Experimental Details

### 4.1 General Instrumentation

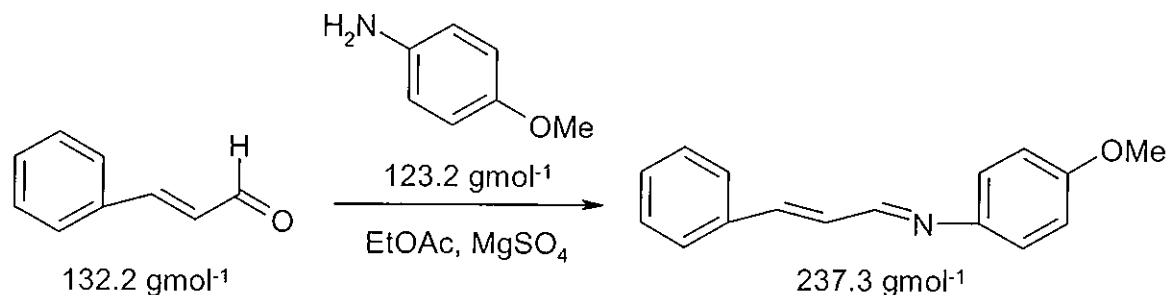
NMR spectra were recorded in deuterated chloroform with tetramethylsilane (TMS) as an internal reference unless otherwise stated. A Gemini 200 instrument operating at 200 MHz was used for  $^1\text{H}$  NMR spectra and at 50 MHz for  $^{13}\text{C}$  NMR spectra. Some  $^1\text{H}$  NMR experiments were carried out in University College Dublin on Varian instruments operating at either 400 MHz or 500 MHz. Melting points were recorded using an Electrothermal 9100 series melting point apparatus and are uncorrected. Microanalyses were carried out by the Microanalytical Unit, School of Chemistry and Chemical Biology, University College Dublin. Silica gel (Merck, Grade 9385, 230-300 Mesh, 60 Angstrom) was used for all purification by flash chromatography which was carried out as described by Leonard *et al.*<sup>106</sup> IR spectra were recorded on a Perkin Elmer Paragon Series FTIR 1000 instrument. Thin layer chromatography was carried out using aluminium-backed or plastic-backed Merck Kieselgel F<sub>254</sub> plates.

### 4.2 Synthesis of Organic Substrates for Kinetic and Equilibrium Measurements

#### 4.2.1 ( $\eta^5$ -Cyclohexadienyl)dicarbonyltriphenylphosphineiron Hexafluorophosphate

The title compound was synthesised in four steps according to the methods of Knölker *et al.*,<sup>45</sup> Pearson and Raithby<sup>107</sup> and Birch *et al.*<sup>66</sup> as follows:

- (i) 1-(4-methoxyphenyl)-4-phenyl-1-azabuta-1,3-diene (tricarbonyliron transfer reagent)

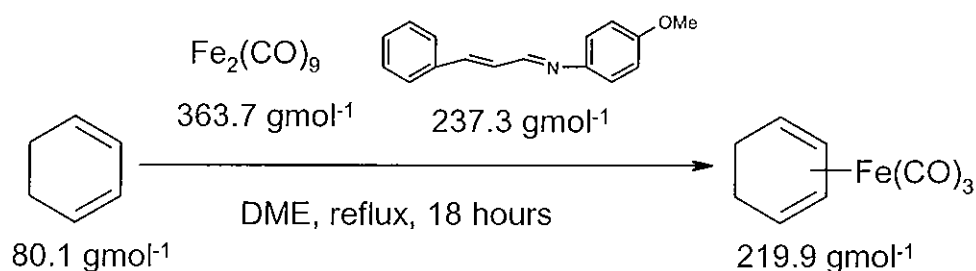


*Trans*-cinnamaldehyde (11.03 g, 83 mmol) and *p*-anisidine (9.77 g, 79 mmol) were dissolved in ethyl acetate (150 ml). Magnesium sulfate (4 g) was added and the mixture (a light brown/very dark red solution with an off white suspension) was stirred for 4 hours under a nitrogen atmosphere to yield a light brown solution with suspended yellow crystals and hydrated magnesium sulphate. At this point, TLC analysis showed that all of the *p*-anisidine had reacted (2:1 40-60 petroleum ether / diethyl ether, R<sub>f</sub> of *p*-anisidine, 0.07). The solution was filtered to yield a solid residue, which was washed with ethyl acetate (3 x 50 ml). The filtrate and washes were combined and evaporation of solvent using the rotary evaporator was carried out slowly at a water bath temperature of 40 °C until crystallisation began. Pentane (100 ml) was then added to the warm solution and, on cooling in an ice bath, crystals formed. Filtering under vacuum and washing with cold pentane (50 ml) yielded the product as light green crystals (5.88 g), m.p. 121 – 122°C (lit.,<sup>45</sup> 122 °C).

The filtrate was sealed under nitrogen in a round bottomed flask, placed in an ice bath and stirred for one hour. Filtration under vacuum yielded a further portion of product (1.45 g, m.p 120-122°C). The product was stored in a freezer under a nitrogen atmosphere (39% total yield).

$\nu_{\max} / \text{cm}^{-1}$ (KBr disc):	3050 ( $sp^2$ C-H), 1655 (C=N), 1627 (C=C), 1600 (aromatic C=C), 1503 (aromatic C=C), 1252 (C-O), 1030 (C-N)
$\delta_{\text{H}} / \text{ppm}$ (200 MHz, $\text{CDCl}_3$ ):	3.79 (3H, s, $\text{OCH}_3$ ), 6.90 (2H, br d, $J = 8.8$ hz, aromatic CHs), 7.09 (2H, m), 7.20 (2H, br d, $J = 8.8$ hz, aromatic CHs), 7.36 (3H, m, aromatic CHs), 7.51 (2H, m), 8.26 (1H, d, HC=N)
$\delta_{\text{C}} / \text{ppm}$ (50 MHz, $\text{CDCl}_3$ ):	55.32 ( $-\text{OCH}_3$ ), 114.29 (2 x CH, methoxyphenyl), 122.12 (2 x CH, methoxyphenyl), 127.26 (2 x CH, phenyl), 128.63 (CH, phenyl), 128.77 (2 x CH, phenyl), 129.26 (CH, Ph-CH=C), 135.63 (C, phenyl), 142.90 (Ph-CH=C), 144.39 (C, methoxyphenyl), 158.28 (C, methoxyphenyl), 159.34 (C=N)

(ii) ( $\eta^4$ -cyclohexa-1,3-diene)tricarbonyliron



1-(4-methoxyphenyl)-4-phenyl-1-azabut-1,3-diene, the transfer reagent, (0.98 g, 4.15 mmol), 1,3-cyclohexadiene (3.02 g, 37.75 mmol) and nonacarbonyldiiron<sup>‡</sup> (5.07 g, 13.94 mmol) were dissolved in 1,2-dimethoxyethane (180 ml, anhydrous) and refluxed for 18 hours under argon or nitrogen. The solvent was then evaporated to yield

<sup>‡</sup> On storing, nonacarbonyldiiron can decompose resulting in pyrophoric iron particles being produced. An aqueous hydrochloric acid solution (~1M) was on hand to neutralise the pyrophoric iron if the need arose.



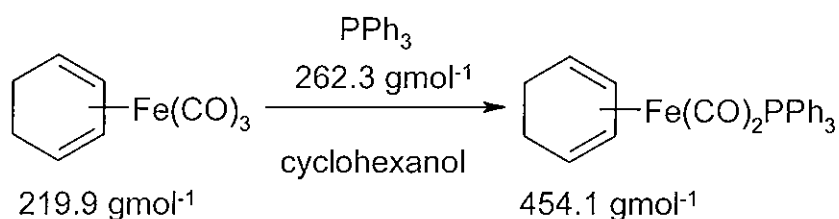
a dark brown residue (12.04 g). The crude product was purified by flash chromatography (9:1 pentane/ethyl acetate, several columns were necessary,  $R_f = 0.71$ ) on silica gel to yield the irontricarbonyl complex as a yellow oil (2.96 g, 48%).<sup>45</sup>

$\nu_{\max} / \text{cm}^{-1}$  (liquid film): 3070 ( $sp^2$  C-H), 2985 ( $sp^3$  C-H), 2053 (C=O), 1944 (C=O), 1466, 1330, 1180

$\delta_{\text{H}} / \text{ppm}$  (200 MHz,  $\text{CDCl}_3$ ): 1.56-1.78 (4H, m,  $2 \times \text{CH}_2$ ), 3.22 (2H, s<sup>§</sup>,  $2 \times \text{CH}_2\text{CH}=\text{CH}$ ), 5.31 (2H, dd,  $2 \times \text{CH}_2\text{CH}=\text{CH}$ )

$\delta_{\text{C}} / \text{ppm}$  (50 MHz,  $\text{CDCl}_3$ ): 23.83 ( $2 \times \text{CH}_2$ ), 62.55 ( $2 \times \text{CH}_2\text{CH}=\text{CH}$ ), 85.39 ( $2 \times \text{CH}_2\text{CH}=\text{CH}$ ), 212.65 ( $\text{Fe}(\text{CO})_3$ )

(iii)  $(\eta^4\text{-cyclohexa-1,3-diene})\text{triphenylphosphinedicarbonyliron}$



$(\eta^4\text{-cyclohexa-1,3-diene})\text{-tricarbonyliron}$  (2.01 g, 9.16 mmol) and triphenylphosphine (2.54 g, 9.68 mmol) were dissolved in cyclohexanol (58 ml) and refluxed under nitrogen for 14 hours. The reaction mixture (dark green solution) was allowed to cool, petroleum ether (b.p. 40 - 60°C, 100 ml) was added and the mixture was stirred in an ice bath for 2 hours. The resulting precipitate (a complex of  $\text{Fe}(\text{CO})_3(\text{PPh}_3)_2$ ) was removed by filtration. The petroleum ether was removed from the filtrate by evaporation on the rotary evaporator. The cyclohexanol was then removed by distillation at 10 mbar to give a yellowish residue. The residue was recrystallised from

<sup>§</sup> A singlet was observed but a multiplet would be expected. Gibson (S.E. Gibson, *Transition Metals in Organic Synthesis*, Oxford University Press, 1997) has noted that, in ironcarbonyl complexes, paramagnetic iron salts can be present which result in broadening of NMR spectra.

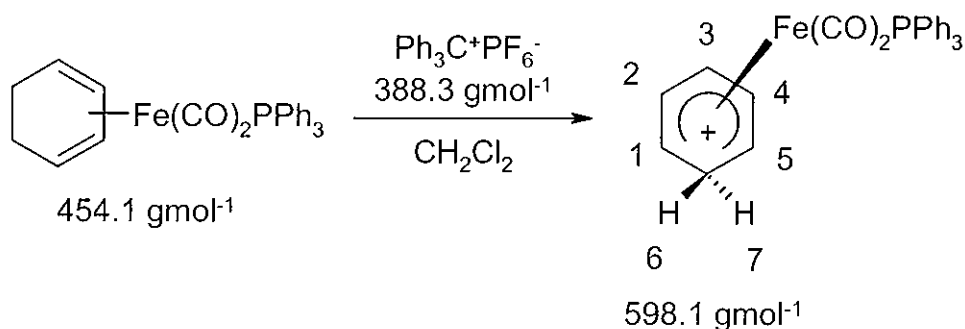
hexane to yield the desired triphenylphosphine complex as yellow crystals (1.80 g, 43%,) m.p. 120.1-122.0 °C (lit., <sup>107</sup>120.0-121.0 °C).

$\nu_{\max}$  /  $\text{cm}^{-1}$  (KBr disc): 1967.5 (C=O), 1907.0 (C=O)

$\delta_{\text{H}}$  / ppm (200 MHz,  $\text{CDCl}_3$ ): 1.44-1.71 (4H, m, 2 x  $\text{CH}_2$ ), 2.50 (2H, s\*\*, 2 x  $\text{CH}_2\text{CH}=\text{CH}$ ), 4.84 (2H, s\*\*, 2 x  $\text{CH}_2\text{CH}=\text{CH}$ ), 7.39 (15H, m, aromatic CH's)

$\delta_{\text{C}}$  / ppm (50 MHz,  $\text{CDCl}_3$ ): 24.58 ( $\underline{\text{C}}\text{H}_2\text{CH}=\text{CH}$ ), 61.09 ( $\text{CH}_2\underline{\text{C}}\text{H}=\text{CH}$ ), 84.63 ( $\text{CH}_2\text{CH}=\underline{\text{C}}\text{H}$ ), 128.06, 128.25, 129.55, 129.53 132.94, 133.16, 135.89 (quaternary C), 136.65 (quaternary C) (aromatic carbons)

(iv) ( $\eta^5$ -cyclohexadienyl)dicarbonyltriphenylphosphineiron hexafluorophosphate



( $\eta^4$ -cyclohexa-1,3-diene)dicarbonyltriphenylphosphineiron (1.00 g, 2.21 mmol) and triphenylcarbenium hexafluorophosphate (2.03 g, 5.22 mmol) were dissolved in dichloromethane (70 ml) and stirred for 3 hours. Diethyl ether (180 ml) was then added to produce two distinct layers. Vigorous stirring for two hours resulted in the formation of a yellow precipitate. The precipitate was collected by vacuum filtration to yield the complex salt as yellow crystals (1.31 g, 99%), m.p. 179-181 °C (lit., <sup>66</sup>180-181 °C).

\*\* A multiplet would be expected. Gibson (S.E. Gibson, *Transition Metals in Organic Synthesis*, Oxford University Press, 1997) has noted that the presence of paramagnetic salts in similar complexes which causes line broadening of NMR spectra.

$\delta_{\text{H}}$  / ppm (400 MHz,  $\text{CD}_3\text{CN}$ ): 1.72 (1H, br d, 7-H), 2.83 (1H, br d, 6-H), 3.61 (2H, s<sup>††</sup>, 1-H, 5-H), 5.17 (2H, s<sup>††</sup>, 2-H, 4-H), 6.98 (1H, s<sup>††</sup>, 3-H), 7.43-7.63 (15 H, m, aromatic CH's)

Analysis found: C, 51.63; H, 3.59

$\text{C}_{26}\text{H}_{22}\text{F}_6\text{FeO}_2\text{P}_2$  requires: C, 52.21; H, 3.71

### 4.3 Other Organic Substrates for Kinetic and Equilibrium Measurements

( $\eta^5$ -cyclohexadienyl)tricarbonyliron tetrafluoroborate (Aldrich, 97%) was used without further purification. Purity was checked by  $^1\text{H}$  NMR spectroscopy. A sample was also recrystallised from water to check for any effect on kinetic measurements as a result of increased purity of the substrate. None was observed.

( $\eta^5$ -2-methoxycyclohexadienyl)tricarbonyliron tetrafluoroborate (Aldrich, 99%) was used without further purification. Purity was checked by  $^1\text{H}$  NMR spectroscopy.

( $\eta^5$ -4-methoxy-1-methylcyclohexadienyl)tricarbonyliron hexafluorophosphate (Aldrich, 99%) was used without further purification. Purity was checked by  $^1\text{H}$  NMR spectroscopy.

### 4.4 Reagents Used for Kinetic and Equilibrium Measurements

#### 4.4.1 Solvents

Water used for kinetic and equilibrium measurements was doubly distilled and deionised and stored in brown glass bottles. HPLC grade water was also used. It was obtained from Romil (Super Purity Solvent).

---

<sup>††</sup> A multiplet would be expected. Gibson (S.E. Gibson, *Transition Metals in Organic Synthesis*, Oxford University Press, 1997) has noted the presence of paramagnetic salts in similar complexes causes line broadening of NMR spectra.

The methanol and acetonitrile used were HPLC grade.

DCI and D<sub>2</sub>O were > 99 % atom isotopic purity (Aldrich).

#### 4.4.2 *Acids and Bases*

Hydrochloric acid solutions were prepared by dilution of BDH Aristar grade concentrated HCl (~ 12 M) and standardised with sodium hydroxide solution using phenolphthalein as indicator.

Perchloric acid solutions were prepared from BDH Analar grade concentrated acid (60% or 70%) and standardised with sodium hydroxide solution using phenolphthalein as an indicator.

Sodium hydroxide solutions were prepared from pellets (Sigma-Aldrich, ≥8%), which were washed with water to remove sodium (bi) carbonate. The solutions were then standardised with hydrochloric acid using phenolphthalein as an indicator.

Sodium hydroxide and hydrochloric acid solutions for standardisation were prepared using “Fixanal” ampoules but were not considered pure enough for kinetic measurements particularly as any dissolved plasticiser may be UV-active and the HCl solutions are normally stabilised with mercuric chloride.

#### 4.4.3 *Buffers*

Buffer solutions were prepared by partial neutralisation of the base with hydrochloric acid or by partial neutralisation of the acid with sodium hydroxide. Commercial reagents were used without further purification. All pK<sub>a</sub> values for buffers were obtained from Perrin and Dempsey.<sup>108</sup>

Acetate buffers were prepared from sodium acetate trihydrate (Riedel de Haën, 99.5%) and hydrochloric acid.

Carbonate buffers were prepared from sodium carbonate (Fluka, 99.5%) and sodium hydrogen carbonate (Fluka, 99%).

Borate buffers were prepared using boric acid (Aldrich, 99.9%) and sodium hydroxide, or by using sodium tetraborate decahydrate (Riedel de Haën, 99.5%) and hydrochloric acid.

Cacodylate buffers were prepared using either cacodylic acid (Aldrich, 98%) and sodium hydroxide or sodium cacodylate (Fluka, 98%) and hydrochloric acid.

Chloroacetate buffers were prepared using chloroacetic acid (Sigma Aldrich, 99%) and sodium hydroxide.

Methoxyacetate buffers were prepared using methoxyacetic acid (Aldrich, 98%) and sodium hydroxide.

Phosphate buffers were prepared from sodium dihydrogen phosphate (Sigma-Aldrich, 99%) and sodium hydroxide.

#### ***4.4.4 Inorganic Reagents***

Sodium Chloride (for adjusting ionic strength): Aldrich, Gold Label, 99.999%

The nitrogen gas used was oxygen free. In experiments where the reagents or products were very sensitive to the presence of oxygen, high purity dry argon was used instead.

#### ***4.4.5 Deuterated Buffer Solutions***

Acetate and cacodylate buffer solutions were used in this study during an investigation to determine the isotope effect for the hydrolysis of ( $\eta^5$ -cyclohexadienyl)tricarbonyliron. The solutions were prepared by partial neutralisation of the buffer base with deuterium chloride (DCI) in deuterium oxide (D<sub>2</sub>O). Kinetic and

equilibrium measurements determined using the deuterated buffer solutions were obtained by the same methods as for the aqueous solutions outlined in Section 4.6.

The pD values ( $-\log[D^+]$ ) of the buffer solutions were calculated using Equation 4.1, where B and  $HB^+$  represent the buffer base and buffer acid respectively.

$$pD = pK_a + \log ([B] / [HB^+]) \quad (4.1)$$

The ratio of buffer base to acid was known for each buffer solution prepared and this was combined with the literature value for the  $pK_a$  of the buffer in  $D_2O$ .<sup>108</sup>

## 4.5 Instrumentation

### 4.5.1 pH Measurement

Measurements of pH were made using a Jenway 3310 pH meter with a combination glass electrode or using a Metrohm 827 pH meter with a glass electrode using  $c(KCl) = 3 \text{ mol / L}$  as the reference electrolyte. Calibration was carried out with standard buffer solutions of pH values 4.00 and 10.00. In the case of buffers, measurements were generally carried out at a temperature other than that used for kinetics (*i.e.*  $\neq 25^\circ\text{C}$ ) and the reading was corrected using the  $pK_a/dT$  value for the buffer, as reported by Perrin and Dempsey.<sup>108</sup>

### 4.5.2 UV Spectrophotometry

A Varian Cary 50 scan spectrophotometer was used which covered the range 190 - 800 nm with a Xenon lamp as light source. The instrument could be operated in either spectral or single wavelength monitoring modes. The spectrophotometer was a single beam instrument and was equipped with an eighteen cell changer compartment. One cm wide quartz cuvettes fitted with Teflon caps were used and the temperature in the cell compartment was maintained at  $25.0 \pm 0.1 \text{ }^\circ\text{C}$  by circulating water from a thermostatted water bath (Julabo, ED5).

#### *4.5.3 UV-Vis Spectrophotometry Using a Fast Mixing Apparatus*

To monitor reactions of which the lifetime is measured in seconds, a fast mixing accessory must be used. In this study a RX 2000 rapid kinetics stopped-flow mixing accessory (Applied Photophysics) was used. This apparatus allows for the monitoring of reactions which are up to a thousand times faster than those which can be examined when manual mixing is performed. A schematic of the RX 2000 accessory is given in Figure 4.1.

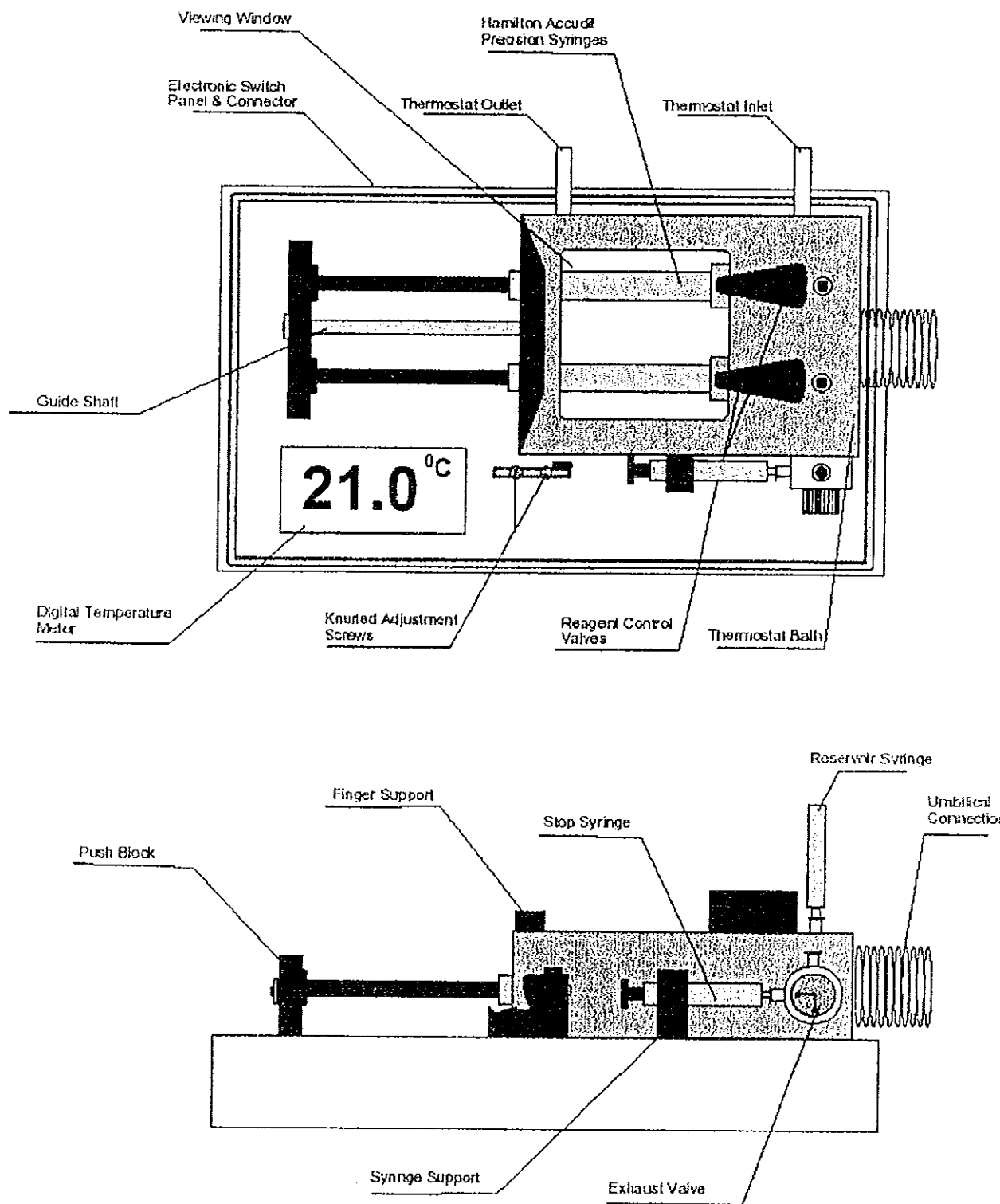


Figure 4.1 Schematic of the RX 2000 Rapid Kinetics Stopped-Flow Mixing Accessory (Applied Photophysics).<sup>\*\*</sup>

<sup>\*\*</sup> Illustration from Applied Photophysics RX.2000 User Manual



A thermostatted water bath was connected to the RX 2000 accessory to maintain the temperature of the sample at  $25.0 \pm 0.1$  °C. The reagent system contains two Hamilton syringes, which, along with an inlet tube from the water bath, are connected to a specialised cuvette *via* an umbilical. The specialised cell is constructed with standard dimensions of 10 x 10 mm in order to be readily connected to standard instrumentation with a cuvette compartment of equal size. The cell is a micro-cell fitted with four observation windows and is made of silica. It can be used with a pathlength of 2 or 10 mm. For experiments carried out in this study, a pathlength of 10 mm was used.

## 4.6 Kinetic and Equilibrium Measurements

All measurements were made at 25 °C in aqueous solution unless otherwise stated. The ionic strength and pH of the solutions were carefully controlled.

### 4.6.1 Equilibrium Measurements

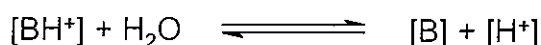
The  $pK_R$  value obtained for the hydrolysis of the ( $\eta^5$ -cyclohexadienyl)dicarbonyltriphenylphosphineiron cation was determined spectrophotometrically by the method of Albert and Serjeant.<sup>109</sup> Spectra were recorded for the fully ionised species and fully unionised species and also for the partially ionised species. The equilibrium constant was calculated according to the method detailed in Chapter 2 (Section 2.1.1).

For the hydrolysis reaction of the ( $\eta^5$ -cyclohexadienyl)tricarbonyliron cation, the equilibrium constant,  $pK_R$ , was determined from spectroscopic and kinetic measurements performed in aqueous solution (Sections 2.2.3 and 2.2.4) and solutions of deuterium oxide (Sections 2.2.5 and 2.2.6). The spectroscopic method involved plotting the absorbance change that occurred for a kinetic time scan at a single wavelength against pH (or pD). The  $pK_R$  value was determined from the inflection point on this plot. The  $pK_R$  values determined for the methanolysis reaction of the ( $\eta^5$ -cyclohexadienyl)tricarbonyliron cation (Sections 2.3.1 and 2.3.2) were determined in a similar way.

#### 4.6.2 Calculation of Data for Equilibrium Measurements Using SigmaPlot Software

Using an equilibrium method, determination of the equilibrium constant,  $pK_R$ , for formation of the coordinated benzene hydrates examined in this study involved manipulating the data to provide plots of absorbance (or absorbance change) versus pH (or pD) using SigmaPlot software. The best fit line through the data points was required in order for the  $pK_R$  values to be obtained at the point of inflection. The equations governing the best fit lines were derived as shown below.

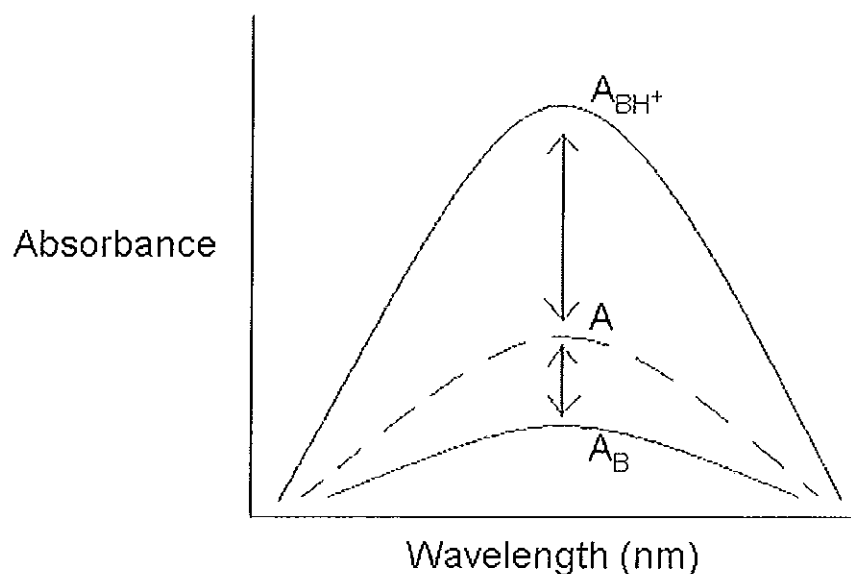
The equilibrium constant,  $K_R$ , for the reaction expressed in Scheme 4.1 is given in equation 4.2, where [B] is the concentration of the coordinated benzene hydrate and  $[BH^+]$  is the concentration of the coordinated cyclohexadienyl cation.



Scheme 4.1

$$K_R = [B] [H^+] / [BH^+] \quad (4.2)$$

Figure 4.2 shows the hypothetical absorbances that would be observed when the coordinated cyclohexadienyl cation ( $A_{BH^+}$ ) and the coordinated benzene hydrate ( $A_B$ ) are in their fully formed states respectively. The absorbance, A, refers to any absorbance measured when an incomplete reaction has been observed from either the cation to hydrate or from the hydrate to the cation



**Figure 4.2** A diagram of absorbance versus wavelength showing the hypothetical spectra of  $A_{BH^+}$  (a coordinated cyclohexadienyl cation),  $A_B$ , (a coordinated benzene hydrate) and  $A$  (the observed absorbance for an incomplete conversion of cation to hydrate or vice versa).

Assuming the total concentration of  $[BH^+]$  and  $[B]$  remains constant, the ratio of the observed absorbances is related to the concentrations as shown in equation 4.3.

$$(A_{BH^+} - A) / (A - A_B) = [B] / [BH^+] \quad (4.3)$$

Substituting for  $[B] / [BH^+]$  in Equation 4.2 using Equation 4.3 provides Equation 4.4, which, when rearranged to express the equation in terms of  $A$ , affords Equation 4.5.

$$K_R = [H^+] \{(A_{BH^+} - A) / (A - A_B)\} \quad (4.4)$$

$$A = \{K_R A_B + A_{BH^+} [H^+]\} / \{K_R + [H^+]\} \quad (4.5)$$

The absorbance,  $A$ , can be calculated for each pH value if  $[H^+]$ ,  $A_B$ ,  $K_R$  and  $A_{BH^+}$  are known. These constraints are iterated to provide a best fit of calculated to observed values of  $A$ , showing the calculated values as a continuous plot of  $A$  versus pH.

Equation 4.5 is the equation that governs the absorbance versus pH plots shown in Figures 2.24 and 2.26 in Sections 2.3.1 and 2.3.2 respectively.

The equation governing the absorbance change versus pH (and pD) plots shown in Figures 2.16 and 2.18 in Sections 2.2.4 and 2.2.6 respectively is a simplified version of Equation 4.5 and is given in Equation 4.7.

$$A = K_R A_B / \{K_R + [H^+]\} \quad (4.6)$$

$$\Delta Abs = A_\infty \times \{K_R / (K_R + [H^+])\} \quad (4.7)$$

In Equation 4.6, the term of Equation 4.5 which relates to the absorbance of the fully formed coordinated cyclohexadienyl cation ( $A_{BH^+}[H^+]$ ) has been removed as the value  $A_{BH^+}$  can be estimated to be zero. This estimation is based on the observed experimental data. The reaction being monitored was hydrolysis of the tricarbonyliron coordinated cyclohexadienyl cation (**72**) to the coordinated cyclohexadiene hydrate (**102**) in aqueous and deuterated acetate buffer solutions. As the pH (or pD) of the acetate buffers decreased, the absorbance change observed when the cation solution was injected decreased and eventually became so small it could be estimated at zero. Equation 4.6 can therefore be rewritten as Equation 4.7 where  $A$ , represents the absorbance change being observed during the reaction and  $A_\infty$  is the limiting absorbance for the fully for product of the reaction.

#### 4.6.3 Kinetic Measurements

Kinetic measurements were made by accurately pipetting 2.0 ml of aqueous buffer, acid or base solution into a 1 cm spectrophotometric cell that was allowed to reach constant temperature in the cell compartment of the spectrometer for 10 minutes. The reaction was initiated by injecting the substrate solution into the reaction solution

using a Hamilton microlitre syringe. The concentration of the substrate solution was usually  $10^{-2}$  -  $10^{-3}$  M in spectroscopic grade methanol or acetonitrile.

#### 4.6.4 Calculations for Kinetic Measurements

##### First and Second Order Kinetics

First order rate constants,  $k_{\text{obs}}$ , determined by UV spectrophotometry were calculated in two ways:

(i) By inputting all of the absorbance versus time measurements into Sigmaplot v 8.0 software and using the regression wizard to fit the first order plot to a regression equation. For a first order increase in absorbance with time, the data were fitted to an exponential rise to maximum as in equation:

$$y = y_0 + a(1 - e^{-bx}) \quad (4.7)$$

where  $x$  = time,  $y$  = absorbance and  $b = k_{\text{obs}}$ . For a first order decrease in absorbance, the data were fitted to an exponential decay Equation:

$$y = y_0 + ae^{-bx} \quad (4.8)$$

where  $x$  = time,  $y$  = absorbance and  $b = k_{\text{obs}}$ .

(ii) By using the UV-Vis spectrophotometer software, Cary Win UV Scanning Kinetics program v 3.0 or Cary Win UV Kinetics program v 3.0 and selecting the “analyse data” function to fit the first order plot to a regression equation. Results from this software were compared to those obtained using Sigmaplot v 8.0 and they agreed.

Second order rate constants were obtained as  $k_2 = k_{\text{obs}} / [\text{OH}^-]$  or more often from a plot of  $k_{\text{obs}}$  versus  $[\text{OH}^-]$ .

## References

### Abbreviations:

Adv. Phys. Org. Chem.	Advances in Physical Organic Chemistry
Angew. Chem.	Angewandte Chemie
Annalen der Physik und Chemie	Annalen der Physik und Chemie
Ann. Rev. Biochem.	Annual Review of Biochemistry
Aust. J. Chem.	Australian Journal of Chemistry
Biochem. J.	Biochemical Journal
Can. J. Chem.	Canadian Journal of Chemistry
Chem. Comm.	Chemical Communications
Chem. Rev.	Chemical Reviews
C.R. Hebd. Seances. Acad. Sci.	Comptus Rendus Hebdomadaires des Seances de l'Academie des Sciences
Croat. Chem. Acta.	Croatica Chemica Acta
Drug. Metab. Rev.	Drug Metabolism Reviews
Eur. J. Inorg. Chem.	European Journal of Inorganic Chemistry
Inorg. Chem.	Inorganic Chemistry
J. Am. Chem. Soc.	Journal of the American Chemical Society
J. Biol. Chem.	Journal of Biological Chemistry
J. Chem. Ed.	Journal of Chemical Education
J. Chem. Soc.	Journal of the Chemical Society
J. Chem. Soc. Chem. Comm.	Journal of the Chemical Society, Chemical Communications
J. Chem. Soc. Dalton. Trans.	Journal of the Chemical Society, Dalton Transactions
J. Chem. Soc. Perkin Trans.	Journal of the Chemical Society, Perkin Transactions
J. Liebig. Ann. Chem.	Justus Liebig's Annalen der Chemie
J. Molec. Cat. B: Enzymatic	Journal of Molecular Catalysis B: Enzymatic
J. Org. Chem.	Journal of Organic Chemistry
J. Organometallic Chem.	Journal of Organometallic Chemistry
Mini-Rev. Org. Chem.	Mini-Reviews in Organic Chemistry
Nat. Prod. Rep.	Natural Product Reports
Tetrahedron Lett.	Tetrahedron Letters

- 
- 1 Boyd, D.R. and Sheldrake, G.N., *Nat. Prod. Rep.* **1998**, 15, 309
  - 2 Gibson, D.T., Koch, J.R. and Kallio, R.E., *Biochemistry*, **1968**, 7, 2653
  - 3 Sheldrake, G.N. in *Chirality in Industry*, ed. Collins, A.N., Sheldrake, G.N. and Crosby, J., Wiley and Sons, **2000**, Chapter 6.
  - 4 Humphreys, J.L., Lowes, D.J., Wesson, K.A. and Whitehead, R.C., *Tetrahedron*, **2006**, 62, 5099
  - 5 Jerina, D.M., Daly, J.W., Witkop, B., Zaltmann-Nirenberg, P. and Udenfried, S., *Biochemistry*, **1970**, 9, 147
  - 6 Nelson, D.L. and Cox, M.M. in *Lehninger Principles of Biochemistry*, 4th edition, W.H. Freeman and Co., New York, **2004**, Chapter 19
  - 7 Omura, T. and Sato, R., *J. Biol. Chem.* **1962**, 237, 1375
  - 8 White, R.E. and Coon, M.J., *Ann. Rev. Biochem.* **1980**, 49, 315
  - 9 Guroff, G., Daly, J.W., Jerina, D.M., Renson, J., Witkop, B. and Udenfriend, S., *Science*, **1967**, 157, 1524
  - 10 Bruice, P.Y. in *Organic Chemistry*, 5<sup>th</sup> edition, Prentice Hall, **2006**, Chapter 11
  - 11 Levin, W., Wood, A., Chang, R., Ryan, D., Thomas, P., Yagi, H., Thakker, D., Vyas, C., Boyd, D.R., Chu, S.-Y., Conney, A.H. and Jerina, D., *Drug Metab. Rev.*, **1982**, 13, 555
  - 12 Boyland, E. and Levi, A.A., *Biochem. J.*, **1936**, 30, 1225
  - 13 Sello, G. and Orsini, F., *Mini-Rev. Org. Chem.*, **2004**, 1, 77
  - 14 Hudlicky, T., Gonzalez, D. and Gibson, D.T., *Aldrichimica Acta.* **1999**, 32, 35
  - 15 Hudlicky, T., Tian, X., Köningsberger, K., Maurya, R., Rouden J., and Fan, B., *J. Am. Chem. Soc.*, **1996**, 118, 10752
  - 16 Orsini, F., Sello, G., Travaini, E. and Di Gennaro, P., *Tetrahedron Asymmetry*, **2002**, 13, 253
  - 17 Boyd, D.R. and Sharma, N.D., *J. Molec. Cat. B: Enzymatic*, **2002**, 19-20, 31
  - 18 Bamberger E. and Loder, W., *J. Liebig. Ann. Chem.*, **1895**, 100
  - 19 Staroscik, J. and Rickborn, B., *J. Am. Chem. Soc.*, **1971**, 93, 3046
  - 20 Boyland. E. and Soloman, J.B., *Biochem. J.*, **1955**, 59, 518
  - 21 Boyd, D.R., McMordie, R.A.S., Sharma, N.D., Dalton, H., Williams P. and Jenkins, R.O., *J. Chem. Soc., Chem. Comm.*, **1989**, 339
  - 22 Agarwal, R., Boyd, D.R., McMordie, R.A.S., O’Kane, G.A., Porter, P., Sharma,

- 
- N.D., Dalton, H. and Gray, D.J., *J. Chem. Soc., Chem. Comm.*, **1990**, 1711
- 23 Boyd, D.R., McMordie, R.A.S., Sharma, N.D., More O'Ferrall, R.A. and Kelly, S.C., *J. Am. Chem. Soc.*, **1990**, 112, 7822-7823
- 24 More O'Ferrall, R.A. and Rao, S.N., *Croat. Chem. Acta.*, **1992**, 65, 593
- 25 Richard, J.P., Rothenberg M.E. and Jencks, W.P., *J. Am. Chem. Soc.*, **1984**, 106, 1361
- 26 Kealy, T.J. and Pauson, P.L., *Nature*, **1951**, 168, 1039
- 27 Zeise, W.C., *Annalen der Physik und Chemie*, **1831**, 21, 497
- 28 Monde, L. and Quincke, F., *J. Chem. Soc.*, **1891**, 59,604
- 29 Bertholet, M., *C.R. Hebd. Seances Acad. Sci*, **1891**, 112, 1343
- 30 Pearson, A.J. in *Iron Compounds in Organic Synthesis*, Academic Press, London, 1994
- 31 Reihlen, H., Gruhl, A., Von Hessling, G. and Pfrengle, O., *J. Liebig Ann. Chem.*, **1930**, 482, 161
- 32 Hallam, B.F. and Pauson, P.L., *J. Chem. Soc.*, **1958**, 642
- 33 Arnett, J.E. and Pettit, R., *J. Am. Chem. Soc.*, **1961**, 83, 2985
- 34 Cais, M. and Maoz, N., *J. Organometallic Chem.*, **1966**, 5, 370
- 35 Knölker, H.J., Ahrens, B., Gonser, P., Heininger, M. and Jones, P.G., *Tetrahedron*, **2000**, 56, 2259
- 36 Knölker, H.J., *Chem. Rev.*, **2000**, 100, 2941
- 37 Stark, K., Lancaster, J.E., Murdoch, H.D. and Weiss, E.Z., *Naturforsch*, **1964**, 19b, 284
- 38 Howell, J.A.S., Johnson, B.F.G., Josty, P.L. and Lewis, J., *J. Organometallic Chem.*, **1972**, 39, 329
- 39 Brookhart, M. and Nelson, G.O., *J. Organometallic Chem.*, **1979**, 164, 193
- 40 Fleckner, H., Grevels, F.-W. and Hess, D., *J. Am. Chem. Soc.*, **1984**, 106, 2027
- 41 Otsuka, S., Yoshida, T. and Nakamura, A., *Inorg. Chem.* **1967**, 6, 20
- 42 Brodie, A.M., Johnson, B.F.G., Josty, P.L. and Lewis, J., *J. Chem. Soc. Dalton Trans.* **1972**, 2031
- 43 Knölker, H.J. and Gonser, P., *Synlett*, **1992**, 517
- 44 Knölker, H.J., Gonser, P. and Jones, P.G., *Synlett*, **1994**, 405
- 45 Knölker, H.J., Baum, G., Foitzik, N., Goesmann, H., Gonser, P., Jones, P.G. and



- 
- Röttele, H., *Eur. J. Inorg. Chem.*, **1998**, 993
- 46 Knölker, H.J., Hermann, H. and Herzberg, D., *Chem. Comm.* **1999**, 831
- 47 Barton, D.H.R., Gunatilaka, A.A.L., Nakanishi T., Patin, H., Widdowson, D.A., and Worth, B.R., *J. Chem. Soc. Perkin Trans.* **1976**, 1, 821
- 48 Franck-Neumann, M. and Martina, D., *Tetrahedron Lett.* **1975**, 1759
- 49 Pearson, A.J. and Srinivasan, K., *J. Org. Chem.* **1992**, 57, 3965
- 50 Pearson, A.J., Lai, Y-S. and Srinivasan, K., *Aust. J. Chem.* **1992**, 45, 109
- 51 Semmelhack, M.F. and Herndon, J.W., *Organometallics*, **1983**, 2, 363
- 52 Birch, A.J., Cross, P.E., Lewis, J., White, D.A. and Wild, S.B., *J. Chem. Soc.(A)*, **1968**, 332
- 53 McCormack, A., McDonnell, C., More O'Ferrall, R.A., O'Donoghue, A.C. and Rao, S.N., *J. Am. Chem. Soc.*, **2002**, 124, 8575
- 54 Fischer, E.O. and Fischer, R.D., *Angew. Chem.* **1960**, 72, 919
- 55 Pettit, R. and Emerson, G.F. in *Advances in Organometallic Chemistry*, West. R. and Stone, F.G.A., Ed., Academic Press, New York, N.Y. **1964**
- 56 Jones, D., Pratt, L. and Wilkinson, G., *J. Chem. Soc.*, **1962**, 4458
- 57 Kane-Maguire, L.A.P., Honig, E.D. and Sweigart, D.A., *Chem. Rev.*, **1984**, 84, 525
- 58 Eisenstein, O., Butler, W.M. and Pearson. A.J., *Organometallics*, **1984**, 3, 1151
- 59 (a) Knölker, H.J., Baum, E. and Reddy, K.R., *Tetrahedron Lett.* **2000**, 41, 1171.  
(b) Knölker, H.J. and Fröhner, W., *Tetrahedron Lett.* **1997**, 38, 1535. (c)  
Knölker, H.J. and Wolpert, M., *Tetrahedron Lett.* **1997**, 38, 533
- 60 Malkov, A.V., Mojovic, L., Stephenson, G.R., Turner, A.T. and Creaser, C.S., *J. Organometallic. Chem.* **1999**, 589, 103
- 61 Bandara, B.M.R., Birch, A.J. and Kelly, L.F., *J. Org. Chem.*, **1984**, 49, 2496
- 62 Spessard, G.O. and Miessler, G.L. in *Organometallic Chemistry*, Prentice Hall, Upper Saddle River, New Jersey, **1996**
- 63 Elschenbroich, Ch. and Salzer, A. in *Organometallics A Concise Introduction*, 2nd edition, Teubner, B.G., Stuttgart, **1991**
- 64 Cotton, F.A. and Wilkinson, G., in *Advanced Inorganic Chemistry*, 6<sup>th</sup> ed. Wiley, New York, **1999**
- 65 Pearson, A.J. and Yoon, J., *Tetrahedron Lett.*, **1985**, 26, 2399
- 66 Birch, A.J., Raverty, W.D., Hsu, S-Y. and Pearson, A.J., *J. Organometallic*

- 
- Chem.*, **1984**, 260, C59
- 67 Guillou, C., Millot, N., Reboul, V. and Thal, C., *Tetrahedron Lett.*, **1996**, 37, 4515
- 68 Howell, J.A.S., Walton, G., Tirvengadam, M-C., Squibb, A.D., Palin, M.G., McArdle, P., Cunningham, D., Goldschmidt, Z., Gottlieb, H. and Strul, G., *J. Organometallic Chem.*, **1991**, 401, 91
- 69 Holmes, J.D. and Pettit, R., *J. Am. Chem. Soc.*, **1963**, 85, 2531
- 70 Shvo, Y. and Hazum, E., *J. Chem. Soc. Chem. Comm.*, **1974**, 336
- 71 Courtney, M.C., MacCormack, A.C., and More O'Ferrall, R.A., *J. Phys. Org. Chem.*, **2002**, 15, 529
- 72 Ritchie, C.D., *Acc. Chem. Res.*, **1972**, 5, 348
- 73 Mathivanan, N., McClelland, R.A. and Steenken, S., *J. Am. Chem. Soc.*, **1990**, 112, 8454
- 74 Cox, R.A. and Yates, K., *Can. J. Chem.*, **1983**, 59, 2116
- 75 Cox, R.A. and Yates, K., *Can. J. Chem.*, **1983**, 61, 2225
- 76 (a) Richard, J.P. and Jencks, W.P., *J. Am. Chem. Soc.*, **1982**, 104, 4689, (b) Richard, J.P. and Jencks, W.P., *J. Am. Chem. Soc.*, **1982**, 104, 4691 (c) Richard, J.P., Rothenberg, M.E. and Jencks, W.P., *J. Am. Chem. Soc.*, **1984**, 106, 1361
- 77 (a) McClelland, R.A., Banait, N. and Steenken, S.J., *J. Am. Chem. Soc.*, **1986**, 108, 7023, (b) McClelland, R.A., Kanagasabapathy, V.M. and Steenken, S., *J. Am. Chem. Soc.*, **1988**, 110, 6913 (c) McClelland, R.A., Kanagasabapathy, V.M., Banait, N.S. and Steenken, S., *J. Am. Chem. Soc.*, **1989**, 111, 3966
- 78 Atton, J.G. and Kane-Maguire, L.A.P., *J. Organometallic Chem.*, **1983**, 246, C23 – C26
- 79 Hine, J., *J. Am. Chem. Soc.*, **1971**, 3701
- 80 Bunting, J.W., *Adv. Heterocycl. Chem.*, **1979**, 25, 1
- 81 Loudon, G.M., *J. Chem. Ed.*, **1991**, 68, 12, 973
- 82 Cotton, F.A. and Wilkinson, G., in *Advanced Inorganic Chemistry*, 4<sup>th</sup> ed. Wiley, New York, **1980**, pg 1062
- 83 Kresge, A.J., More O'Ferrall, R.A. and Powell, M.F. in *Isotope Effects in Organic Chemistry*; Buncl, E., Lee, C.C. Eds, Elsevier, Amsterdam, **1987**, Vol 7, pp 177-273.
- 84 Gibson, S.E. in *Transition Metals in Organic Synthesis*, 1<sup>st</sup> ed. Oxford

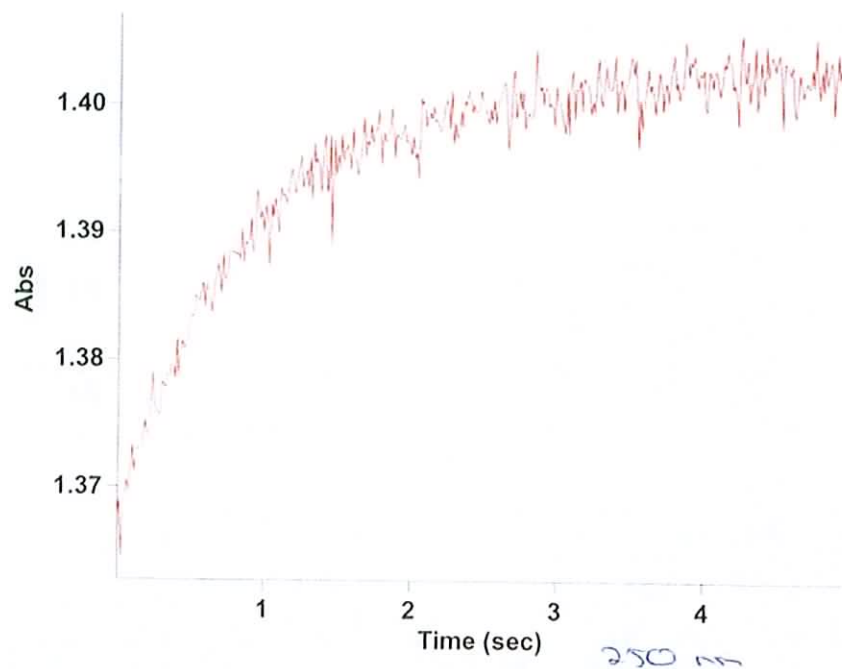
- 
- University Press, **1997**
- 85 Pelet, S. and More O'Ferrall, R.A., *unpublished results*
- 86 Kruck, T. and Noack, M., *Chem. Ber.*, **1964**, 97, 1693
- 87 Muetterties, E.L., *Inorg. Chem.*, **1965**, 4, 1841
- 88 Loudon, G.M., *J. Chem. Ed.*, **1991**, 68, 12, 973
- 89 El-Mabrouk M.A. Salama., *PhD Thesis, University College Dublin*, **1990**
- 90 Grice, N., Kao, S.C. and Pettit, R., *J. Am. Chem. Soc.*, **1979**, 110, 1627
- 91 Gold, V. *Adv. Phys. Org. Chem.*, **1969**, 7, 259
- 92 Hine, J. and Weimer, R.D.Jr., *J. Am. Chem. Soc.*, **1965**, 87, 3387
- 93 Perdoncin, G. and Scorrano, G., *J. Am. Chem. Soc.*, **1977**, 99, 6983
- 94 Mahler, J.E., Jones, D.A.K. and Pettit, R., *J. Am. Chem. Soc.*, **1964**, 86, 3589
- 95 Mayr, H., Müller, K-H., Ofial, A.R. and Bühl, M., *J. Am. Chem. Soc.*, **1999**, 121, 2418
- 96 Jia, Z.S. and Thibblin, A., *J. Chem. Soc. Perkin Trans.*, **2001**, 247
- 97 Schanfele, H., Hu, D., Pritzkow, H. and Zenneck, U., *Organometallics*, **1989**, 8, 396
- 98 Manuel, T.A., *Inorg. Chem.*, **1964**, 1794
- 99 McClelland, R.A., *Tetrahedron*, **1996**, 52, 6823
- 100 Ritchie, C.D. and Fleischhauer, H.J., *J. Am. Chem. Soc.* **1972**, 94, 3481
- 101 Lawlor, D.A., More O'Ferrall, R.A. and Nagaraja Rao, S. *unpublished results*
- 102 Hine, K.E., Johnson, B.F.G. and Lewis, J., *J. Chem. Soc. Chem. Comm.*, **1975**, 81
- 103 O'Meara, C., McDonnell, C. and More O'Ferrall, R.A., *unpublished results*
- 104 MacCormack, A. and More O'Ferrall, R.A., *unpublished results*
- 105 Stephenson, G.R., Howard, P.W. and Taylor, S.C., *J. Org. Chem.*, **1988**, 339, C5-C8
- 106 Leonard, J., Lygo, B. and Procter, G. in *Advanced Practical Organic Chemistry*, Stanley Thornes Ltd, Cheltenham, United Kingdom, **1998**
- 107 Pearson, A.J. and Raithby, P.R., *J. Chem. Soc. Dalton Trans.*, **1981**, 884
- 108 Perrin, D.D. and Dempsey, B. in *Buffers for pH and Metal Ion Control*, Chapman and Hall, London, **1974**
- 109 Albert, A. and Serjeant, E.P. in *The Determination of Ionisation Constants*, 3<sup>rd</sup> edition, Chapman and Hall, London, **1984**

## Appendix

1. *Kinetic Determination of  $pK_R$  of ( $\eta^5$ -cyclohexadienyl)tricarbonyliron in Deuterated Solution* 179
2. *Publications* 183

### *1. Kinetic Determination of $pK_R$ of ( $\eta^5$ -cyclohexadienyl)tricarbonyliron in Deuterated Solution*

The data point for pD 4.32 with a  $[D^+]$  of  $3.1 \times 10^{-5}$  M and observed rate constant ( $k_{obs}$ ) of  $1.47 \text{ s}^{-1}$  in Table 2.18 (Section 2.2.5) was omitted on plotting of a best fit straight line in Figure 2.17. This was rationalised on the grounds the absorbance change for the kinetic scan collected at 250 nm was only 0.036 absorbance units and the scan appears noisy as can be seen in Figure A1. The other data points collected in Table 2.18, were obtained from kinetic scans with an absorbance change greater than 1 absorbance unit and have very little noise. An example is given in Figure A2. With the data point included, the best fit straight line is shown in Figure A3. A  $pK_R$  value of 5.55 is obtained



**Figure A1** Kinetic scan at 250 nm recorded for the hydrolysis of ( $\eta^5$ -cyclohexadienyl)tricarbonyliron in acetate buffer prepared in deuterium oxide at a pD of 4.32, substrate concentration of  $2 \times 10^{-4}$  M and 25°C.

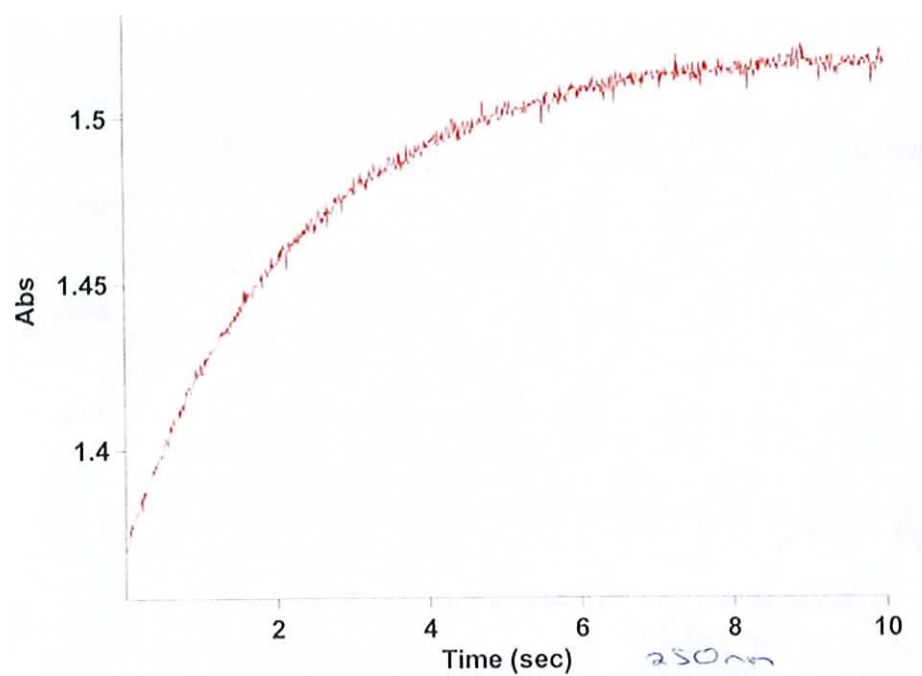
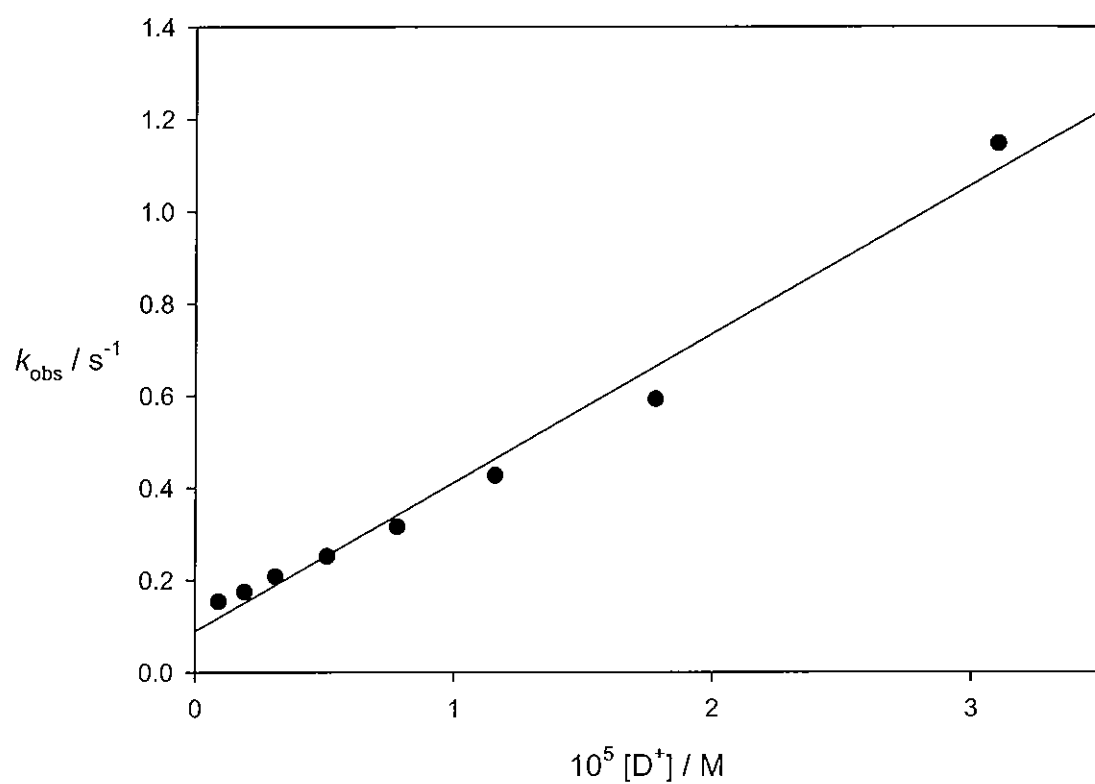


Figure A2

Kinetic scan at 250 nm recorded for the hydrolysis of ( $\eta^5$ -cyclohexadienyl)tricarbonyliron in acetate buffer prepared in deuterium oxide at a pD of 4.86, substrate concentration of  $2 \times 10^{-4}$  M and 25°C.



**Figure A3** Plot of first order rate constants against  $[D^+]$  for the hydrolysis of  $(\eta^5\text{-cyclohexadienyl})\text{tricarbonyliron}$  in aqueous acetate and cacodylate buffer solutions prepared in deuterium oxide at  $25^\circ\text{C}$ .

## 2. Publications

### Oral Presentation

“Kinetic and Equilibrium Studies on Some Co-ordinated Cyclohexadiene Cations”, M. Galvin, C. Mc Donnell and R. More O’Ferrall, *Abstracts of Papers, 57<sup>th</sup> Irish Universities Chemistry Research Colloquium*, NUI Maynooth, June 2005.

### Poster Presentations

“Kinetic and Equilibrium Studies on Some Co-ordinated Cyclohexadiene Cations : Investigating a Chemoenzymatic Route to Arene *trans*-Dihydrodiols”, M. Galvin, C. Mc Donnell and R. More O’Ferrall, International Symposium on Organocatalysis in Organic Synthesis, University of Glasgow, July 2006.

“Kinetic and Equilibrium Studies on Some Co-ordinated Cyclohexadiene Cations : Investigating a Chemoenzymatic Route to Arene *trans*-Dihydrodiols”, M. Galvin, C. Mc Donnell and R. More O’Ferrall, Recent Advances in Synthesis and Chemical Biology Symposium, University College Dublin, December 2005.

“Kinetic and Equilibrium Studies on Some Co-ordinated Cyclohexadiene Cations”, M. Galvin, C. Mc Donnell and R. More O’Ferrall, 10<sup>th</sup> European Symposium on Organic Reactivity, Rome, July 2005.

“Kinetic and Equilibrium Studies on Some Co-ordinated Cyclohexadiene Cations”, M. Galvin, C. Mc Donnell and R. More O’Ferrall, Organic Reaction Mechanisms VII International Conference, University College Dublin, July 2004.

“Kinetic and Equilibrium Studies on Some Iron Tricarbonyl and Iron Dicarbonyl Triphenylphosphine Coordinated Cyclohexadiene Cations,” M. Galvin, C. Mc Donnell and R. More O’Ferrall, Royal Society of Chemistry European Postgraduate Industry Tour, London Gatwick Hotel, November 2003.